

Ana Patrícia Barreira Marques

## ROLE OF HYPOXIA AND FIBROSIS IN ADIPOSE TISSUE

Tese de Doutoramento em Biologia Experimental e Biomedicina, ramo de Biologia Molecular, Celular e do Desenvolvimento, orientada pela Professora Doutora Cláudia Margarida Gonçalves Cavadas e pela Doutora Joana Margarida Rosmaninho Salgado, apresentada ao Instituto de Investigação Interdisciplinar da Universidade de Coimbra.

Outubro 2016



UNIVERSIDADE DE COIMBRA



# **Role of hypoxia and fibrosis in adipose tissue**

**Ana Patrícia Barreira Marques**

Outubro 2016



UNIVERSIDADE DE COIMBRA



# Role of hypoxia and fibrosis in adipose tissue

Ana Patrícia Barreira Marques

PhD thesis presented to the Institute for Interdisciplinary Research of the University of Coimbra (IIIUC) in fulfillment of the requirements for a Doctoral degree in Experimental Biology and Biomedicine, specialization in Molecular, Cellular and Developmental Biology.

Tese de Doutoramento apresentada ao Instituto de Investigação Interdisciplinar da Universidade de Coimbra (IIIUC), para cumprimento dos requisitos necessários à obtenção do grau de Doutor em Biologia Experimental e Biomedicina, no ramo de Biologia Molecular, Celular e do Desenvolvimento.

This work was performed at the Center for Neuroscience and Cell Biology, University of Coimbra, Portugal, under the supervision of Professor Cláudia Margarida Gonçalves Cavadas and Joana Margarida Rosmaninho Salgado.

This work was supported by FEDER funds through the Operational Programme Factors Competitiveness - COMPETE 2020 and by National Funds through FCT - Foundation for Science and Technology under the Strategic Project (UID/NEU/04539/2013), PTDC/SAU-FCF/102415/2008, SFRH/BD/51674/2011; by QREN – Projeto Mais Centro – "Aging, Stress And Chronic Diseases: From Mechanisms To Therapeutics" and by a Project Grant for Obesity investigation provided by the Portuguese Society of Endocrinology and Metabolism (SPEDM) and Abbot; L'Oreal Women for Science Program (FCT/UNESCO-Portugal).

Este trabalho foi realizado no Centro de Neurociências e Biologia Celular da Universidade de Coimbra, Portugal, sob orientação da Professora Doutora Cláudia Margarida Gonçalves Cavadas e da Joana Margarida Rosmaninho Salgado.

Este trabalho foi financiado por fundos FEDER através do Programa Operacional Factores de Competitividade – COMPETE, por fundos nacionais, através da FCT - Fundação para a Ciência e Tecnologia pelo projeto estratégico UID/NEU/04539/2013, PTDC/SAU-FCF/102415/2008, SFRH/BD/51674/2011; pelo QREN – Projeto Mais Centro – "Aging, Stress And Chronic Diseases: From Mechanisms To Therapeutics" e pelo projecto para o estudo da obesidade através da Sociedade Portuguesa de Endocrinologia, Diabetes e Metabolismo (SPEDM) e Abbot; L'Oréal Portugal para as Mulheres na Ciência (FCT/UNESCO-Portugal).



C · IIIUC

INSTITUTO DE INVESTIGAÇÃO  
INTERDISCIPLINAR  
UNIVERSIDADE DE COIMBRA



UNIÃO EUROPEIA  
Fundo Europeu  
de Desenvolvimento Regional





**COVER:** Image of differentiated 3T3-L1 adipocytes immunostained for peroxisome proliferator-activated receptor  $\gamma$  (PPAR $\gamma$ , green) and with lipids stained with Oil red-O (red). Nuclei were visualized with Hoechst 33342 (blue).





*"It was the best of times, it was the worst of times, it was the age of wisdom, it was the age of foolishness, it was the epoch of belief, it was the epoch of incredulity, it was the season of light, it was the season of darkness, it was the spring of hope, it was the winter of despair."*

Charles Dickens, *A Tale of Two Cities*



## **Agradecimentos/Acknowledgements**

Ao Centro de Neurociências e Biologia Celular por me ter acolhido e proporcionado todas as condições para desenvolver a parte prática deste trabalho.

À Professora Doutora Cláudia Cavadas agradeço a disponibilidade em me aceitar como aluna de Doutorado e por me ter acompanhado neste desafio e orientado ao longo deste trabalho. Obrigada, também, pelo seu apoio, disponibilidade, e pela ajuda que me deu na realização deste trabalho sempre com boa disposição e optimismo.

Agradeço à Doutora Joana Salgado pela orientação, ensinamentos, incentivo, e empenho que contribuíram para a realização deste trabalho. Mas quero agradecer acima de tudo a amizade. Obrigada por todos os momentos divertidos, por todos os conselhos, pela disponibilidade para me ouvires mesmo nos momentos mais difíceis. Obrigada!

A todo o Grupo de Neuroendocrinologia e Envelhecimento pela ajuda e boa disposição constante: Professora Caetana Carvalho, Professor Paulo Santos, Professor Armando Cristovão, Inês Araújo, Inês Morte, Bruno Carreira, Ana Carvalho, Fábica Vicente, Jorge Pascoal, Alexandra Gonçalves, Ana Isabel Santos, Sofia Lourenço, Vanessa Machado, Gabriel Costa, Mariana Correia, Pedro Gomes, Joana Neves, Dina Pereira, Liliana Santos, Helena Leal, Marta Quatorze, Ana Leal, Ana Samões e Joana Pereira.

Quero deixar um agradecimento especial à Célia Avelaira pelo apoio, à Magda Santana por estar sempre lá, à Janete Santos pela companhia na secretária mas também pela amizade, pelos conselhos e desabafos, à Vera Cortez pela amizade e por todos os momentos divertidos que passámos, à Marta Estrada por ser a “Muffin” e por toda a ajuda que me deu no laboratório, à Marianinha pelo carinho e amizade, à Marisa e Sara pela boa disposição no laboratório e pela alegria que vos caracteriza, à Lígia Ferreira pela contribuição e apoio na realização deste trabalho e também pela amizade, à Joana Vindeirinho por toda a sabedoria que partilhou sempre connosco e pela boa disposição, à Ana Rita Álvaro pela simpatia, carinho e disponibilidade, à Laetitia pela amizade e alegria e ao Pedro pelos conselhos e opiniões sempre tão positivos.

A todas as pessoas do “aquário”, obrigada pelo bom ambiente, companheirismo e boa disposição. Quero agradecer em especial à Taty por ser uma pessoa especial e passar isso para todas as pessoas que a rodeiam. Um especial agradecimento à Mariline por todos os almoços, lanches, gelados, cafezinhos que apesar de às vezes não serem assim tão saudáveis, tão bem que faziam à alma.

Ao Grupo do Professor Luís Pereira de Almeida, obrigada pela simpatia e disponibilidade para ajudar sempre que necessário. Quero agradecer em especial à Sara Lopes pela amizade e pela sua boa disposição contagiante. Obrigada também ao Rui Nobre pela ajuda na realização deste trabalho. Um obrigada também a todos aqueles com quem me cruzei diariamente nos corredores.

Agradeço aos meus colegas do BEB, ao André, António, Catarina, Dominique, Joana, João, Marcelo, Mariline, Sara, Sofia, Tânia, por fazerem aquele nosso primeiro ano tão mais fácil de ultrapassar. Obrigada a todos por tudo, tanto aos que se mantiveram mais próximos como àqueles que estão mais longe.

À Luisa Cortes, Margarida Caldeira, Isabel Dantas e Isabel Nunes agradeço o apoio técnico e disponibilidade.

Agradeço à Diana Graça, à Sara Lopes, à D. Céu, à D. Isabel e à Elisabete toda a ajuda técnica.

A todos os amigos fora do laboratório, obrigada pela amizade e apoio ao longo desta viagem. Obrigada por estarem por perto.

Agradeço ao Bruno, por me ter acompanhado, e acreditado sempre em mim. Pelo teu amor, carinho, amizade e enorme paciência! Por seres o meu porto de abrigo e me dares força mesmo nos momentos mais difíceis. Obrigada por tudo!

Obrigada à minha família, por me apoiar e incentivar.

Obrigada ao meu irmão e à minha cunhada por todo o apoio ao longo destes anos e obrigada ao Diogo por me deixar com um sorriso na cara em qualquer situação.

Obrigada aos meus pais pela dedicação, a paciência, o apoio incondicional em todos os momentos e toda a confiança que sempre depositaram em mim. Obrigada por tudo.. Um agradecimento especial à minha avó por também ela ser uma pessoa especial. Por fim, um agradecimento especial à Margarida, Mimi e Miminho.

## Table of Contents

<b>List of abbreviations.....</b>	<b>xvii</b>
<b>Resumo.....</b>	<b>xxi</b>
<b>Abstract.....</b>	<b>xxiii</b>
<b>CHAPTER 1 General Introduction .....</b>	<b>xxv</b>
<b>1. General Introduction .....</b>	<b>27</b>
<b>1.1 Obesity.....</b>	<b>27</b>
<b>1.2 Adipose tissue .....</b>	<b>29</b>
1.2.1 White and brown adipose tissue .....	29
<b>1.3 Adipogenesis .....</b>	<b>31</b>
1.3.1. Factors Positively Regulating Adipogenesis.....	33
1.3.1.1 Peroxisome Proliferator-Activated Receptor $\gamma$ .....	33
1.3.1.2 CCAAT/Enhancer-Binding Proteins.....	34
1.3.1.3 The Krüppel-Like Factor Family .....	35
1.3.1.4 Sterol Regulatory Element-Binding Protein 1 .....	36
1.3.1.5 cAMP Response Element-Binding Protein.....	36
1.3.2 Factors Negatively Regulating Adipogenesis .....	36
1.3.2.1 The Krüppel-Like Factor Family .....	36
1.3.2.2 GATA2 and GATA3.....	37
1.3.2.3 Preadipocyte Factor-1 .....	37
1.3.3 Other regulators of adipogenesis .....	38
1.3.3.1 MicroRNAs .....	38
1.3.3.1.1 MicroRNA miR-27 .....	41
1.3.3.2 Autophagy .....	41
1.3.3.2.1 Autophagy in adipose tissue .....	44
<b>1.4 Metabolic function of adipose tissue.....</b>	<b>44</b>
1.4.1 Lipogenesis .....	45
1.4.2 Lipolysis.....	46

<b>1.5 Endocrine function .....</b>	<b>47</b>
<b>1.6 Adipose tissue changes in obesity .....</b>	<b>50</b>
1.6.1 Adipose tissue hypoxia .....	52
1.6.1.1 Vasculature in adipose tissue.....	52
1.6.1.2 Hypoxia hypothesis .....	53
1.6.1.3 Hypoxia signaling pathways.....	54
1.6.1.4 Glucose metabolism and insulin resistance .....	56
1.6.1.5 Lipid metabolism .....	57
1.6.1.6 Fibrosis.....	58
1.6.2 Adipose tissue fibrosis.....	59
1.6.2.1 Extracellular matrix properties and functions .....	59
1.6.2.2 Extracellular matrix and adipose tissue development .....	61
1.6.2.3 Extracellular matrix remodeling and fibrosis in obesity .....	62
1.6.2.4 Modulation of extracellular matrix components in obese mouse models.....	64
1.6.2.5 Underlying mechanisms of fibrosis formation in white adipose tissue .....	66
<b>1.7 Dipeptidyl peptidase IV .....</b>	<b>67</b>
1.7.1 Non-enzymatic function of dipeptidyl peptidase IV.....	68
1.7.2 Enzymatic (catalytic) function of dipeptidyl peptidase IV.....	69
1.7.2.1 Incretins.....	70
1.7.2.2 Non-incretin substrates .....	72
1.7.3 Dipeptidyl peptidase in adipose tissue .....	72
1.7.4 Dipeptidyl peptidase inhibitors.....	74
1.7.4.1 Vildagliptin.....	76
1.7.5 Effect of dipeptidyl peptidase inhibition on adipose tissue and obesity .....	76
1.7.6 Role of dipeptidyl peptidase IV inhibitor in fibrosis in non-adipose tissues	78
<b>1.8 Neuropeptide Y .....</b>	<b>81</b>
1.8.1 Neuropeptide Y in adipose tissue.....	84

<b>CHAPTER 2 Objectives .....</b>	<b>87</b>
<b>2. Main objectives .....</b>	<b>89</b>
<b>CHAPTER 3 Hypoxia mimetic induces lipid accumulation through mitochondrial dysfunction and stimulates autophagy in murine preadipocyte cell line .....</b>	<b>91</b>
<b>3.1 Abstract .....</b>	<b>93</b>
<b>3.2 Introduction.....</b>	<b>94</b>
<b>3.3 Materials and Methods .....</b>	<b>96</b>
3.3.1 Cell culture .....	96
3.3.2 Cell Differentiation protocol .....	96
3.3.3 Experimental Conditions .....	96
3.3.4 Lipid accumulation quantification by Oil red-O staining.....	96
3.3.5 Oil Red-O fluorescent staining .....	97
3.3.6 Immunofluorescence .....	97
3.3.7 Mitotracker and Mitosox .....	97
3.3.8 Western blotting.....	97
3.3.9 Quantitative real-time PCR for PPAR $\gamma$ 2 .....	98
3.3.10 Lactate measurements.....	99
3.3.11 Determination of ATP content .....	99
3.3.12 Reactive oxygen species measurements.....	99
3.3.13 Quantitative real-time PCR for miRNA 27a and 27b analysis .....	99
3.3.14 Statistical analysis .....	100
<b>3.4 Results.....</b>	<b>101</b>
3.4.1 Hypoxia mimetic agent CoCl <sub>2</sub> induces lipid accumulation without PPAR $\gamma$ 2 expression .....	101
3.4.2 Adipocyte differentiation is blocked by miR-27a and miR-27b induction..	104
3.4.3. Mitochondrial dysfunction and reactive oxygen species are responsible for lipid accumulation induced by hypoxia mimetic.....	104
3.4.4 Hypoxia mimetic induces autophagy .....	107
<b>3.5 Discussion.....</b>	<b>109</b>

<b>CHAPTER 4 DPP-IV inhibition prevents fibrosis in adipose tissue of obese mice</b>	<b>113</b>
<b>4.1 Abstract</b>	<b>115</b>
<b>4.2 Introduction</b>	<b>116</b>
<b>4.3 Materials and Methods</b>	<b>118</b>
4.3.1 <i>In vivo</i> experiments	118
4.3.2 Animals	118
4.3.3 Intraperitoneal Glucose Tolerance Test	118
4.3.4 Tissue collection	118
4.3.5 Serum Triglycerides and Cholesterol determination	119
4.3.6 Serum leptin and insulin quantification	119
4.3.7 Tissue preparation for histological processing	119
4.3.8 Hematoxylin and eosin staining	119
4.3.9 Adipocyte diameter quantification	119
4.3.10 Hydroxyproline quantification	120
4.3.11 Viral Vectors Production	120
4.3.12 Engineering of short hairpin RNA	120
4.3.13 Cell culture of 3T3-L1 preadipocyte cell line	121
4.3.14 Preadipocyte differentiation	121
4.3.15 Immunofluorescence	121
4.3.16 Protein quantification and sample preparation	122
4.3.17 Western blotting	122
4.3.18 Statistical analysis	123
<b>4.4 Results</b>	<b>124</b>
4.4.1 Vildagliptin has no effect on body weight of HFD mice, but reduces serum triglycerides and total cholesterol	124
4.4.2 Vildagliptin decreases blood glucose and improves glucose tolerance	125
4.4.3 Vildagliptin does not alter epididymal adipose tissue weight nor adipocyte diameter	126



4.4.4 Vildagliptin prevents fibrosis markers in adipose tissue of HFD mice .....	127
4.4.5 Vildagliptin prevents collagen and matrix markers deposition in TGFβ1-stimulated 3T3-L1 cell line.....	129
4.4.6 Vildagliptin abrogates the TGFβ1-induced alterations in ECM through NPY Y <sub>1</sub> receptor activation .....	131
<b>4.5 Discussion.....</b>	<b>134</b>
<b>CHAPTER 5 Concluding Remarks .....</b>	<b>137</b>
<b>5. Concluding remarks .....</b>	<b>139</b>
<b>CHAPTER 6 References .....</b>	<b>141</b>
<b>6. References .....</b>	<b>143</b>



## List of abbreviations

<b>AC</b>	Adenylate cyclase
<b>ACC</b>	Acetyl-CoA carboxylase
<b>ACS</b>	Acyl-CoA synthase
<b>ADA</b>	Adenosine deaminase
<b>ADD1</b>	Adipocyte determination and differentiation-dependent factor 1
<b>ADRP</b>	Adipose differentiation-related protein
<b>AF-1</b>	Activation function-1
<b>AF-2</b>	Activation function-2
<b>Ago2</b>	Argonaute2
<b>AMPK</b>	AMP-activated protein kinase
<b>ANOVA</b>	Analysis of variance
<b>aP2</b>	Adipocyte protein 2
<b>β-AR</b>	β-adrenergic receptor
<b>Atg</b>	Autophagy related genes
<b>ATGL</b>	Adipose triglyceride lipase
<b>ATP</b>	Adenosine Triphosphate
<b>BAT</b>	Brown Adipose Tissue
<b>BMI</b>	Body Mass Index
<b>BSA</b>	Bovine serum albumin
<b>cAMP</b>	Cyclic adenosine monophosphate
<b>CBP</b>	CREB binding protein
<b>cDNA</b>	Complementary DNA
<b>C/EBP</b>	CCAAT/Enhancer-Binding Protein
<b>CoA</b>	Coenzyme A
<b>CPON</b>	C-terminal flanking peptide of NPY
<b>CREB</b>	Cyclic AMP response Element-binding protein
<b>Ct</b>	Cycle threshold
<b>DAG</b>	Diacylglycerol
<b>DFO</b>	Deferoxamine mesylate
<b>DGCR8</b>	DiGeorge syndrome chromosomal region 8
<b>DMEM-HG</b>	Dulbecco's Modified Eagle Medium with high glucose
<b>DNA</b>	Deoxyribonucleic acid
<b>DPP-IV</b>	Dipeptidyl peptidase IV
<b>DTT</b>	Dithiothreitol
<b>ECF</b>	Enhanced chemifluorescence
<b>ECM</b>	Extracellular matrix
<b>EID-1</b>	EP300-interacting inhibitor of differentiation 1
<b>EMA</b>	European Medicine Agency
<b>ERK</b>	Extracellular Signal-regulated Kinase-1
<b>FA</b>	Fatty acid
<b>FABP</b>	Fatty acid binding protein
<b>FAS</b>	Fatty acid synthase
<b>FATP1</b>	Fatty acid transport protein 1
<b>FDA</b>	Food and Drug Administration
<b>FIH</b>	Factor inhibiting HIF
<b>FIP200</b>	Focal adhesion kinase family-interacting protein of 200 kDa

<b>GABA</b>	$\gamma$ -aminobutyric acid
<b>GATA</b>	GATA binding protein
<b>GIP</b>	Gastric inhibitory polypeptide
<b>GIPR</b>	GIP receptor
<b>GLP-1</b>	Glucagon-like peptide-1
<b>GLP-1R</b>	Glucagon-like peptide 1 receptor
<b>GLUT</b>	Glucose transporter type
<b>GSH</b>	Glutathione
<b>GTPase</b>	Guanosine triphosphatase
<b>hASC</b>	Human adipose-derived stem cell
<b>HE</b>	Hematoxylin and eosin
<b>HFD</b>	High-fat diet
<b>HIF-1</b>	Hypoxia-inducible factor-1
<b>HIF-1<math>\alpha</math></b>	Hypoxia-inducible factor-1 $\alpha$
<b>HIF-1<math>\beta</math></b>	Hypoxia-inducible factor-1 $\beta$
<b>HRE</b>	Hypoxia-response element
<b>HSL</b>	Hormone-sensitive lipase
<b>IBMX</b>	3-isobutyl-1-methylxanthine
<b>IGF</b>	Insulin-like growth factor
<b>I<math>\kappa</math>B</b>	Inhibitor $\kappa$ B
<b>IL</b>	Interleukin
<b>iNOS</b>	Inducible nitric oxide synthase
<b>ipGTT</b>	Intraperitoneal glucose tolerance test
<b>IR</b>	Insulin receptor
<b>KLF</b>	Krüppel-like factor
<b>LAMP2A</b>	Lysosome-associated membrane protein 2A
<b>LC3B</b>	Microtubule associated protein-1 light chain-3B
<b>LDL</b>	Low density lipoproteins
<b>LPL</b>	Lipoprotein lipase
<b>MAG</b>	Monoacylglycerol
<b>MAPK</b>	Mitogen-activated protein kinase
<b>MCP-1</b>	Monocyte chemoattractant protein 1
<b>MCT1</b>	Monocarboxylate transporter 1
<b>MCT4</b>	Monocarboxylate transporter 4
<b>MEF</b>	Mouse embryonic fibroblast
<b>MGL</b>	Monoacylglycerol lipase
<b>MIF</b>	Macrophage migration inhibitory factor
<b>miRISC</b>	miRNA-induced silencing complex
<b>miRNAs, miRs</b>	MicroRNAs
<b>MMP</b>	Matrix metalloproteinase
<b>mRNA</b>	Messenger RNA
<b>MSC</b>	Mesenchymal stem cell
<b>mTOR</b>	Mammalian target of rapamycin
<b>mTORC</b>	Mammalian target of rapamycin complex
<b>NADH</b>	Nicotinamide adenine dinucleotide
<b>NF<math>\kappa</math>B</b>	Factor nuclear $\kappa$ B
<b>NPY</b>	Neuropeptide Y
<b>OD</b>	Optical density

<b>OPN</b>	Osteopontin
<b>p62 or SQSTM1</b>	Sequestosome 1
<b>PAI-1</b>	Plasminogen activator inhibitor-1
<b>PBS</b>	Phosphate buffered saline
<b>PC</b>	Prohormone convertase
<b>PDK1</b>	Pyruvate dehydrogenase kinase 1
<b>PE</b>	Phosphatidylethanolamine
<b>PET</b>	Positron emission tomography
<b>PGC-1<math>\alpha</math></b>	Peroxisome proliferator-activated receptor $\gamma$ coactivator-1 $\alpha$
<b>PHD</b>	prolyl hydroxylase domain enzymes
<b>PI3K</b>	Phosphatidylinositol 3-kinase
<b>PI3KC3</b>	Phosphatidylinositol-3-kinase class III
<b>PKA</b>	Protein kinase A
<b>PKB</b>	Protein kinase B
<b>PMSF</b>	Phenylmethylsulfonyl fluoride
<b>pO<sub>2</sub></b>	Interstitial partial pressure of oxygen
<b>PP</b>	Pancreatic polypeptide
<b>PPAR<math>\gamma</math></b>	Peroxisome proliferator-activated receptor $\gamma$
<b>PPAR<math>\gamma</math>2</b>	Peroxisome proliferator-activated receptor $\gamma$ 2
<b>Pref-1</b>	Preadipocyte factor-1
<b>Pre-miRNA</b>	Precursor miRNA
<b>Pri-miRNA</b>	Primary miRNA
<b>PVDF</b>	Polyvinylidene fluoride
<b>pVHL</b>	Von Hippel-Lindau tumor suppressor
<b>PYY</b>	Peptide YY
<b>qPCR</b>	Quantitative real-time PCR
<b>RBP-4</b>	Retinol-binding protein 4
<b>RNA</b>	Ribonucleic acid
<b>RNase</b>	Ribonuclease
<b>ROS</b>	Reactive oxygen species
<b>Runx2</b>	Runt-related transcription factor 2
<b>sDPP-IV</b>	Soluble dipeptidyl peptidase IV
<b>SDS</b>	Sodium dodecylsulphate
<b>SDS-PAGE</b>	SDS-polyacrylamide gel electrophoresis
<b>SEM</b>	Standard error of the mean
<b>shRNA</b>	Short hairpin RNA
<b><math>\alpha</math>SMA</b>	$\alpha$ -smooth muscle actin
<b>SPARC</b>	Secreted protein acidic and rich in cysteine
<b>SREBP</b>	Sterol regulatory element-binding protein
<b>STZ</b>	Streptozotocin
<b>SVF</b>	Stromal vascular fraction
<b>TAG</b>	Triglyceride
<b>TBS-T</b>	Tris-buffered saline
<b>TCF7L2</b>	Transcription factor 7-like 2
<b>TGF<math>\beta</math></b>	Transforming growth factor $\beta$
<b>TGFBR2</b>	Transforming growth factor $\beta$ receptor 2
<b>TIMP</b>	Tissue inhibitor of metalloproteinase
<b>TIP47</b>	Tail-interacting protein 47

<b>TNF-<math>\alpha</math></b>	Tumor necrosis factor- $\alpha$
<b>t-PA</b>	Tissue-type plasminogen activator
<b>TRBP</b>	Trans-activation response RNA-binding protein
<b>TSP1</b>	Thrombospondin-1
<b>TZD</b>	Thiazolidinedione
<b>UCP-1</b>	Uncoupling protein-1
<b>ULK</b>	Unc-51 like kinase
<b>u-PA</b>	Urokinase-type plasminogen activator
<b>UPS</b>	Ubiquitin-proteasome system
<b>UTR</b>	Untranslated region
<b>VEGF</b>	Vascular endothelial growth factor
<b>VLDL</b>	Very low density lipoproteins
<b>Vps</b>	Vacuolar protein sorting-associated protein
<b>WAT</b>	White adipose tissue
<b>WHO</b>	World Health Organization

## Resumo

A obesidade é um problema de saúde pública que leva a um aumento da morbidade e mortalidade. É caracterizada por um aumento excessivo de tecido adiposo branco (WAT). Durante a obesidade ocorre hipertrofia dos adipócitos, levando ao desenvolvimento de hipóxia local no WAT. No entanto, o papel da hipóxia na regulação do tecido adiposo ainda é controverso.

Desta forma, o primeiro objectivo desta tese foi investigar o papel da hipóxia na função dos adipócitos em pré-adipócitos de murganho (linha celular 3T3-L1) através da avaliação da acumulação lipídica, marcadores de pré-adipócitos e adipócitos, microRNA (miR)-27, alterações mitocondriais e autofagia.

Os resultados mostram que o cloreto de cobalto ( $\text{CoCl}_2$ ), um mimético de hipóxia, aumenta a acumulação lipídica sem expressão do receptor activado pelo proliferador do peroxissoma  $\gamma 2$  (PPAR $\gamma 2$ ), perilipina e com diminuição da proteína factor de pré-adipócito-1 (Pref-1). Além disso, o mimético de hipóxia induz a expressão dos microRNAs, miR-27a e miR-27b, que como já foi descrito inibem a expressão de PPAR $\gamma 2$ . Observou-se ainda que o  $\text{CoCl}_2$  induz disfunção mitocondrial e aumenta a produção de espécies reactivas de oxigénio (ROS). O tratamento das células com glutathiona, um agente antioxidante, previne a acumulação lipídica induzida por  $\text{CoCl}_2$ . Por outro lado, o mimético de hipóxia aumenta a autofagia. Em conjunto estes resultados mostram que o  $\text{CoCl}_2$  bloqueia a diferenciação dos adipócitos, enquanto induz a autofagia e também estimula a acumulação de lípidos através de disfunção mitocondrial e acumulação de ROS.

Durante o desenvolvimento da obesidade a expansão de WAT conduz também a uma desregulação e uma acumulação excessiva da matriz extracelular (ECM), levando à formação de fibrose. Por outro lado, alguns estudos mostraram que os inibidores da dipeptidil peptidase IV (DPP-IV), as gliptinas, previnem a fibrose no coração, fígado e rim em modelos animais.

Desta forma, o segundo objectivo da presente tese foi investigar se o inibidor da DPP-IV, a vildagliptina, previne a fibrose que ocorre no WAT num modelo de obesidade induzida por uma dieta rica em gordura (HFD) em murganhos C57BL/6 e também estudar os seus mecanismos, usando uma linha celular de pré-adipócitos, 3T3-L1. Murganhos C57BL/6 foram submetidos a uma dieta standard ou a uma dieta HFD (40% de gordura durante 7 semanas) e tratados com vildagliptina (30 mg/kg/day in water) durante 7 semanas. O peso corporal e a ingestão de alimentos foram avaliados duas vezes por semana. Os níveis de glicose no sangue e de triglicérideos, colesterol total,

leptina e insulina no soro foram investigados e um teste de tolerância à glucose foi realizado.

Os resultados mostraram que a vildagliptina melhora a resposta à glicose nos murganhos submetidos a HFD, e reduz os níveis séricos de triglicéridos, colesterol total e leptina, sem alterar os níveis séricos de insulina. A vildagliptina não altera o peso corporal, peso do WAT e o diâmetro dos adipócitos. Por outro lado, a vildagliptina previne o aumento da fibrose, conteúdo de colagénio e os níveis de actina do músculo liso  $\alpha$  ( $\alpha$ SMA) e fibronectina no WAT de murganhos submetidos a HFD. No estudo *in vitro*, a vildagliptina previne a deposição de ECM induzida por TGF- $\beta$ 1, prevenindo o aumento dos níveis de colagénio total,  $\alpha$ SMA e fibronectina, através da activação do receptor NPY Y<sub>1</sub>. A inibição da DPP-IV por abordagens farmacológicas e genéticas deram origem a resultados semelhantes. Este estudo sugere assim que a vildagliptina inibe a deposição de ECM e a formação de fibrose no WAT num modelo de obesidade em murganhos induzido pela dieta e em pré-adipócitos 3T3-L1, pelo menos, parcialmente através do NPY e da activação dos receptores Y<sub>1</sub>.

Em conclusão, com os resultados desta tese conseguimos uma melhor compreensão sobre o efeito da hipóxia na fisiologia do adipócito e do metabolismo lipídico. Por outro lado, a redução da fibrose pela vildagliptina poderá melhorar a expandibilidade do tecido adiposo no tratamento da obesidade e complicações associadas.

**Palavras-chave:** obesidade, hipóxia, adipogénese, espécies reactivas de oxigénio, autofagia, fibrose, matriz extracelular, inibidores da DPP-IV, vildagliptina, NPY, receptor NPY Y<sub>1</sub>.



## **Abstract**

Obesity is one of the most immediate health threats in industrialized countries, increasing morbidity and mortality. It is characterized by an excessive increase of white adipose tissue (WAT). As adipocyte hypertrophy develops, local adipose tissue hypoxia may occur within WAT of obese humans and mice. However, its role in adipose tissue regulation is still controversial.

Therefore, the first aim of this study was to investigate the role of hypoxia on adipocyte function in murine preadipocytes (3T3-L1 cell line) by evaluating lipid accumulation, preadipocyte and adipocyte markers, microRNA (miR)-27, mitochondrial changes and autophagy.

The results show that the hypoxia mimetic cobalt chloride (CoCl<sub>2</sub>) increases lipid accumulation with no expression of peroxisome proliferator-activated receptor  $\gamma$ 2 (PPAR $\gamma$ 2), perilipin and with decrease in preadipocyte factor-1 (Pref-1). Furthermore, using qPCR we observed that the hypoxia mimetic upregulates both miR-27a and miR-27b, which are known to block PPAR $\gamma$ 2 expression. CoCl<sub>2</sub> induces mitochondrial dysfunction, and increases the production of reactive oxygen species (ROS). Moreover, an antioxidant agent, glutathione, prevents lipid accumulation induced by hypoxia mimetic indicating that ROS are responsible for hypoxia-induced lipid accumulation in these cells. Furthermore, we also observed that CoCl<sub>2</sub> increases autophagy activity. These results demonstrate that CoCl<sub>2</sub> blocks differentiation, while inducing autophagy and lipid accumulation through mitochondrial dysfunction and ROS accumulation.

During the development of obesity the expansion of WAT leads also to a dysregulation and an excessive remodeling of extracellular matrix (ECM), leading to fibrosis formation. Moreover, dipeptidyl peptidase IV (DPP-IV) inhibitors (gliptins) were shown to prevent fibrosis in other tissues, such as heart, liver and kidney.

Therefore, the second aim of this study was to investigate whether vildagliptin, a DPP-IV inhibitor, can be beneficial in preventing fibrosis in WAT in a model of diet-induced obesity, high-fat diet (HFD)-fed C57BL/6 mice and also to study its mechanisms, using a 3T3-L1 preadipocyte cell line. C57BL/6 mice were maintained on either a standard rodent chow diet or a HFD (40% fat for 7 weeks) and treated with vildagliptin (30 mg/kg/day in water) for 7 weeks. Body weight and food intake were assessed twice a week. Blood glucose, serum triglycerides, total cholesterol, leptin and insulin levels were also assessed and an oral glucose tolerance test was performed.

The results show that vildagliptin improves glucose response, reduces serum triglycerides, total cholesterol and leptin and has no effect on serum insulin. Vildagliptin

also has no effect in body weight, WAT weight and adipocyte diameter. However, vildagliptin prevents the increase of collagen content,  $\alpha$  smooth muscle actin ( $\alpha$ SMA) and fibronectin levels in WAT of HFD-fed mice. In the *in vitro* study, vildagliptin prevents ECM deposition-induced by TGF $\beta$ 1, preventing collagen content,  $\alpha$ SMA and fibronectin levels, through NPY and NPY Y<sub>1</sub> receptor activation. Inhibition of DPP-IV by pharmacological and genetic approaches results in similar results. These results suggest that vildagliptin can prevent ECM deposition and fibrosis formation in WAT of a diet-induced obesity mice model and 3T3-L1 preadipocytes at least partially through NPY and NPY Y<sub>1</sub> receptor activation.

Overall, these results deepen our knowledge about the effect of hypoxia in adipocyte physiology and in lipid metabolism. Moreover, the decrease in adipose tissue fibrosis by vildagliptin may improve adipose tissue expandability in the treatment of obesity and associate diseases.

**Keywords:** obesity, hypoxia, adipogenesis, reactive oxygen species, autophagy, fibrosis, extracellular matrix, DPP-IV inhibitor, vildagliptin, NPY, NPY Y<sub>1</sub> receptor.

# **CHAPTER 1**

---

## **General Introduction**



## 1. General Introduction

### 1.1 Obesity

Obesity is a relevant public health problem. According to World Health Organization (WHO), worldwide obesity has more than doubled since 1980. In 2014, 39% of adults aged 18 years and over were overweight, and 13% were obese (Figure 1.1). According to WHO, overweight and obesity are defined as abnormal or excessive fat accumulation that presents a risk to health [1].

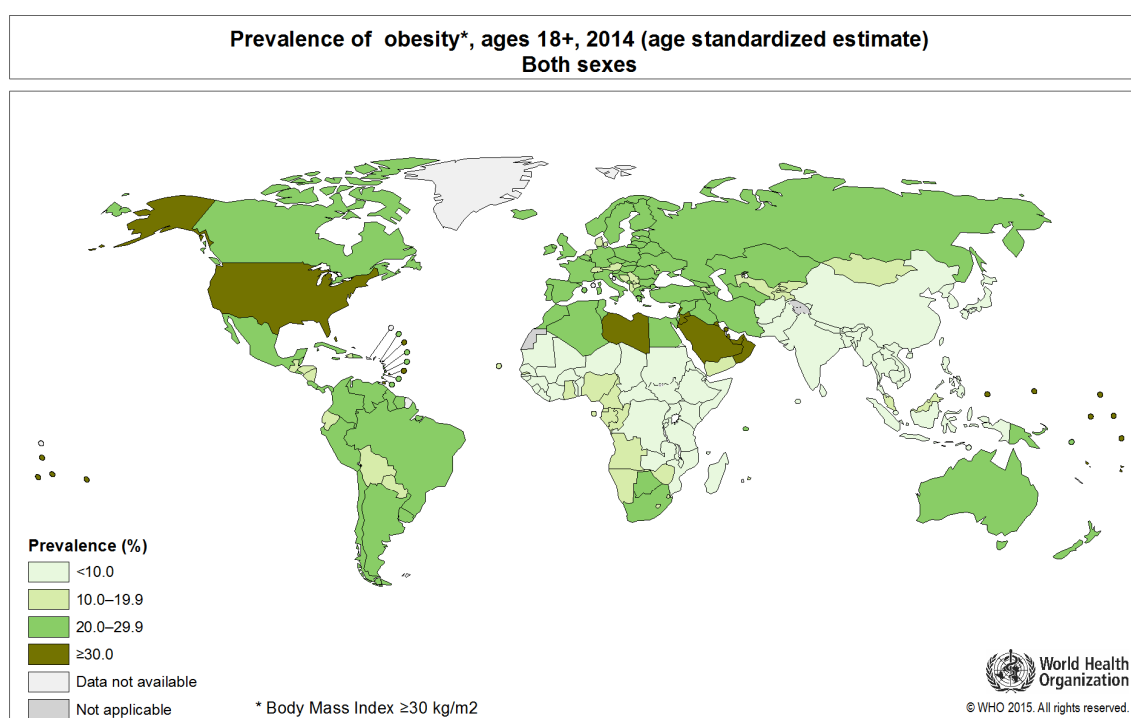


**Figure 1.1 – Prevalence of obesity (body mass index  $\geq 30$  kg/m<sup>2</sup>) of population aged 18-plus in 2014.** Data from World Health Organization.

Although with some limitations the body mass index (BMI) is the more acceptable parameter to define levels of obesity. It is defined as body weight (in kilograms) divided by the square of the height (in meters) [2]. A BMI of 30 or higher corresponds to an obese person [2].

Obesity is a major risk factor for several chronic diseases, including type 2 diabetes mellitus [3], cardiovascular diseases [4] and cancer [5] and it is closely linked to the metabolic syndrome with all the pathological consequences [6].

The fundamental cause of obesity is a long-standing energy imbalance between energy intake and energy expenditure [1]. In fact, obesity is a multifactorial and complex disorder with both genetic and non-genetic causes [1]. Most of monogenic causes of obesity affect

hypothalamic pathways and thereby the regulation of food intake, such as leptin and pro-opiomelanocortin [7] or the receptors, such as leptin receptor [8,9] and melanocortin-4 receptor [10]. However, monogenic cases are rare and genetic predisposition to obesity is in most of the cases polygenic [11,12].

Weight loss of 5-10% in obese people improves overall health, regarding obesity-related comorbidities [13,14]. The most effective way to ameliorate obesity is a change in lifestyle, which includes balanced healthy eating and regular physical activity [15]. However, long-term maintenance of these lifestyle changes is low [16]. Surgery is a very effective treatment with clinically significant and relatively sustained weight loss in subjects with morbid obesity associated with comorbidities [16]. However, it is an expensive therapy with risk of complications, being unsuitable as a solution for obesity epidemics [16]. Pharmacological interventions might be suitable for patients with a BMI of 30 or greater or for patients with a BMI of 27 or greater but with other health complications [16]. Pharmacotherapy has different ways of action and has limited effectiveness, resulting usually in modest weight loss and adverse effects [16] (Table 1.1). Overall, more research is needed to address the underlying causes of obesity and to obtain more effective treatments for obesity and associated comorbidities.

**Table 1.1 – Anti-obesity therapeutics approved by Food and Drug Administration (FDA) and European Medicine Agency (EMA). Adapted from [17].**

Drug	Brand (Manufacturer)	Year approved	Mechanism of action	BW loss (%)	Refs
Orlistat	Xenical® (Roche) Ali® (GlaxoSmithKline)	1998 EMA 1999 FDA	Pancreatic and gastric lipase inhibitor	5-11	[18]
Lorcaserin	Belviq® (Arena Pharmaceuticals)	2012 FDA	Serotonin agonist (5-HT <sub>2C</sub> receptor agonist)	3-5	[19]
Phentermine + topiramate	Qsymia® (Vivus)	2012 FDA	γ-Aminobutyric acid (GABA) receptor modulation + norepinephrine releasing agent	9-11	[20]
Naltrexone + bupropion	Contrave® (Takeda Pharmaceuticals) Mysimba® (Orexigen)	2014 FDA 2015 EMA	Reuptake inhibitor of dopamine + norepinephrine and opioid antagonist	<5	[21]
Liraglutide	Saxenda® (Novo Nordisk)	2014 FDA 2015 EMA	Glucagon-like peptide-1 (GLP-1) receptor agonist	5-12	[22,23]

## 1.2 Adipose tissue

Obesity is characterized by an increase of adipose tissue volume. Adipose tissue is composed mainly of adipocytes. Adipose tissue is a connective tissue, so it has high quantity of extracellular matrix (ECM) proteins. It consists also of a variety of other cell types, collectively known as stromal vascular fraction (SVF), which is also important for normal function of adipose tissue. Cells of SVF include immune cells (macrophages and mast cells), preadipocytes, vascular tissue cells, neural tissue cells and fibroblasts (Figure 1.2).

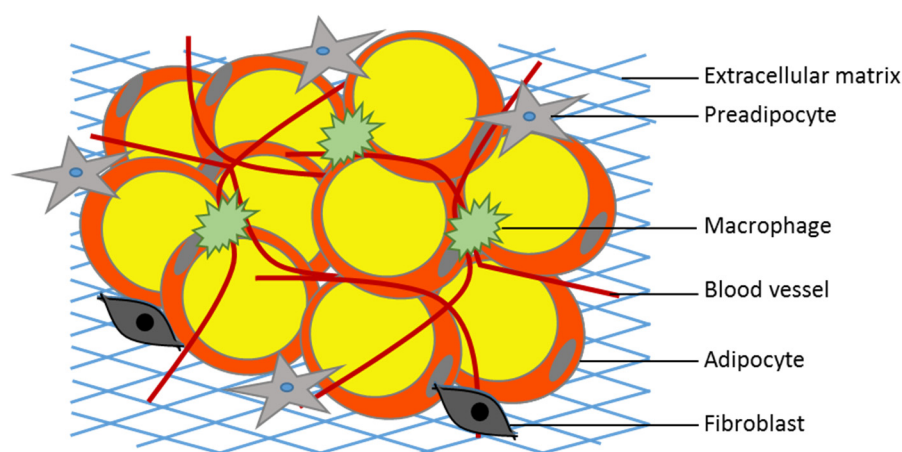


**Figure 1.2 – Composition of adipose tissue.** Adipose tissue is composed of adipocytes, the main cellular component; preadipocytes, precursor cells; fibroblasts; vascular cells, from blood vessels; macrophages, immune cells; and extracellular matrix. Adapted from [24].

The different types of adipose tissue, their different functions and localizations in the body and also its adipogenic processes are tightly regulated in physiological and pathophysiological conditions.

In obesity, several alterations occur in adipose tissue, namely in its architecture and function and thereby it becomes dysregulated [25]. Therefore, adipose tissue is very important in the development of obesity and is reviewed below.

### 1.2.1 White and brown adipose tissue

In mammals, adipose tissue is composed of two different types: white adipose tissue (WAT) and brown adipose tissue (BAT) [26]. WAT is both functionally and morphologically distinct from BAT.

Adipocytes in WAT are larger and unilocular with one single large lipid droplet and a thin cytoplasm [26]. Due to WAT wide distribution throughout the body, it provides protection against mechanical impact and insulation [27]. Moreover, WAT regulates energy balance through its high capacity for storing excess energy in the body and releasing it when

needed [27]. However, WAT is more than a simple storage organ and has important endocrine functions, by secreting cytokines and other compounds [27].

The primary function of BAT is to generate body heat (thermogenesis) [28]. It is especially abundant in fetus and newborns and was thought to be absent in adults being considered irrelevant for energy expenditure. However, using positron emission tomography (PET) scanning, it was demonstrated that adults have several discrete areas of metabolically active BAT that have a more important role in human metabolism than it was previously appreciated [29]. In humans, BAT depots can be found in the supraclavicular, perirenal, paravertebral regions and in the neck [29]. Brown adipocytes are smaller than adipocytes of WAT and have numerous, but small, cytoplasmic lipid droplets and relatively abundant cytoplasm [28]. Brown adipocytes possess numerous mitochondria containing the uncoupling protein-1 (UCP-1), whose main function is related to heat release via oxidation of fatty acids (FAs) [28]. UCP-1 is found in the inner mitochondrial membrane and acts as a proton channel, allowing protons that have been pumped into the intermembrane space to return to the mitochondrial matrix. This mechanism decreases adenosine triphosphate (ATP) production, allowing it to be dissipated as heat [30].

More recently, the transdifferentiation from WAT to BAT has been reported in different species, including humans, forming a different type of adipocyte, referred to as beige or “brite” (brown in white) [31,32]. This is an intermediate type of adipocyte that has a distinct gene expression pattern from white or brown adipocytes [31,32] (Figure 1.3).

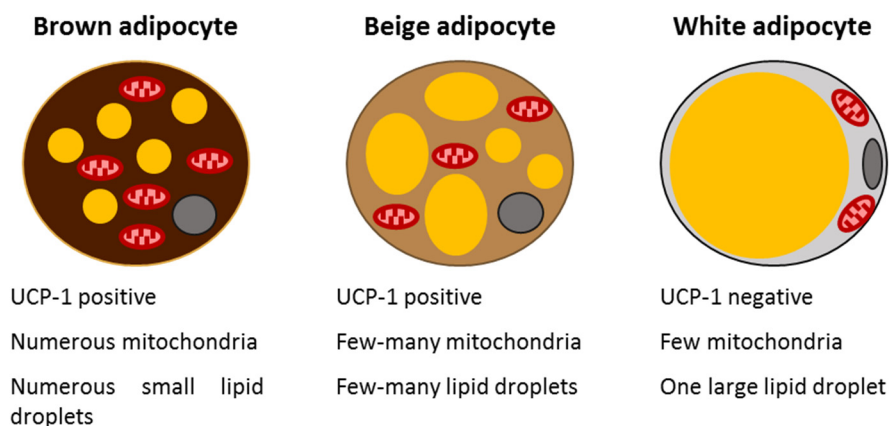


**Figure 1.3 – Morphology of brown, beige, and white adipocytes.** Brown, beige and white adipocytes possess different uncoupling protein-1 (UCP-1) expression, mitochondria density and number and size of lipid droplets. Adapted from [33].

The major focus of this study will be on the biological activities associated with WAT. WAT is distributed throughout the body in different regions called depots (Figure 1.4). Adipose tissue can be classified based on their location that seems to contribute



differently to metabolic and cardiovascular risk [34,35]. The main WAT depots are subcutaneous adipose tissue (beneath the skin), and visceral adipose tissue (around internal organs) [30]. Subcutaneous adipose tissue can be divided in superficial and deep subcutaneous [30]. Visceral adipose tissue surrounds the inner organs and can be divided in omental (near the stomach and spleen), mesenteric (attached to the intestine), retroperitoneal (surrounding the kidney), gonadal (attached to the uterus and ovaries in females and epididymis and testis in men), and pericardial (near the heart) [30].

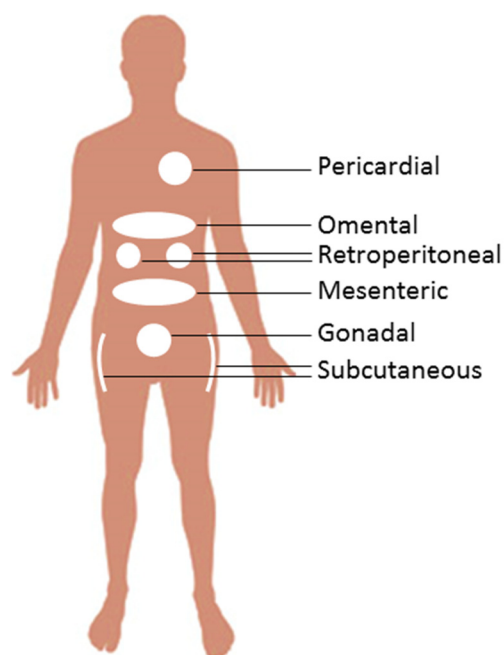


**Figure 1.4 – Adipose tissue distribution throughout the body.** The main white adipose tissue depots are subcutaneous and visceral. The latter can be divided in pericardial, omental, retroperitoneal, mesenteric and gonadal adipose tissue. Adapted from [30].

Visceral adipose depots have been associated with higher levels of lipolysis and lower rates of triglycerides (TAGs) storage [34,35]. Abdominal visceral adipose tissue increases the risk of obesity-related diseases, while subcutaneous adipose tissue seems to be protective through short-term and long-term storage of TAGs [34,35].

Subcutaneous WAT is protective while visceral WAT is associated with an increased risk of obesity-related diseases. WAT distribution is an important factor for the risk of obesity-related diseases development.

### 1.3 Adipogenesis

Adipogenesis of white adipocytes refers to the process of differentiation of the precursor cells into mature adipocytes. Adipocytes have origin in mesenchymal stem cells (MSCs) that can also differentiate into chondrocytes, osteoblasts, and myocytes [36]. MSCs

differentiate into preadipocytes, and finally into mature adipocytes [37]. MSCs have the capacity to differentiate into lipid-storing adipocytes, changing from fibroblastic to round shape cells [37]. WAT expansion takes place rapidly after birth and results from an increase of both adipocyte size and number. The capacity of cells to differentiate into mature adipocytes is maintained throughout all lifespan [38]. The molecular events leading to the commitment of the embryonic stem cell precursor to the adipocyte lineage are not well known. However, the molecular and cellular events that occur from undifferentiated preadipocytes into fully differentiated adipocytes have been extensively studied *in vitro* [39].

During adipocyte differentiation, cells not only suffer changes in morphology, but also in the ECM and cytoskeletal components that are required for change in cell shape, adipocyte-specific gene expression and lipid accumulation [37]. Adipogenesis is a process regulated by a cascade of transcription factors and cell-cycle proteins regulating gene expression and leading to adipocyte development. This process comprises four main steps: growth arrest, mitotic clonal expansion, early differentiation and terminal differentiation [40]. When committed, preadipocytes reach confluence and proliferative preadipocytes become growth-arrested by contact inhibition [40]. Then in mitotic clonal expansion phase, cells re-enter the cell cycle after hormonal induction and undergo cell division [37,40]. Cells then stop proliferating again and undergo early and terminal adipocyte differentiation. Below are reviewed the main positive and negative regulators of this network that are represented in Figure 1.5.

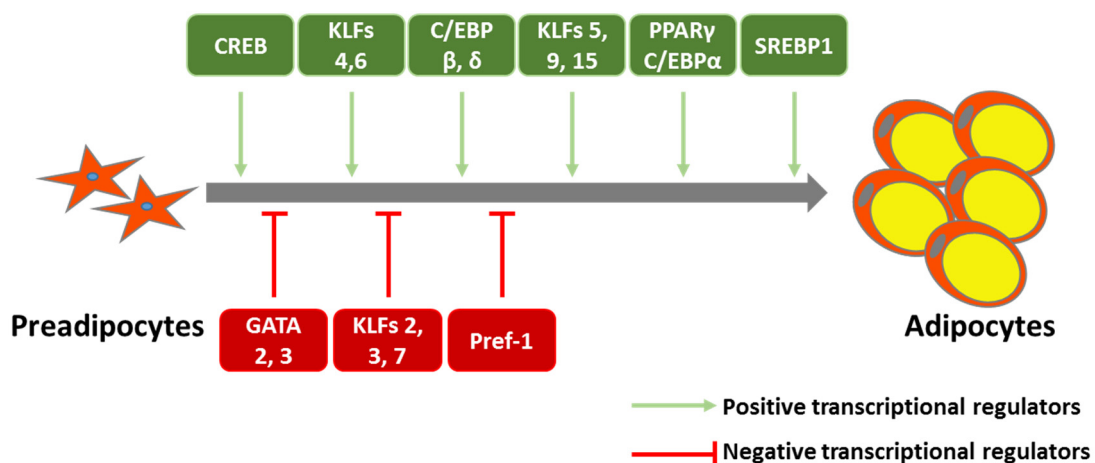


**Figure 1.5 – Regulation of differentiation of preadipocytes into adipocytes.** Adipogenesis is a highly regulated process by both positive and negative regulators. cAMP Response Element-Binding Protein (CREB), Krüppel-Like Factor Family (KLF) 4, 5, 6, 9 and 15, CCAAT/Enhancer-Binding Proteins (C/EBP)  $\alpha$ ,  $\beta$  and  $\delta$  and Sterol Regulatory Element-Binding Protein-1 (SREBP-1) are some relevant transcriptional factors that induce adipogenesis. There are also other factors that inhibit adipocyte differentiation, namely GATA binding protein (GATA) 2 and 3, KLF 2, 3 and 7 and also preadipocyte factor-1 (Pref-1). Adapted from [41].

### 1.3.1. Factors Positively Regulating Adipogenesis

Adipogenesis is a complex and tightly regulated process by a cascade of transcription factors and cell-cycle proteins regulating gene expression. This sequence of events includes activation of Peroxisome Proliferator-Activated Receptor  $\gamma$  (PPAR $\gamma$ ), CCAAT/Enhancer-Binding Proteins (C/EBPs), Krüppel-Like Factor Family (KLF), Sterol Regulatory Element-Binding Protein-1 (SREBP-1) and cyclic adenosine monophosphate (cAMP) Response Element-Binding Protein (CREB) [40].

#### 1.3.1.1 Peroxisome Proliferator-Activated Receptor $\gamma$

PPAR $\gamma$  belong to a nuclear hormone receptor super family that acts as ligand inducible activated transcription factors and is known as the master regulator of adipogenesis [42]. A variety of genes are under control of PPAR $\gamma$  and are involved in FA metabolism, adipogenesis, and insulin sensitivity [43]. The PPAR $\gamma$  structure consists of a non-conserved N-terminal regulatory domain, a highly conserved deoxyribonucleic acid (DNA) binding domain, a hinge region and a C-terminal ligand binding domain [44,45] (Figure 1.6).



**Figure 1.6 – Peroxisome Proliferator-Activated Receptor  $\gamma$  (PPAR $\gamma$ ) has conserved structural and functional domains.** The A/B domain is the hypervariable region that has the activation function-1 (AF-1) domain. Human PPAR $\gamma 2$  contains 28 additional amino acids in the amino terminal region that arise from differential promoter use and splicing. C-domain contains the DNA binding domain with two zinc-fingers. The D-domain (Hinge region) allows for conformational change following ligand binding. The hinge region is important for cofactor docking. The E/F region contains the ligand binding domain and the activation function-2 (AF-2) domain. Adapted from [46].

To bind DNA, PPAR $\gamma$  heterodimerizes with another nuclear receptor, Retinoid X Receptor and recruits transcriptional machinery, leading to the remodeling of chromatin and to increased transcription [47]. Because PPAR $\gamma$  has a ligand-binding domain with a promiscuous nature with a markedly open conformation, a wide range of molecules, such as FAs and prostaglandins have been reported to act as PPAR ligands, binding and activating PPAR $\gamma$  [48-50]. Additionally, synthetic full agonists of the receptor, named thiazolidinediones (TZDs), also activate PPAR $\gamma$  [51]. TZDs are currently used in the

treatment of hyperglycemia in patients with type 2 diabetes mellitus, improving insulin sensitivity, increasing glucose uptake and decreasing glycemia [51].

PPAR $\gamma$  is expressed in two isoforms: PPAR $\gamma$ 1 and PPAR $\gamma$ 2, which are generated by alternative promoter usage and splicing [52]. Both isoforms are identical peptides, although PPAR $\gamma$ 2 has an extension of 28 amino acids at the N-terminus in humans [52]. While PPAR $\gamma$ 1 is expressed in multiple other tissues, including intestine, kidney and liver, PPAR $\gamma$ 2 is expressed almost exclusively in WAT and BAT [53,54]. PPAR $\gamma$  is the master regulator of adipocyte differentiation being necessary to adipogenesis [55-57]. The functional differences between these two PPAR $\gamma$  isoforms in adipocyte differentiation have also been described. A study showed that knockdown of PPAR $\gamma$ 1 and 2 in 3T3-L1 cells using artificial zinc finger repressor proteins inhibits adipogenic differentiation, but exogenous PPAR $\gamma$ 2 restores adipogenesis, while exogenous PPAR $\gamma$ 1 has no effect on adipogenesis [58]. In contrast, a study in PPAR $\gamma$ -null cells showed that both PPAR $\gamma$ 1 and PPAR $\gamma$ 2 can promote differentiation in fibroblasts, although PPAR $\gamma$ 2 has a more robust effect [59].

No factor has been described to induce adipogenesis in the absence of PPAR $\gamma$  and most of adipogenesis inducers seem to act at least partially through PPAR $\gamma$  activation. The importance of PPAR $\gamma$  in adipogenesis was first showed in 1994 in two independent studies [47,60]. These studies demonstrated that PPAR $\gamma$  is predominantly expressed in adipocytes and is increased during adipogenesis [47,60]. It was also shown that forced expression of PPAR $\gamma$ 2 induces adipogenesis in fibroblasts in the presence of PPAR $\gamma$  agonists [55]. In addition, PPAR $\gamma$ -null embryonic stem cells fail to differentiate into adipocytes [61]. Adipose-specific PPAR $\gamma$  knockout mice have decreased fat pads [62,63]. Moreover, PPAR $\gamma$  silencing does not induce 3T3-L1 adipocyte dedifferentiation [64]. In contrast, overexpression of a dominant negative mutant PPAR $\gamma$  in mature 3T3-L1 adipocytes results in dedifferentiation, with the decrease of lipid accumulation and adipogenic markers [65]. Dedifferentiation of adipocytes in the absence of PPAR $\gamma$  demonstrates the importance of PPAR $\gamma$  for both differentiation and maintenance of differentiated adipocytes.

### **1.3.1.2 CCAAT/Enhancer-Binding Proteins**

C/EBPs belong to a family of basic leucine zipper transcription factors [66]. This family consists of six C/EBP isoforms,  $\alpha$ ,  $\beta$ ,  $\delta$ ,  $\gamma$ ,  $\epsilon$ , and  $\zeta$ , from which C/EBPs  $\alpha$ ,  $\beta$ , and  $\delta$  were shown to promote adipocyte differentiation both *in vitro* and *in vivo* [66].

C/EBP $\alpha$  and PPAR $\gamma$  are very important in adipogenic differentiation program, in which PPAR $\gamma$  plays a dominant role [55]. C/EBP $\alpha$  is important in the terminal differentiation

process of adipocytes [67]. C/EBP $\alpha$  knockout mice are almost devoided of WAT and C/EBP $\alpha$  plays an important role in insulin sensitivity *in vitro* [68]. Several studies of gain and loss of function were performed to demonstrate the importance of C/EBP $\beta$  and C/EBP $\delta$  in adipogenesis. C/EBP $\beta$  and C/EBP $\delta$  are induced during an early phase of adipogenesis, and lead to a later induction of C/EBP $\alpha$  and PPAR $\gamma$  [67]. Mouse embryonic fibroblasts (MEFs) from C/EBP $\beta$  knockout mice show impaired adipogenesis [69]. C/EBP $\beta$  and  $\delta$ -null embryonic fibroblasts were described to be unable to differentiate and do not express C/EBP $\alpha$  and PPAR $\gamma$  [70]. In contrast, an *in vivo* study showed that C/EBP $\beta$  and C/EBP $\delta$ -null mice express C/EBP $\alpha$  and PPAR $\gamma$  but have significantly reduced fat pads, suggesting C/EBP $\alpha$  and PPAR $\gamma$  are not sufficient for complete adipocyte differentiation in the absence of C/EBP $\beta$  and C/EBP $\delta$  [70].

#### **1.3.1.3 The Krüppel-Like Factor Family**

Besides PPAR $\gamma$  and C/EBP $\alpha$ , several other transcription factors are involved in adipocyte differentiation regulation, namely the KLFs. The KLFs are a large family of zinc-finger transcription factors. KLF4, KLF5, KLF6, KLF9 and KLF15 are induced during adipogenesis in 3T3-L1 cell line and were described to promote adipocyte differentiation [71-74]. KLF4 is expressed in an early phase of adipocyte differentiation in 3T3-L1 preadipocytes [71]. KLF4 knockdown in 3T3-L1 cells results in adipogenesis inhibition [71]. KLF5 is also expressed during the early phase of adipogenesis [75] and KLF5 inhibition decreases adipogenesis in 3T3-L1 cell line [75]. Moreover, overexpression of KLF5 induces adipocyte differentiation [75]. In fact, KLF5 binds directly to the PPAR $\gamma$ 2 promoter and cooperate with C/EBPs to induce PPAR $\gamma$ 2 expression [75]. *In vivo* studies showed that KLF5 knockout heterozygous mice have less fat mass and when challenged with high-fat diet (HFD) these mice gain less weight than wild type mice [75]. KLF6 induces adipogenesis by repressing preadipocyte factor-1 (Pref-1), an important adipogenesis inhibitor. Pref-1 is suppressed by forced expression of KLF6 and silencing of KLF6 prevents adipogenesis [76]. KLF9 expression is upregulated in the middle stage through the later stage of differentiation [73] and its inhibition suppresses adipogenesis [73]. On the other hand, KLF9 overexpression is required for adipogenesis but it does not upregulate C/EBP $\alpha$  or PPAR $\gamma$  levels [73]. Furthermore, KLF15 expression is also an important regulator of the later phase of adipogenesis [74] and its inhibition leads to suppression of adipogenesis in 3T3-L1 preadipocytes [74]. Furthermore, KLF15 overexpression in 3T3-L1 preadipocytes and ectopic expression of KLF15 in NIH 3T3 cells induce PPAR $\gamma$  expression [74].

#### **1.3.1.4 Sterol Regulatory Element-Binding Protein 1**

The SREBP-1 was originally termed adipocyte determination and differentiation-dependent factor 1 (ADD1) and is a basic helix-loop-helix regulatory molecule [77]. Three isoforms of SREBP were described: SREBP-1a, SREBP-1c, and SREBP-2 [78]. SREBP-1c is the predominantly isoform expressed in WAT [79].

Ectopic expression of a dominant-negative form of SREBP-1 that contains a point mutation within the DNA-binding domain inhibits adipocyte differentiation and expression of adipocyte-specific genes in 3T3-L1 preadipocytes [80]. Furthermore, the ectopic expression of SREBP-1 increases adipocyte differentiation in NIH 3T3 fibroblasts [80]. SREBP-1 was shown to be required for adipocyte differentiation.

#### **1.3.1.5 cAMP Response Element-Binding Protein**

CREB also seems to have a role in the control of adipogenesis. Differentiation-inducing compounds promote expression of CREB [81]. Moreover, CREB was shown to be sufficient to induce adipogenesis in 3T3-L1 preadipocytes and silencing of this protein suppresses adipocyte differentiation [81]. CREB was described to promote expression of C/EBP $\beta$  [82], and it was also demonstrated to bind and promote PPAR $\gamma$ 2 gene transcription [83].

### **1.3.2 Factors Negatively Regulating Adipogenesis**

Several factors were described to inhibit adipogenesis in different models. These factors include KLFs, GATA binding protein (GATA) 2 and 3, and Pref-1. Regulation of these factors could be a good strategy in the treatment of obesity and obesity-associated diseases.

#### **1.3.2.1 The Krüppel-Like Factor Family**

Although some members of KLF family promote adipogenesis, others like KLF2, KLF3 and KLF7 inhibit adipogenesis [84]. KLF2 is highly expressed in preadipocytes but its expression decreases during adipogenesis [85]. KLF2 overexpression in 3T3-L1 preadipocytes inhibits lipid accumulation and PPAR $\gamma$ , C/EBP $\alpha$  and SREBP-1 expression [85]. KLF2 inhibits adipocyte differentiation by binding directly to PPAR $\gamma$ 2 promoter, repressing its promoter activity [85]. KLF3 is highly expressed in 3T3-L1 preadipocytes and decreases during adipogenic stimulation [86]. Overexpression of KLF3 inhibits 3T3-L1 preadipocyte differentiation [86]. Conversely, MEFs from KLF3 knockout mice show increased lipid accumulation compared to wild type [86]. The KLF7 protein is abundant

in 3T3-L1 preadipocytes and its expression decreases during adipogenesis, but their levels are restored at day 7 of differentiation [87-89]. KLF7 overexpression inhibits PPAR $\gamma$ , C/EBP $\alpha$ , adipocyte protein 2 (aP2), and adipisin [87], and also inhibits adipogenesis of human preadipocytes [87-89].

### **1.3.2.2 GATA2 and GATA3**

GATA2 and GATA3 belong to the GATA family of transcription factors that are zinc-finger DNA binding proteins involved in developmental processes [90]. GATA2 and GATA3 are expressed in preadipocytes of WAT and are decreased during adipogenesis [91]. Forced expression of GATA2 decreases adipogenesis and GATA2-null embryonic stem cells exhibit increased adipocyte differentiation [91]. Constitutive expression of GATA2 and GATA3 inhibits adipogenesis and cells are maintained at preadipocyte stage [91].

### **1.3.2.3 Preadipocyte Factor-1**

Pref-1 is a transmembrane protein that contains epidermal-growth-factor-like repeats and is activated by proteolytic cleavage [92]. Pref-1 is highly expressed in preadipocytes but the levels of this protein decrease during adipocyte differentiation and it is absent in mature adipocytes [92]. Constitutive expression of Pref-1 in 3T3-L1 cells by stable transfection downregulates PPAR $\gamma$  and C/EBP $\alpha$  and blocks adipocyte differentiation [92,93]. Moreover, decreasing Pref-1 expression by transfection of antisense RNA promotes adipocyte differentiation [94]. Pref-1 knockout mice exhibit an increase in adipose tissue mass [95]. Moreover, transgenic mice overexpressing Pref-1 in adipose tissue show a reduction in adipose tissue mass [96,97]. These studies show that Pref-1 regulates adipogenesis negatively.

The Pref-1 inhibitory effect on adipogenesis was demonstrated to occur through inhibition of insulin-like growth factor (IGF) receptor signaling of Extracellular Signal-regulated Kinase-1 (ERK)–Mitogen-activated protein kinase (MAPK) activation [98]. Downregulation of Pref-1 induces IGF-1-dependent ERK activation [99]. Treatment of Pref-1-null MEFs with Pref-1 shows that Pref-1 inhibitory effects occur through ERK1/2–MAPK pathway [100]. Furthermore, it was described that Sox9 downregulation is required for adipocyte differentiation and that Sox9 directly binds to the promoter regions of C/EBP $\beta$  and C/EBP $\delta$  blocking adipocyte differentiation. Furthermore, it was also demonstrated that Pref-1 inhibits differentiation of mesenchymal cells into adipocytes by induction of Sox9. Moreover, Sox9 is induced by ERK activation, and Sox9 induction is prevented by ERK activation inhibition [101]. These studies suggest that Pref-1 maintains

preadipocyte expression of Sox9 via ERK activation, which suppresses C/EBP $\beta$  and C/EBP $\delta$  expression by binding to their promoter regions.

### 1.3.3 Other regulators of adipogenesis

#### 1.3.3.1 MicroRNAs

MicroRNAs (miRNAs or miRs) are small single stranded non-coding ribonucleic acids (RNAs) that bind to regulatory sites of target messenger RNA (mRNA) and regulate their expression by translational repression or by targeting mRNA degradation, resulting in decreased protein production [102].

miRNAs are highly conserved and stable, and have multiple targets [103-105]. They regulate a wide range of biological processes, such as development, cell proliferation, differentiation, apoptosis and cell metabolism [106]. miRNA dysregulation has also been implicated in different human diseases [107].

miRNA biogenesis is a multiple step process that occurs in the nucleus and subsequently in the cytoplasm (Figure 1.7). Transcription of primary miRNA (pri-miRNA) from different genes is mostly catalyzed by RNA Polymerase II but can be also catalyzed by RNA Polymerase III [108,109]. Pri-miRNAs processing begins in the nucleus by Drosha and its cofactor, DiGeorge syndrome chromosomal region 8 (DGCR8), a RNA type III endonuclease, originating double stranded precursor miRNA (pre-miRNA) [110]. DGCR8 function is to act in substrate recognition and as a molecular anchor to properly position Drosha's catalytic site [110]. After processing pri-miRNA to pre-miRNA, it is transported to the cytoplasm by Exportin 5 [111]. In the cytoplasm pre-miRNA is processed by ribonuclease (RNase) III enzyme Dicer coupled to trans-activation response RNA-binding protein (TRBP) near the terminal loop, creating a miRNA duplex [112]. The double stranded miRNA is loaded onto Argonaute2 (Ago2), generating the miRNA-induced Silencing Complex (miRISC). Target RNAs are then identified and regulated by miRNA and miRISC proteins, by binding specific complementary base pairs [108,109]. miRNAs bind sequences in the 3' untranslated region (UTR) or more rarely in the 5' UTR of mRNAs and can target promoter regions or the coding-region of genes [102]. Total complementarity between the miRNA and target mRNA sequence cleaves the mRNA while absence of total complementarity prevents translation. Moreover, the target mRNA and the miRNA are able to regulate each other [108,109].



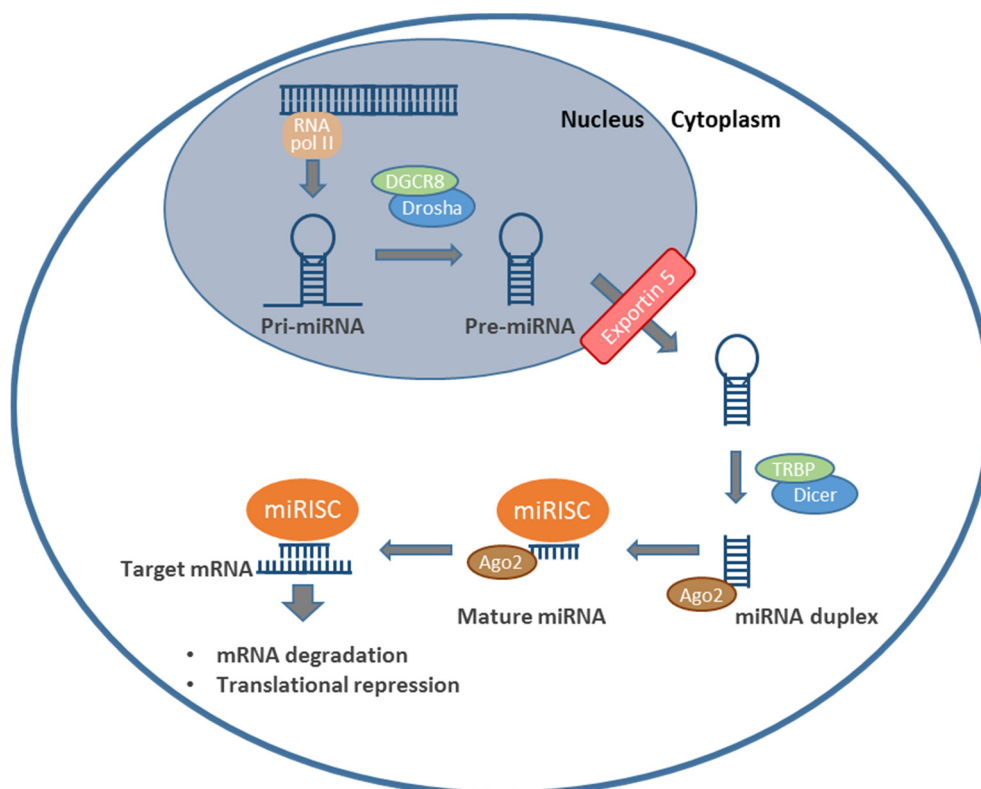


**Figure 1.7 - MiRNA biogenesis process.** Pri-miRNA transcript is mostly synthesized by RNA Pol II and processed in the nucleus by Drosha coupled to DGCR8 leading to a pre-miRNA. Pre-miRNA is exported to the cytoplasm by Exportin 5 and processed by Dicer coupled to TRBP into a double stranded mature miRNA. Ago2 integrates the mature miRNA in the miRISC, where miRNA-directed targeting of mRNAs takes place, and inhibits its processing by mRNA degradation or by translational repression. Abbreviations: Pri-miRNA, Primary RNA; Pre-miRNA, Precursor miRNA; RNA Pol II, RNA Polymerase II; DGCR8, DiGeorge syndrome chromosomal region 8; TRBP, Trans-activation response RNA-binding protein; Ago2, Argonaute2; miRISC, miRNA-induced Silencing Complex. Adapted from [113].

Some studies have already performed suppression of Drosha and Dicer demonstrating the importance of miRNAs in adipogenesis [114-116]. Several miRNAs have been implicated in adipogenesis since the first miRNA, miR-143, was shown to regulate this process [117]. Some miRNAs appear to increase adipocyte differentiation while others inhibit adipogenesis in various models, as summarized in Table 1.2.

**Table 1.2 MicroRNAs that regulate adipogenesis.** Adapted from [118].

microRNAs	Target	Function	Experimental model	Refs
miR-8	TCF	Pro-adipogenic	MSCs	[119]
miR-17-92	Rb2/p130	Pro-adipogenic	3T3-L1	[114]
miR-21	TGFBR2	Pro-adipogenic	3T3-L1, MSCs	[120]
miR-27a	PPAR $\gamma$	Anti-adipogenic	3T3-L1, MSCs	[121,122]
miR-27b	PPAR $\gamma$	Anti-adipogenic	MSCs, hASCs	[122,123]
miR-29	PKB	Anti-adipogenic	3T3-L1	[124]
miR-31	C/EBP $\alpha$	Anti-adipogenic	MSCs, hASCs	[125,126]
miR-103	PDK1	Pro-adipogenic	3T3-L1, MSCs, preadipocytes	[127,128]
miR-107		Pro-adipogenic	3T3-L1, MSCs, preadipocytes	[128]
miR-124	CREB	Anti-adipogenic	3T3-L1	[129]
miR-130	PPAR $\gamma$	Anti-adipogenic	Primary human preadipocytes	[130]
miR-138	EID-1	Anti-adipogenic	hASCs	[131]
miR-143	ERK5	Pro-adipogenic	3T3-L1, MSCs	[117,132]
miR-155	C/EBP $\beta$	Anti-adipogenic	3T3-L1	[133]
miR-200		Pro-adipogenic	MSCs	[119,134]
miR-204 miR-211	Runx2	Pro-adipogenic	MSCs	[135]
miR-210	TCF712 Wntless CG32767	Pro-adipogenic	3T3-L1	[136]
miR-221 miR-222		Anti-adipogenic	3T3-L1	[127]
miR-320	PI3K	Anti-adipogenic	3T3-L1	[137]
miR-326	C/EBP $\alpha$	Anti-adipogenic	MSCs	[125]
miR-335		Pro-adipogenic	3T3-L1, MSCs	[138]
miR-375	ERK1/2	Pro-adipogenic	3T3-L1	[139]
miR-378		Pro-adipogenic	3T3-L1, MSCs	[140,141]
miR-448	KLF5	Pro-adipogenic	3T3-L1	[142]

Abbreviations: TGFBR2, Transforming Growth Factor  $\beta$  Receptor 2; PPAR, Peroxisome Proliferator-Activated Receptor; PKB, Protein kinase B; C/EBP, CCAAT/enhancer-binding protein; PDK1, Pyruvate dehydrogenase kinase 1; CREB, Cyclic AMP response Element-binding protein; EID-1, EP300-interacting inhibitor of differentiation 1; ERK, Extracellular Signal-regulated Kinase; Runx2, Runt-related transcription factor 2; TCF712, Transcription factor 7-like 2; PI3K, Phosphatidylinositol 3-kinase; KLF, Krüppel-like factor; hASC, Human Adipose-Derived Stem Cell; MSC, Mesenchymal Stem Cell.

### **1.3.3.1.1 MicroRNA miR-27**

The miR-27 family consists of miR-27a and miR-27b, which are transcribed from different chromosomes. miR-27a and miR-27b are two highly conserved isoforms that have identical seed sequences and differ in only one nucleotide [143].

Both miR-27a and miR-27b levels are elevated in adipose tissue of genetically obese *ob/ob* mice [122]. However, the levels of pri-miR-27a are downregulated in mature adipocytes of HFD-fed obese mice comparing to chow diet-fed lean mice [121]. Moreover, the microRNAs miR-27a and miR-27b were described to impair adipocyte differentiation [121,122,144].

At the molecular level, it was demonstrated that miR-27a and miR-27b binds the 3'UTR of PPAR $\gamma$  mRNA and that both decrease during adipocyte differentiation of 3T3-L1 preadipocytes [121,123]. However, in 3T3-L1 preadipocytes, overexpression of miR-27a and miR-27b also inhibits adipogenesis by inhibiting the expression of PPAR $\gamma$  mRNA but with no alteration in PPAR $\gamma$  protein levels [122]. Additionally, miR-27 was described to suppress adipogenesis by also targeting prohibitin [144]. Prohibitin increases during differentiation and its silencing inhibits adipogenesis in 3T3-L1 preadipocytes [145]. Overexpression of miR-27a and miR-27b decreases both mRNA and protein levels of prohibitin and impairs adipocyte differentiation [144].

### **1.3.3.2 Autophagy**

Autophagy is an intracellular degradation system that targets cytoplasmic substrates for lysosomal degradation [146]. Three types of mammalian autophagy have been described: chaperone-mediated autophagy, microautophagy and macroautophagy [147]. Chaperone-mediated autophagy targets specific proteins that contain a pentapeptide motif (KFERQ) [148]. This motif is recognized by a chaperone complex that transfers the proteins to the lysosomal through the receptor lysosome-associated membrane protein 2A (LAMP2A) [149]. The proteins are degraded in the lysosomal lumen. Microautophagy involves the direct engulfment of cytosolic cargo by invagination or evagination into the lysosomal lumen for degradation [150,151]. Macroautophagy, referred here as autophagy, is the best studied type of autophagy in which cells form a double-membraned vesicle named autophagosome. Autophagosomes form around a portion of cytoplasm that engulfs proteins and organelles degrading them after fusion with the lysosome [152,153].

Autophagosome formation comprises several steps: induction of autophagosome formation; nucleation of the membrane; autophagosomal elongation; cargo selection; and autophagosome maturation and cargo degradation (Figure 1.8).

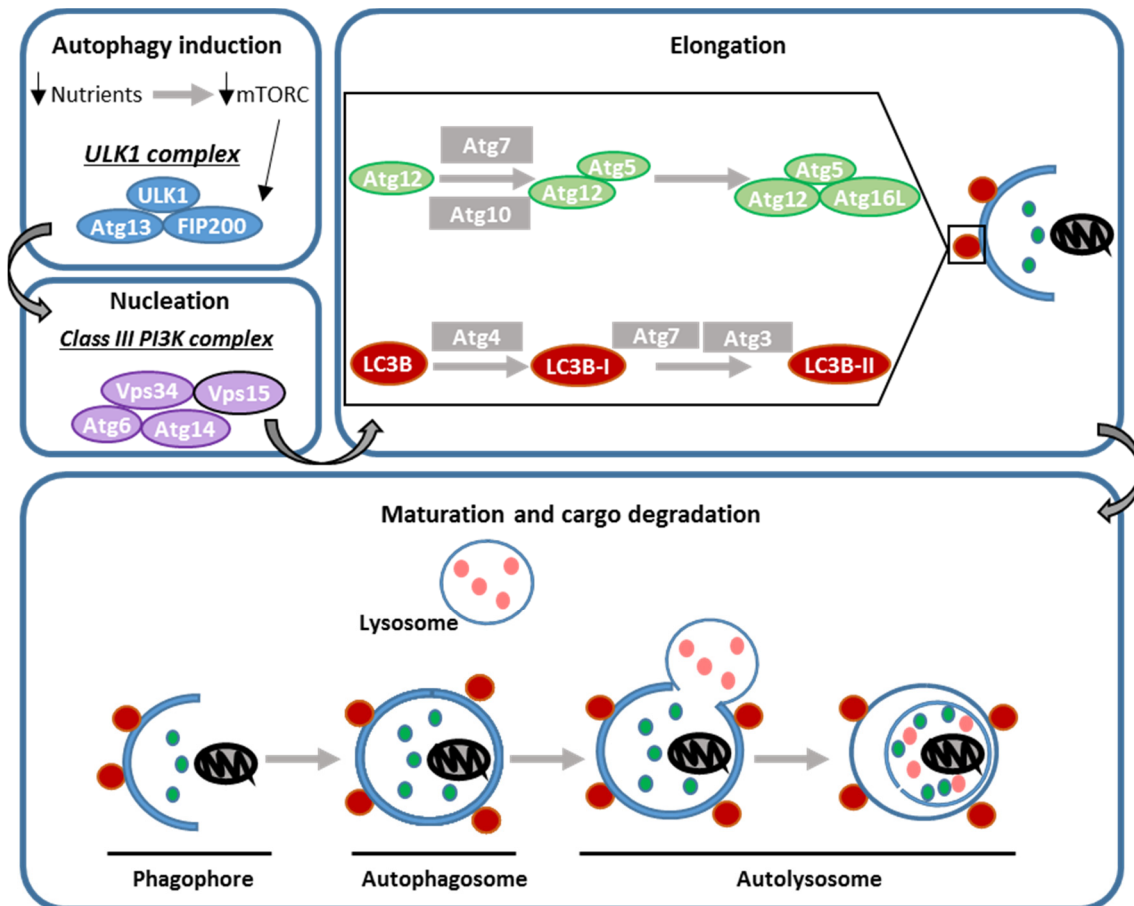


**Figure 1.8 - The core molecular machinery of autophagy in mammalian cells.** Autophagy induction: during cellular and metabolic stress the mTORC1 is inactivated, which allows ULK complex activation. Nucleation: ULK1 phosphorylates Ambra1, interacting with the class III PI3K (PIK3C3) complex. Then, the PIK3C3 complex generates phosphatidylinositol-3-phosphate (PI3P), which recruits Atg proteins to the site of autophagosome formation. Elongation: two ubiquitin-like processes are carried out. Atg7 and Atg10 mediate Atg5-Atg12 complex formation. This Atg5-Atg12 complex subsequently binds to Atg16L1, generating the Atg16L1 complex. LC3 cleaved by Atg4 generates LC3-I, which is then conjugated to phosphatidylethanolamine (PE), to generate LC3-II, a process mediated by Atg7, Atg10 and the Atg16L1 complex. Maturation and cargo degradation: after the completion of autophagosome formation, the autophagic cargo is released into the lysosomal lumen by the fusion of the outer autophagosomal membrane with the lysosome, and the content is degraded. Abbreviations: mTORC, Mammalian target of rapamycin complex; Atg, Autophagy related genes; ULK, Unc-51 like kinase; FIP200, Focal adhesion kinase family-interacting protein of 200 kDa; PI3K, Phosphatidylinositol 3-kinase; Vps, Vacuolar protein sorting-associated protein; LC3B, Microtubule associated protein-1 light chain-3B. Adapted from [154].

Induction of autophagosome formation step can occur dependent or independently of mammalian target of rapamycin (mTOR) [154]. The mTOR is a multidomain serine/threonine kinase that forms the catalytic subunit of two structurally distinct complexes: the mTOR complex (mTORC) 1 and mTORC2 [155]. In nutrient-rich conditions, mTORC1 downregulates autophagy. Inversely, nutrient starvation inhibits mTORC1 inducing autophagy. Autophagy is regulated via mTOR by several signaling

molecules, such as insulin, phosphatidylinositol 3-kinase (PI3K) and protein kinase B (PKB), also known as Akt [156,157]. Autophagy can also be activated through an mTOR-independent pathway by stimulation with the phosphatidylinositol-3-kinase class III (PI3KC3) or Autophagy related gene (Atg) 6, also known as Beclin-1.

The nucleation step starts with the phagophore, which is a small portion of membrane, whose source is unclear. This step initiates with the interaction between the unc-51 like kinase (ULK) complex (ULK, Atg13 and Focal adhesion kinase family-interacting protein of 200 kDa (FIP200)) and the class III PI3K complex that contains the proteins Vacuolar protein sorting-associated protein (Vps) 34, Atg6, Atg14 and Vps15 (p150) [158,159].

The nucleation is followed by autophagosomal elongation step that consists of two ubiquitylation-like reactions. In the first reaction, Atg12 is conjugated to Atg5 by Atg7 (ubiquitin-activating-enzyme (E1)-like) and Atg10 (ubiquitin-conjugating-enzyme (E2)-like). Covalently bound Atg5-Atg12 also interacts non-covalently with Atg16L, forming Atg12-Atg5-Atg16L) [160,161], which is localized in the outer portion of the autophagosomal membrane [162]. In the second ubiquitylation-like reaction, microtubule associated protein-1 light chain-3B (LC3B), synthesized from the precursor, Pro LC3, is cleaved at its C-terminal by Atg4, a cysteine protease, forming LC3B-I [163]. LC3B-I conjugates with lipid phosphatidylethanolamine (PE) to form LC3B-II. The unconjugated form, LC3B-I, translocates from cytoplasm to the autophagosomal membrane, originating the conjugated form LC3B-II, which is very effective as an important autophagy marker. This process requires Atg7 (E1-like) and Atg3 (E2-like) [163,164]. The Atg proteins are released from the autophagosome after its formation is complete.

In the cargo selection step, sequestosome 1 (SQSTM1, also called p62) mediates autophagy selectivity related to ubiquitinated substrates [165,166]. The p62 is a signaling-adaptor protein which has a multidomain structure that interacts with several proteins, including ubiquitinated proteins for ubiquitin-proteasome system (UPS) degradation and it also co-localizes with ubiquitinated protein aggregates, LC3B and lysosomes [167,168]. p62 also binds to LC3B during autophagosome formation, being both degraded by the autophagy pathway at late stages [169].

The autophagosome maturation and cargo degradation involves the sealing of the membrane and the fusion between autophagosomes and lysosomes, to form autolysosomes [170]. The contents of the two vesicles are mixed and the cargo is degraded. Because autophagosomes are associated with the microtubules network, this is a dynamic process regulated by the cytoskeleton. Autophagosome maturation and degradation requires the LAMP-2 and the guanosine triphosphatase (GTPase), Rab7 [171]. After autolysosome formation, the inner membrane and cargo are degraded,

including LC3B-II, and are released to the cytosol, where they can activate mTOR [170,172].

Importantly, an increased number of autophagosomes may not correspond to an increase of autophagic activity but to a blockage in the autophagy pathway downstream of autophagosome formation [173].

#### **1.3.3.2.1 Autophagy in adipose tissue**

Some studies suggest that autophagy has a relevant role in adipogenesis [174-176]. Autophagy increases during adipocyte differentiation in 3T3-L1 cell line and MEFs [175,176]. MEFs derived from adipose tissue-specific Atg5 knockout mice and from Atg7 knockout mice show drastically reduced adipogenesis efficiency [175,176]. Additionally, the knockdown of Atg5 and Atg7 in 3T3-L1 preadipocytes impairs adipocyte differentiation by decreasing adipocyte markers [174]. These results were confirmed with pharmacological inhibitors, 3-methyladenine and chloroquine [174]. Newborn Atg5 knockout mice show less subcutaneous adipocytes than wild-type, demonstrating that autophagy is relevant in adipose tissue development [176]. The importance of autophagy in adipogenesis *in vivo* was also confirmed in adipocyte-specific Atg7 knockout mice [174,175]. Adipocyte-specific Atg7 knockout mice are leaner, have decreased WAT mass and have adipocytes with features characteristic of brown adipocytes, smaller, containing multilocular lipid droplets and increased cytoplasmic volume [174,175]. These cells also have increased number of mitochondria and increased  $\beta$ -oxidation of FAs [174,175]. No weight gain occurs in these mice when fed a HFD, associated with increased thermogenesis and energy expenditure. Furthermore these mice exhibit improved insulin sensitivity, lower TAGs, cholesterol, and leptin levels [174].

Furthermore, human adipose tissue and adipocytes of obese individuals show increased autophagy [177]. However, functional consequence of increased autophagy in adipose tissue of obese individuals is not known.

### **1.4 Metabolic function of adipose tissue**

Adipose tissue have an important function in energy storage and energy release [178]. In periods of negative energy balance, there is the release of FAs in order to suppress energetic needs of tissues [178]. In times of overnutrition, energy is stored in the form of TAGs in lipid droplets in adipocytes [178]. This process prevents ectopic lipid deposition and lipotoxicity in other tissues. Ectopic lipid accumulation causes severe deleterious effects to other tissues such as liver, muscle and pancreas. Lipid accumulation by liver and muscle can cause insulin resistance [179,180] and in the pancreas it is responsible

for  $\beta$ -cell death by apoptosis [181]. The energy storage function of adipose tissue is very important to prevent these lipotoxic insults. Energy storage, in the form of TAGs, is determined by the balance between lipogenesis and lipolysis (Figure 1.9).

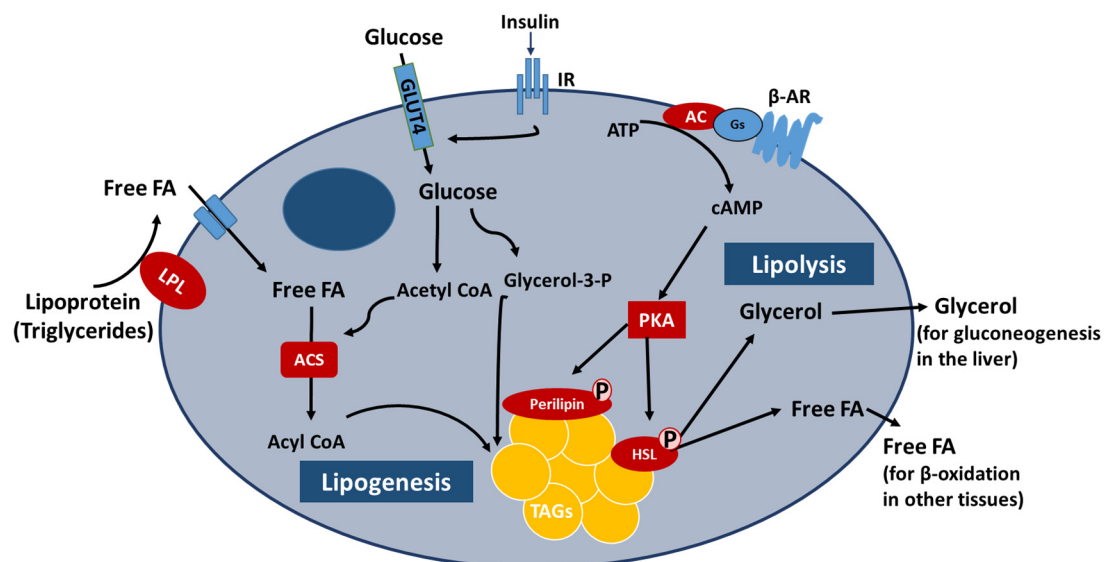


**Figure 1.9 - Lipid metabolism in adipocytes.** In mammals, adipocytes store excess energy in the form of TAGs in lipid droplets and release it when energy is needed. When there is excess of energy, insulin stimulates lipogenesis and through the action of LPL, triglycerides of lipoproteins are degraded in free FA. Then, free FA enter the cell and suffer several reactions, occurring esterification with glycerol-3-P, synthesizing TAGs that are stored in lipid droplets and protected by perilipin. When energy is needed,  $\beta$ -adrenergic stimulation induces lipolysis and TAGs are catabolized by HSL to generate free FA and glycerol that will be transported to other tissues and used in  $\beta$ -oxidation. Abbreviations: AC, adenylate cyclase; ACS, acyl-CoA synthase;  $\beta$ -AR,  $\beta$ -adrenergic receptor; FA, fatty acid; GLUT, glucose transporter; HSL, hormone-sensitive lipase; IR, insulin receptor; LPL, lipoprotein lipase; PKA, protein kinase A; TAG, triglyceride. Adapted from [182].

#### 1.4.1 Lipogenesis

In response to overnutrition, adipocytes store excess energy as TAGs in a single lipid droplet in the cytoplasm [183]. TAGs are composed of three molecules of FAs and one of glycerol. Adipocytes can either synthesize FAs *de novo* or accumulate them from the dietary lipids [178].

To be accumulated from dietary lipids, they are transported in blood plasma as non-esterified FAs bound to plasma albumin or as TAGs in lipoprotein transport particles, the chylomicrons [184] or very low density lipoproteins (VLDL) [185] and to a lesser extent low density lipoproteins (LDL) [186], to the adipose tissue [178]. In order to enter the cell, TAGs are digested by lipoprotein lipase (LPL) into FAs [187] and their uptake by adipocytes requires specific processes. The proteins fatty acid transport protein 1

(FATP1) and CD36 are implicated in the uptake of FAs by adipocytes [188,189]. Intracellularly, FAs are transported by fatty acid binding proteins (FABPs) into the acyl coenzyme A (CoA) synthase reaction site [190]. This enzyme catalyses the reaction of FAs with an acetyl-CoA, originating fatty acyl-CoA [191].

*De novo* lipogenesis is the synthesis of FAs from non-lipid substrates, mainly carbohydrates. Insulin stimulates the translocation of glucose transporter type (GLUT) 4 to the membrane that takes up glucose into adipocytes [192]. During the FAs *de novo* synthesis, the acyl-CoA molecule comes from an acetyl-CoA molecule via acetyl-CoA carboxylase (ACC) and the multifunctional enzyme fatty acid synthase (FAS) [191]. Afterwards, this molecule reacts with glycerol-3-P, which is produced from glucose during glycolysis, originating the TAGs molecules on the endoplasmic reticulum [191]. TAGs are incorporated in lipid droplets that are protected by a protein named perilipin [193].

Perilipin belongs to a family called PAT family that also includes adipocyte differentiation-related protein (ADRP), S3-12, OXPAT, and tail-interacting protein 47 (TIP47) [194]. Perilipin has three isoforms in humans: perilipin A, perilipin B and perilipin C, that result from mRNA splicing of a single perilipin gene [195]. Perilipin A is the most abundant protein associated with the adipocyte lipid droplets. Perilipin A coats lipid droplets and is the main mechanism protecting TAGs from hydrolysis by lipases [196]. When energy is needed, perilipin from surface of lipid droplets is phosphorylated by cAMP-dependent protein kinase A (PKA). Then perilipin suffers a conformational change, allowing the action of lipases, leading to lipolysis [197]. Perilipin sequence has multiple consensus sites for the phosphorylation of serine residues by PKA. Perilipin A has five sites in humans [198] and six in rats and mice [195,199]. Perilipin besides preventing lipolysis it also facilitates this process. Perilipin knockout mice have significantly less fat mass and increased basal lipolysis [200,201]. Perilipin also provides a docking site for hormone-sensitive lipase (HSL). Perilipin-null MEFs have adipophilin surrounding lipid droplets but HSL is not able to dock to it after the stimulation of  $\beta$ -adrenergic receptors ( $\beta$ -ARs) [202]. Moreover, perilipin expression is upregulated in obese humans and mice [203].

#### 1.4.2 Lipolysis

During fasting and exercise, lipolysis of TAGs is stimulated [204]. Lipolysis is a controlled process of hydrolysis of TAGs, via diacylglycerol (DAG) and monoacylglycerol (MAG) with consequent release of one glycerol and providing three FA molecules to be used as energy source by other tissues, such as heart and skeletal muscles [204]. The lipid droplets of TAGs are surrounded by a phospholipid monolayer with structural proteins and metabolic enzymes that are specific to the adipocyte [178]. TAGs hydrolysis is a



process driven by three enzymes: adipose triglyceride lipase (ATGL), HSL and monoacylglycerol lipase (MGL). The major signaling pathways activating lipolysis is  $\beta$ -adrenergic stimulation induced by catecholamines. The  $\beta$ -ARs are Gs-protein coupled receptors, which activate adenylate cyclase that catalyses the formation of cAMP from ATP [205]. cAMP binds and activates PKA [205]. Subsequently, PKA phosphorylates serine hydroxyl groups of HSL, resulting in its activation and translocation from the cytosol to the lipid droplet. HSL begins to hydrolyze TAGs, DAGs, and MAGs [205]. As described above, Perilipin A is found in the outer surface of the lipid droplet preventing lipases from reaching TAGs, thus inhibiting lipolysis [196]. The presence and phosphorylation of perilipin is essential for HSL translocation and the lipolytic activity [202].

A second enzyme involved in the hydrolysis of TAGs is ATGL although the mechanisms that regulate it in response to  $\beta$ -adrenergic stimulation are not well known [206,207]. The other hydrolase located in adipocytes is MGL which is located in adipocytes that acts specifically on MAG, unlike ATGL and HSL [208]. FAs are transported in the bloodstream to energy-requiring tissues bound to albumin [209].

## 1.5 Endocrine function

WAT was first thought to be a relatively inert tissue, specialized in energy storage and release. The discovery of leptin, a satiety factor, in 1994 that is produced mainly by adipocytes changed the view about WAT physiological functions [210]. WAT was then recognized as a dynamic endocrine organ that is fundamental for regulating metabolism. Adipose tissue was identified to be responsible for synthesis and secretion of several other proteins, called adipokines. Adipokines are endocrine, paracrine, and autocrine factors that signal to several tissues, including hypothalamus, pancreas, liver, skeletal muscle and kidney. Adipokines have effects on multiple biological systems like regulation of lipid and carbohydrate metabolism, appetite, thermogenesis and blood pressure (Table 1.3). Some adipokines are reviewed briefly below.

**Table 1.3 - Factors secreted by adipose tissue into the bloodstream and respective function/effect in their targets.**

Adipokine	Function/Effect	Levels in response to obesity	Refs
Leptin	Regulates food intake and energy expenditure	↑	[211]
Adiponectin	Regulates glucose and lipid metabolism, insulin sensitivity and food intake	↓	[212]
Visfatin	Insulin-mimetic effects	↑	[213]
Resistin	Regulates inflammation, increases insulin resistance	↑	[214]
Adipsin	Enhances fat storage	↑	[215]
Vaspin	Improves glucose tolerance, insulin sensitivity, and reduces food intake	↑	[216]
Omentin	Enhances insulin-stimulated signals and glucose uptake but not insulin-mimetic	↓	[217]
RBP-4	Reduces insulin sensitivity, impairs insulin action in muscle	↑	[218]
Apelin	Regulates feeding behavior, involved in stimulating gastric cell proliferation	↑	[219]
DPP-IV	Plays a major role in glucose metabolism	↑	[220]
TNF- $\alpha$	Pro-inflammatory, inhibits insulin signaling	↑	[221]
IL-6	Pro-inflammatory, lipolytic, reduces insulin sensitivity	↑	[222]
TGF $\beta$	Regulates cell growth, cell proliferation, cell differentiation and apoptosis	↑	[223]
PAI-1	Inhibits endothelial plasminogen activator, blocking fibrinolysis	↑	[224]

↑ : increase, ↓ : decrease; abbreviations: RBP-4, Retinol-binding protein 4; DPP-IV, Dipeptidyl peptidase IV; TNF- $\alpha$ , Tumor necrosis factor- $\alpha$ ; IL, Interleukin; TGF $\beta$ , Transforming growth factor  $\beta$ ; PAI-1, Plasminogen activator inhibitor-1.

### **Leptin**

Leptin is a 16 kDa polypeptide that contains 167 amino acids and is primarily secreted by adipocytes [225]. Leptin is also secreted in low levels by placenta, skeletal muscle, gastric and mammary epithelium and the brain [226]. Leptin is encoded by the *ob* gene and exerts its effects by binding to its receptor in several peripheral tissues [210]. Leptin is a major satiety signal and suppresses food intake through activation of leptin receptor in the hypothalamus, reducing the release of orexigenic peptides, neuropeptide Y (NPY) and agouti-related protein, resulting in reduced food intake [227]. Leptin also modulates reproduction, angiogenesis, immunoresponse, blood pressure and osteogenesis [226]. Mice deficient in leptin (*ob/ob*) and mice deficient in the leptin receptor (*db/db*) show an increase of food consumption due to the disruption of leptin signaling, leading to an obese phenotype [228,229].

**Adiponectin**

Adiponectin was discovered in 1995 by four independent groups, shortly after the discovery of leptin, and it was originally named Acrp30, AdipoQ, apM1, and GBP28 [230-233]. Adiponectin is a 30 kDa polypeptide that contains 244 amino acids and is secreted primarily by WAT but is also secreted to a lesser extent by myocytes and skeletal muscle [231]. Adiponectin has a N-terminal collagen-like domain and a C-terminal globular domain that mediates multimerization [231]. This protein circulates in trimeric, hexameric and higher order complexes in plasma and exerts its effects through two adiponectin receptors, AdipoR1 and AdipoR2 [234]. AdipoR1 acts through AMP-activated protein kinase (AMPK) phosphorylation and is mainly expressed in the muscle, while AdipoR2 acts through activation of PPAR $\alpha$ , and is mainly expressed in the liver [234]. Adiponectin plasma levels are negatively correlated to fat mass, obesity, and type 2 diabetes mellitus, both in humans and animal models [231,235,236]. Adiponectin was reported to improve whole-body insulin sensitivity in models of genetic and diet-induced obesity [237,238], and genetic deletion of adiponectin in mice causes insulin resistance [239,240]. Other properties of adiponectin include insulin sensitizing, cardioprotective, satiety, anti-inflammatory, anti-atherogenic and hepatoprotective effects [241-243].

**Resistin**

Resistin was first described in 2001 [244]. Resistin, also known as FIZZ3, is a 12.5 kDa polypeptide rich in cysteines that contains 108 amino acids [244]. Resistin acts in several tissues, including WAT, liver and muscle. It has been reported that neutralization of resistin with antibodies in an obese mouse model restores insulin sensitivity [244]. Intraperitoneal injections of resistin causes glucose intolerance in normal mice [244]. Moreover, mice lacking resistin show low blood glucose levels after fasting, due to a reduced hepatic glucose production [245]. This study indicates that resistin acts by increasing hepatic gluconeogenesis. Moreover, resistin induces adipogenesis in 3T3-L1 preadipocyte cell line [246]. Resistin silencing decreases lipid accumulation with no alteration in PPAR $\gamma$  expression in 3T3-L1 preadipocyte cell line [247]. Resistin is also positively associated with cardiovascular risk [248].

**Omentin**

Omentin is primarily expressed in visceral rather than in subcutaneous adipose tissue [249,250]. It acts as an insulin sensitizer rather than insulin mimetic, resulting in positive effects in glucose uptake [249]. Omentin was described to improve glucose uptake in human adipose tissue [249]. Omentin levels are reduced in obesity and insulin resistance [217].

### **Retinol-binding protein 4**

Retinol-binding protein 4 (RBP-4) is a member of the lipocalin superfamily [251]. RBP-4 is associated with insulin resistance [251]. Serum levels of RBP-4 are elevated in obese humans and rodents [251]. Moreover, overexpression of RBP-4 and injections of recombinant RBP-4 in mice leads to the development of insulin resistance [251]. Additionally, RBP-4 knockout mice that were fed a HFD are resistant to obesity [251].

### **1.6 Adipose tissue changes in obesity**

Adipose tissue is a tissue with high plasticity, having the ability to expand throughout the entire lifespan [38]. The expansion of adipose tissue that occurs in obesity has been described to be related to several dysfunctions such as ectopic lipid accumulation, insulin resistance, mitochondrial dysfunction, altered adipokine profile, inflammation, hypoxia and fibrosis [25] (Figure 1.10).

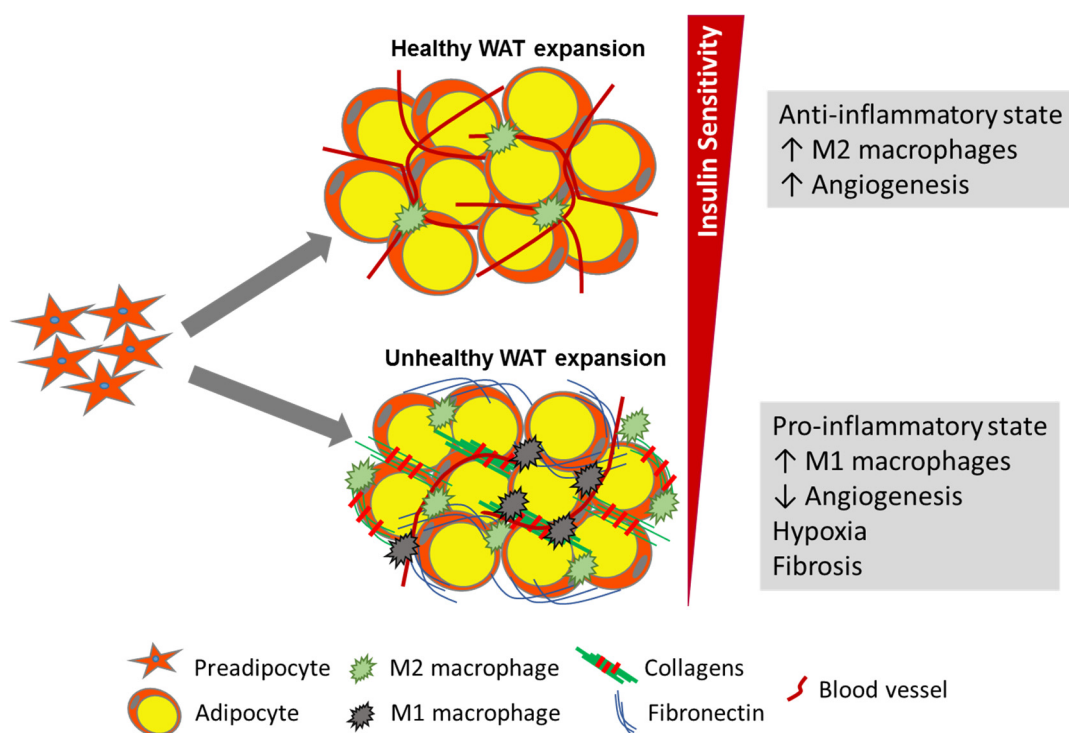


**Figure 1.10 – Schematic overview of “healthy” and “unhealthy” expansion of adipose tissue during obesity development.** In “unhealthy” expansion of adipose tissue, there is a switch from an anti-inflammatory state to a pro-inflammatory state, it occurs a decrease in angiogenesis, contributing to hypoxia and it is also observed fibrosis formation. Adapted from [17].

Adipose tissue expansion occurs by hyperplasia (increase in adipocyte number) and hypertrophy (increase in adipocyte volume) [25]. Adipose tissue is the main storage

compartment in the body having an important function in releasing stored energy when needed but also to store energy in the form of TAGs in times of overnutrition. In obesity, when energy intake exceeds adipose tissue storage capacity, it becomes saturated and unable to store more lipids, increasing lipolysis [252]. This dysfunction leads to ectopic deposition of lipids in non-adipose tissues, such as the liver, skeletal muscle and pancreas [252]. Moreover, ectopic accumulation in the liver leads to hepatic steatosis, which is associated with hepatic insulin resistance, through the inability of insulin to activate hepatic glycogen synthesis and suppress hepatic glucose production [179]. Moreover, ectopic accumulation in the muscle is also associated with insulin resistance and is a good predictor for insulin resistance in lean nondiabetic offspring of type 2 diabetic patients [180,253]. Furthermore, FAs were also shown to induce pancreatic  $\beta$ -cell death by apoptosis [181].

Obesity also impairs mitochondria in adipose tissue [254]. Mitochondria is important in adipogenesis, FA synthesis and esterification, and lipolysis [254]. Mitochondria dysfunction decreases ATP production, and leads to overproduction of reactive oxygen species (ROS) [255,256].

Low-grade, chronic inflammation in WAT also occurs in obesity. Macrophage infiltration in obese WAT has been described in humans and mice [257]. Moreover, it was shown an increase of M1 classically activated pro-inflammatory macrophages and decrease of M2 alternatively activated macrophage fraction [258]. There is also a major alteration in adipokine profile. Inflammatory cytokines are highly upregulated in adipose tissue of obese subjects, such as monocyte chemoattractant protein 1 (MCP-1) leading to massive macrophage infiltration, tumor necrosis factor- $\alpha$  (TNF- $\alpha$ ), interleukin (IL)-1 $\beta$ , IL-6 and C-reactive protein [25,259]. There is also a concomitant reduction in anti-inflammatory factors, such as IL-10 and adiponectin [25,259].

Angiogenesis is an important process during adipose tissue enlargement. In obesity, adipocytes become very large and the vasculature of adipose tissue is unable to grow along to provide oxygen to adipocytes, leading to local adipose tissue hypoxia. Hypoxia results in stabilization of hypoxia-inducible factor-1 $\alpha$  (HIF-1 $\alpha$ ), the main regulator of hypoxic response [260]. Overexpression of HIF-1 $\alpha$  in adipocytes stimulates fibrosis and local inflammation [261].

The ECM is a non-cellular component of all tissues that provides a scaffold that is very important in the expandability of WAT. It is well known that, unhealthy expansion of WAT leads to a dysregulation of ECM, and an excessive synthesis and accumulation of ECM, leading to fibrosis formation [25,262]. Fibrosis formation contributes to the WAT dysfunction that occurs in obesity, because it might hinder WAT growth and it contributes to increased lipotoxicity, ectopic lipid accumulation and insulin resistance [25,262]. In

fact, mice lacking collagen VI, an important component of WAT ECM, have increased weight gain and fat depots but improved local inflammation, and whole-body glucose and lipid homeostasis [263].

Some of these alterations that occur in adipose tissue in obesity are described in more detail below.

### **1.6.1 Adipose tissue hypoxia**

Hypoxia was reported to occur in WAT in obese mice and humans [264-266]. Hypoxia is associated with several dysfunctions in WAT, such as altered adipokine profile, inflammation, fibrosis, and altered glucose and lipid metabolism [260].

#### ***1.6.1.1 Vasculature in adipose tissue***

White adipose is a highly plastic tissue which expands and reduces its size throughout all life span [38]. WAT is also a very active metabolic organ and both expansion and metabolic processes of WAT require an efficient blood supply [267,268]. WAT is a high-vascularized tissue with a dense capillary network with every adipocyte surrounded by at least one capillary. Moreover, adipose tissue expansion requires angiogenesis, which is the formation of new blood vessels that is needed for tissue growth [269]. Vasculature has several important roles in WAT (Figure 1.11). Adipose vasculature is important in the transport of lipids, growth factors and cytokines, nutrients and oxygen [269]. Vasculature also contributes to WAT expansion by being a source of adipocyte progenitor cells [270]. Vasculature is also involved in the transport and infiltration of immune cells, such as macrophage cells, contributing to the inflammatory state, typically observed in obese condition but it also contributes to remove waste products from WAT, such as metabolic products [269].

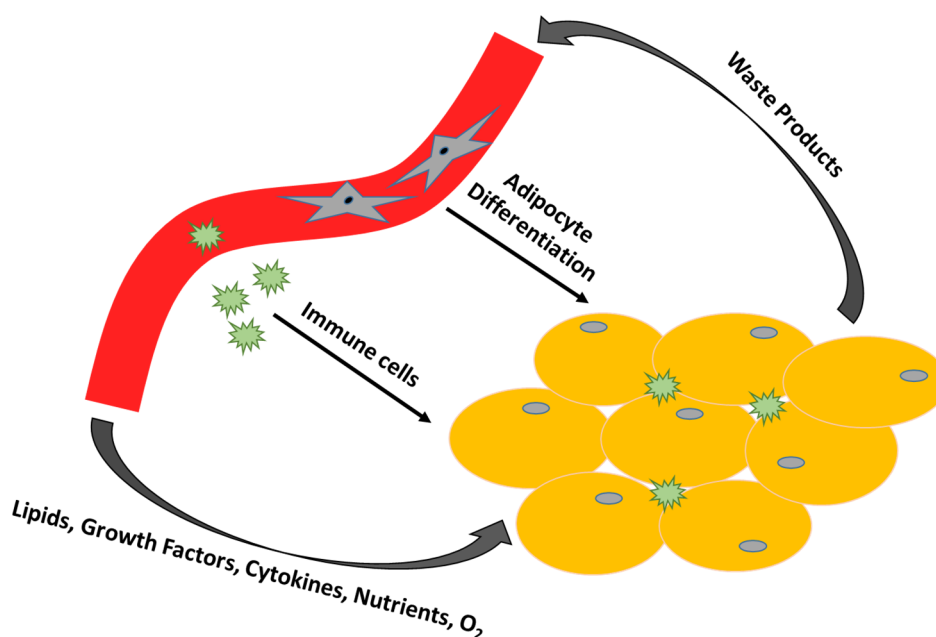


**Figure 1.11 – Functions of adipose tissue vasculature.** Vasculature of adipose tissue is important in providing lipids, growth factors, cytokines, nutrients and O<sub>2</sub>; it also provides progenitor cells for adipocyte differentiation; transports immune cells and removes waste products. Adapted from [271].

### 1.6.1.2 Hypoxia hypothesis

Hypoxia as a main contributor for the link between obesity and inflammation was first proposed by Trayhurn, in 2004 [272]. Localized hypoxia was suggested to develop in expanding adipocytes furthest removed from blood supply [272]. Some arguments can provide circumstantial support for hypoxia in WAT in obesity [272]. Reduction of capillary density [266,273], accompanied by larger blood vessels [273] was observed in obese mice, which can contribute to hypoxia. An inverse relationship between adipose tissue blood flow and fat cell size was observed in dogs [274]. The high increase of adipocyte size in obesity, up to 140–180  $\mu\text{m}$  of diameter [275], may decrease the ability of oxygen to reach the cells, because the oxygen diffusion distance is 100–120  $\mu\text{m}$  [276]. Therefore, oxygen may not be able to reach the cells, causing hypoxia. Furthermore, the WAT mass is increased in the obese state but the total blood flow and cardiac output does not rise to match the WAT increasing needs [264,277–280]. Moreover, in obese subjects there is no increase in postprandial blood flow to WAT as occurs in lean subjects [281,282].

Direct evidence of adipose tissue hypoxia in obesity was observed in different studies in obese animal models – genetically obese *ob/ob*, KKAy mice, and HFD induced obese mice [264,265,283–285]. Hypoxia was demonstrated in adipose tissue in these studies by employing O<sub>2</sub> microelectrodes, measuring the interstitial partial pressure of oxygen

(pO<sub>2</sub>) [265,283-285]. Adipose hypoxia was also demonstrated by staining adipose tissue of obese mice with the chemical hypoxic probe, pimonidazole hydrochloride, which reacts with proteins in a low-oxygen environment leading to the generation of new protein adducts [264,265,283]. Another method to evaluate hypoxia is to study hypoxia-responsive genes such as HIF-1 $\alpha$  [265,283]. Lactate concentration was also used as an indirect indicator of hypoxia in adipose tissue [264].

There are also studies in humans that are consistent with the results in rodents, indicating that hypoxia develops in growing adipocytes in adipose tissue. Two studies showed a lower pO<sub>2</sub> in subcutaneous [277] and visceral adipose tissue [266] in obese individuals compared to lean individuals. However, one study showed that pO<sub>2</sub> is elevated in obese patients but it was also observed a reduction in blood flow and impaired capillarization [282]. Another study did not observe evidences of hypoxia, despite the reduced delivery and consumption of O<sub>2</sub> and increased lactate release [286].

### **1.6.1.3 Hypoxia signaling pathways**

Hypoxia-inducible factor-1 (HIF-1) is a heterodimeric transcription factor that mediates the cellular response to hypoxia [287] (Figure 1.12). Factor nuclear  $\kappa$  B (NF $\kappa$ B) transcription factor pathway is also involved in hypoxia response in adipose tissue [288,289]. NF $\kappa$ B binds the inhibitory protein inhibitor kappa B (I $\kappa$ B) in the cytoplasm being inactivated [289]. Several stress-mediated pathways lead to the degradation of I $\kappa$ B, activating NF $\kappa$ B [289]. HIF-1 has received more attention and is better studied. HIF-1 is a heterodimer composed of two subunits:  $\alpha$  and  $\beta$ . The hypoxia-inducible factor-1 $\beta$  (HIF-1 $\beta$ ) is a constitutively expressed aryl hydrocarbon receptor nuclear translocator and is not sensitive to O<sub>2</sub> [290]. HIF-1 $\alpha$  expression is upregulated during hypoxia and can be considered a hypoxia sensor [290]. Under normal conditions of O<sub>2</sub>, HIF-1 $\alpha$  is continuously synthesized but is rapidly degraded via the ubiquitin pathway [290]. Under hypoxia, HIF-1 $\alpha$  is stabilized and translocated to the nucleus, where it binds to HIF-1 $\beta$  to form the active transcription factor [290]. HIF-1 binds to hypoxia response elements (HRE) on target genes and activate transcription [290]. HIF-1 transcriptionally activates a wide number of genes, involved in glucose and energy metabolism, cell proliferation, apoptosis and angiogenesis [291].



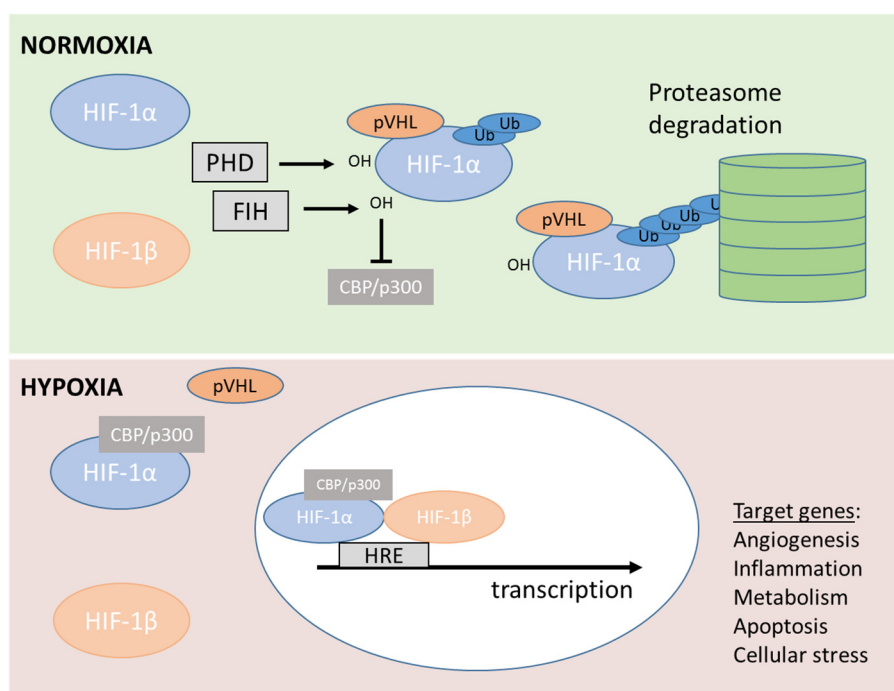


**Figure 1.12 – Regulation of hypoxia-inducible factor-1 (HIF-1).** In the presence of oxygen, prolyl hydroxylase domains (PHD), and factor inhibiting HIF, (FIH) inactivate HIF-1α. PHD enzymes hydroxylate a prolyl residue in the amino- and the carboxy-terminal oxygen-dependent degradation domains and promote von Hippel-Lindau tumor suppressor (pVHL)-dependent proteolysis. FIH hydroxylates an asparaginyl residue in the carboxy-terminal activation domain, which blocks CREB binding protein (CBP)/p300 co-activator recruitment and results in the inactivation of HIF-1α-subunit transcriptional activity. These processes lead to degradation of HIF-1α subunits via the ubiquitin (ub) pathway. In hypoxia, PHD and FIH are inactive so there is no degradation of HIF-1α subunits that is translocated to the nucleus and heterodimerizes with HIF-1β, and binds to hypoxia-response elements (HRE) in the regulatory regions of target genes, allowing the formation of a transcriptionally active complex. Adapted from [292].

Several studies using human and mouse preadipocytes and adipocytes were performed to investigate their molecular and cellular response to reduced O<sub>2</sub> tension. HIF-1α is increased in adipocytes in cell-culture studies in response to low O<sub>2</sub> or with incubation of chemical hypoxia mimetic agents, namely cobalt chloride (CoCl<sub>2</sub>) and deferoxamine [293,294]. Both chemical hypoxia mimetic agents act by stabilizing HIF-1 even in normoxia by inhibiting prolyl hydroxylase domain (PHD) enzymes [293,294]. CoCl<sub>2</sub> and deferoxamine are often used to mimic hypoxia. CoCl<sub>2</sub> inhibits PHD enzymes, which are oxygen sensors through replacement of Fe<sup>2+</sup> with Co<sup>2+</sup>. Fe<sup>2+</sup> is an essential cofactor that along with PHD degrades HIF-1α. So these enzymes are then unable to mark HIF-1α for degradation. Deferoxamine has a similar effect on the iron pool [295]. These hypoxia mimetics only mimic HIF-1 accumulation, therefore they are the most widely used hypoxia mimetics and are frequently used to study alterations in gene expression regulated by HIF-1 [295-299].

Several studies were performed to investigate the effect of hypoxia on selected genes and proteins, namely adipokines and adipogenesis regulators. In murine cell models under hypoxia or hypoxia mimetic treatment, several genes were observed to be increased namely, genes encoding leptin, vascular endothelial growth factor (VEGF), matrix metalloproteinase (MMP)-2 and MMP-9, plasminogen activator inhibitor-1 (PAI-1), IL-6 and macrophage migration inhibitory factor (MIF) and decreased genes encoding adiponectin [264,283,300,301]. It was also observed an increase of protein levels of leptin, VEGF, PAI-1 and a decrease in adiponectin [300,301]. Similar results were observed in human adipocytes [302].

Hypoxia and hypoxia mimetic agents were described to block adipocyte differentiation by decreasing the expression of several regulators of adipogenesis. The positive regulators, PPAR $\gamma$ , the isoforms C/EBP $\alpha$ ,  $\beta$  and  $\delta$  and also SREBP-1c are all inhibited *in vitro* following adipogenic stimulation, indicating adipocyte differentiation inhibition by hypoxia [264,298,303,304]. Moreover, Pref-1, an inhibitor of adipogenesis that is expressed in preadipocytes, is not altered in preadipocytes submitted to hypoxia and induced to differentiate [304].

#### **1.6.1.4 Glucose metabolism and insulin resistance**

Oxygen is a major regulator of cell metabolism and gene expression. Low oxygen induces physiological adaptations in adipocytes. It also reduces oxidative phosphorylation and Krebs cycle rates leading to a shift to anaerobic metabolism [276,305].

Hypoxia is described to increase glucose uptake both in human subcutaneous preadipocytes [306] and 3T3-L1 adipocytes [307]. These alterations were described to be blocked by inhibiting facilitative GLUTs with cytochalasin B [306]. GLUTs are a wide group of membrane proteins that facilitate the transport of glucose across the plasma membrane. GLUT1, which is ubiquitous and responsible for basal glucose uptake by most cells, was shown to be upregulated by hypoxia in murine and human adipocytes [306,308]. In contrast, prolonged exposure to hypoxia downregulates GLUT4 and GLUT8 [308,309]. Moreover, HIF-1 $\beta$  knockdown mice and 3T3-L1 adipocytes showed a decrease in GLUT1 and GLUT4 [310].

In accordance to the anaerobic shift that occurs in response to hypoxia, it was observed the upregulation of genes encoding enzymes involved in glycolytic pathways, including hexokinase 1 and 2, glucose-6-phosphate isomerase, phosphofructokinase, and aldolase C [311-313]. In accordance to these results, an increase of lactate production, an end product of glycolysis, was also observed in human and murine cells subjected to

hypoxia [300,314]. Moreover, an increase of lactate production in WAT of obese animals was also described [264]. The expression of the lactate transporters, monocarboxylate transporter 1 (MCT1) and monocarboxylate transporter 4 (MCT4), are upregulated in human fat cells exposed to hypoxia [314]. Lactate has several important functions as a signaling molecule, contributing to insulin resistance in skeletal muscle, increase of inflammation and decrease of lipolysis [315,316].

Several studies suggest that hypoxia has a role in the development of type 2 diabetes mellitus in obesity. Hypoxia alters the expression of several adipokines. It decreases adiponectin [283] and upregulates leptin and IL-6 [300,302,308]. Adiponectin is involved in insulin sensitivity so the decrease of this protein contributes to insulin resistance [236,237]. On the other hand, leptin is involved in insulin action inhibition and IL-6 is involved in insulin resistance [317]. Another action of hypoxia that might contribute to insulin resistance is GLUT4 downregulation, inhibiting the insulin-stimulated uptake of glucose through this transporter [308]. Moreover, 3T3-L1 adipocytes under hypoxia show insulin signaling inhibition as revealed by a decrease in the phosphorylation of insulin receptor [285,318]. Adipocyte-specific disruption of HIF-1 in HFD-fed mice improves insulin sensitivity and decreases adiposity [319].

#### **1.6.1.5 Lipid metabolism**

The increased glucose utilization through the glycolytic pathway in hypoxia accompanies a decrease in aerobic metabolism, decreasing oxidation of glucose through the citric acid cycle [276,305]. Hypoxia induces strong alterations in lipid oxidation and lipolysis in adipocytes [311,313]. Hypoxia was described to have no effect on basal lipolysis [300]. However, other studies described an increase of basal lipolysis and a decrease of FAs uptake in adipocytes in response to hypoxia [285,320]. Hypoxia was also described to attenuate lipogenesis [320]. These results show that hypoxia impairs the buffering capacity of adipocytes and contributes to the increase of plasma free FAs and lipotoxicity that occurs in obesity [320,321]. In accordance, it was described a decrease in several genes encoding proteins involved in mitochondrial metabolism and oxidative phosphorylation, namely cytochrome b, cytochrome c oxidase subunit Va, and ATP synthase, in human adipocytes subjected to hypoxia [322]. Moreover, hypoxia inhibits peroxisome proliferator-activated receptor  $\gamma$  coactivator-1 $\alpha$  (PGC-1 $\alpha$ ) in human adipocytes, a protein involved in mitochondrial biogenesis [311,313]. Hypoxia and hypoxia mimetic agents were described to decrease ATP production, mitochondrial membrane potential and nicotinamide adenine dinucleotide (NADH) dehydrogenase activity in 3T3-L1 adipocytes [322].

### **1.6.1.6 Fibrosis**

Fibrosis consists of an excessive accumulation of ECM components [323]. ECM is a very important component in the architecture and function of WAT, so changes in ECM may induce WAT dysfunction [263,324,325]. Fibrosis has been described to occur in WAT in obesity and a link between hypoxia and fibrosis has been proposed [326].

The study of the effect of hypoxia on global gene expression in human adipocytes showed the increase of genes that encode ECM proteins, including COL13A1 (encodes collagen type XIII  $\alpha$ ) and LOX (encodes the enzyme lysyl oxidase, which initiates the cross-linking of collagen and elastin) [311]. A proteomic study of the secretome of human adipocytes showed that a hypoxia mimetic induces alterations associated with ECM protein dysregulation [327]. However, mice lacking Hif-1 $\beta$  in WAT show no alteration in fibrosis in WAT [310]. Respiratory hypoxia in mice (10% O<sub>2</sub>) was reported to increase genes that encode for ECM proteins in WAT, namely COL13A1 and COL1A1 (encodes collagen type 13 $\alpha$ 1 and 1 $\alpha$ 1) [261]. Adipocyte-specific disruption of HIF-1 decreases expression of fibrosis related genes in HFD-fed mice [319]. Furthermore, treatment of HFD-fed mice with a selective HIF-1 $\alpha$  inhibitor, PX-478, effectively inhibited HIF-1 $\alpha$  and reduced fibrosis in WAT [284]. Similar results were obtained in adipose tissue-specific, doxycycline-inducible dominant negative HIF-1 $\alpha$  mice [284]. Moreover, a transgenic model with overexpression of a constitutively active form of HIF-1 $\alpha$  shows fibrosis formation in WAT [261].

The major effects of hypoxia on the key functions of white adipocytes are summarized in figure 1.13.

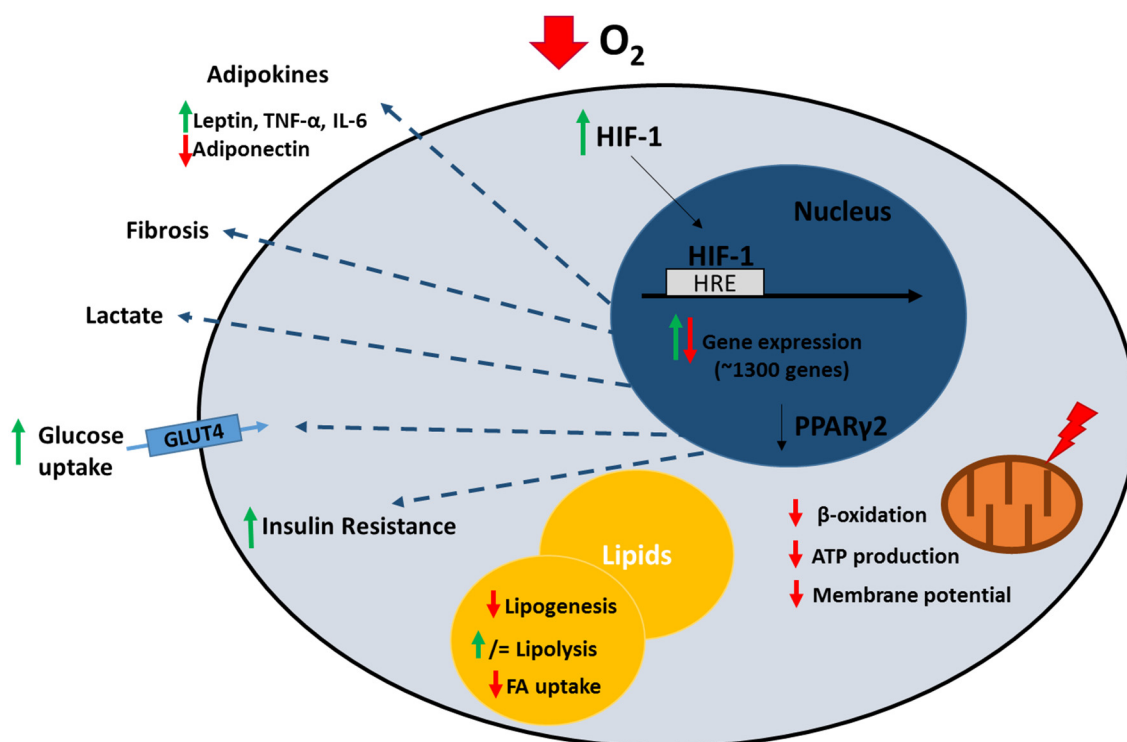


**Figure 1.13 – Schematic illustration of the major effects of hypoxia on white adipocyte functions.** Hypoxia is associated with several dysfunctions such as altered adipokine profile, inflammation, fibrosis, insulin resistance, mitochondrial dysfunction, increased glucose uptake, decreased lipogenesis and FAs uptake, and lipolysis was described to be increased or not altered. Abbreviations: TNF- $\alpha$ , Tumor necrosis factor- $\alpha$ ; IL, Interleukin; HIF-1, Hypoxia-inducible factor-1; PPAR, Peroxisome Proliferator-Activated Receptor; HRE, hypoxia-response elements; GLUT, Glucose transporter type; FA, Fatty acid. Adapted from [328].

## 1.6.2 Adipose tissue fibrosis

### 1.6.2.1 Extracellular matrix properties and functions

ECM is the non-cellular component of a tissue that has an important role in maintaining the architecture of the tissue and in other important biological functions, such as morphogenesis, differentiation and homeostasis [329]. ECM is composed of two main macromolecules: proteoglycans and fibrous proteins [325] (Figure 1.14).

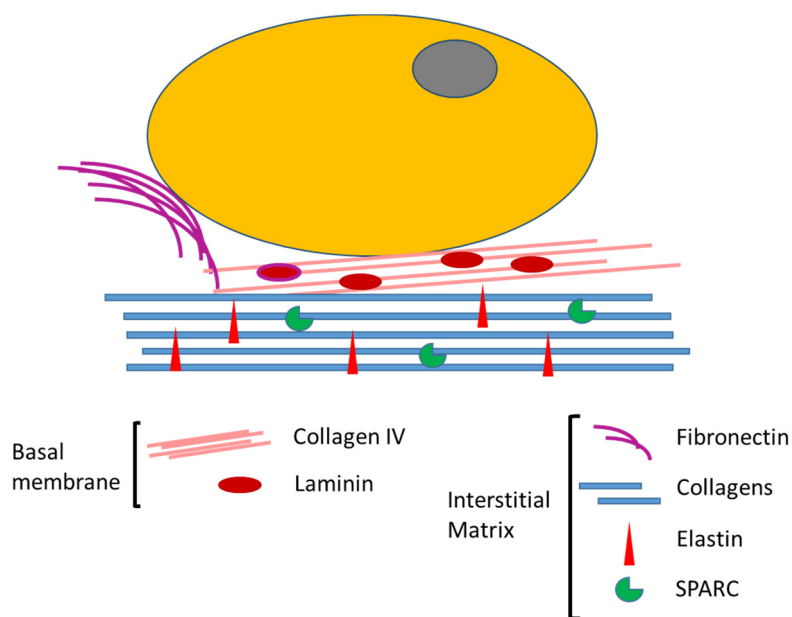


**Figure 1.14 – Adipocyte extracellular matrix (ECM) proteins.** ECM of adipose tissue is composed of a basal membrane formed by collagen IV and laminin; and it is also composed of the interstitial matrix formed by fibronectin, several collagens, elastin and secreted protein acidic and rich in cysteine (SPARC). Adapted from [330].

Proteoglycans are glycosaminoglycans that attach to proteins that fill most of the extracellular space forming a hydrated gel that provide mechanical support [331]. Fibrous proteins include structural proteins such as collagens and also adhesion proteins, such as fibronectin, laminin and elastin [325].

Collagen is the most abundant fibrous protein and provide strength, regulate cell adhesion, support chemotaxis and migration, and direct tissue development [332]. Several isoforms of collagen exist but type I, III and VI are the most associated with fibrosis [333]. Collagen associates with elastin and provide recoil to tissues that undergo repeated stretch [332].

Another important fibrous protein is fibronectin that directs the organization of ECM and has an important role in cell attachment and function [334].

Basal lamina is composed of type IV collagen and laminin [334]. Basal lamina has a structural function but it is also involved in cell polarity, metabolism, and migration and promote cell survival, proliferation, or differentiation [334].

The ECM is essential for wound healing and regeneration. ECM composition varies between different tissues and has several different functions besides structural support. These functions include anchorage for cells, intercellular communication, and is also involved in the most basic functions of cells, from cell proliferation, adhesion and migration, to cell differentiation and cell death [325]. Cell-to-ECM communication is regulated by specific heterodimeric transmembrane receptors named integrins [335].

Different integrins expression determine which ECM substrate can bind to the cell and further regulate the downstream signaling events. Integrins are directly linked to the cytoskeleton [335]. Any changes in the ECM can interact with integrins having an impact on cell movement during development and proliferation, differentiation, apoptosis and gene induction [335].

Proteoglycans can sequester several molecules, including MMPs and growth factors. MMPs are proteolytic enzymes that degrade components of the ECM [336]. Specific members of MMP family degrade specific components of ECM, helping in maintaining ECM structure, release of active molecules and it can also facilitate cell migration and produce activated substrates [336]. One important activated substrate of MMP-2 and MMP-9 is the transforming growth factor  $\beta$  (TGF $\beta$ ) [337,338]. TGF $\beta$  isoforms are multifunctional cytokines that play a central role in wound healing and in tissue repair [339]. TGF $\beta$  stimulates the production of various ECM proteins and inhibits their degradation [323]. However, in pathological situations excessive TGF $\beta$  contributes to tissue fibrosis by promoting the synthesis of collagen I [323].

#### **1.6.2.2 Extracellular matrix and adipose tissue development**

WAT has a high capacity to adapt its size according to the energetic needs of the body. ECM was shown to be important in normal adipocyte differentiation and development of WAT.

ECM network of WAT was first described in 1963 [340]. Since then, it was shown that ECM of WAT is composed by different collagen fibrils as well as various classes of adhesion proteins, such as fibronectin, laminin, elastin and proteoglycans [341,342]. Although several isoforms of collagen were described in WAT, the most expressed is collagen VI [263,341].

The importance of ECM in adipocyte differentiation was demonstrated. It was shown that fibronectin expression decreases during 3T3-F442A [343] and 3T3-L1 adipocytes [344] adipogenesis. In an *in vivo* study, it was observed that fibronectin is not expressed in differentiated adipocytes whereas collagen IV, laminin and heparan sulfate are detectable around single adipocytes in subcutaneous WAT [334]. However, type I-VI collagens, laminin and fibronectin increase in differentiating adipocytes compared with undifferentiated cells [345]. 3T3-L1 preadipocytes cultures on a fibronectin-rich matrix are inhibited to differentiate [346], while culturing human preadipocytes on a matrigel (mainly composed of basement membrane components) or laminin (the main basement membrane component) leads to increased adipocyte differentiation [347].

### **1.6.2.3 Extracellular matrix remodeling and fibrosis in obesity**

Fibrosis is defined as an excessive accumulation of ECM components, which is a result of degradation impairment and an excess synthesis of fibrillar components. Fibrosis occurs as a result of a reparative process where dead or injured cells are replaced. However, if the damage and this reparative process persist, then cells are activated and secrete ECM components, such as collagens, to replace the normal parenchymal tissue, leading to fibrosis formation [329].

During the development of obesity, WAT suffers several modifications as a result of hypertrophy and hyperplasia. WAT expansion leads to ECM remodeling with degradation of the existing ECM and the production of new ECM components (Table 1.4).

In HFD-fed mice, it was shown WAT remodeling, with increased collagen deposition observed by Gomori trichrome staining [348]. Collagens, specifically collagen I, II, III, IV, V and VI are highly upregulated in adipose tissue of obese and diabetic *db/db* mice [263,349]. Upregulation of collagen VI was observed in *ob/ob* mice. The transcriptomic signature of WAT of obese subjects was evaluated in two different studies and overexpression of many ECM components was reported in obese compared to lean WAT [324,350]. One of these studies describes alterations in 40 genes that encode components of the ECM or molecules involved in ECM remodeling and regulation, including several collagens [324]. Collagen IV, V and XII are increased in obese subjects, while collagen I is decreased [324]. Other study also described an increase in collagen V in WAT of obese individuals with a decrease in elastin [273]. Fibrotic areas in WAT are also increased in obese individuals [326,351], specifically, increased collagen VI which is associated with BMI and negatively associated with insulin sensitivity [326]. Other study also showed that WAT of obese subjects, when compared with lean individuals, has higher levels of collagens I, III and VI, and this omental WAT fibrosis is negatively correlated with omental adipocyte diameters and TAG levels [352]. Adipocyte size was also demonstrated to correlate inversely with transcript levels of COL1A1, COL6A1 (encode for collagen I and VI) in visceral adipose tissue and with fibrosis measured by Sirius Red staining in visceral and subcutaneous adipose tissue [353]. Moreover, subcutaneous WAT fibrosis correlates negatively with fat mass loss after bariatric surgery [351,352]. Several collagen genes were also evaluated and similar results were shown. COL6A3 expression (encoding for collagen VI) is correlated with BMI and fat mass [354]. In obese subjects, transcript levels of COL3A1, COL5A2 and COL6A3 (encode for collagen II, V and VI, respectively) are lower in omental and subcutaneous adipose tissue in individuals with metabolic syndrome compared to the healthy obese [355]. In contrast with these results, COL6A3 expression was reported to be lower in obesity in



subcutaneous and omental WAT, whereas weight loss increased COL6A3 expression in subcutaneous WAT [356]. Secreted protein acidic and rich in cysteine (SPARC) is a matrix-associated protein that regulates cell shape, cell-cycle progression, and synthesis of ECM [357]. SPARC was described to be upregulated in WAT in several mouse models of obesity: GTG mice, *ob/ob* mice, AKR mice [357] and *db/db* mice and in humans [358]. Thrombospondin-1 (TSP1) is an ECM glycoprotein that influences cell adhesion, motility, and growth [359]. TSP1 was described to be upregulated in WAT of *ob/ob* mice and C57Bl/6 mice fed a HFD [360]. TSP1 is also associated with obesity and insulin resistance in humans [359]. Osteopontin (OPN), an ECM protein, was also reported to be increased in WAT of obese individuals [361,362] and mice [362,363].

HFD upregulates MMP-3, 12, 14 and tissue inhibitor of metalloproteinase 1 (TIMP1) expression in adipose tissue of *db/db* mice [349]. MMP-3, 11, 12, 13, 14 and TIMP1 are upregulated while MMP-7, 9, 16, 24 and TIMP4 are downregulated in adipose tissue from *ob/ob* and diet-induced obese mice [364]. Two genetic models of obesity (*ob/ob* and *db/db* mice) and a diet-induced model of obesity (AKR mice) show increase of MMP-2, 3, 12, 14, 19, and TIMP1 and decrease in MMP-7 and TIMP3 [365]. TIMP2 expression is downregulated in HFD-fed mice [366]. Adipocyte size was shown to be inversely correlated with MMP-2, MMP-14, and TIMP1 transcript levels, and positively correlated with MMP-9 in visceral adipose tissue [353]. Moreover, MMP-9 is upregulated in obese subjects [367]. It was observed an increase of several integrins, namely integrins  $\beta 1$  and  $\beta 3$  in obese humans [324,368,369] and  $\beta 1$ ,  $\beta 2$  and  $\beta 3$  obese mice [368,369].

Fibroblasts are the main cells producing ECM components but the precise contribution of each cell type of WAT to ECM alterations is not known. *In vitro* studies suggest that preadipocytes in contact with pro-inflammatory macrophages overexpress several ECM components, namely collagen I, tenascin-C, fibronectin and its receptor  $\alpha 2\beta 1$  integrin, and activin A [370]. Adipocytes can also contribute to fibrosis formation based on the relationship described between adipocyte and pericellular fibrosis surrounding adipocytes [352].

**Table 1.4 - The extracellular matrix (ECM), ECM modifiers and ECM receptors alteration in adipose tissue in obesity.** Adapted from [371].

Proteins		Mice	Human	Refs
<b>ECM</b>	Collagens I, III, IV, V, VI	↑	↑	[263,273,349]
	SPARC	↑	↑	[357,358]
	Osteopontin	↑	↑	[362,363]
	Thrombospondin-1	↑	↑	[359,360]
	MMP-2, 3, 11, 12, 13, 14,19	↑		[364,365]
<b>ECM modifiers</b>	MMP-7, 16, 24	↓		[364]
	MMP-9	↓	↑	[364,367]
	TIMP1	↑		[364]
	TIMP2	↓		[366]
	TIMP3	↓		[365]
	TIMP4	↓		[364]
<b>ECM receptors</b>	β1, β3 integrins		↑	[324]
	β2 integrin	↑	↑	[368,369]

↑ : increase, ↓ : decrease; abbreviations: ECM, Extracellular matrix; SPARC, Secreted protein acidic and rich in cysteine; MMP, Metalloproteinase; TIMP, Tissue inhibitor of metalloproteinase.

#### **1.6.2.4 Modulation of extracellular matrix components in obese mouse models**

The adipose tissue expandability hypothesis states that WAT has a limited expandability for any given individual [372]. During adipose tissue expansion, WAT can reach its storage capability limit [372], and lipids that cannot be stored in adipose tissue are accumulated in ectopic depots like skeletal muscle, heart, liver and pancreas, causing lipotoxic insults and cardiometabolic derangements, including insulin resistance and inflammation, leading to obesity-associated diseases [372]. The mechanisms that determine adipose tissue expandability are not known, but ECM remodeling is of great importance because if there is an excessive ECM and fibrosis formation there is an inadequate expansion ability of adipocytes. Fibrosis formation was described to occur in WAT in obesity but the impact of ECM alterations are not well understood and only few studies focused on the effect of specific ECM proteins in carbohydrate and lipid metabolism (Table 1.5).

**Table 1.5 Phenotype of mice lacking extracellular matrix (ECM) and ECM modifiers.**

Mice		Phenotype	Refs
<b>ECM</b>	Collagen V <sup>-/-</sup>	Resistant to HFD-induced weight gain, hyperglycemic and insulin resistant.	[373]
	Collagen VI <sup>-/-</sup>	Increased adipocyte cell size, decreased blood triglycerides, glycemia, WAT inflammation, liver triglycerides in <i>ob/ob</i> mice.	[263]
	SPARC <sup>-/-</sup>	Increased adipocyte size and number, subcutaneous and epididymal adipose tissue weight with no alterations in body weight gain.	[374]
	OPN <sup>-/-</sup>	Improved insulin sensitivity, reduced WAT inflammation with no alterations in adipose tissue and body weight.	[363]
	TSP1 <sup>-/-</sup>	Resistant to HFD-induced insulin resistance and WAT inflammation.	[375]
<b>ECM modifiers</b>	t-PA <sup>-/-</sup>	Increased HFD-induced adipocyte diameter, subcutaneous weight and body weight gain.	[376]
	u-PA <sup>-/-</sup>	No alterations in body weight gain and in adipose tissue development.	[376]
	MMP-14 <sup>+/-</sup>	Lower body weight gain and adipose tissue weight.	[377]
	MMP-14 <sup>-/-</sup>	Lipodystrophy.	[378]
	TIMP1 <sup>-/-</sup>	Increased adipocyte size and number, body weight and adipose tissue weight.	[379]
	TIMP2 <sup>-/-</sup>	Obese with normal glucose tolerance and insulin sensitivity.	[366]

ECM, Extracellular matrix; SPARC, Secreted protein acidic and rich in cysteine; OPN, Osteopontin; TSP1, Thrombospondin-1; t-PA, tissue-type plasminogen activator; u-PA, urokinase-type plasminogen activator; MMP, Metalloproteinase; TIMP, Tissue inhibitor of metalloproteinase.

In fact, the absence of collagen V in mice (Female Col5a3<sup>-/-</sup> mice) induces resistance to HFD-induced weight gain [373], and male and female Col5a3<sup>-/-</sup> mice are hyperglycemic and insulin resistant [373]. Moreover, the absence of collagen VI results in increased expansion of individual adipocytes but improves the metabolic phenotype in *ob/ob* mice, including the increase of glucose and lipid clearance [263]. These mice also show reduced inflammation in adipose tissue [263]. Furthermore, SPARC-null mice were reported to have a great reduction in collagen and have a larger epididymal fat pad and an increased number and size of adipocytes [374]. Obese mice lacking OPN show no differences in body composition or energy expenditure but display improved insulin sensitivity and decreased WAT inflammation [363]. Despite HFD-fed TSP1 knockout mice develop obesity, they are protected against inflammation and insulin resistant associated with obesity [375].

Moreover, tissue-type plasminogen activator (t-PA) deficient mice fed a HFD have higher body weight, subcutaneous adipose tissue and adipocyte diameter [376]. However,

urokinase-type plasminogen activator (u-PA) deficient mice in HFD showed no differences in weight gain and adipose tissue development [376]. Mice in HFD and treated with a synthetic MMP inhibitor show lower body weight gain, lower WAT weight and higher number of adipocytes but smaller [380]. Moreover, MMP-14+/- mice have lower weight gain and decreased fat pads [377]. Another study showed that the absence of matrix metalloproteinase MMP-14 causes an increase in collagen content and lipodystrophy in mice by impairing WAT development [378]. Furthermore, mice lacking TIMP1 show increased body weight and adipose tissue weight accompanied by increased adipocyte number and size [379]. Chow-fed TIMP2 knockout mice are obese maintaining normal glucose tolerance and insulin sensitivity. Obesity is exacerbated when fed a HFD with hyperglycemia, hyperinsulinemia, and hyperleptinemia [366]. All together, these data are consistent with the notion that increased collagen restricts expansion of adipocytes and that decreased collagen allows higher adipocyte expansion resulting in metabolic improvements.

#### ***1.6.2.5 Underlying mechanisms of fibrosis formation in white adipose tissue***

As previously mentioned, hypoxia and HIF-1 $\alpha$  are thought to significantly contribute to fibrogenic progression [261,273]. However, several studies also demonstrated that the increased deposition of ECM components that lead to fibrosis in the adipose tissue in obesity is associated with inflammation and insulin resistance.

Obesity is associated with a low-grade inflammation in adipose tissue, with infiltration of macrophages [381], neutrophils [382], lymphocytes [383], and mast cells [384] promoting a local pro-inflammatory environment. Adipose tissue macrophages are known to undergo a phenotypic switch from an anti-inflammatory M2 state to a pro-inflammatory M1 polarization state [258]. M2 macrophages express IL-10 or arginase, increasing the anti-inflammatory profile, while M1 macrophages express TNF- $\alpha$ , TGF $\beta$ , IL-1 $\beta$ , IL-6 or inducible nitric oxide synthase (iNOS), increasing the inflammatory profile and contributing to insulin resistance [258]. M1 macrophages were observed in a crown-like structure surrounding necrotic adipocytes in human and mice [385].

COL6A3 expression was described to be associated with adipose tissue macrophage chemotaxis and inflammation [354]. Moreover, others showed that Collagen VI-null mice have reduced inflammation in epididymal adipose tissue [263]. These studies suggest that collagen VI and ECM contribute to adipose tissue inflammation [263,354]. Inversely, inflammatory preadipocytes exhibit overexpression of ECM genes [370]. Moreover, transcriptomic studies in subcutaneous WAT in obese human subjects, driven by the analysis of transcriptional interactions, reported that a pro-inflammatory environment can

lead to excessive synthesis of ECM components [324]. A strong relationship linking inflammatory processes to ECM remodeling components and fibrosis formation is well established. However, the time-course of the events and a causal relationship between inflammation and fibrosis is not yet fully established in the context of obesity.

### **1.7 Dipeptidyl peptidase IV**

Dipeptidyl peptidase IV (DPP-IV; EC 3.4.14.5), also known as CD26, is a 766 amino acids and 110 kDa glycoprotein [386]. DPP-IV was first characterized by Hopsu-Havu and Glenner in 1966 in rat liver homogenates [387]. DPP-IV belongs to the prolyl oligopeptidase family, a group of atypical serine proteases able to hydrolyze the prolyl bond.

DPP-IV is a type II transmembrane protein that consists of a short N-terminal cytoplasmic domain (6 residues) that is linked to the cell membrane by a single hydrophobic segment, a transmembrane domain (22 residues) and a large C-terminal extracellular domain (738 residues) [386] (Figure 1.15). The extracellular domain of DPP-IV is composed of a glycosylation domain, a cysteine-rich domain, and a catalytic domain [388]. This enzyme is a membrane-bound protein that contains a noncleavable signal sequence in contrast to classical secreted proteins that cleave off the signal sequence [388]. The signal sequence is located at the N-terminal that serves as a membrane anchor and targets them to the rough endoplasmic reticulum [388].

DPP-IV can also be found as a soluble circulating form (sDPP-IV) that lacks the cytoplasmic and transmembrane domain [389]. sDPP-IV is cleaved from the cell membrane and released into the circulation in a process called shedding that involves MMPs [390]. sDPP-IV exhibit intact enzymatic and cysteine-rich region and have both enzymatic and non-enzymatic functions with paracrine and endocrine effects [220].

DPP-IV exists as a monomer and a dimer and can also form tetramers between two soluble DPP-IV and two membrane-bound DPP-IV proteins [391]. Dimerization is needed for catalytic function of this enzyme and is the most common form [391].

DPP-IV is an ubiquitous multifunctional enzyme that has the catalytic function of cleaving N-terminal dipeptides from proteins containing proline or alanine in the penultimate position [392]. Besides this catalytic function, DPP-IV also has non-enzymatic functions, such as being a binding partner for numerous peptides, including adenosine deaminase (ADA) and ECM proteins, it also has cell surface co-receptor activity to mediate viral entry, and regulates intracellular signal transduction coupled to the control of cell migration and proliferation [393]. Dysregulation of DPP-IV has been implicated in several

diseases, such as cancer, inflammatory diseases as well as in obesity and diabetes [394-397].

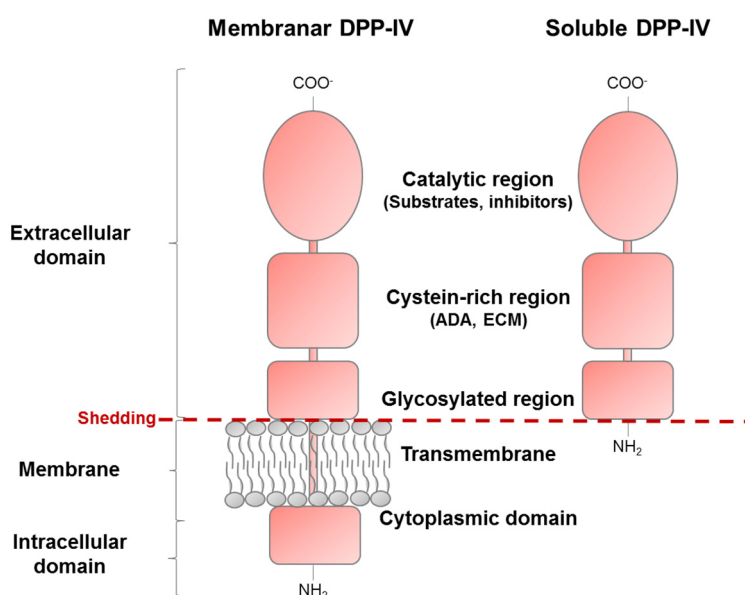


**Figure 1.15** – Dipeptidyl peptidase IV (DPP-IV) has two forms: membranar and soluble. Both have an extracellular domain composed by a catalytic region (substrates and inhibitors binding site), a cysteine-rich region (adenosine deaminase, collagen and fibronectin binding site) and a glycosylated region. The membranar DPP-IV has also a transmembranar and a cytoplasmic domain. Adapted from [220].

### 1.7.1 Non-enzymatic function of dipeptidyl peptidase IV

DPP-IV binds several ligands in the cysteine-rich region and it provides different functions to this enzyme. DPP-IV binding partners include ADA [398], fibronectin [399], and collagen [400] that are reviewed briefly below.

#### Adenosine deaminase

DPP-IV binds ADA and this DPP-IV interaction is the most studied one. It was suggested that tetramerization of DPP-IV and proper glycosylation is a mechanism for ADA binding control [401]. ADA is an enzyme involved in purine metabolism. ATP or ADP is initially converted to AMP to produce adenosine which is then converted to inosine by ADA [402]. DPP-IV-ADA interaction preserves enzymatic function of both molecules [401]. DPP-IV-ADA complex activates plasminogen-2 that leads to the increase of plasmin levels, leading to degradation of ECM proteins and activation of MMPs [403,404]. This indicates an involvement of DPP-IV and ADA interaction in tissue remodeling [395]. Only the ADA bound to DPP-IV on the cell surface was functional and was more resistant to the inhibitory effect of elevated extracellular adenosine [405,406].

### **ECM proteins: Fibronectin and Collagen**

DPP-IV binds ECM components, preferentially fibronectin and collagens I and III [399,400]. Due to its interaction with ECM proteins, such as collagen and fibronectin, DPP-IV can be considered a cell adhesion molecule. DPP-IV was reported to bind fibronectin using nitrocellulose binding assays in rat hepatocytes. It was shown that DPP-IV plays a role in interaction of hepatocytes with ECM and in matrix assembly [407]. Both interaction of DPP-IV with fibronectin and collagen are independent of its enzymatic activity because the binding site is located at the C-terminal portion of the molecule, separated from the catalytic site [399,400]. It is thought that the ability of DPP-IV to interact with the ECM can influence the biology and clinical behavior of tumors [399,408-410]. Several studies report that DPP-IV affects the invasiveness of many tumor cells. However, different results were observed in different cancers.

A positive correlation between DPP-IV expression and metastasis development was observed in primary colorectal cancer, thyroid cancer and gastrointestinal stromal tumors in humans [408,411,412]. Additionally, CD26-positive cells show higher adhesion to fibronectin and type I collagen than CD26-negative cells in primary colorectal cancer [408]. Moreover, serum DPP-IV is positively associated with colorectal cancer, and is significantly higher in patients with metastatic colorectal disease [413]. Treatment with peptides that inhibit DPP-IV interaction with fibronectin decreased pulmonary metastasis of tumor cells [399]. DPP-IV inhibition by using an anti-DPP-IV antibody decreases binding to collagen and fibronectin and inhibits tumor growth in renal cell carcinoma [409].

In contrast with these studies, DPP-IV present in lung endothelial cells specifically binds to fibronectin in breast cancer cell surface, and this interaction inhibits tumor metastasis in animal models [414]. DPP-IV overexpression decreases the invasive potential of ovarian carcinoma cell lines [408] and prostate cancer cells [415]. Furthermore, inhibition of DPP-IV promotes metastasis in prostate cancer [410].

DPP-IV was shown to be associated with decreased cancer invasiveness in some cancers, while in others DPP-IV is associated with increased cancer progression. These contrary results might occur due to the pleiotropic effects of DPP-IV.

#### **1.7.2 Enzymatic (catalytic) function of dipeptidyl peptidase IV**

DPP-IV exhibits catalytic activity by cleaving peptides at the N-terminal region proline or alanine in the penultimate position [392]. The substrates of DPP-IV include several types of molecules, including incretins, neuropeptides and chemokines as described in Table 1.6. The action of DPP-IV on its substrates can lead to inactivation of peptides, change

of receptor specificity, and can also enhance substrate activity. There are several predicted DPP-IV substrates but only some have been proved to be cleaved by DPP-IV, *in vivo*.

**Table 1.6** – Incretins, neuropeptides and chemokines cleaved by dipeptidyl peptidase-IV (DPP-IV) and consequences.

	DPP-IV Substrates	Consequences	Refs
<b>Incretins</b>	Glucagon-like peptide 1	Substrate inactivation	[416]
	Glucagon-like peptide 2	Substrate inactivation	[417]
	Gastric inhibitory peptide	Substrate inactivation	[416]
<b>Neuropeptides</b>	Neuropeptide Y	Change of receptor affinity	[418]
	Peptide YY	Change of receptor affinity	[418]
	Endomorphin	Change of receptor affinity	[419]
	Substance P	Substrate inactivation	[420]
	$\beta$ -casomorphin	Substrate inactivation	[421]
	Vasoactive intestinal peptide	Substrate inactivation	[422]
	Pituitary adenylate-cyclase-activating polypeptide	Substrate inactivation	[422]
<b>Chemokines</b>	Stromal cell-derived factor-1 $\alpha$	Substrate inactivation	[423]
	Monokine induced by $\gamma$ interferon	Substrate inactivation	[424]
	Interferon-inducible protein-10	Substrate inactivation	[424]
	Regulated on activation, normal T-cell expressed and secreted	Change of receptor affinity	[425]
	LD78 $\beta$	Enhanced substrate activity	[426]
	Macrophage inflammatory protein-1 $\beta$	Change of receptor affinity	[427]
	Eotaxin	Substrate inactivation	[428]
	Interferon-inducible T-cell $\alpha$ chemoattractant	Substrate inactivation	[429]

### 1.7.2.1 Incretins

One of the most important DPP-IV substrates are incretins that have an important role in maintaining glucose homeostasis [430]. Incretins, such as glucagon-like peptide-1 (GLP-1) and gastric inhibitory polypeptide (GIP), are released from the gut after food intake, and are responsible for 60% of insulin secretion that occurs [431]. Incretins can bind to receptors in pancreas to stimulate insulin secretion and also to suppress glucagon release as a response to increased blood glucose [431,432]. One of the major characteristics of these incretins is that plasma levels return to baseline within a couple of minutes because they are rapidly inactivated by DPP-IV [433].



GLP-1 is an incretin hormone secreted from intestinal L-cells to the blood stream. GLP-1 delays gastric emptying, being a regulator of satiety and appetite [434]. This peptide appears to be responsible for the majority of the incretin effects on pancreatic  $\beta$ -cell function and is responsible for an important part of the insulin response to glucose [430]. Some conflicting results describe the effect of GLP-1 in adipocyte differentiation and lipolysis. GLP-1 was described to stimulate adipogenesis in 3T3-L1 preadipocytes and primary preadipocytes through glucagon-like peptide 1 receptor (GLP-1R) [435,436]. However, GLP-1 was shown to inhibit adipogenesis in human bone marrow-derived MSCs [437]. On the other hand, treatment of differentiated 3T3-L1 and human primary adipocytes with GLP-1 stimulates lipolysis through GLP-1R [438]. In contrast, subcutaneous injections of GLP-1 in adipose tissue in humans and GLP-1 treatment of human primary adipocytes have no lipolytic effect [439]. Intracerebroventricular infusion of GLP-1 in mice decreases fat storage via direct modulation of adipocyte metabolism, independently of food intake but this effect is blunted in obese mice [440]. Moreover, GLP-1 agonist, liraglutide, is described to decrease appetite, visceral adiposity and body weight in humans, rats and mice [441-444].

GIP is synthesized by K cells, which are found in gastrointestinal tract. It is transported in blood stream and bind to G-protein-coupled receptors found on  $\beta$ -cells in the pancreas leading to increased cAMP [445]. Circulating GIP levels are decreased in type 2 diabetes mellitus patients and are negatively associated with the severity of insulin resistance [446]. Besides being insulinotropic, another important role of GIP is to regulate adipocytes function. The GIP receptor (GIPR), is increased during adipocyte differentiation [447-449]. GIP was described to promote adipogenesis and glucose uptake [447,449]. GIP stimulates LPL activity and TAGs accumulation in the presence of insulin in 3T3-L1 and human adipocytes [450]. Moreover, GIP stimulates lipolysis [451,452] but attenuates isoproterenol-induced lipolysis [452]. Other study demonstrated that GIP inhibits lipolysis in 3T3-L1 adipocytes [453]. GIP was also demonstrated to lower plasma free FAs, although it does not reduce plasma TAGs in humans [453]. Furthermore, mice lacking the GIPR, mice lacking GIP and mice treated with a GIPR antagonist when fed a HFD are protected against obesity and insulin resistance [454-458]. GIP administration during hyperinsulinemic-hyperglycemic clamp increases adipose tissue blood flow, glucose uptake, and free FA re-esterification, leading to lipid accumulation in abdominal subcutaneous adipose tissue [459].

### **1.7.2.2 Non-incretin substrates**

#### **Neuropeptide Y**

NPY is a 36 amino acid peptide that can be metabolized by DPP-IV, from NPY<sub>1-36</sub> to NPY<sub>3-36</sub> [418]. NPY is a neuropeptide highly expressed in hypothalamus but it is also expressed in peripheral tissues, including adipose tissue [460,461].

NPY regulates energy balance, food intake, memory, and learning [462]. NPY levels are increased in obesity [461]. Hypothalamic NPY overexpression causes hyperphagia and obesity in rats [463] and knockdown of NPY in the hypothalamus ameliorates these alterations [464]. NPY was described to suppress glucose-induced insulin secretion [465], to stimulate adipogenesis [466,467] and to have an anti-lipolytic effect in 3T3-L1 preadipocytes [468,469].

When NPY is cleaved by DPP-IV, the resulting cleavage product has different affinity to NPY receptors, altering its biological functions. NPY will be discussed with more detail in section 1.8.

#### **Substance P**

Substance P is metabolized by DPP-IV *in vivo* [470]. DPP-IV sequentially convert substance P<sub>1-11</sub> to substance P<sub>3-11</sub> and substance P<sub>5-11</sub> [470]. It is a member of the tachykinin neuropeptide family and can act as a neurotransmitter and as a neuromodulator. Substance P is also associated with inflammatory processes. Although it was described that substance P has an orexigenic effect in mice [471] it was also reported that substance P is associated with development of obesity and type 2 diabetes mellitus [472]. However, another study demonstrated that substance P is decreased in diabetic patients [473],

Substance P was described to increase viability, reduce apoptosis, and stimulate proliferation of human mesenteric preadipocytes [474]. In 3T3-L1 preadipocytes, substance P treatment decreases lipid accumulation, increases adipokine secretion, decreases differentiation and blocks insulin-mediated action [475].

### **1.7.3 Dipeptidyl peptidase in adipose tissue**

Most clinical studies focus mainly in DPP-IV inhibitors effect on GLP-1 metabolism and glucose homeostasis. However, DPP-IV was demonstrated to have also other important roles in the periphery, namely in adipose tissue.

DPP-IV was described to be expressed in both human omental adipose tissue [476] and also in visceral and epididymal adipose tissue [468]. DPP-IV is also expressed in

preadipocytes and adipocytes in mice and humans [397,467] and DPP-IV is upregulated as adipocytes differentiate [397,477]. In contrast, other studies reported that DPP-IV expression is upregulated during human adipocyte dedifferentiation *in vitro* [478] and DPP-IV expression is decreased during 3T3-L1 adipocyte differentiation [479]. Moreover, adipose tissue explants from obese subjects release more sDPP-IV than adipose tissue explants of lean subjects and sDPP-IV is decreased after weight lost [397,480]. Moreover, DPP-IV was demonstrated to be increased both in subcutaneous and visceral adipose tissue of obese individuals and its levels are positively correlated with adipocyte size and all parameters of the metabolic syndrome [397,480,481]. In contradiction with this result, DPP-IV expression was described to be decreased in subcutaneous adipose tissue of obese individuals [468]. Moreover, DPP-IV activity is increased in plasma but decreased in visceral adipose tissue in obese rats fed a HFD [482].

Other studies investigated the effect of DPP-IV in adipocyte differentiation and adiposity. DPP-IV treatment stimulates lipid accumulation and PPAR $\gamma$ 2 expression through cleavage of NPY, indicating that it stimulates 3T3-L1 adipocyte differentiation [467]. Moreover, HFD-fed mice lacking DPP-IV shows protection against obesity, insulin resistance and increased adiposity [483]. This protection is associated with reduced food intake and increased energy expenditure [483]. In addition, the lack of DPP-IV leads to activation of the PPAR pathway and down-regulation of SREBP-1 expression, thereby increasing lipid oxidation and reducing lipogenesis [483]. HFD-fed DPP-IV-deficient rats gain more weight and visceral fat mass [484]. Moreover, the adipose tissue of these rats shows a higher adipocyte maturation and increased expression of enzymes involved in TAGs uptake and synthesis, namely LPL and FAS [484]. These animals also exhibit reduced adipose tissue inflammation and improved insulin resistance [484]. Several DPP-IV knockout rodent models show increased glucose tolerance, lower plasma glucose, and increased plasma insulin and GLP-1 [485-488]. These results suggest that DPP-IV activation might be responsible for hyperglycemia and lipid metabolism, which are characteristic of diabetic and obese subjects [485-488]. A role of DPP-IV in insulin signaling was described in a study that showed that treatment of human adipocytes with DPP-IV results in insulin-stimulated Akt phosphorylation, showing insulin-signaling impairment [397]. These studies use whole-body knockout animals but to study the specific role of DPP-IV in adipose tissue, it would be important to study adipose tissue-specific knockout models.

### 1.7.4 Dipeptidyl peptidase inhibitors

DPP-IV inhibitors, also called gliptins, are a class of oral antidiabetic drugs used in the treatment of type 2 diabetes mellitus [489]. Type 2 diabetes mellitus is characterized by hyperglycemia and insulin resistance. The main targets of DPP-IV inhibitors as antidiabetic agents are incretins. The predominant incretins are GLP-1 and GIP. The mechanism of action of DPP-IV inhibitors is illustrated in Figure 1.16.

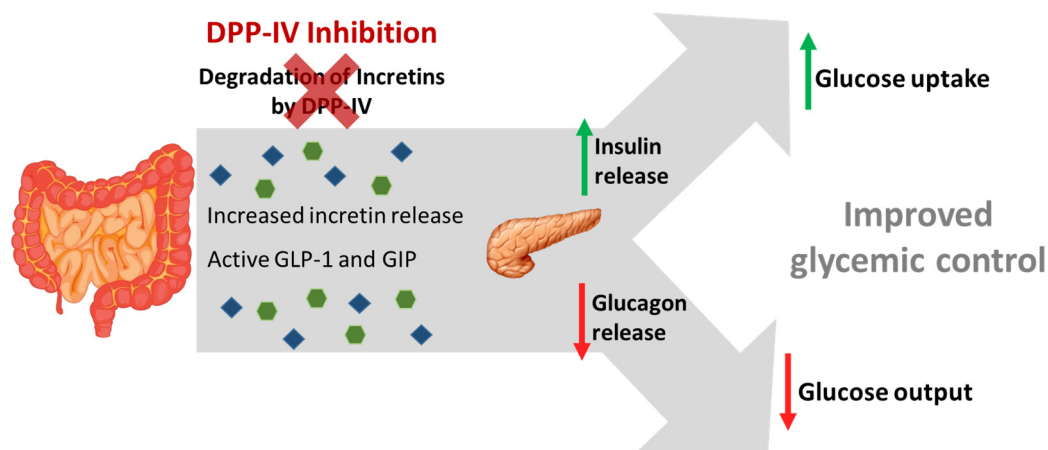


**Figure 1.16 – Mechanism of action of dipeptidyl peptidase IV (DPP-IV) inhibitors in glycemic control.** DPP-IV inhibition prevents the enzymatic inactivation of glucagon-like peptide-1 (GLP-1) and gastric inhibitory polypeptide (GIP). Then, GLP-1 and GIP increase insulin secretion and inhibit glucagon secretion by the pancreas, resulting in increased glucose uptake and decreased glucose output. Adapted from [490].

GLP-1 and GIP have very short half-time life, being rapidly metabolized by DPP-IV [433]. GLP-1 and GIP, unlike other insulinotropic agents, stimulate insulin release from the pancreatic islets in a glucose dependent manner [431]. GLP-1 has several actions that contribute to its glucose-lowering effects, namely suppression of post-prandial glucagon release, delay gastric emptying, enhancement of  $\beta$ -cell mass and increase of satiety [431,434,491]. DPP-IV inhibitors prevent the inactivation of incretins by DPP-IV, increasing their half-time life. Enhanced endogenous GLP-1 and GIP activity ultimately results in the potentiation of insulin secretion by pancreatic  $\beta$ -cells and subsequent lowering of blood glucose levels, HbA1c, glucagon secretion and liver glucose production [431,492]. DPP-IV inhibitors also have effects on pancreatic  $\beta$ -cells, including increased  $\beta$ -cell survival and expansion of  $\beta$ -cell mass [493]. DPP-IV inhibitors do not pass the blood–brain barrier and do not alter gastric emptying or satiety [494]. Importantly, these inhibitors are associated with low risk of hypoglycemia and weight loss or neutrality and are well tolerated [495].

Several inhibitors are already commercially available and are listed in Table 1.7.

**Table 1.7 – Dipeptidyl peptidase IV inhibitors approved for the treatment of type 2 diabetes.**

Inhibitor	Brand (Manufacturer)	Year approved	Type of action	Recommended dose	Refs
Sitagliptin	Januvia® (Merck & Co.); Tesavel® (Merck & Co.); Xelevia® (Merck & Co.); Ristaben® (Merck & Co.)	2006 (FDA) 2007 (EMA)	Reversible non-covalent bond	100 mg QD	[496]
Vildagliptin	Galvus® (Novartis); Jalra® (Novartis); Xiliarx® (Novartis)	2007 (EMA)	Reversible covalent bond	50 mg BID	[497]
Saxagliptin	Onglyza® (AstraZeneca)	2009 (FDA) 2009 (EMA)	Reversible covalent bond	5 mg QD	[498]
Linagliptin	Trajenta® (Boehringer Ingelheim)	2011 (FDA) 2011 (EMA)	Reversible non-covalent bond	5 mg QD	[499]
Gemigliptin	Zemiglo® (LG Life Sciences)	2012 (Korea)	Reversible non-covalent bond	50 mg QD	[500]
Anagliptin	Suiny® (Sanwa Kagaku Kenkyusho Co.)	2012 (Japan)	Reversible bond	200 mg QD	[501]
Alogliptin	Nesina® (Takeda); Vipidia® (Takeda)	2013 (FDA) 2013 (EMA)	Reversible non-covalent bond	25 mg QD	[502]
Teneligliptin	Tenelia® (Mitsubishi Tanabe Pharma Corporation)	2012 (Japan)	Reversible covalent bond	20 mg QD	[503]
Trelagliptin	Zafatek® (Takeda)	2015 (Japan)	Reversible non-covalent bond	100 mg QW	[504]
Omarigliptin	Marizev® (Merck & Co.)	2015 (Japan)	Reversible bond	25 mg QW	[505]
Evogliptin	Suganon® (Dong A-ST)	2016 (Korea)	Reversible non-covalent bond	5 mg QD	[506]

Abbreviations: FDA, Food and Drug Administration; EMA, European Medicines Agency; QD, once daily; BID, twice daily; QW, once weekly.

Five DPP-IV inhibitors have been approved by Food and Drug Administration (FDA) and/or European Medicine Agency (EMA): sitagliptin, vildagliptin, saxagliptin, linagliptin and alogliptin. Five other DPP-IV inhibitors were approved in Japanese and Korean markets. Our work will focus on vildagliptin that was one of the first DPP-IV inhibitors to be approved.

All the inhibitors have the same mechanism of action but differ in pharmacodynamics and pharmacokinetics [489]. DPP-IV inhibitors are competitive reversible inhibitors with similar efficacy (70–90%) but different potency with an *in vitro* half maximal inhibitory

concentration (IC<sub>50</sub>) of 1, 19, 62, 50, and 24 nM for linagliptin, sitagliptin, vildagliptin, saxagliptin and alogliptin, respectively [507].

Besides the role of DPP-IV inhibitors in lowering glucose levels, several other pleiotropic effects of these drugs have been described, such as in lipid profile, blood pressure and on inflammation. The effects of DPP-IV inhibitors in adipose tissue and also its effects on fibrosis formation in non-adipose tissue are reviewed in sections 1.7.5. and 1.7.6, respectively.

#### 1.7.4.1 Vildagliptin

Vildagliptin (Galvus®, Jalra®, Xiliarx®), also known as LAF237, was first approved for treatment of type 2 diabetes mellitus patients in 2007 and is commercialized in more than 100 countries [508]. The structure of vildagliptin is represented in Figure 1.17. Vildagliptin is a selective inhibitor of DPP-IV that is indicated in the European Union for the treatment of type 2 diabetes more commonly used in combination with metformin, and more rarely as monotherapy [508]. This DPP-IV inhibitor binds reversibly and covalently DPP-IV. Vildagliptin functions as a substrate for DPP-IV with a dissociation half-life of 55 minutes [508]. This drug has an *in vitro* IC<sub>50</sub> of 62 nM and a K<sub>i</sub> value of 10 nM [507].

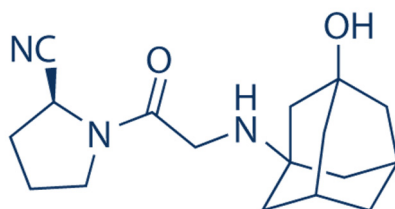


**Figure 1.17 – Chemical structure of vildagliptin.** Vildagliptin is a cyanopyrrolidine-based dipeptidyl peptidase-IV inhibitor.

#### 1.7.5 Effect of dipeptidyl peptidase inhibition on adipose tissue and obesity

DPP-IV inhibitors have important effects in adipose tissue (Table 1.8).

**Table 1.8 – Dipeptidyl peptidase IV inhibition effects in adipose tissue in several models of obesity.**

Models		Inhibitor	Inhibitor effect	Refs
<b><i>In vivo</i></b> <b>studies</b>	Zucker diabetic rats	FE 999011	Improved glucose tolerance and reduced circulating free FAs and TAGs levels.	[509]
	HFD-fed mice	Sitagliptin	Reduced fasting blood glucose without changes in body weight and epididymal and retroperitoneal fat mass; increased number of small adipocytes; reduced number of the very large adipocytes; reduced inflammation in the adipose tissue and pancreatic islet.	[510]
	HFD-fed mice	Des-fluoro-sitagliptin	Decreased weight gain and improved glucose and insulin levels after an oral glucose tolerance test.	[511]
	HFD-fed mice	Sitagliptin	Increased insulin sensitivity, decreased body weight, and adipocyte hypertrophy.	[512]
	HFD-fed mice	Teneligliptin	Improved insulin resistance, reduced body weight and adipocyte hypertrophy.	[513]
	HFD-fed mice	Des-fluoro-sitagliptin	Decreased serum glucose and insulin levels, attenuated epididymal adiposity, and decreased serum leptin levels.	[514]
	Wild type mice	Vildagliptin	Reduced levels of cholesterol and triglycerides, reduced hepatic expression of genes important for cholesterol synthesis and FA oxidation	[515]
	Gck+/-mice	Des-fluoro-sitagliptin	Ameliorated linoleic acid-induced adipose tissue hypertrophy and prevented inflammation and fatty liver.	[516]
	HFD-fed mice	Llinagliptin	Increased insulin sensitivity, reduced liver fat content, and lower expression of the macrophage marker F4/80.	[517]
<b><i>In vitro</i></b> <b>studies</b>	3T3-L1 preadipocytes	Vildagliptin	Reduced lipid accumulation by inhibiting adipogenesis, through NPY cleavage and NPY Y <sub>2</sub> receptor activation	[467]
	3T3-L1 preadipocytes	Sitagliptin	No effect on adipocyte differentiation.	[479]

HFD, High-fat diet; FA, Fatty acid; TAG, Triglyceride; NPY, Neuropeptide Y.

Several studies showed that treatment with DPP-IV inhibitors decreases blood glucose and improves insulin sensitivity in Zucker diabetic rats and HFD-fed mice [509-511,513,514,517]. Additionally, circulating free FAs and TAGs levels are also decreased after DPP-IV inhibitors, FE 999011 and vildagliptin, treatment in Zucker diabetic rats and wild type mice [509,515].

Moreover, C57Bl/6J mice fed a high-fat and treated with sitagliptin show no body weight and epididymal and retroperitoneal fat mass changes [510]. It was also described that sitagliptin treatment increases the number of small adipocytes and reduces the number

of the very large adipocytes [510]. In contrast, mice fed a HFD when treated with different DPP-IV inhibitors show decreased body weight [511-513], adiposity [514], and adipocyte hypertrophy [512,513]. Vildagliptin treatment also reduces the hepatic expression of genes important for cholesterol synthesis and FA oxidation, namely phospho-mevalonate kinase, acyl-coenzyme dehydrogenase medium chain, mevalonate (diphospho)decarboxylase, and Acyl-CoA synthetase [515]. DPP-IV inhibitors prevent adipose tissue inflammation and fatty liver in C57BL/6 mice fed a HFD [510,517] and  $\beta$ -cell-specific glucokinase haploinsufficient (Gck(+/-)mice, a model of non-obese type 2 diabetes mellitus [516].

DPP-IV inhibitor effects were also evaluated in humans. Besides the antidiabetic effects of DPP-IV inhibitors, other effects were observed in adipose tissue. DPP-IV inhibition with vildagliptin increases postprandial lipid mobilization and oxidation in patients with type 2 diabetes mellitus [518]. This effect was suggested to occur through sympathetic activation rather than a direct effect on metabolic status [518]. Sitagliptin improved glycemic control, and reduces intrahepatic lipid content and total body fat in overweight Japanese patients with type 2 diabetes mellitus [519]. However, clinical trials with vildagliptin, sitagliptin and saxagliptin, reported no significant changes in body weight [520].

However, it was reported that DPP-IV inhibitors regulate adipocyte differentiation [467]. The effect of DPP-IV inhibitor, vildagliptin, in adipogenesis was studied *in vitro* in a murine preadipocyte cell line, 3T3-L1 cells [467]. Vildagliptin reduces lipid accumulation by inhibiting adipogenesis, through NPY cleavage and subsequent NPY Y<sub>2</sub> receptor activation without affecting lipolysis [467]. In contrast, it was described that DPP-IV inhibitor, sitagliptin, has no effect on adipocyte differentiation as seen by Oil Red-O assay [479].

#### **1.7.6 Role of dipeptidyl peptidase IV inhibitor in fibrosis in non-adipose tissues**

Besides the already described beneficial effects of DPP-IV inhibitors, other protective effects were demonstrated in heart, liver, kidney and pancreas. DPP-IV was found to prevent fibrosis in several organs, including cardiac, hepatic, and kidney fibrosis both *in vitro* and *in vivo* (Table 1.9).



**Table 1.9 – Effects of dipeptidyl peptidase IV inhibitors in fibrosis in the liver, heart and kidney in different animal models.**

Tissue	Animal model	DPP-IV inhibitor treatment	Effect in fibrosis	Refs
Liver	STZ-treated mice fed a HFD	Linagliptin	↓	[521]
	Porcine serum mouse model	Sitagliptin	↓	[522]
Heart	Pressure-overloaded cardiac hypertrophy mouse model	Vildagliptin	↓	[523]
	Type 2 diabetes GK mouse model	Sitagliptin	↓	[524]
	Isoproterenol-infused rat model	Vildagliptin	↓	[525]
	Ischemia-reperfusion injury mouse model	Sitagliptin	↓	[526]
	<i>db/db</i> mouse model	Sitagliptin	↓	[527]
	Western diet-induced obesity mice	MK0626	↓	[528]
	Experimental autoimmune myocarditis mouse model	Linagliptin	↓	[529]
	5/6-nephrectomized mouse model	Linagliptin	↓	[529]
	STZ-treated rats	Sitagliptin	↓	[530]
Kidney	Zucker rats	Sitagliptin	↓	[531]
	STZ-treated mice	Linagliptin	↓	[532]
	STZ-treated rats	Vildagliptin	↓	[533]
	Endothelial nitric oxide synthase knockout mice	Linagliptin	↓	[534]
	Unilateral ureteral obstruction mouse model	Gemigliptin	↓	[535]
	Apolipoprotein knockout mice	Sitagliptin	↓	[536]

↓ : decrease; abbreviations: STZ, Streptozotocin; HFD, High-fat diet.

### **Liver Fibrosis**

Two independent cohort studies showed that circulating DPP-IV activity is positively associated with liver fibrosis severity in populations with diabetes and/or obesity [537]. Another study reported that linagliptin treatment of HFD-fed mice treated with streptozotocin (STZ) decreases liver fibrosis, by lowering collagen deposition and  $\alpha$ -

smooth muscle actin ( $\alpha$ SMA) expression (ECM proteins-synthesizing activated cells marker). In this study, the decrease of liver fibrosis by linagliptin is independent of GLP-1 effects on blood glucose [521]. Moreover, it was also demonstrated that sitagliptin prevents liver fibrosis in a rat model of liver fibrosis, by decreasing TGF $\beta$ 1, TIMP1 and  $\alpha$ SMA-positive cells [522]. Furthermore, *in vitro* studies using activated hepatic stellate cells demonstrated a decrease of TGF $\beta$ 1 and  $\alpha$ 1(I)-procollagen [522]. In both of these studies it was also observed an amelioration of liver inflammation and steatosis [521].

### **Cardiac Fibrosis**

A cardiac hypertrophy mouse model, induced by transverse aortic constriction, shows cardiac fibrosis and vildagliptin improves glucose tolerance and reduces fibrosis [523]. Others showed that sitagliptin reduces cardiac fibrosis in a rat model of type 2 diabetes (GK) [524]. Moreover, an *in vitro* study showed that GLP-1 reduces fibrosis of cardiomyocytes and cardiac fibroblasts [524]. This study also suggests that the cardioprotective effects induced by sitagliptin may occur via GLP-1 activation [524]. An isoproterenol-infused rat model exhibits perivascular fibrosis, cardiac hypertrophy and inflammation that are prevented by the treatment with vildagliptin [525]. Ischemia-reperfusion injury in mice treated with sitagliptin and also mice lacking DPP-IV were also studied. Both sitagliptin-treated mice and DPP-IV lacking mice show reduction of cardiac fibrosis [526]. Treatment with sitagliptin improves myocardial fibrosis and oxidative stress in *db/db* mice, a model of diabetes and obesity [527]. Other study showed that the treatment with the DPP-IV inhibitor, MK0626, also reduces fibrosis in another mouse model of obesity, western diet induced obesity [528]. Moreover, an experimental autoimmune myocarditis model in Balb/c mice treated with linagliptin exhibits suppressed cardiac fibrosis [538]. The mRNA levels of heart tissue fibrosis markers are increased in a rat model of chronic renal failure, 5/6-nephrectomized and are normalized by linagliptin [529]. It was also observed an increase of GLP-1 that is suggested to be involved in linagliptin cardioprotective effects. In Diabetic type 1 rats, sitagliptin reduces cardiac fibrosis but has no effect in plasma glucose, suggesting that this cardioprotective effect is GLP-1-independent [530].

### **Kidney fibrosis**

In Zucker rats, a model of type 2 diabetes mellitus, sitagliptin has anti-fibrotic, anti-inflammatory and anti-apoptotic effect in the kidney [531]. Linagliptin decreases renal fibrosis in STZ-induced type 1 diabetic mice model and vildagliptin has the same effect in a STZ-induced type 1 diabetic rat model [532,533]. Treatment of endothelial nitric oxide synthase knockout mice with linagliptin has an antifibrotic effect in the kidney,

independently of glucose lowering [534], suggesting that this protective effect is GLP-1 independent. A mouse model of renal fibrosis, subjected to unilateral ureteral obstruction, when treated with the DPP-IV inhibitor gemigliptin shows decreased renal fibrosis and inflammation, independent of mechanisms mediated by GLP-1 because GLP-1 and GLP-1 receptors are not altered by DPP-IV inhibitor treatment [535]. Sitagliptin reverts the renal dysfunction and structural damage induced by dyslipidemia in dyslipidemia-related kidney injury in apolipoprotein knockout mice, including renal fibrosis [536].

Taking all these studies into account, it is clear that DPP-IV plays an important role in adipose tissue metabolism and that DPP-IV inhibitors have a beneficial effect in obesity and obesity-associated complications. In Figure 1.18 is represented a schematic overview of the impact of DPP-IV inhibitors in obesity-relevant organs/tissues, including adipose tissue. Moreover, some studies suggested GLP-1 action to be responsible for the metabolic response to DPP-IV inhibition, derived from sympathetic nervous system activation or directly from adipose tissue [509,518], but DPP-IV has many substrates besides GLP-1 that can play a role in DPP-IV inhibitor effects. The underlying mechanisms of these effects are not well known and more studies are required.

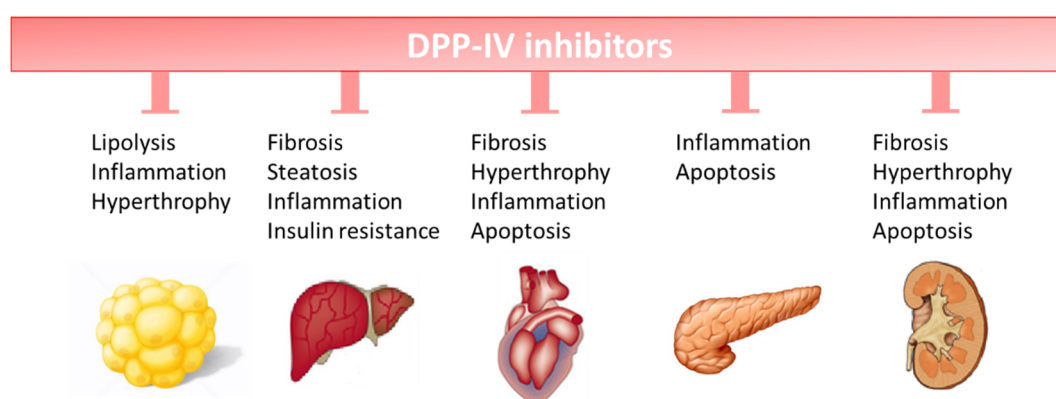


**Figure 1.18 – Schematic overview of protective actions of dipeptidyl peptidase-IV (DPP-IV) inhibitors in obesity-relevant tissues, namely adipose tissue, liver, heart, pancreas and kidney.** Adapted from [220].

## 1.8 Neuropeptide Y

NPY was first isolated from porcine brain and sequenced by Tatamoto and colleagues in 1982 [539]. NPY belongs to NPY family or “PP-fold” family which also includes peptide YY (PYY) and pancreatic polypeptide (PP), with whom shares 70 and 50% homology, respectively [539-541]. NPY is one of the most conserved neuropeptide among species [541]. NPY consists of 36 amino acid residues with a total of five tyrosine residues

including one at its amino and other one at its carboxyl terminal [542] (Figure 1.19). The carboxyl terminal of NPY is responsible for its biological activity, while the amino terminal is involved in receptor affinity. NPY is one of the most abundant and widespread peptides in the central nervous system, mainly in hypothalamus in the brain. NPY is also highly expressed in peripheral nervous system and in peripheral tissues [460,542]. Among other functions, NPY is involved in the regulation of food intake and energy expenditure, control of learning and memory, locomotion, reproduction, thermoregulation and circadian rhythm [462].

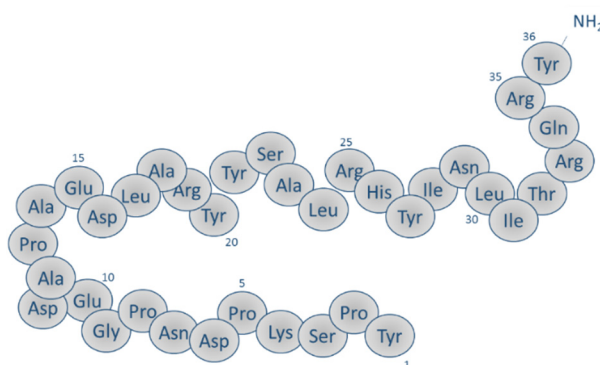


**Figure 1.19 – Structure of neuropeptide Y (NPY).** NPY is composed of 36 amino acid residues, from which five are tyrosine residues (Tyr). Adapted from [541].

Like all polypeptides and proteins, NPY becomes active after the processing of a precursor peptide that is synthesized in ribosomes and transported into the lumen of the endoplasmic reticulum and then to the Golgi complex (Figure 1.20). The precursor peptide of NPY is pre-pro-neuropeptide Y, a 97 amino acid precursor [97]. The 28 amino acids signal peptide of Prepro-NPY is cleaved by signal peptidase enzyme producing pro-NPY. Afterwards, proconverting enzymes, prohormone convertase (PC) 1/3 and/or PC2, process 69 amino acids pro-NPY by cleaving the 30 amino acids peptide called the C-terminal flanking peptide of NPY (CPON). NPY<sub>1-39</sub> is further cleaved by carboxypeptidase like enzyme and amidated by peptidyl-glycine  $\alpha$ -amidating monooxygenase to originate the mature and biological active form NPY<sub>1-36</sub> or simply NPY [543]. Although this peptide is already in its biologically active form it can be further cleaved by aminopeptidase P or DPP-IV to originate NPY<sub>2-36</sub> and NPY<sub>3-36</sub>, respectively. In addition, the NPY<sub>3-36</sub> can be further cleaved into NPY<sub>3-35</sub> by enzyme kallikrein but it does not bind to any of NPY receptors. Because these different peptides have different selectivity to NPY receptors, they also have different functions [540,543].

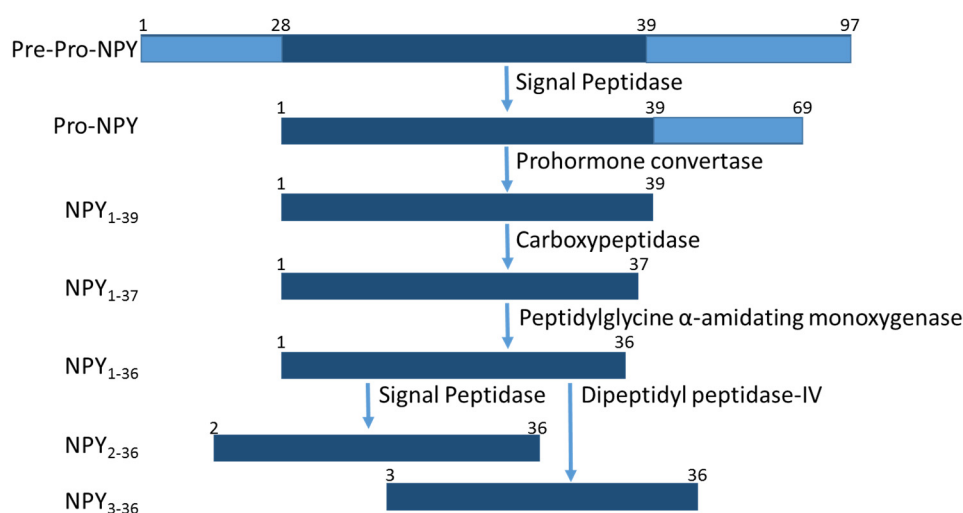


**Figure 1.20 – Scheme of synthesis and processing of neuropeptide Y (NPY).** The steps of the process and enzymes involved are represented. Adapted from [544].

NPY activates G-proteins coupled receptors [542,545]. NPY receptors are Gi/Go coupled receptors that when activated inhibit the action of adenylyl cyclase. Inhibition of adenylyl cyclase leads to decreased cAMP levels, preventing PKA activation. Activation of NPY receptors also increases intracellular calcium levels [546].

All NPY family members, NPY, PP and PYY, bind to the same family of NPY receptors. To date seven different NPY receptors (Y<sub>1</sub>-Y<sub>8</sub>) have been described in vertebrates. Five of these receptors are present in mammals (Y<sub>1</sub>, Y<sub>2</sub>, Y<sub>4</sub>, Y<sub>5</sub> and y<sub>6</sub>) and only Y<sub>1</sub>, Y<sub>2</sub>, Y<sub>4</sub> and Y<sub>5</sub> receptors are functional in all mammals, while the y<sub>6</sub> receptor is non-functional in several mammals. Subtypes Y<sub>1</sub>, Y<sub>2</sub> and Y<sub>5</sub> preferentially bind NPY and PYY, whereas the Y<sub>4</sub> binds preferentially to PP [547,548]. The Y<sub>1</sub> receptor was the first NPY receptor to be cloned [549]. The Y<sub>1</sub> receptor has high affinity to NPY<sub>1-36</sub> and PYY, but its affinity is largely decreased as the N-terminal of the peptide is cleaved by peptidases [550]. Cleaving the C-terminal on the other hand does not affect NPY affinity for this receptor. The Y<sub>2</sub> receptor was first cloned in 1995 [551]. The Y<sub>2</sub> receptor has high affinity for NPY and PYY, but it is resistant to N-terminal deletions in contrast with Y<sub>1</sub> receptor [550]. Y<sub>4</sub> receptor was first cloned in 1995 and binds preferentially PP, while NPY and PYY have lower affinity [552,553]. The cloning of Y<sub>5</sub> receptor was first described in 1996 [554]. Like Y<sub>1</sub> and Y<sub>2</sub> receptors, Y<sub>5</sub> receptor has higher affinity for NPY and PYY than for PP. Similarly to Y<sub>2</sub> receptor, it maintains its high affinity for both N-terminal truncated NPY and PYY, such as NPY<sub>3-36</sub> and PYY<sub>3-36</sub> [554] (Figure 1.21).

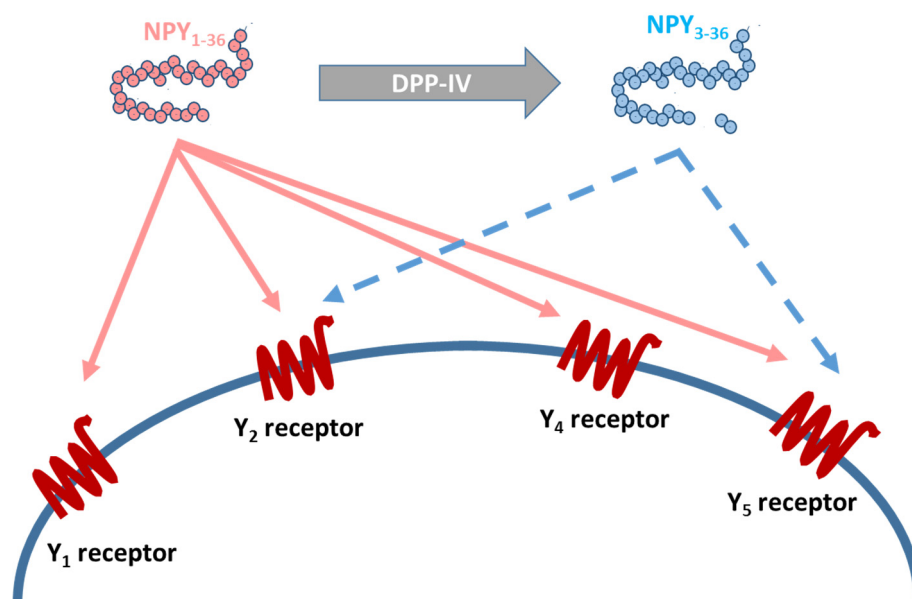


**Figure 1.21 – NPY<sub>1-36</sub> and NPY<sub>3-36</sub> affinity for NPY receptors: Y<sub>1</sub>, Y<sub>2</sub>, Y<sub>4</sub>, and Y<sub>5</sub> receptors.** Abbreviations: NPY, Neuropeptide Y; DPP-IV, Dipeptidyl Peptidase IV. Adapted from [489].

### 1.8.1 Neuropeptide Y in adipose tissue

NPY regulates adipose tissue functions through NPY released from nerve endings but also through local synthesis of NPY in adipose tissue. Different studies provided evidence that NPY is secreted by adipocytes isolated from human and mouse abdominal subcutaneous fat. NPY and some of its receptors are synthesized in human [555], pig [556] and mouse [461] adipose tissue and also in 3T3-L1 preadipocyte cell line [461,557]. NPY levels are increased in visceral WAT in an early-life programmed rat model of increased visceral adiposity [461]. Moreover, NPY is increased in visceral adipose tissue in obese Zucker rats [461].

Several studies investigated the effect of NPY in adipose tissue in different models. Local intra-fat injections of NPY in mice and monkeys stimulate adipose tissues weight and volume by 50%, demonstrating that NPY can promote *de novo* adipose tissue formation [558]. Moreover, NPY improves long-term human fat graft survival and vascularity in the athymic mice, which was shown to occur through increased cell survival and not through increased adipose tissue formation [558].

Furthermore, some studies also evaluated the involvement of different NPY receptors in NPY effects in adipose tissue. Conditional knockdown of Y<sub>2</sub> receptor in peripheral tissues (including WAT) results in protection against diet-induced obesity, reduced weight gain and adiposity and amelioration in glucose tolerance [559]. Genetically obese B6.V-Lepob/J mice show upregulated plasma NPY levels and upregulated NPY and Y<sub>2</sub> receptor expression in subcutaneous abdominal fat, compared with control C57BL/6J

mice. Moreover, the weight and volume of adipose tissue in both obese and lean mice are increased with subcutaneous abdominal fat-delivered NPY treatment. The NPY-induced adipose tissue weight and volume are prevented with injections with an Y<sub>2</sub> receptor antagonist (BIIE0246). The Y<sub>2</sub> receptor antagonist also decreases vascularity and increases apoptosis in the abdominal fat pads [466]. Mice treated with local administration of Y<sub>2</sub> receptor antagonist in WAT, germline Y<sub>2</sub> knockout mice, and also mice with conditional Y<sub>2</sub> knockdown in WAT show reduced stress-induced abdominal fat [466]. The results of this study suggest that the increase of adipogenesis and angiogenesis occur through Y<sub>2</sub> receptor activation [466]. In mice, stress activates Y<sub>2</sub> receptor in a glucocorticoid-dependent manner in abdominal fat, adipogenesis and angiogenesis, leading to obesity and metabolic syndrome, that is prevented by intra-fat inactivation of Y<sub>2</sub> receptor [560].

Furthermore, some *in vitro* studies evaluated NPY effect in proliferation and differentiation of adipocytes and the receptor involved. NPY treatment induces proliferation of 3T3-L1 preadipocytes, and this effect is prevented by Y<sub>2</sub> receptor antagonist [466,561] and also by Y<sub>5</sub> receptor antagonist [561]. NPY was also observed to stimulate preadipocyte proliferation but this effect occurred through Y<sub>1</sub> receptor [461]. All these *in vitro* studies observed that NPY stimulates preadipocyte proliferation but the NPY receptor involved is still controversial. Regarding the effect of NPY in adipocyte differentiation, no alterations were observed in lipid accumulation and PPAR $\gamma$  in NPY-treated 3T3-L1 preadipocytes [461]. In contrast, NPY mimics the effects of insulin by increasing lipid accumulation that is prevented with Y<sub>2</sub> receptor antagonist [466]. Moreover, other study showed that NPY stimulates lipid accumulation and PPAR $\gamma$ 2 through Y<sub>2</sub> and Y<sub>5</sub> receptors [561].

Several studies reported an inhibitory effect of NPY on lipolysis [468,469,562-567]. However, in one study it was reported that NPY has no effect on lipolysis in non-stimulated conditions but increases  $\beta$ -adrenergic-induced stimulation of lipolysis [568]. The inhibitory effect of NPY on lipolysis were shown to occur mainly through Y<sub>1</sub> receptor [569] or through both Y<sub>1</sub> and Y<sub>2</sub> receptors activation [555].

All together, these studies show that NPY has hyperplastic, adipogenic and antilipolytic effects in adipose tissue. These effects were described to occur mainly through Y<sub>1</sub> and/or Y<sub>2</sub> receptors but Y<sub>5</sub> receptors have also been implicated in these processes.





## **CHAPTER 2**

---

### **Objectives**



## 2. Main objectives

Obesity is characterized by an excessive increase of WAT. During the development of obesity, adipocytes become hypertrophic, which leads to a reduction of oxygenation causing local hypoxia in WAT [264,265,277,283]. Hypoxia has a high impact in WAT homeostasis, contributing to adipose tissue dysfunction in obesity.

Oxygen is critical for energy homeostasis and cell differentiation. In addition, hypoxia regulates adipocyte differentiation, inhibiting PPAR $\gamma$ 2 expression [298,570]. However, the effect of hypoxia on lipid accumulation in adipocytes is controversial and its impact on adipocyte physiology is not fully understood.

Besides the development of hypoxia, other adipose tissue dysfunctions occur as a consequence of hypertrophy of adipocytes in obesity. The increase of adipocyte size leads to increased deposition of ECM components, causing fibrosis formation in adipose tissue in obesity [326]. Alterations of specific components of ECM were described to have a high impact in adipose tissue metabolism [263]. Another study reported that fibrosis in subcutaneous WAT is negatively associated with fat mass loss after bariatric surgery [352].

DPP-IV inhibitors are used as oral drugs for the treatment of type 2 diabetes mellitus. Besides the effect of DPP-IV inhibitors on glucose control, these drugs also exhibit other protective effects in other non-adipose tissues, namely in preventing fibrosis in several organs, such as heart, liver and kidney, both *in vitro* and *in vivo* [522,528,532].

Taking this into account, our work focused in two main objectives:

- 1 – To investigate the role of hypoxia in adipogenesis and adipocyte function using 3T3-L1 preadipocytes as an *in vitro* model.
- 2 – To evaluate the impact of vildagliptin, a DPP-IV inhibitor, on fibrosis formation in adipose tissue of HFD-induced obese mice and to investigate the possible underlying mechanisms using 3T3-L1 preadipocytes.



## **CHAPTER 3**

---

**Hypoxia mimetic induces lipid accumulation through mitochondrial dysfunction and stimulates autophagy in murine preadipocyte cell line**



### **3.1 Abstract**

Hypoxia occurs within adipose tissue of obese human and mice. However, its role in adipose tissue regulation is still controversial. The aim of the present work is to study the role of hypoxia in adipocyte function by evaluating lipid accumulation, PPAR $\gamma$ 2 expression, microRNAs, mitochondrial changes and autophagy in murine preadipocytes (3T3-L1 cell line).

Our results show that the hypoxia mimetic cobalt chloride (CoCl<sub>2</sub>, 100  $\mu$ M) increases lipid accumulation with no expression of PPAR $\gamma$ 2. Furthermore, using quantitative real-time PCR (qPCR) we observed that the hypoxia mimetic increases microRNAs miR-27a and miR-27b, which are known to block PPAR $\gamma$ 2 expression. In contrast, the hypoxia mimetic cobalt chloride induces mitochondrial dysfunction, and increases production of ROS and autophagy. Moreover, an antioxidant agent, glutathione, prevents lipid accumulation induced by hypoxia mimetic indicating that ROS are responsible for lipid accumulation induced by hypoxia in these cells.

All these results taken together suggest that hypoxia mimetic blocks differentiation, induces autophagy and increases lipid accumulation through mitochondrial dysfunction and ROS accumulation.

### 3.2 Introduction

Obesity is characterized by an excessive increase of WAT, which is associated with an oxygenation reduction of the adipose tissue in mice and humans [264,265,277,283]. Adipocytes become hypertrophic during the development of obesity, becoming larger than the diffusion distance limit of oxygen [275,571]. Therefore, oxygen is not able to reach the cells causing local hypoxia in expanding adipocytes. Cellular response to hypoxia is manifested by the activation of HIF-1, a heterodimeric transcription factor that is considered a molecular oxygen sensor [287]. HIF-1 mediates the cellular response to hypoxia, regulating several target genes that encode for proteins involved in angiogenesis, cell proliferation, apoptosis and energy metabolism [572]. It is clear that hypoxia is an important condition that regulates WAT homeostasis, being a major contributor for adipose tissue dysfunction in obesity.

The formation of adipose tissue is dependent on preadipocyte differentiation to adipocytes, which are mature cells specialized in lipid accumulation. This differentiation process is called adipogenesis and it is driven by the coordinated expression of various transcription factors, such as the PPAR $\gamma$ 2 [57]. Given the importance of oxygen levels for energy homeostasis and cell differentiation, hypoxic condition regulates adipocyte differentiation [298,570]. The effect of hypoxic status on lipid accumulation is controversial, since there are conflicting reports, which describe hypoxia as both increasing and decreasing cytoplasmic lipid accumulation [298,303,304,573]. It has been demonstrated that hypoxia inhibits adipogenesis through decreasing PPAR $\gamma$ 2 expression [298,570]. In addition, HIF-1 $\alpha$  suppresses FA  $\beta$ -oxidation and this mechanism is responsible for adipose tissue expansion attenuation [574]. Furthermore, most of the studies about the role of hypoxia on adipocytes describe its effect either on lipid accumulation or on PPAR $\gamma$  expression. However, hypoxia may also lead to changes in other intracellular pathways, in particular mitochondrial dysfunction, production of ROS, and also the formation of microRNAs, which can modify differentiation and lipid accumulation within adipocytes. In fact, it has been reported that microRNAs modulate adipocyte differentiation [117,130]. The miR-143 induces preadipocytes 3T3-L1 differentiation and the miR-130 is involved in the blockage of PPAR $\gamma$  expression [117,130,575]. In addition, miR-27a and miR-27b levels are higher in adipose tissue of obese *ob/ob* mice than in lean animals [122]. However, it was also described that miR-27a is down-regulated in mature adipocytes of HFD-fed obese mice comparing to normal chow diet-fed lean mice [121]. Although there are some works about the effect of miRs on adipocyte differentiation, the effect of hypoxia on miRs regulation in adipose tissue is not well known.



Autophagy is known to be necessary to normal adipocyte differentiation [176]. Moreover, it is known that hypoxia can induce autophagy in other non-adipose cells [576,577] but few works report the effect of autophagy in adipose tissue [176]. Using either the 3T3-L1 cell line or MEFs, it was shown that normal adipogenesis is associated with increased autophagic activity [174,176], but autophagy is increased in the adipose tissue of obese individuals [177].

The aim of this work is to evaluate the role of hypoxia mimetic, cobalt chloride, on the normal physiology of adipocytes, by determining lipid accumulation, PPAR $\gamma$ 2 expression, miRNA expression, mitochondrial changes and autophagy. We hypothesized that lipid accumulation in adipocytes, induced by hypoxia mimetic, is due to mitochondrial dysfunction and autophagy increase.

### **3.3 Materials and Methods**

#### **3.3.1 Cell culture**

3T3-L1, a murine preadipocyte cell line (American type Culture Collection – LGC Promochem) was plated in 22.1 cm<sup>2</sup> flasks and were maintained in Dulbecco's Modified Eagle Medium with high glucose (4.5 g/L D-glucose) (DMEM-HG; Sigma) with phenol red, supplemented with 10% (vol/vol) heat-inactivated fetal bovine serum, 100 U/mL penicillin, 100 µg/mL streptomycin, 2.5 mM L-glutamine and 1.5 g/L NaHCO<sub>3</sub> at 37 °C and 5% CO<sub>2</sub>/air.

#### **3.3.2 Cell Differentiation protocol**

Preadipocytes were plated in 24-well plates (25000 cells/well) until they reached confluence (day 0). After 2 days, the medium was removed and replaced by DMEM-HG supplemented with a cell differentiation cocktail: 3-isobutyl-1-methylxanthine (IBMX, 0.5 mM) and dexamethasone (0.25 µM) (day 2) (Sigma). After 3 days (day 5), the culture medium was changed to DMEM-HG without the differentiation cocktail. Every 2 days, the medium was renewed until day 9.

#### **3.3.3 Experimental Conditions**

For the positive control it was used insulin (1 µg/mL) (Sigma). To evaluate the effect of hypoxia mimetic on adipogenesis, 3T3-L1 preadipocytes were treated with CoCl<sub>2</sub> (100 µM) or deferoxamine mesylate (DFO) (100 µM) (Sigma), hypoxia mimetic agents. Our group has also previously demonstrated, by immunofluorescence against HIF-1 $\alpha$  (Abcam), that cells treated with CoCl<sub>2</sub> 100 µM or DFO express HIF-1 $\alpha$  in the nucleus, and thereby confirming that those CoCl<sub>2</sub> and DFO can act as hypoxia mimetic agents. Mitochondrial complex I inhibitor, rotenone (1 µM) or glutathione (GSH) (50 µM) (Sigma) were added to the medium (without insulin) to evaluate their effect on adipocyte differentiation.

#### **3.3.4 Lipid accumulation quantification by Oil red-O staining**

Seven days after induction of preadipocyte differentiation, cells were washed twice with phosphate buffered saline (PBS) and fixed with p-formaldehyde (4% in PBS) for 30 minutes at room temperature. Cells were then washed twice with PBS, once with distilled water, and stained with Oil Red-O dye (6:4, 0.6% Oil red-O dye in water) (Sigma) for one hour before being washed three times with water. Finally, Oil red-O staining was dissolved in 200 µL of isopropanol, and the absorbance measured at 500 nm.

### **3.3.5 Oil Red-O fluorescent staining**

Prior to the permeabilization step of immunofluorescence protocol, cells were washed twice with PBS and fixed with p-formaldehyde (4% in PBS) for 30 minutes at room temperature. Cells were then washed twice with PBS and stained with Oil Red-O dye (6:4, 0.6% Oil red-O dye in water) for one hour before being washed three times with PBS.

### **3.3.6 Immunofluorescence**

Following fixation with p-formaldehyde (4% in PBS) and permeabilization with Triton-X100 (1% in PBS), nonspecific binding was blocked with 3% bovine serum albumin (BSA) and 0.2% Tween20 in PBS. Cells were incubated overnight at 4 °C with the following primary antibodies, anti-PPAR $\gamma$  (1:500) (Santa Cruz Biotechnology), anti-perilipin A (1:100) (Cell Signalling) or anti-Pref-1 (1:500) (Abcam). After rinsing with PBS, the cells were incubated with the appropriate secondary antibody (Molecular Probes, Invitrogen) for 1 hour (1:200), at room temperature. All antibodies were prepared in blocking solution (PBS containing 3% of BSA). Nuclei were labeled with Hoechst 33342 (1  $\mu$ g/ml) (Molecular Probes, Invitrogen) for 3 minutes, after incubation with the secondary antibody and coverslips were mounted on glass slides. Cells were visualized using the laser scanning microscope LSM 510 META (Zeiss, Jena, Germany).

### **3.3.7 Mitotracker and Mitosox**

For direct labeling of mitochondria, cells were stained with 500 nM MitoTracker Red CMXRos (Molecular Probes, Invitrogen) for 30 minutes, and fixed with p-formaldehyde (4% in PBS). Alternatively, for detection of superoxide in the mitochondria of live cells, cells were stained with 5  $\mu$ M MitoSOX (Molecular Probes, Invitrogen) for 10 minutes at 37 °C. Cells were counterstained with Hoechst 33342 (1  $\mu$ g/ml) for 3 minutes. Coverslips were mounted on glass slides, the cells were visualized using a fluorescence microscope (Carl Zeiss Axio Observer Z1) and the images were acquired with the Carl Zeiss Zen software or in a laser scanning microscope LSM 510 META (Zeiss, Jena, Germany).

### **3.3.8 Western blotting**

Cells were rinsed twice with ice-cold PBS and then lysed with RIPA buffer (50 mM Tris-HCl pH 8, 150 mM NaCl, 1% Triton X-100, 0.5% sodium deoxycholate, 0.1% sodium dodecylsulphate (SDS)) containing 100  $\mu$ M phenylmethylsulfonyl fluoride (PMSF), 1 mM

dithiothreitol (DTT), 1 µg/mL quimostatin, 1 µg/mL leupeptin, 1 µg/mL antiparin, 5 µg/mL pepstatin A and 1 mM ortovanadate, pH 7.4. Lysates were centrifuged at 12,000 x g, for 15 minutes at 4 °C. Protein concentration was determined by the Bradford assay (Biorad). The same amount of protein were separated by electrophoresis in the presence of SDS-polyacrylamide gel electrophoresis (SDS-PAGE). Following electrophoresis, proteins were transferred electrophoretically to polyvinylidene fluoride (PVDF) membranes for 90 minutes at 750 mA. The membranes were blocked with 5% (m/vol) non-fat milk in Tris-buffered saline (TBS-T; 137 mM NaCl, 20 mM Tris·HCl, pH 7.6) containing 0.1% Tween 20 for 60 minutes at room temperature. Membranes were incubated overnight at 4 °C with the primary antibody. The primary antibodies were used as follows: rabbit anti-PPAR $\gamma$  (1:500), anti-perilipin (1:500), anti-Pref-1 (1:1,000), anti-LC3B (1:1000) (Cell Signalling) or anti-p62 (1:1000) (Cell Signalling) in 1% (m/v) of non-fat milk in TBS-T. After washing for 30 minutes in TBS-T, membranes were incubated with an alkaline phosphatase-conjugated anti-rabbit or anti-mouse antibody (1:20000) diluted in a solution of 1% (m/v) of non-fat milk in TBS-T, for 30 minutes at room temperature. Membranes were washed with TBS-T for 30 minutes and immunoreactive bands were detected by chemifluorescence with enhanced chemifluorescence (ECF) substrate (GE Healthcare) in a VersaDoc Imaging System (Bio-Rad). To control for protein loading, membranes were probed with anti- $\beta$ -actin antibody (1:10000). Band intensity was quantified by Quantity One (Biorad).

### 3.3.9 Quantitative real-time PCR for PPAR $\gamma$ 2

Total RNA was isolated according to the manufacturer's instructions using commercially available kit (Macherey-Nagel). Total RNA amount was quantified by optical density (OD) measurements using a ND-1000 Nanodrop Spectrophotometer (Thermo Scientific), and the purity was evaluated by measuring the ratio of OD at 260 and 280 nm. Complementary DNA (cDNA) was then obtained by conversion of total RNA with iScript Selected cDNA Synthesis kit (Bio-Rad) according to manufacturer's instructions. cDNA was stored at -20 °C. qPCR was performed in the StepOnePlus Real-Time PCR thermocycler (Applied Biosystems, Life Technologies Corporation, USA) using 96-well microtiter plates and SsoAdvanced SYBR Green Supermix (Bio-Rad). Primers for mouse PPAR $\gamma$ 2 and  $\beta$ -actin were designed using PrimerBlast Software. Primers for PPAR $\gamma$ 2 (forward/reverse): 5'GCCTATGAGCACTTCACAAGAAAT3' and 5'GGAATGCGAGTGGTCTTCCA3'. Primers for  $\beta$ -actin (forward/reverse): 5'CAGCAAGCAGGAGTA3' and 5'GGTGTAAAACGCAG 3'. Appropriate negative controls were also prepared. All reactions were performed in duplicate and according to

the manufacturer's recommendations: 95 °C for 30 sec, followed by 45 cycles at 95 °C for 5 sec and 60 °C for 30 sec. The amplification rate for each target was evaluated from the cycle threshold (Ct) numbers obtained with cDNA dilutions, with correction for  $\beta$ -actin levels. The mRNA fold increase or fold decrease with respect to control samples was determined by the Pfäffl method.

### **3.3.10 Lactate measurements**

Lactate was measured in cell supernatants using a Lactate Colorimetric Assay Kit (Abcam), according to the manufacturer's protocol. Data were normalized in terms of protein concentration determined by the Bradford assay (Biorad).

### **3.3.11 Determination of ATP content**

Cells were disrupted with lysis buffer on ice. Extracts were centrifuged at 13000 x g for 10 minutes at 4 °C and supernatants were collected. ATP was measured using the ATP Bioluminescence assay kit CLS II (Roche Diagnostics GmbH, 1699 695, Mannheim, Germany), according to the manufacturer's protocol. Light emission was recorded for 30 seconds by a photon counting luminometer. Relative ATP levels were normalized in terms of protein concentration determined by the Bradford assay (Biorad).

### **3.3.12 Reactive oxygen species measurements**

Cells were washed twice with PBS, and incubated with a cell-permeant indicator for ROS (5  $\mu$ M H<sub>2</sub>DCFDA, Invitrogen) in PBS for 30 minutes at 37 °C. The fluorescent signal was read at excitation of 492 nm and emission of 517 nm in a microplate reader. ROS levels were normalized in terms of protein concentration determined by the Bradford assay (Biorad).

### **3.3.13 Quantitative real-time PCR for miRNA 27a and 27b analysis**

Total RNA was isolated using the miRCURY RNA Isolation Kit - Cell & Plant content (Exiqon, Vedbaek, Denmark) according to the manufacturer's instructions. Total RNA amount was quantified by OD measurements using a ND-1000 Nanodrop Spectrophotometer (Thermo Scientific), and the purity was evaluated by measuring the ratio of OD at 260 and 280 nm. After RNA quantification, cDNA conversion for miRNA quantification was performed using the Universal cDNA Synthesis Kit (Exiqon, Vedbaek, Denmark). For each sample, cDNA for miRNA detection was produced from 20 ng total RNA according to the following protocol: 60 minutes at 42 °C followed by heat-

inactivation of the reverse transcriptase for 5 minutes at 95 °C. The cDNA was diluted 80 times with the nuclease free water before quantification by qPCR. The primers were mmu-miR-27a (target sequence): UUCACAGUGGUAAGUCCGC and mmu-miR-27b (target sequence): UUCACAGUGGCUAAGUUCUGC.

qPCR was performed in an iQ5 thermocycler (Bio-Rad, CA, USA) using 96-well microtitre plates. For miRNA quantification the miRCURY LNA Universal RT microRNA PCR system (Exiqon, Vedbaek, Denmark) was used in combination with pre-designed microRNA LNA PCR primers (Exiqon, Vedbaek, Denmark) for miR-27a, miR-27b and miR-103 (reference gene) according to the manufacturer's recommendations. Briefly, for each reaction, 10 µL of SYBR Green master mix and 2 µL of PCR primer mix were added to 8 µL of diluted cDNA template. All reactions were performed in duplicate at a final volume of 20 µL per well, using the iQ5 Optical System Software (Bio-Rad, CA, USA). The reaction conditions consisted of polymerase activation/denaturation and well factor determination at 95 °C for 10 minutes, followed by 40 amplification cycles at 95 °C for 10 seconds and 65 °C for 1 minute (ramp-rate 1.6 °C/s). A melting curve protocol was started immediately after amplification and consisted of 1 minute heating at 55 °C followed by 80 steps of 10 seconds, with a 5 °C increase at each step. Threshold values for Ct determination were generated automatically by the iQ5 Optical system software (Bio-Rad, CA, USA). The amplification efficiency for each primer pair and the threshold values for Ct determination were determined automatically by the iQ5 Optical System Software (Bio-Rad). Relative mRNA quantification was performed according to Pfäffl method.

#### **3.3.14 Statistical analysis**

Results are expressed as mean ± standard error of the mean (SEM). Data were analyzed using one-way analysis of variance (ANOVA), or t-test, as indicated in figure legends. A value of  $p < 0.05$  was considered significant. Prism 6.0 (GraphPad Software, San Diego, CA) was used for all statistical analysis.

### **3.4 Results**

#### **3.4.1 Hypoxia mimetic agent CoCl<sub>2</sub> induces lipid accumulation without PPAR $\gamma$ 2 expression**

Adaptation to low oxygen is mediated by the transcription factor HIF-1 $\alpha$  [287]. Hypoxia stabilizes HIF-1 $\alpha$ , which induces the expression of several genes [287,572]. Hypoxia (1% O<sub>2</sub>), CoCl<sub>2</sub> and DFO can stabilize HIF-1 $\alpha$  through inhibition of HIF-1 $\alpha$  hydroxylation by prolyl and arginyl hydroxylases [293,294]. Therefore, CoCl<sub>2</sub> and DFO are widely used as hypoxia mimetics [293,294]. We used both CoCl<sub>2</sub> and DFO, as hypoxia mimetics, to evaluate the impact of hypoxia in adipocyte differentiation. As expected, we observed that both CoCl<sub>2</sub> and DFO increase HIF-1 $\alpha$  immunoreactivity in the nucleus of 3T3-L1 preadipocytes (data not shown). The effect of hypoxia mimetic in adipocyte differentiation was evaluated by measuring PPAR $\gamma$ , a transcription factor critical in the differentiation process, and also lipid accumulation, characteristic of mature adipocytes. CoCl<sub>2</sub> decreases PPAR $\gamma$  mRNA levels by  $88.6 \pm 7.3\%$ , compared to control (Figure 3.1A). By Western blotting, we observed that the adipogenic marker PPAR $\gamma$ 2 is present in adipocytes incubated with insulin but it is not detected when preadipocytes are submitted to hypoxic mimetic conditions (Figure 3.1B). As expected, insulin (1  $\mu$ g/mL)-treated preadipocytes differentiate into adipocytes as showed by the two well-known adipogenic markers: increase of cytoplasmic lipid droplets coupled with PPAR $\gamma$  staining in the nuclei (Figure 3.1C). Hypoxic mimetic conditions (CoCl<sub>2</sub>) increases cytoplasmic lipid droplet accumulation but no nuclear PPAR $\gamma$  staining is observed (Figure 3.1C). Moreover, these lipid droplets are smaller, more numerous, and have a diffuse pattern compared to lipid droplets in adipocytes under control conditions (Figure 3.1D). Lipid accumulation was measured by Oil red-O staining and hypoxia increases lipid accumulation by  $63.2 \pm 10.5\%$ , compared to control (Figure 3.1E).

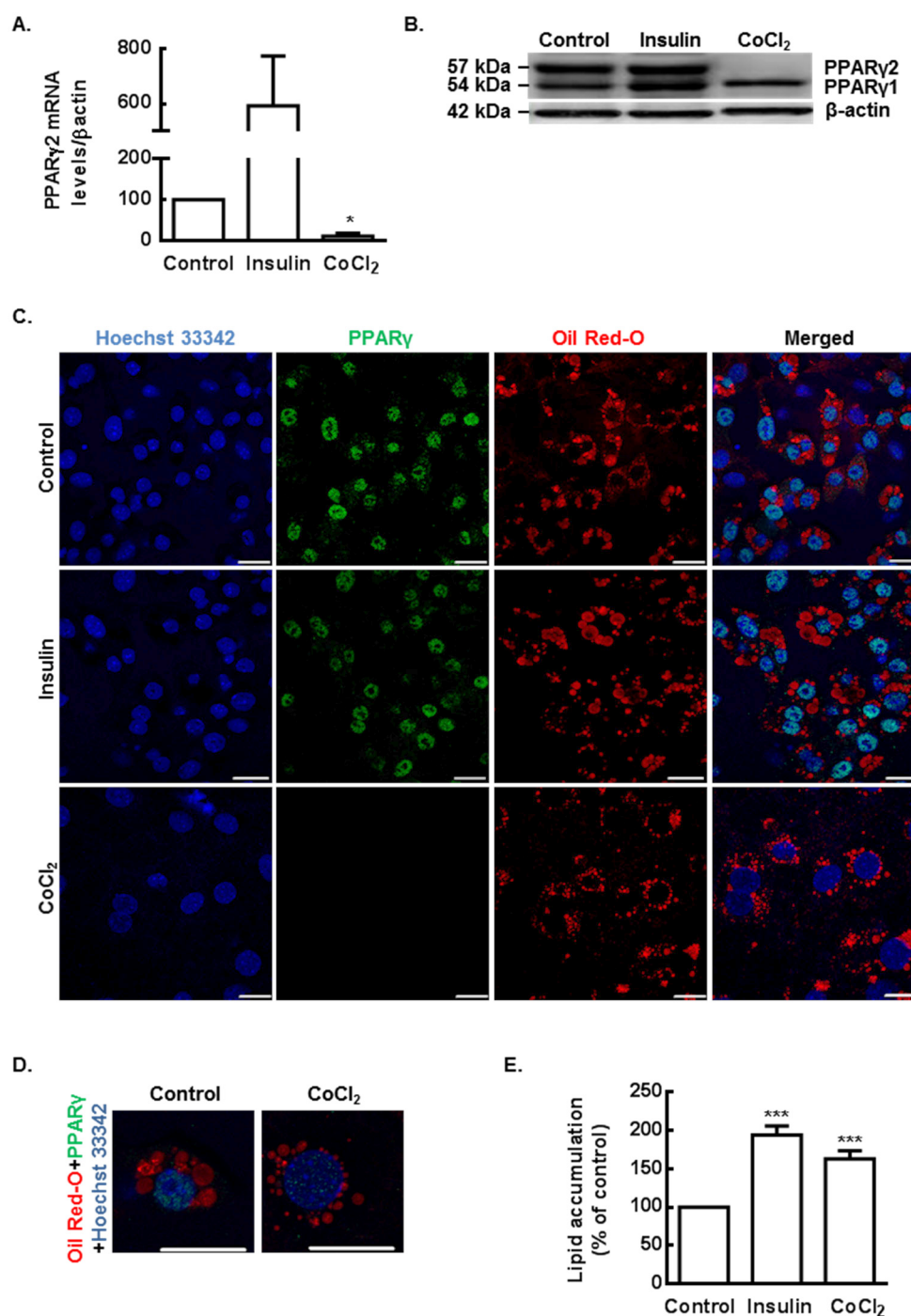


**Figure 3.1 – Hypoxia mimetic inhibits PPAR $\gamma$ 2 expression but induces lipid accumulation.** 3T3-L1 preadipocytes were induced to differentiate and were treated with insulin (1  $\mu$ g/mL) or cobalt chloride (100  $\mu$ M) for seven days. (A) qPCR to determine the expression of PPAR $\gamma$ 2 mRNA. n =3 \*p<0.05 compared to control. One-way ANOVA was used as statistical test. (B) Representative image of western blotting for PPAR $\gamma$  and  $\beta$ -actin (loading control). (C and D) Representative images of immunofluorescence for PPAR $\gamma$  (green) performed after Oil red-O that stains the lipid droplets (red). Nuclei were stained with Hoechst 33342 (blue). Scale bar: 20  $\mu$ m. (E) Oil red-O staining to quantify lipid accumulation. n =9 \*\*\*p < 0.001, significantly different from control group. One-way ANOVA was used as statistical test.



*Hypoxia mimetic induces lipid accumulation through mitochondrial dysfunction and stimulates autophagy in murine preadipocyte cell line*

Because hypoxia mimetic induces lipid accumulation without differentiation we investigated perilipin expression, which is an adipocyte-specific protein that coats lipid droplets. Adipocytes differentiated with insulin (1  $\mu\text{g}/\text{mL}$ ) show an increase in perilipin expression, while in hypoxic mimetic conditions perilipin is not detected (Figure 3.2A and B). Since lipid droplets are present in these adipocytes with no PPAR $\gamma$  or perilipin expression, we decided to evaluate whether preadipocytes under hypoxia mimetic condition are arrested in the preadipocyte state. To address that, we evaluated the expression of the preadipocyte marker Pref-1 [92]. As expected, we observed, by western blotting and immunofluorescence, that insulin decreases Pref-1 immunoreactivity (Figure 3.2C and D). Hypoxia mimetic conditions also inhibit Pref-1 expression (Figure 3.2C and 2D), suggesting that hypoxia mimetic does not arrest preadipocytes in an undifferentiated state.

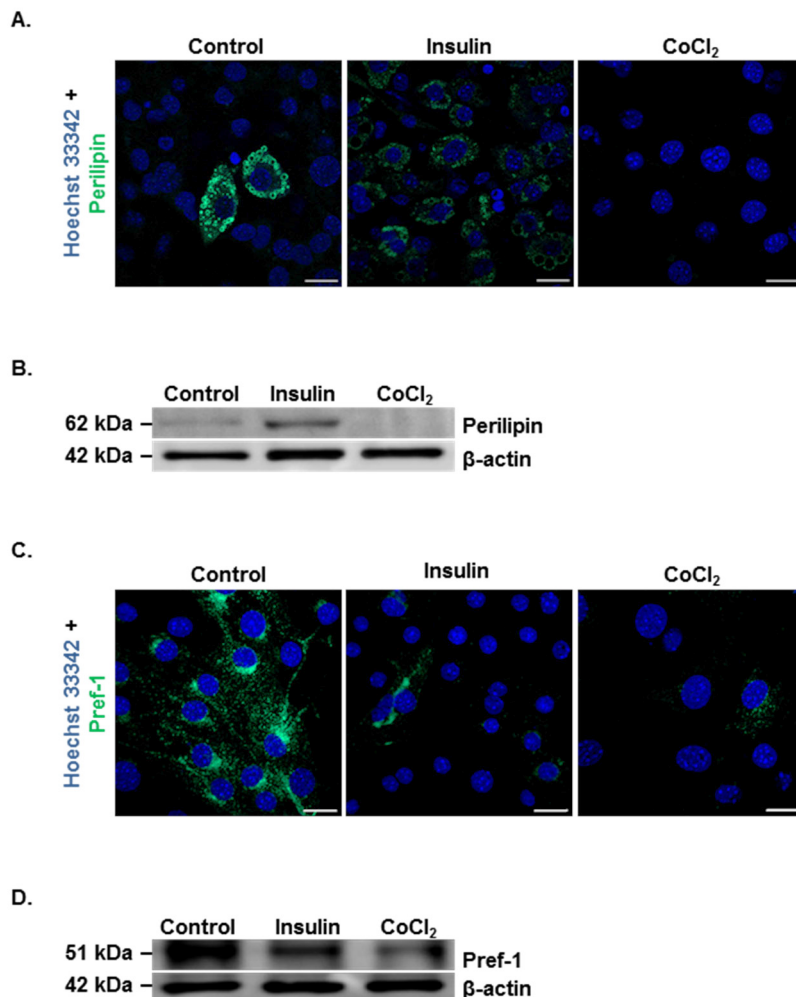


**Figure 3.2 – Hypoxia mimetic inhibits perilipin and Pref-1 protein levels.** 3T3-L1 preadipocytes were induced to differentiate and were treated with insulin (1  $\mu\text{g}/\text{ml}$ ) or cobalt chloride (100  $\mu\text{M}$ ) for seven days. (A and C) Representative images of immunofluorescence for (A) perilipin (green) or (C) Pref-1 (green). Nuclei were stained with Hoechst 33342 (blue). Scale bar: 20  $\mu\text{m}$ . (B and D) Representative image of western blotting for (B) perilipin or (D) Pref-1 and  $\beta$ -actin (loading control).

### 3.4.2 Adipocyte differentiation is blocked by miR-27a and miR-27b induction

It has been reported that miR-27a and miR-27b are downregulated during adipogenesis and that their overexpression impairs adipocyte differentiation by inhibiting PPAR $\gamma$  expression [121-123]. We hypothesized that hypoxia mimetic inhibits adipocyte differentiation by miR-27a and miR-27b increase, which in turn inhibits PPAR $\gamma$ 2 expression. To test whether inhibition of PPAR $\gamma$ 2 expression by the hypoxia mimetic CoCl $_2$  is modulated by miR-27a and miR-27b expression, we measured the levels of miR-27a and miR-27b under hypoxic mimetic conditions. As shown in Figure 3, both microRNAs are increased when cells are under hypoxic mimetic conditions (CoCl $_2$ : 341.7  $\pm$  32.2 and 446.0  $\pm$  55.8% of control, respectively; Figure 3.3). These results show that hypoxia increases miR-27a and miR-27b, which probably will impair adipocyte differentiation.

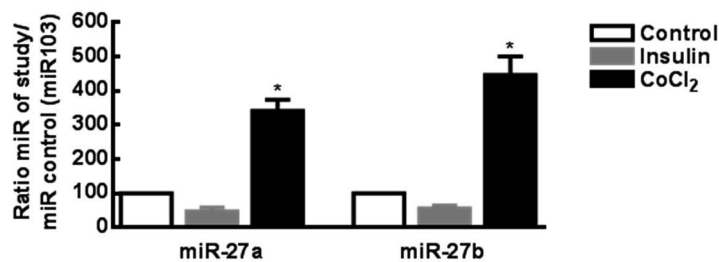


**Figure 3.3 – Hypoxia mimetic increases mir-27a and mir-27b expression.** 3T3-L1 preadipocytes were induced to differentiate and were treated with insulin (1  $\mu$ g/ml) or cobalt chloride (100  $\mu$ M) for seven days. Real-time PCR for miR-27a and miR-27b was performed. The control miR was considered the miR103. Results are expressed as the ratio miR-27a/miR103 or miR-27b/miR103 levels. n=3 \*p<0.05 compared to control. One-way ANOVA was used as statistical test.

### 3.4.3. Mitochondrial dysfunction and reactive oxygen species are responsible for lipid accumulation induced by hypoxia mimetic

Hypoxia may induce other cellular dysfunctions in preadipocytes, such as mitochondrial dysfunction [578]. In agreement, we observed that hypoxic mimetic condition decreases the number of normal and energized mitochondria and induces a disrupted mitochondrial network with fewer interconnections (Figure 3.4A). We also observed that hypoxic mimetic condition increases lactate production by 40.7  $\pm$  5.3% (Figure 3.4C), decreases the cellular ATP content by 66.5  $\pm$  4.0% (Figure 3.4D) and also increases the production of ROS by 110.2  $\pm$  7.9%, compared to control (Figure 3.4E).

*Hypoxia mimetic induces lipid accumulation through mitochondrial dysfunction and stimulates autophagy in murine preadipocyte cell line*

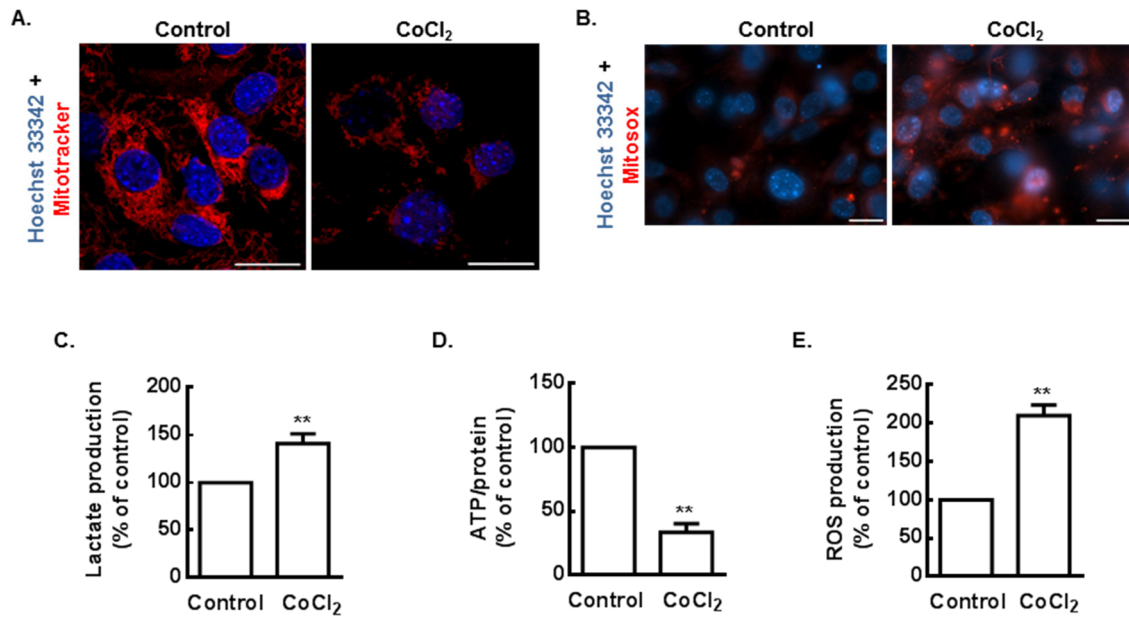


**Figure 3.4 – Hypoxia mimetic induces mitochondrial dysfunction.** 3T3-L1 preadipocytes were induced to differentiate and were treated with cobalt chloride (100  $\mu$ M) for seven days. (A) Mitochondrial network was evaluated by using MitoTracker Red CMXRos stained (red). (B) Mitochondrial superoxide production was evaluated by using MitoSOX Red (red). Hoechst 33342 labels the nuclei (blue). A representative image is showed in this figure. Scale bar: 20  $\mu$ m (C) The lactate production was quantified. (D) Intracellular ATP was evaluated. (E) The release of reactive oxygen species (ROS) to the medium was evaluated. Values were normalized by amount of protein. n=3-4 \*\*p<0.01 compared to control. t-test was used as statistical test.

To establish a link between mitochondrial dysfunction and adipogenesis, cells were treated with an inhibitor of mitochondrial complex I, rotenone (1  $\mu$ M). As also seen in hypoxic mimetic conditions, rotenone increases lipid accumulation by  $48.4 \pm 7.2\%$ , compared to control, without the adipocyte differentiation markers, PPAR $\gamma$ 2 and perilipin (Figure 3.5). Taken together, these results suggest that mitochondrial inhibition caused by hypoxia mimetic condition is contributing to lipid accumulation increase.

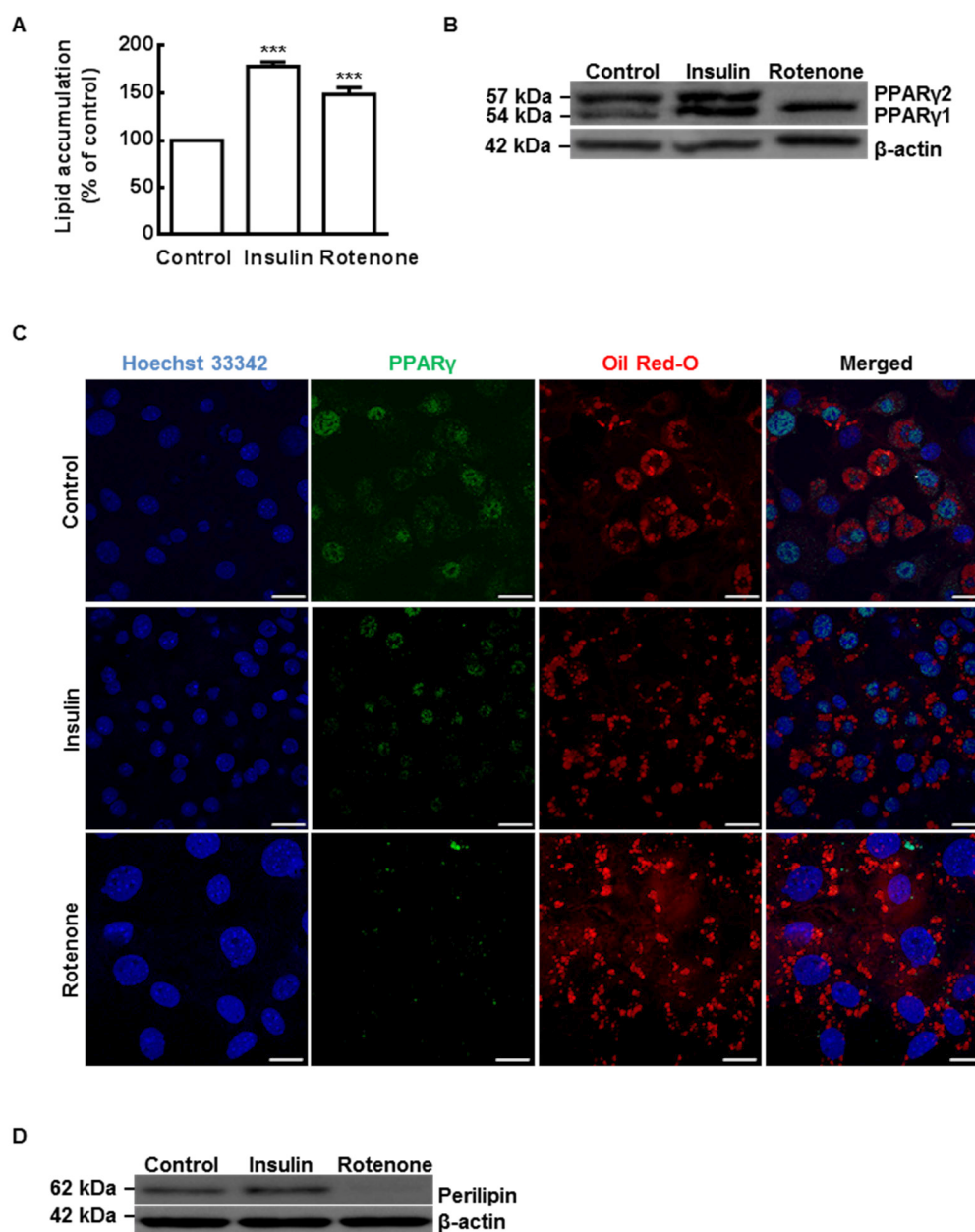


**Figure 3.5 – Mitochondrial dysfunction is involved on lipid accumulation and PPAR $\gamma$  inhibition induced by hypoxia mimetic.** 3T3-L1 preadipocytes were induced to differentiate and were treated with insulin (1  $\mu$ g/ml) or rotenone (1  $\mu$ M) for seven days. (A) Oil red-O staining to quantify lipid accumulation.  $n = 8$  \*\*\* $p < 0.001$ , significantly different from control group. One-way ANOVA was used as statistical test. (B) Representative image of western blotting for PPAR $\gamma$  and  $\beta$ -actin (loading control). (C) Representative images of immunofluorescence for PPAR $\gamma$  (green) performed after Oil red-O that stains the lipid droplets (red). Nuclei were stained with Hoechst 33342 (blue). Scale bar: 20  $\mu$ m (D) Representative image of western blotting for perilipin and  $\beta$ -actin (loading control).

In order to investigate whether ROS production was due to mitochondrial dysfunction, we evaluated the production of superoxide by mitochondria using MitoSOX Red. MitoSOX Red selectively targets mitochondria, being oxidized by superoxide but not by other ROS and reactive nitrogen species. We observed that  $\text{CoCl}_2$  increases superoxide

production by mitochondria when compared to control (Figure 3.4B). This provides direct evidence that CoCl<sub>2</sub>-induced ROS production is derived from mitochondria. To further study the contribution of ROS to lipid accumulation induced by hypoxia mimetic, we treated cells with CoCl<sub>2</sub> in the presence or absence of glutathione which is an antioxidant, reducing ROS availability. We observed that glutathione prevents 37.8 ± 3.2% lipid accumulation induced by CoCl<sub>2</sub> (Figure 3.6). This result suggests that ROS production is responsible for lipid accumulation induced by hypoxia mimetic.

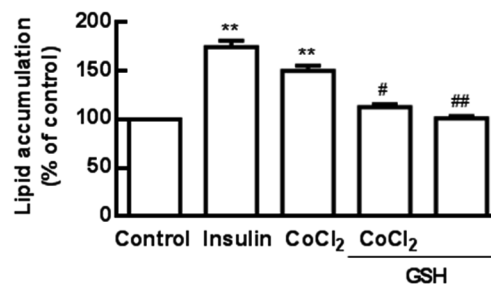


**Figure 3.6 – Reactive oxygen species are responsible for hypoxia-induced lipid accumulation that occurs in 3T3-L1 preadipocytes.** 3T3-L1 preadipocytes were induced to differentiate and were treated with cobalt chloride (100 μM) in the presence or absence of glutathione (50 μM) for seven days. (A) Oil red-O staining to quantify lipid accumulation. n =4 \*\*p < 0.01, significantly different from control group; #p < 0.05, ##p<0.01, significantly different from CoCl<sub>2</sub>. One-way ANOVA was used as statistical test.

#### **3.4.4 Hypoxia mimetic induces autophagy**

Autophagy is a physiological protective mechanism that is also described to occur as a consequence of cell stress. Autophagy can be induced in response to a hypoxic condition [576,577]. Moreover, ROS was also shown to mediate autophagy induction [579]. To investigate whether hypoxia regulates autophagy in 3T3-L1 preadipocyte cell line, we measured the protein levels of the transient autophagosomal membrane-bound form of LC3B (LC3B-II) and p62, widely used as markers for monitoring the autophagic process [173]. Hypoxia mimetic (CoCl<sub>2</sub>) decreases LC3B-II levels by 65.7 ± 10.2% (Figure 3.7A) and also decreases p62 levels by 49.8 ± 6.0% (Figure 3.7B), when compared to control. These results suggest an increase of autophagic clearance in this hypoxia mimetic condition.

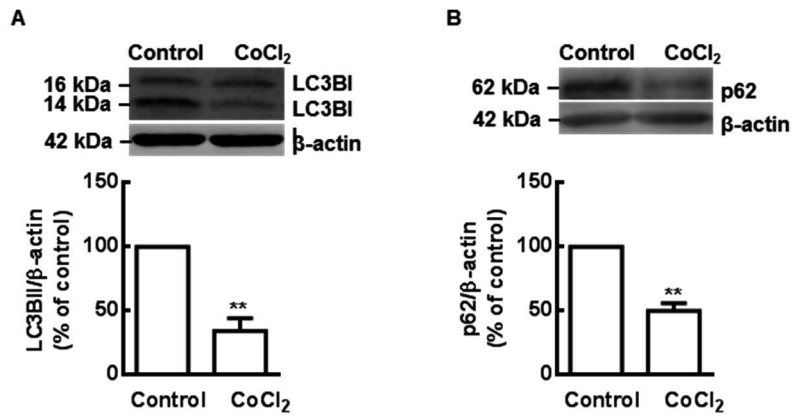


**Figure 3.7 – Hypoxia mimetic-treatment induces autophagy.** 3T3-L1 preadipocytes were induced to differentiate and were treated with cobalt chloride (100 μM) for seven days. Whole-cell extracts were assayed for (A) LC3B or (B) p62 and β-actin (loading control) immunoreactivity by Western blotting. n=4-6 \*\*p<0.01 compared to control. t-test was used as statistical test.

### **3.5 Discussion**

The present work shows that the hypoxia mimetic, CoCl<sub>2</sub> (100 μM) induces lipid accumulation without expression of PPARγ2, perilipin or the preadipocyte marker, Pref-1. In addition, the absence of PPARγ2 expression can be related to an increase of microRNAs miR-27a and miR-27b that was described to inhibit PPARγ2. Since we observed that CoCl<sub>2</sub> induces mitochondrial dysfunction and increased ROS production, we suggest that the lipid droplets induced by hypoxia mimetic condition could be a consequence of the mitochondrial dysfunction and, consequently, lead to inhibition or dysfunction of adipocyte differentiation and can be prevented by an antioxidant agent, glutathione. Furthermore, hypoxia and ROS have been reported as inducers of autophagy [576,577,579]. We observed that hypoxia mimetic is also responsible for autophagy induction in these cells.

Most works that studied the effect of hypoxia on adipocyte differentiation described the effect of hypoxia in PPARγ expression [573] or in lipid accumulation [573], and use very different hypoxic treatment durations. Our results are in agreement with other works that have shown PPARγ2 expression inhibition by hypoxia or hypoxia mimetics, suggesting that hypoxia inhibits adipocyte differentiation [285,298,303,304,570,580]. However, other studies showed that hypoxia or hypoxic mimetic also inhibits lipid accumulation [298,304,570]. Our results are in agreement with a study that shows that CoCl<sub>2</sub> induces cytoplasmic lipid accumulation in 3T3-L1 preadipocytes [573]. Increased lipid accumulation was also described in bone marrow stromal cells under hypoxic conditions [581]. Another group showed similar results in human bone marrow stromal cells, hMSC-TERT [303], where hypoxia induces an atypical nature of lipid accumulation with no change in marker genes characteristic of mature adipocytes, such as PPARγ2 [303]. The authors suggest that adipogenesis may occur through PPARγ2-dependent and -independent pathways [303]. Moreover, it was described that adipocyte-derived exosomes from hypoxic conditions, which contain lipogenic enzymes, promote lipid accumulation in non-stressed, normoxic cells [582].

Moreover, we hypothesized that the inhibition of PPARγ2 in hypoxic mimetic conditions most probably occurs due to an increase of specific miRNAs. In fact, it has been previously described that some miRNAs regulate adipogenesis: the mir-143 induces differentiation of murine 3T3-L1 and human preadipocytes [117,575], while miR-27 and miR-130 families inhibit this process [121-123,130]. In addition, miR-27a overexpression in 3T3-L1 preadipocytes suppresses PPARγ expression and adipocyte differentiation [121,122]. Another family member, miR-27b, is down-regulated during adipocyte differentiation, and binds to the 3'UTR of PPARγ while repressing PPARγ2 protein levels

[123]. miR-27 was also shown to have a role in repressing adipogenic lineage commitment in C3H10T1/2 cells [583]. Interestingly, in mature adipocytes from obese mice lower miR-27a expression was found, compared to mature adipocytes of lean mice, indicating that down-regulation of miR-27a is necessary for adipocyte hypertrophy [121]. On the other hand, it was also described that expression levels of both miR-27a and miR-27b are significantly increased in the adipose tissue of *ob/ob* mice, as compared with the genetically matched lean mice [122]. In addition, it has also been reported that hypoxia induces a 2-fold and 1.5-fold increase of miR-27a and miR-27b levels, respectively [122]. These results suggest that miR-27 functions by inhibiting PPAR $\gamma$  expression and, consequently, preventing adipocytes from entering into the stage of differentiation [122]. From these observations, we evaluated the effect of the hypoxia mimetic CoCl<sub>2</sub> on miR-27a and miR-27b expression and observed that the expression of these microRNAs miR-27a and miR-27b increase and may consequently inhibit PPAR $\gamma$ 2 expression. These results may explain the fact that preadipocytes treated with CoCl<sub>2</sub> have an increase in cytoplasmic lipid droplet accumulation without increasing PPAR $\gamma$ 2. We have further investigated other mechanisms that could explain the lipid droplet accumulation induced by hypoxia mimetic condition. Since some studies have already showed that alterations in mitochondrial function lead to an increase in lipid accumulation [584,585], we studied the putative role of mitochondrial changes on lipid droplet accumulation induced by hypoxia mimetic. In fact, as with CoCl<sub>2</sub>, we also observed that, rotenone, an inhibitor of mitochondrial electron transport of complex I, increases lipid droplet accumulation in adipocyte cytoplasm without nuclear PPAR $\gamma$ 2 expression. Furthermore, we also observed that the antioxidant glutathione prevents the lipid accumulation induced by CoCl<sub>2</sub>. Mitochondrial dysfunction induced by hypoxia mimetic is also strongly supported by the decrease in mitochondrial network, increase in lactate release in the medium, decrease in ATP production and increased ROS production induced by CoCl<sub>2</sub>. One of the initial steps in the response of cells to hypoxia is adaptation at the mitochondrial level by reducing the amount of the high O<sub>2</sub>-consuming process of oxidative phosphorylation [571]. As a consequence, there is a switch to anaerobic glycolysis for energy production [571]. A decrease in ATP production and increase in lactate production then occur [571]. The increase of ROS was described to modulate adipocyte differentiation [586,587]. The high levels of ROS in adipocytes have already been shown in adipocytes isolated from obese mice [588,589], and also during the differentiation of 3T3-L1 preadipocytes into adipocytes [587]. Others have also shown that mitochondrial dysfunction in adipocytes leads to increased TAG storage [584,585]. Moreover, the glutathione prevention of hypoxia-induced lipid accumulation is in agreement with a study in other cell model, in which the inhibition of mitochondrial



oxidative damage induces lipid- $\beta$ -oxidation recovery accompanied by a decrease on FA incorporation into triglycerides [590].

Autophagy constitutes an important protective mechanism that allows cells to eliminate damaged components to maintain nutrient and energy homeostasis. Moreover, several forms of stress can also activate autophagy. Hypoxia has been described as a stimulus for the induction of autophagy in other cell types [576,577]. Autophagy has also been described to occur as a consequence of ROS production [579]. Taking this into account we investigated the effect of hypoxia and consequent ROS production in adipocytes. In the present study, increased autophagic activity was detected in adipocytes under hypoxia mimetic treatment. To the best of our knowledge, this is the first study to report the effects of hypoxia on autophagy induction in adipocytes. The role of autophagy on adipocytes development and function were studied by others [175,176]. During adipocyte differentiation of 3T3-L1 cell line or primary MEFs, others observed increased autophagy [176]. Moreover, MEFs derived from Atg5 and Atg7 knockout mice exhibit drastically reduced adipogenesis efficiency [175,176]. The knockdown of Atg5 and Atg7 in 3T3-L1 preadipocytes also decreases the markers of adipocyte differentiation, which was confirmed by studies with pharmacological inhibitors, 3-methyladenine and chloroquine [174]. Newborn Atg5 knockout mice have less subcutaneous adipocytes than wild-type, suggesting that autophagy is important for adipose tissue development [176]. The importance of autophagy in adipogenesis *in vivo* was confirmed in adipocyte-specific Atg7 knockout mice [174,175]. These mutant mice are leaner, have decreased WAT mass and have adipocytes with features characteristic of brown adipocytes, smaller, containing multilocular lipid droplets, increased number of mitochondria and increased cytoplasmic volume [174,175]. Furthermore, in obesity, human adipose tissue and adipocytes show increased autophagy [177]. Functional consequence of increased autophagy in adipose tissue of obese people is not known. Taking these results together, the present study both extends our understanding of the effect of hypoxia on adipocyte biology and lipid metabolism, providing a possible explanation for hypoxic lipogenesis. It highlights the importance of preadipocyte response to hypoxia, mitochondrial dysfunction and ROS leading to autophagy and also to lipid accumulation, which might impair adipocyte metabolism and also compromise their normal function, which can be partially reversed by antioxidant treatment. These conclusions need to be further studied for its *in vivo* implications and to validate the results with hypoxic conditions (<1% O<sub>2</sub>).



## **CHAPTER 4**

---

**DPP-IV inhibition prevents fibrosis in  
adipose tissue of obese mice**



#### **4.1 Abstract**

Expansion of WAT in obesity promotes adipose tissue ECM changes, leading to fibrosis. The ECM alterations have high impact on WAT physiology and may change obesity progression and response to diet regimen or therapeutical approaches. Since DPP-IV inhibitors prevent fibrosis in other tissues, such as heart, liver and kidney, the objective of this study was to assess whether vildagliptin, a DPP-IV inhibitor, has beneficial effects in preventing fibrosis in adipose tissue in a mouse model of obesity. The mechanisms underlying fibrosis inhibition by vildagliptin were studied using an *in vitro* model of adipose tissue fibrosis: 3T3-L1 cell line of mouse adipocytes treated with TGF $\beta$ 1.

In HFD-fed mice, vildagliptin reduces blood glucose, and serum triglycerides, total cholesterol and leptin and has no effect on serum insulin, body weight, adipose tissue weight, and adipocyte diameter. Moreover, vildagliptin prevents fibrosis in adipose tissue of HFD mice. In the *in vitro* study, vildagliptin prevents ECM deposition, through NPY and NPY Y<sub>1</sub> receptor activation.

Taken together, these results suggest that vildagliptin prevents fibrosis formation in adipose tissue in obese mice, at least partially through NPY and NPY Y<sub>1</sub> receptor activation. Moreover, the decrease in adipose tissue fibrosis by vildagliptin may improve adipose tissue expandability in the treatment of obesity and associate diseases.

## 4.2 Introduction

Obesity is one of the most common health problems in developed countries and is characterized by an increase of WAT volume. WAT expansion prevents the ectopic lipid accumulation [591]. The ability of WAT expansion is dependent of ECM. Moreover, ECM remodeling is a crucial event to the main WAT biological functions , such as adipogenesis and also for maintenance of tissue architecture [325]. However, in obesity it occurs excessive ECM deposition in adipose tissue, leading to fibrosis [326]. Fibrosis is characterized by deposition of ECM components, mainly collagens, which lead ultimately to organ dysfunction [323]. Several profibrotic factors have been implicated in the development of fibrosis but the most important and potent profibrotic factor is TGF $\beta$ 1 [323]. TGF $\beta$ 1 is an important player in fibrosis development and the decrease of this factor prevents fibrosis [323].

Furthermore, it was also described that subcutaneous WAT fibrosis decreases fat mass loss induced by surgery [352]. Moreover, it was demonstrated that collagen VI-null *ob/ob* mice show ameliorations in glucose and lipid metabolism [263]. Alterations in ECM may have high impact in adipose tissue metabolism [329].

DPP-IV is a multifunctional enzyme, which is involved in cell cycle regulation [592], cell differentiation [593], adhesion [395], immunomodulation [594] and apoptosis [595]. DPP-IV is expressed ubiquitously, including in visceral, epididymal [468] and omental adipose tissue [476]. DPP-IV is a so-called “moonlighting protein” as it functions as a serine protease, a receptor, a costimulatory protein, and as an adhesion molecule for collagen and fibronectin [393]. DPP-IV cleaves peptides at the N-terminal region after X-proline or X-alanine, such as substance P, chemokines, NPY, PYY, GLP-1, GLP-2 and GIP [392,489]. DPP-IV inhibitors mainly act to activate insulin secretion, inhibit glucagon secretion, improve  $\beta$ -cell mass, and to lower glucose [596]. For this reason, several DPP-IV inhibitors are used as oral drugs for the treatment of type 2 diabetes mellitus [596]. Besides DPP-IV inhibitors action in lowering glucose, they have also been shown to have a protective role in other non-adipose tissues [597,598]. DPP-IV inhibitors were demonstrated to have a protective effect in preventing fibrosis in several organs, such as heart, liver and kidney, both *in vitro* and *in vivo* [522,528,532]. DPP-IV inhibitor sitagliptin reduces local inflammation in adipose tissue of obese mice [510]. Vildagliptin inhibits adipogenesis in 3T3-L1 preadipocyte cell line [467]. However, DPP-IV inhibitors were demonstrated to be weight neutral in humans [599]. The role of DPP-IV and its inhibition is not known in the pathogenesis of fibrosis in adipose tissue in obesity. The DPP-IV inhibitors as inhibitors of fibrosis in other tissues led us to hypothesize that it also happens in adipose tissue. Thus, the aim of this study was to clarify the role of DPP-IV

*DPP-IV inhibition prevents fibrosis in adipose tissue of obese mice.*

inhibition in adipose tissue fibrosis in a mouse model of diet-induced obesity and using also a 3T3-L1 preadipocyte cell line.

## **4.3 Materials and Methods**

### **4.3.1 *In vivo* experiments**

All experimental procedures were performed in accordance with the European Union Directive 86/609/EEC for the care and use of laboratory animals. In addition, animals were housed in a licensed animal facility (international Animal Welfare Assurance number 520.000.000.2006) and the CNC animal experimentation board approved the utilization of animals for this project. Moreover, people coordinating the animals studies have received appropriate education (FELASA course) as required by the Portuguese authorities.

### **4.3.2 Animals**

8-weeks old adult male C57BL/6 mice were purchased from Charles River Laboratories and randomly divided into four groups. Mice were housed under a 12h light/dark cycle in a temperature/humidity controlled room with *ad libitum* access to water and food. Mice were divided into four groups and treated for seven weeks: two groups were maintained in normal chow diet (8% fat), one group with and the other without vildagliptin treatment (30 mg/kg/day in water). The animals of the other two groups were maintained in a high fat diet (LabDiet - Western diet for rodents) with 40% fat, also one group with and the other without vildagliptin treatment (30 mg/kg/day in water). Body weight, water and food consumption were measured twice a week for a total of 7 weeks.

### **4.3.3 Intraperitoneal Glucose Tolerance Test**

Intraperitoneal glucose tolerance test (ipGTT) was performed at the sixth week of HFD. The test was performed after an overnight fast (12h). The next morning mice were weighted and glycemia levels were measured using the FreeStyle Precision Neo glucometer (Abbot) (Time 0). Glucose administration was performed via injection (2.0 g/kg, using a 20% glucose solution in saline 0.9% NaCl) into the peritoneal cavity. Glycemia levels were measured at 15, 30, 60, 90 and 120 minutes after glucose administration.

### **4.3.4 Tissue collection**

At week 7, mice were sacrificed with a lethal dose of halothane (2-bromo-2-chloro-1, 1, 1-trifluoroethane) followed by decapitation. Liver and WAT (epididymal fat pad) were collected. The WAT was weighted and, afterwards, samples were collected, immediately



frozen in dry ice and kept at  $-80^{\circ}\text{C}$ . Blood was collected; the serum was separated by centrifugation (2000 g, 15 minutes) and stored at  $-20^{\circ}\text{C}$ .

#### **4.3.5 Serum Triglycerides and Cholesterol determination**

Serum triglyceride and cholesterol levels were quantified using the automatic biochemical analyzer Integra 800 (Roche).

#### **4.3.6 Serum leptin and insulin quantification**

Serum levels were measured for leptin and insulin with commercially available ELISA kits from EMD Millipore. All ELISA-based measurements were performed according to manufacturers' instructions.

#### **4.3.7 Tissue preparation for histological processing**

Mice were sacrificed with an overdose of avertin (2.5 times of  $14\ \mu\text{l/g}$ ,  $250\ \text{mg/kg}$ , intraperitoneally). Transcardial perfusion with phosphate solution and fixation with 4% paraformaldehyde were performed. The epididymal adipose tissue and liver were collected and postfixed in 4% paraformaldehyde and cryoprotected by incubation in 25% sucrose/phosphate buffer. After that, dry tissues were embedded in paraffin, and subsequently cut into  $3\ \mu\text{m}$ -thick sections in a microtome.

#### **4.3.8 Hematoxylin and eosin staining**

For histological analysis of paraffin sections, epididymal adipose tissue and liver were stained with hematoxylin and eosin (HE). Slides were kept for 30 min at  $68^{\circ}\text{C}$  to melt the paraffin. After 2 baths in xylene for 3 and 2 minutes, slides were transferred to a glass coplin jar containing 100% ethanol for 4 minutes and 95% for 2 minutes and rinsed 2 times with distilled water for 30 seconds. Slides were stained in hematoxylin Gill III for 5 minutes and bathed 2 times in distilled water for 2 and 1 minutes. After that, slides were stained with eosin for 1 minute and dehydrated with a fast rinse in  $\text{H}_2\text{O}$ , 95% and 100% of ethanol in  $\text{H}_2\text{O}$ . Glass slides were then mounted.

#### **4.3.9 Adipocyte diameter quantification**

Epididymal adipose tissue sections were stained with HE. The tissue was visualized using a fluorescence microscope (Axioskop 2 Plus, Zeiss, Jena, Germany) and the images were acquired with Axiovision software (release 4.7). Axiovision software was

used to measure adipocyte diameter, which is represented as the average adipocyte diameter (in  $\mu\text{m}$ ). Adipocyte diameter was measured from four groups of mice (>100 cells/group).

#### 4.3.10 Hydroxyproline quantification

Hydroxyproline measurement was done using a modified protocol that was described elsewhere [600]. Briefly, 20 mg of frozen fat or 3T3-L1 cells were heated in 6 N HCl at 110°C overnight in sealed tubes. The samples were then heated at 110°C until dried. Each sample was incubated with chloramine-T (Sigma Aldrich) at room temperature for exactly 20 min and then with p-dimethylaminobenzaldehyde (Fisher Scientific) at 60°C for 15 min. The absorbance was read at 540 nm and the concentration was determined by the standard curve created with cis-4-hydroxy-L-proline (Sigma-Aldrich).

#### 4.3.11 Viral Vectors Production

Lentiviral vectors encoding for a negative short hairpin RNA (LV-PGK-EGFP-H1-shRNA control) and a short hairpin RNA targeting DPP-IV (LV-PGK-EGFP-H1-shRNA DPP-IV) were produced in HEK293T cell line with a four-plasmid system, as previously described [601]. Lentiviral particles were suspended in sterile 1% BSA in PBS. Concentrated viral stocks were stored at -80 °C, until use.

#### 4.3.12 Engineering of short hairpin RNA

A negative short hairpin RNA (shRNA) (control) and shRNA targeting mouse DPP-IV were created. For each one, a pair of oligomers was designed. The sequences of each pair of oligomers used were: shRNA control (top 5' GATCCCCCAACAAGATAAGAGCACCAATTC AAGAGATTGGTGCTCTTCATCTTGTT G3TTTTTA 3' / bot 5' AGCTTAAAAACAACAAGATGAAGAGCACCAATCTCTTGAATT GGTGCTCTTCATCTTGTTGGGG 3') and shRNA DPP-IV (top 5' GATCCCCATAAGATCATCAGCGACAAAGTTCAAGAGACTTTGTCGCTGATGATCTTA TTTTTTA 3' / bot 5' AGCTTAAAAAATAAGATCATCAGCGACAAAGTCTCTTGAAC TTTGTCGCTGATGATCTTATGGG 3'). Each pair of oligomers were annealed and inserted in linearized (with BgIII and HindIII restriction enzymes) pENTR/pSUPER<sup>+</sup> (AddGene 575-1). The H1-shRNA cassette was then transferred, with LR clonase recombination system, into SIN-cPPT-PGK-EGFP-WHV-LTR gateway vector.

#### **4.3.13 Cell culture of 3T3-L1 preadipocyte cell line**

3T3-L1 preadipocytes were obtained from the American type Culture Collection, through LGC Promochem. Cells were maintained in Dulbeccos Modified Eagles Medium with phenol red and supplemented with 2.5 mM L-glutamine, 4.5 g/L glucose, 1.5 g/L NaHCO<sub>3</sub>, 10% heat-inactivated fetal bovine serum (45 °C, 30 min), 100 U/mL penicillin, 100 U/mL streptomycin, and 0.25 µg/mL amphotericin B, at 37 °C with humidified atmosphere containing 5% CO<sub>2</sub>. At 80% confluence, cells were split by 1:10 using trypsin solution (37°C, 5 min) and subcultured in 22.1 cm<sup>2</sup> polystyrene culture plates.

For infected cells: Cells were plated in a six-well plate and 24 hours later were infected with lentiviral vectors encoding for negative shRNA control (LV-PGK- EGFP-H1-shcontrol) or for shRNA targeting DPP-IV (LV-PGK- EGFP-H1-shDPP-IV) with infectious media. At 2 weeks post-infection, cells were plated and induced to differentiate.

#### **4.3.14 Preadipocyte differentiation**

Preadipocytes were plated in 24-well plates (25000 cells/well) until they reached confluence (day 0). After 2 days, the medium was removed and replaced by DMEM-HG supplemented with a differentiation cocktail: IBMX (0.5 mM) and dexamethasone (0.25 µM) (day 2). After 3 days (day 5), the differentiation cocktail was removed and the culture medium changed to DMEM-HG. Every 2 days, the medium was renewed until day 9. The control conditions are cells that were incubated at day 2 with DMEM-HG, together with IBMX (0.5 mM) and dexamethasone (0.25 µM); after that, the cells were incubated every two days with DMEM-HG without any drug. To evaluate the effect of a fibrotic inducer, 3T3-L1 preadipocytes were treated with TGFβ1 (2.5 µg/ml), vildagliptin (2 nM), NPY (100 nM), NPY Y<sub>1</sub> receptor agonist (Leu31Pro34NPY, 100 nM), NPY Y<sub>2</sub> receptor agonist (NPY13-36, 100 nM) or the NPY Y<sub>5</sub> receptor agonist (NPY19-23(Gly1, Ser3, Gln4, Thr6, Ala31, Aib32, Gln34)PP, 100 nM) and NPY neutralizing antibody (6 µg/ml).

#### **4.3.15 Immunofluorescence**

Following fixation and permeabilization, nonspecific binding was blocked with 3% BSA. Cells were incubated with the following primary antibodies, anti-αSMA (1:500), anti-Fibronectin (1:1000) or anti-collagen VI (1:500) overnight, at 4°C. After rinsing with PBS, the cells were incubated with the appropriate secondary antibodies for 1 hour (1:200, anti-rabbit or anti-mouse IgGs conjugated with Alexa Fluor 488 or Alexa Fluor 594), at room temperature. All antibodies were prepared in blocking solution (PBS containing 3%

of BSA). Nuclei were labeled with Hoechst 33342 (1 µg/ml) for 3 minutes, after incubation with the secondary antibodies. Coverslips were mounted on glass slides, the cells were visualized using a fluorescence microscope (Carl Zeiss Axio Observer Z1) and the images were acquired with Carl Zeiss Zen software. Fluorescence was quantified using FIJI (Fiji is Just ImageJ) software (National Institutes of Health) and averaged per image. Five images were analyzed for each condition, and data are representative of at least three independent experiments.

#### **4.3.16 Protein quantification and sample preparation**

Cells were rinsed twice with ice-cold PBS and then lysed with RIPA buffer (50 mM Tris-HCl, pH 7.4; 150 mM NaCl; 5 mM EDTA; 1% Triton X-100; 0.5% deoxycholate; 0.1% SDS; 200 µM PMSF; 1 mM DTT, 1 mM Na<sub>3</sub>VO<sub>4</sub>; 10 mM NaF), supplemented with mini protease inhibitor cocktail tablet (Roche, Germany). Lysates were centrifuged at 12000 x g, for 15 minutes at 4 °C. Protein concentration was determined by the Bradford assay (Biorad) and denatured with the SDS buffer (0.5 M Tris, 30% glycerol, 10% SDS, 0.6 M DTT, 0.012% bromophenol blue). After heating for 5 min at 95 °C, the samples were frozen at -20 °C until use.

Adipose tissue was sonicated at 4°C in RIPA buffer (50 mM Tris-HCl, pH 7.4; 150 mM NaCl; 5 mM EDTA; 1% Triton X-100; 0.5% deoxycholate; 0.1% SDS; 200 µM PMSF; 1 mM DTT, 1 mM Na<sub>3</sub>VO<sub>4</sub>; 10 mM NaF), supplemented with mini protease inhibitor cocktail tablet (Roche, Germany). Lysates were centrifuged at 1000 x g, for 5 minutes at 10°C and the supernatant collected and centrifuged at 3300 x g, for 5 minutes at 4 °C. Protein concentration was determined by the Bradford assay (Biorad) and denatured with the SDS buffer (0.5 M Tris, 30% glycerol, 10% SDS, 0.6 M DTT, 0.012% bromophenol blue). After heating for 5 min at 95°C, the samples were frozen at -20 °C until use.

#### **4.3.17 Western blotting**

Samples were separated in a 4–10% SDS-PAGE followed by electrophoretic transfer onto PVDF membranes. The membranes were blocked with 5% non-fat milk in TBS-T (137 mM NaCl, 20 mM Tris, 0.1% Tween 20, pH 7.6) and incubated overnight at 4°C with a rabbit polyclonal anti-αSMA (1:500), anti-fibronectin (1:1000), anti-β-actin antibody (1:10000) or anti-β-tubulin antibody (1:10000) diluted in blocking solution. After three washes with TBS-T, the membranes were incubated for 1 h, at room temperature, with an alkaline phosphatase-linked secondary antibody, specific to rabbit or mouse

immunoglobulin G (1:20000, Amersham Biosciences, GE Healthcare, UK). Immunoreactive bands were visualized using ECF substrate in the Versa-Doc 3000 imaging system (Bio-Rad, USA). Densitometry of the bands was quantified using Quantity One Software (Bio-Rad, USA).

#### **4.3.18 Statistical analysis**

Results are expressed as mean SEM. Data were analyzed using one-way ANOVA or two-way ANOVA, as indicated in figure legends. A value of  $p < 0.05$  was considered significant. Prism 6.0 (GraphPad Software) was used for all statistical analysis.

## 4.4 Results

### 4.4.1 Vildagliptin has no effect on body weight of HFD mice, but reduces serum triglycerides and total cholesterol

8-week-old C57BL/6 mice were given a standard chow diet or a HFD and were treated with vildagliptin for 7 weeks. Table 4.1 shows some measured parameters for each group. All parameters analyzed (body weight gain, food intake, serum triglycerides and total cholesterol) are not different in vildagliptin-treated chow diet mice, when compared to non-treated mice.

**Table 4.1 – Parameters measured in mice fed a Chow or HFD with or without vildagliptin treatment for 7 weeks.** Mean  $\pm$  SEM, n=4-14 \*p<0.05; \*\*p<0.01; \*\*\*p<0.001 compared to Chow group. #p<0.05; ##p<0.01 compared to HFD group. One-way ANOVA was used as statistical test.

	Chow	Chow+V	HFD	HFD+V
Body weight change (%)	18.9 $\pm$ 1.7	20.6 $\pm$ 1.1	34.0 $\pm$ 2.6***	37.7 $\pm$ 2.4***
Food Intake/mice/day (calories)	9.1 $\pm$ 0.2	8.5 $\pm$ 0.1	17.7 $\pm$ 0.02***	16.6 $\pm$ 0.3***, #
Serum Triglycerides (mg/dL)	72.9 $\pm$ 4.3	86.1 $\pm$ 8.9	184.9 $\pm$ 9.1***	141.2 $\pm$ 10.5***, ##
Serum Cholesterol (mg/dL)	127.9 $\pm$ 31.1	138.6 $\pm$ 38.9	334.8 $\pm$ 35.5**	162.3 $\pm$ 25.4#
Serum Insulin (ng/dL)	0.47 $\pm$ 0.15	0.30 $\pm$ 0.09	2.26 $\pm$ 0.84*	1.51 $\pm$ 0.54
Serum Leptin (ng/dL)	1.6 $\pm$ 0.3	2.7 $\pm$ 0.8	19.2 $\pm$ 4.6***	10.8 $\pm$ 1.8**, #

The mean body weight of all mice assigned to either the HFD or standard chow diet with or without vildagliptin treatment was not different at the beginning of the study. As expected, HFD mice have a significantly increase in percentage weight gain in comparison with chow diet-fed mice, which is not altered with vildagliptin treatment (Table 4.1 and Figure 4.2A). The HFD has higher energy content than the chow diet (4.49 kcal/g vs 2.268 kcal/g); the increased body weight of mice fed HFD is associated to an increased energy intake in comparison to mice fed a chow diet (Table 4.1). In vildagliptin-treated mice total energy intake levels tend to be slightly decreased, compared with HFD group without treatment (Table 4.1). Despite the maintenance of body weight increase, vildagliptin-treated mice fed with HFD have reduced serum triglycerides and total cholesterol levels (Table 4.1) thereby ameliorating the metabolic parameters of animals fed a HFD.

#### 4.4.2 Vildagliptin decreases blood glucose and improves glucose tolerance

Vildagliptin-treated mice fed a chow diet compared to non-treated mice have no difference in fasting blood glucose (Figure 4.1A; chow diet:  $140.2 \pm 5.5$  mg/dL and chow diet with vildagliptin:  $131.8 \pm 4.1$  mg/dL) as well as on glucose kinetics measured by ipGTT (Figure 4.1B-C; area under the curve (AUC): chow diet,  $24431.5 \pm 1046.3$  a.u.; chow diet with vildagliptin,  $21639.0 \pm 944.2$  a.u.). Fasting glucose levels in HFD mice are increased by  $54.9 \pm 9.2$  mg/dL, when compared to chow diet mice. Vildagliptin reverts this effect ( $29.1 \pm 7.0$  mg/dL, in HFD treated with vildagliptin compared to untreated HFD mice; Figure 4.1A). When challenged with an ipGTT, HFD mice treated with vildagliptin demonstrate improved glucose clearance for the duration of the challenge, when compared with non-treated HFD mice (Figure 4.1B-C; AUC: HFD,  $36005.5 \pm 1863.7$  a.u.; HFD with vildagliptin,  $30253.3 \pm 1655.2$  a.u.). Serum insulin levels significantly increase in HFD mice in comparison with chow diet, but no significant alterations were observed in vildagliptin-treated mice (Table 4.1). Serum leptin levels are also significantly increased in HFD mice but this increase is, as expected, prevented with vildagliptin treatment (Table 4.1).

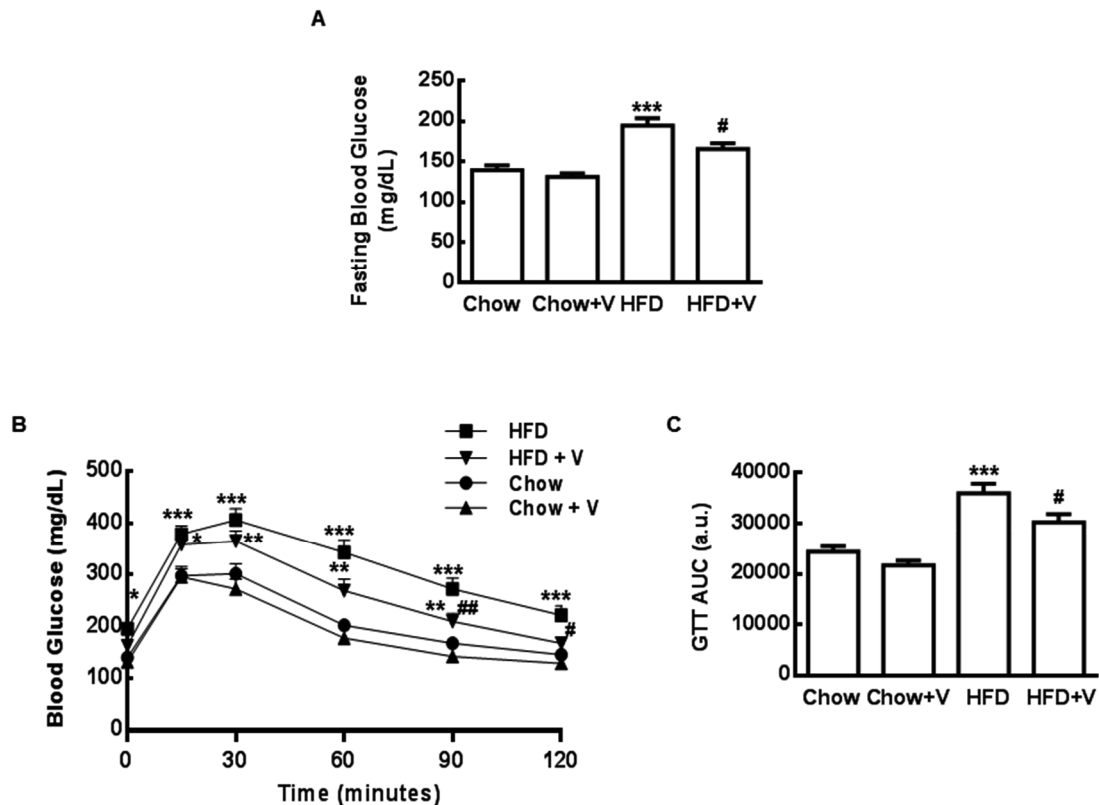


**Figure 4.1 – Vildagliptin decreases blood glucose and improves glucose tolerance.** (A) Fasting blood glucose, (B) blood glucose during intraperitoneal glucose tolerance test, Two-way ANOVA was used as statistical test, (C) area under the curve (0-120 minutes) of blood glucose of intraperitoneal glucose tolerance test in Chow and HFD group with and without vildagliptin treatment (V). n=9-13 \*p<0.05; \*\*p<0.01; \*\*\*p<0.001 compared to Chow group. #p<0.05; ##p<0.01 compared to HFD group. One-way ANOVA was used as statistical test.

#### 4.4.3 Vildagliptin does not alter epididymal adipose tissue weight nor adipocyte diameter

As expected, epididymal adipose tissue weight is significantly higher in the HFD group than in the chow group. And in vildagliptin-treated group, the epididymal adipose tissue weight does not change (Figure 4.2B; Chow:  $443.7 \pm 27.2$  mg; Chow with vildagliptin:  $443.0 \pm 46.1$  mg; HFD:  $1036.9 \pm 199.3$  mg; HFD with vildagliptin:  $1206.2 \pm 167.9$  mg). In agreement, adipocyte diameter is increased in HFD group when compared to chow diet mice and vildagliptin does not change this parameter (Figure 4.2C-D; Chow:  $52.0 \pm 3.3$   $\mu\text{m}$ ; Chow with vildagliptin:  $59.9 \pm 2.9$   $\mu\text{m}$ ; HFD:  $74.3 \pm 4.7$   $\mu\text{m}$ ; HFD with vildagliptin:  $77.4 \pm 4.7$   $\mu\text{m}$ ).

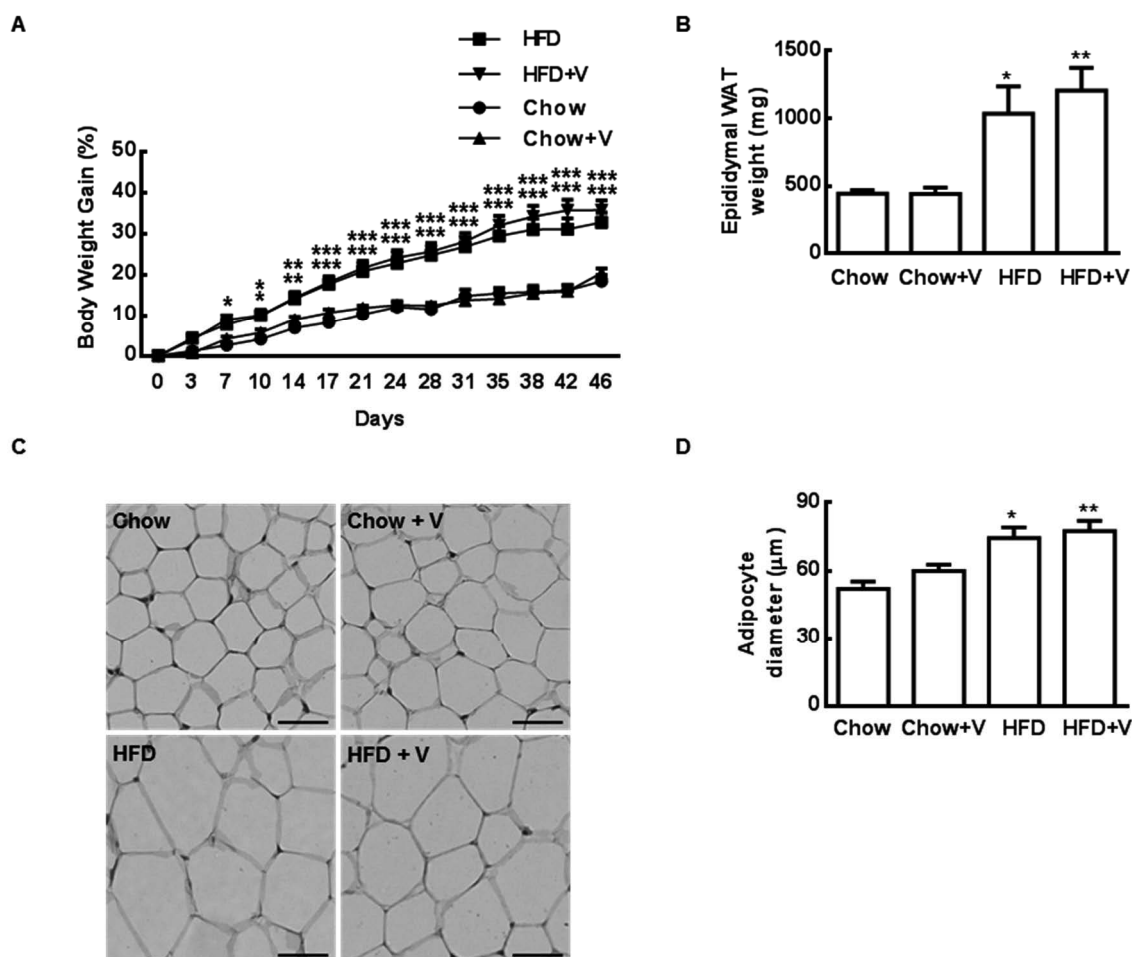


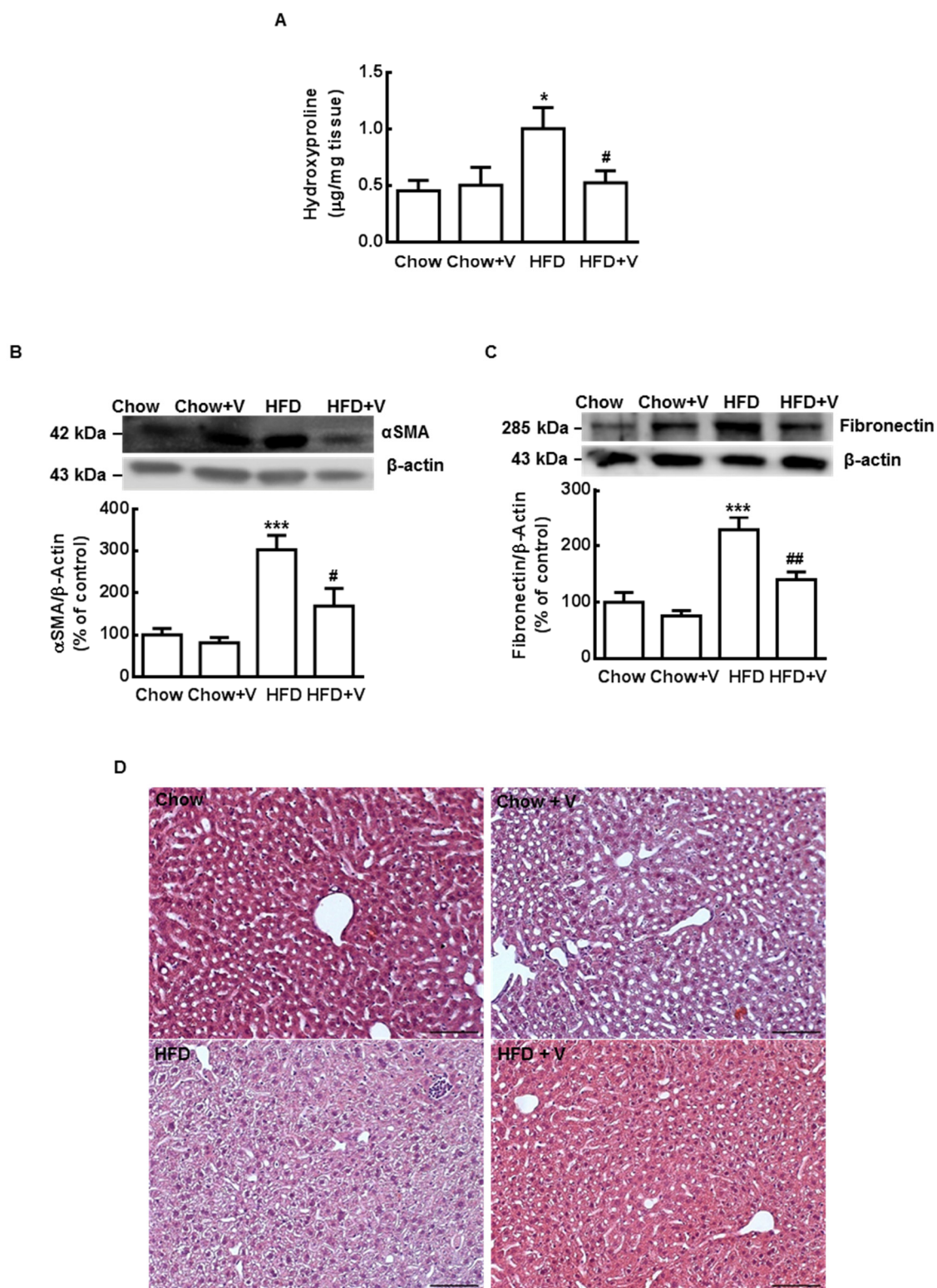
**Figure 4.2 – Vildagliptin has no effect on body weight gain, epididymal white adipose tissue and adipocyte diameter.** (A) Cumulative body weight gain presented as percentage of initial weight (n=10-14), Two-way ANOVA was used as statistical test, (B) epididymal adipose tissue weight (n=7-10), (C) representative image of hematoxylin and eosin staining in epididymal adipose tissue (n=3; Scale bar: 50  $\mu\text{m}$ ), (D) adipocyte diameter in Chow and HFD group with and without vildagliptin treatment (V) (n=3). \* $p < 0.05$ ; \*\* $p < 0.01$ ; \*\*\* $p < 0.001$  compared to Chow group. One-way ANOVA was used as statistical test.



#### **4.4.4 Vildagliptin prevents fibrosis markers in adipose tissue of HFD mice**

Increased collagen and matrix deposition are key features of fibrosis that occur in adipose tissue of obese mice [326]. Since hydroxyproline is a major component of collagen, the measurement of this modified amino acid can be used as an indicator of collagen content [600]. We observed that total collagen is increased in adipose tissue of mice fed a HFD when compared to chow-fed mice, but these levels decrease in vildagliptin-treated HFD mice in comparison with non-treated mice (Figure 4.3A; Chow:  $0.457 \pm 0.092$   $\mu\text{g}/\text{mg}$  tissue; Chow+V:  $0.508 \pm 0.158$   $\mu\text{g}/\text{mg}$  tissue; HFD:  $1.008 \pm 0.186$   $\mu\text{g}/\text{mg}$  tissue; HFD+V:  $0.528 \pm 0.107$   $\mu\text{g}/\text{mg}$  tissue). By western blotting assay we evaluated the expression of  $\alpha\text{SMA}$  and fibronectin, two pro-fibrotic proteins. We observed that adipose tissue of HFD-fed mice has significantly higher  $\alpha\text{SMA}$  and fibronectin levels, we observe an increase of  $202.7 \pm 34.1\%$  and  $128.8 \pm 22.4\%$ , respectively, compared to adipose tissue of chow diet-fed mice (Figure 4.3B-C). Vildagliptin treatment is able to decrease the levels of  $\alpha\text{SMA}$  and fibronectin in adipose tissue of mice fed a HFD, by  $134.4 \pm 42.1\%$  and  $88.6 \pm 13.7\%$ , respectively (Figure 4.3B-C). These results suggest that vildagliptin decreases fibrosis formation in WAT of HFD-induced obese mice.

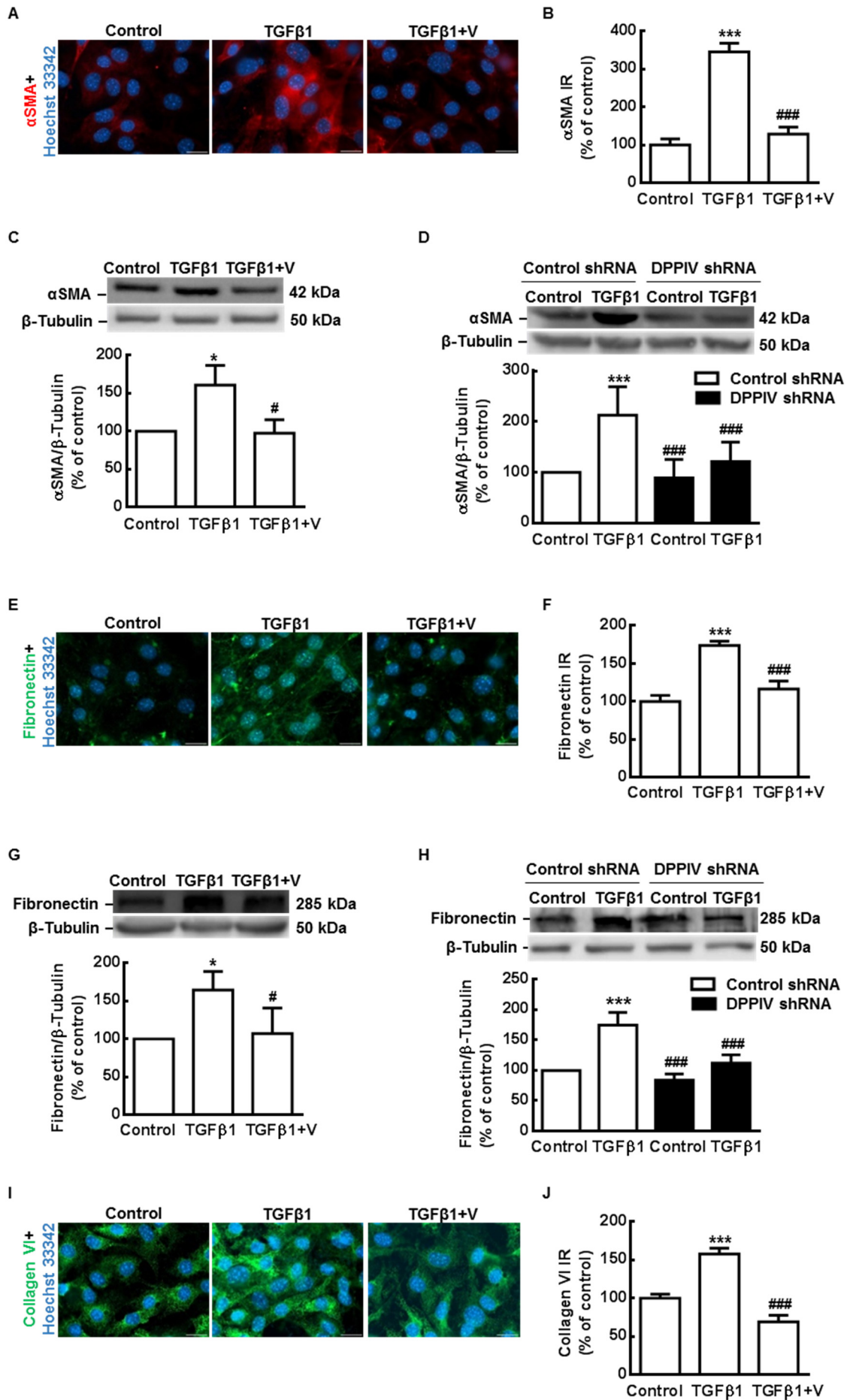
Obesity is often associated with ectopic lipid accumulation due to incapacity of lipid accumulation in adipose tissue and thereby hepatic steatosis can occur. Analysis of livers from control mice on HFD reveal an increase in lipid content compared with mice fed regular chow diet (Figure 4.3D). Moreover, livers from vildagliptin-treated mice on HFD show lower levels of lipid droplet accumulation when compared to livers from non-treated HFD mice (Figure 4.3D).



**Figure 4.3 – Vildagliptin prevents fibrosis formation in the adipose tissue of HFD mice.** (A) Hydroxyproline quantification (n=3-8), (B and C) αSMA or fibronectin and β-actin (loading control) immunoreactivity by Western blotting (n=5-7), (D) representative image of hematoxylin and eosin staining in liver (Scale bar: 100 µm) in Chow and HFD group with and without vildagliptin treatment (V). \*p<0.05; \*\*\*p<0.001 compared to Chow group. #p<0.05; ##p<0.01 compared to HFD group. One-way ANOVA was used as statistical test.

#### **4.4.5 Vildagliptin prevents collagen and matrix markers deposition in TGF $\beta$ 1-stimulated 3T3-L1 cell line**

In order to clarify the mechanism through which vildagliptin can prevent fibrosis in adipose tissue, we first evaluated whether vildagliptin was able to prevent collagen and matrix deposition *in vitro*. We used a preadipocyte cell line, 3T3-L1, and mimicked pathological conditions in which fibrosis is induced by treating cultures with 2.5 ng/ml of TGF- $\beta$ 1 [602]. After 7 days of treatment with the fibrosis inducer, we observed an increase in  $\alpha$ SMA and fibronectin levels by  $60.8 \pm 12.9\%$  and  $64.6 \pm 12.1\%$ , in comparison with control cells, respectively (in Figure 4.4C and G). Moreover, vildagliptin significantly decreases the levels of  $\alpha$ SMA and fibronectin by  $63.2 \pm 8.8$  and  $57.3 \pm 16.6\%$ , respectively, in comparison with TGF- $\beta$ 1-treated cells (Figure 4.4C and G). We also evaluated the levels of  $\alpha$ SMA, fibronectin and collagen VI by immunofluorescence (Figure 4.4A-B, E-F and I-J). TGF- $\beta$ 1 increases the immunoreactivity of  $\alpha$ SMA and this increase is prevented by vildagliptin (Figure 4.4A-B; Control:  $100.0 \pm 16.2\%$ ; TGF- $\beta$ 1:  $345.6 \pm 22.6\%$ ; TGF- $\beta$ 1 and vildagliptin:  $128.7 \pm 18.6\%$ ). Furthermore, in TGF- $\beta$ 1-treated cells, fibronectin immunoreactivity is increased by  $73.9 \pm 5.9\%$ , which is prevented by treatment with vildagliptin by  $57.1 \pm 10.4\%$  (Figure 4.4E-F). Similar results were obtained when we analyzed collagen VI. Immunoreactivity of this protein is increased by TGF- $\beta$ 1 but vildagliptin is able to prevent this increase (Figure 4.4I-J; Control:  $100.0 \pm 5.3\%$ ; TGF- $\beta$ 1:  $158.0 \pm 7.7\%$ ; TGF- $\beta$ 1 and vildagliptin:  $69.2 \pm 8.6\%$ ). Total collagen content was evaluated by determination of hydroxyproline. We also observed a significant increase of total collagen content in cells treated with TGF- $\beta$ 1 by  $82.7 \pm 6.8\%$ . Vildagliptin is able to inhibit TGF- $\beta$ 1-induced total collagen stimulation by  $61.5 \pm 7.3\%$  (Figure 4.4K). To better understand the direct effect of DPP-IV inhibition, by vildagliptin, in ECM deposition and remodeling, we silenced DPP-IV using a shRNA targeting DPP-IV. Fibrosis was induced in 3T3-L1 cells with TGF $\beta$ 1 and DPP-IV was genetically silenced. We evaluated, by western blotting, the protein levels of  $\alpha$ SMA and fibronectin. As expected, we observed that TGF $\beta$ 1 increases  $\alpha$ SMA by  $112.7 \pm 21.1\%$  and fibronectin by  $74.7 \pm 9.5\%$  (Figure 4.4D and H). The DPP-IV silencing significantly decreases both  $\alpha$ SMA and fibronectin levels by  $91.6 \pm 14.5\%$  and by  $62.7 \pm 6.1\%$ , respectively (Figure 4.4D and H). We further studied total collagen content, and we observed that TGF $\beta$ 1 increases by  $54.5 \pm 3.3\%$  the total collagen and when DPP-IV was silenced the levels of total collagen decrease  $51.5 \pm 7.2$  (Figure 4.4L). In conclusions, our results suggest that inhibition of DPP-IV by vildagliptin and by genetic tools prevents collagen and matrix deposition in TGF $\beta$ 1-treated 3T3-L1 cells.



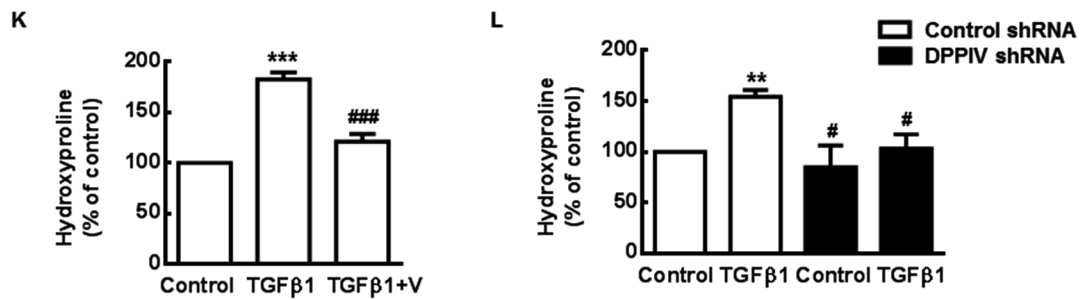


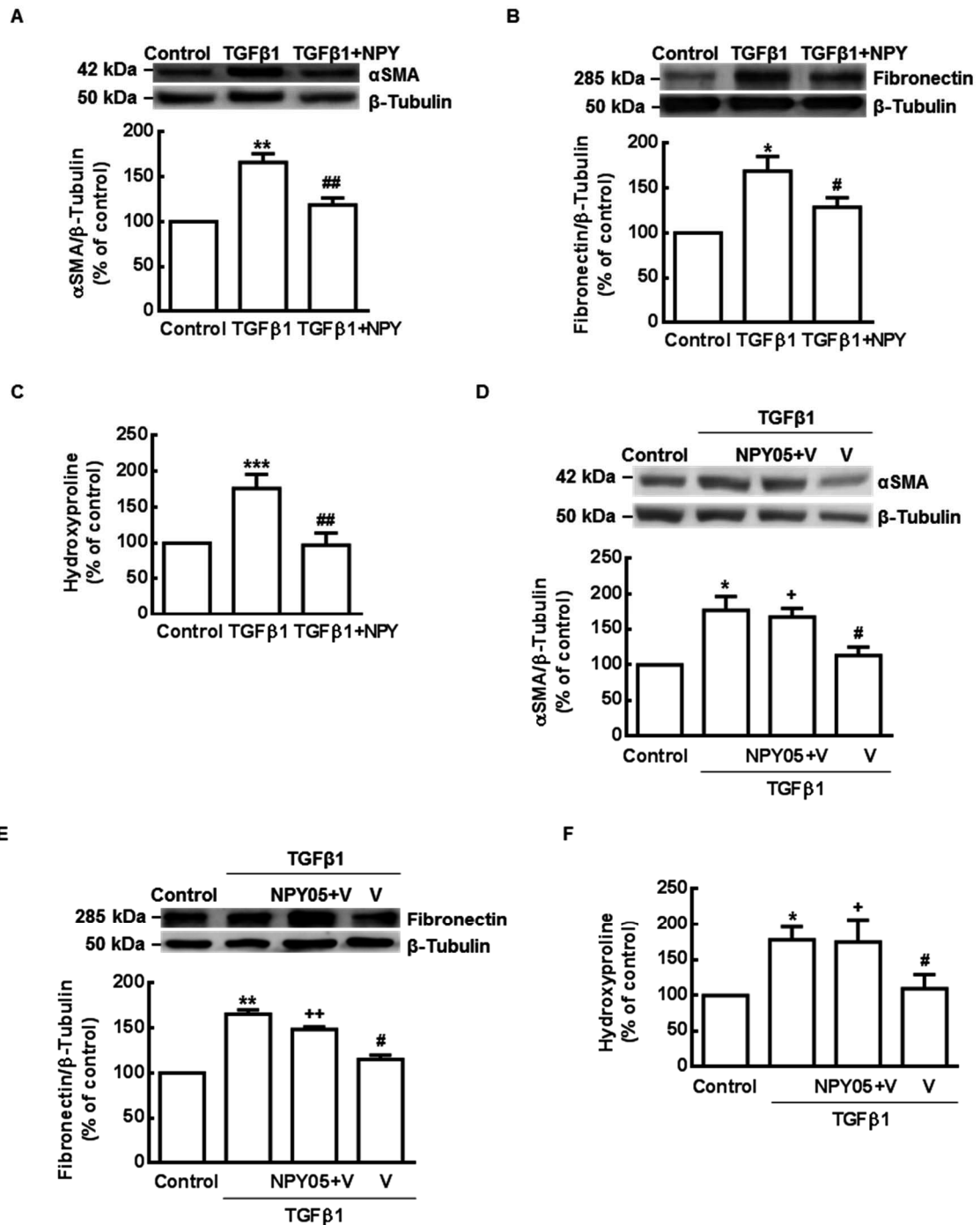
**Figure 4.4 – Vildagliptin and DPP-IV silencing prevent fibrosis formation.** 3T3-L1 preadipocytes were induced to differentiate and were treated with TGFβ1 (2.5 ng/ml) in the presence or absence of vildagliptin (V, 2nM) for seven days. (A, E, I) Representative images of immunofluorescence for αSMA (red), Fibronectin (green) and Collagen VI (green). Nuclei were stained with Hoechst 33342 (blue). Scale bar: 20 μm (B, F, J) Quantification of αSMA, Fibronectin and Collagen VI immunofluorescence immunoreactivity. (C, G) αSMA or fibronectin and β-tubulin (loading control) immunoreactivity by Western blotting. (K) Hydroxyproline quantification. n=3-10 \*p<0.05; \*\*\*p<0.001 compared to control. #p<0.05; ###p<0.001 compared to TGFβ1. One-way ANOVA was used as statistical test. 3T3-L1 preadipocytes were infected with lentivirus encoding a negative short hairpin RNA (control condition) or a short hairpin RNA targeting DPP-IV. (D, H) αSMA or fibronectin and β-tubulin (loading control) immunoreactivity by Western blotting. (L) Hydroxyproline quantification. n=4-7 \*\*p<0.01; \*\*\*p<0.001; compared to control of control shRNA. #p<0.05; ###p<0.001; compared to TGFβ1-treated control shRNA. One-way ANOVA was used as statistical test.

#### 4.4.6 Vildagliptin abrogates the TGFβ1-induced alterations in ECM through NPY Y<sub>1</sub> receptor activation

To further clarify the underlying mechanisms of the relationship between DPP-IV inhibitor vildagliptin and its anti-fibrotic role, we next investigated whether NPY has an effect on ECM. This hypothesis was based in the fact that NPY is a substrate of DPP-IV, and it is implicated in the regulation of fibrosis in a swine model of chronic myocardial ischemia and hypercholesterolemia [603].

To study the effect of NPY on ECM, cells were treated with NPY (100 nM) in the presence of TGFβ1. We observed, by western blotting, that NPY significantly decreases the levels of αSMA and fibronectin induced by TGFβ1,  $47.6 \pm 7.8\%$  and  $40.1 \pm 10.5\%$ , respectively, when compared to TGFβ1 alone (Figure 4.5A-B). NPY also decreases total collagen content in TGFβ1-treated cells by  $79.1 \pm 6.9\%$  (Figure 4.5 C). Moreover, in order to study whether vildagliptin effect occurs through NPY receptor activation by NPY released, cells were treated with TGFβ1 and vildagliptin in the presence of a neutralizing NPY antibody, NPY05 [604]. It was observed that when NPY effect is neutralized, the inhibitory effect of vildagliptin on αSMA, fibronectin and total collagen in TGFβ1-treated cells is partially reverted by  $54.0 \pm 13.4\%$ ,  $33.3 \pm 2.8\%$  and  $65.1 \pm 15.9\%$ , respectively (Figure 4.5D-F). To evaluate which NPY receptors were involved in this anti-fibrotic effect induced by NPY, preadipocytes were incubated with TGFβ1 in the presence of NPY Y<sub>1</sub> receptor agonist

(Leu<sup>31</sup>Pro<sup>34</sup>NPY, 100 nM), NPY Y<sub>2</sub> receptor agonist (NPY13-36, 100 nM) or the NPY Y<sub>5</sub> receptor agonist (NPY19-23(Gly1, Ser3, Gln4, Thr6, Ala31, Aib32, Gln34)PP, 100 nM). We observed that NPY Y<sub>1</sub> receptor agonist decreases  $\alpha$ SMA, fibronectin, total collagen upregulation induced by TGF $\beta$ 1 (Figure 4.5G-I). NPY Y<sub>2</sub> receptor agonist or the NPY Y<sub>5</sub> receptor agonist do not change the levels of  $\alpha$ SMA, fibronectin and total collagen (Figure 4.5G-I). These results show that NPY prevents ECM deposition by NPY Y<sub>1</sub> receptor activation. These results suggest that vildagliptin anti-fibrotic effect occurs partially through preserving NPY that will activate NPY Y<sub>1</sub> receptors.



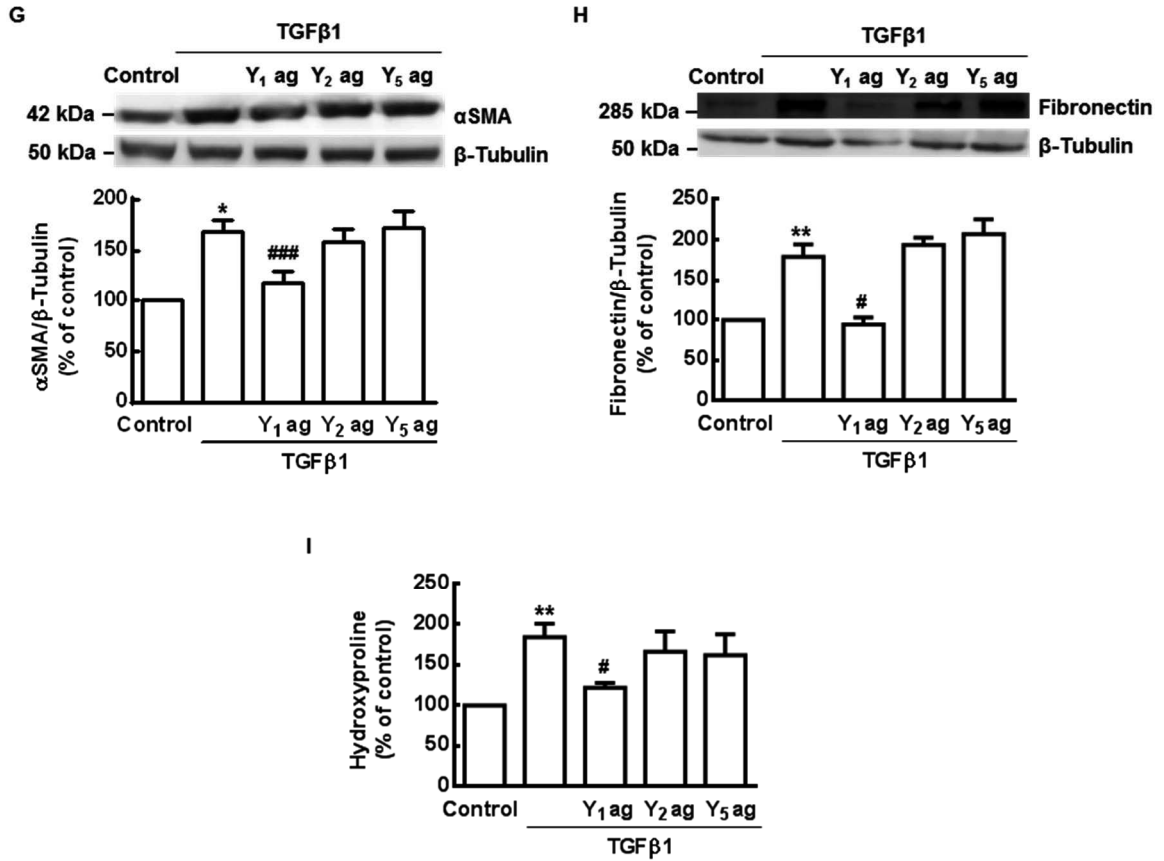


**Figure 4.5 – DPP-IV inhibitor prevents fibrosis through NPY and NPY Y<sub>1</sub> receptor activation.** 3T3-L1 preadipocytes were induced to differentiate and were treated with TGFβ1 (2.5 ng/ml) in the absence or presence of (A-C) NPY; (D-F) vildagliptin (V, 2 nM) with or without NPY neutralizing antibody (NPY05, 6 μg/ml) for seven days; (G-I) NPY Y<sub>1</sub> receptor agonist (Leu31Pro34NPY, 100 nM), NPY Y<sub>2</sub> receptor agonist (NPY13-36, 100 nM) or the NPY Y<sub>5</sub> receptor agonist (NPY19-23(Gly1, Ser3, Gln4, Thr6, Ala31, Aib32, Gln34)PP, 100 nM). (A, D, G) αSMA or (B, E, H) fibronectin and β-tubulin (loading control) immunoreactivity by Western blotting. ((C, F, I) Hydroxyproline quantification. n=4-7 \*p<0.05; \*\*p<0.01; \*\*\*p<0.001 compared to control. #p<0.05; ##p<0.01; ###p<0.001 compared to TGFβ1. †p<0.05; ††p<0.01 compared to TGFβ1+V. One-way ANOVA was used as statistical test.

## 4.5 Discussion

Obesity is associated with an excessive increase of WAT. It has been described an excessive ECM remodeling, that leads to fibrosis formation in adipose tissue in obesity [326]. Adipose tissue fibrosis limits normal expansion of the tissue, leading to metabolic complications in obesity. Vildagliptin is a selective and competitive inhibitor of DPP-IV that is currently being used in the treatment of type 2 diabetes [596]. Moreover, there is evidence that DPP-IV inhibitors have other effects besides glycemic control, such as hypolipidemic effect [605]. Some studies have already described that DPP-IV inhibitors are able to prevent fibrosis formation in the liver, kidney and heart [522,528,532]. Taking this into account, in this study we investigated the potential effect of DPP-IV inhibitor, vildagliptin, in the prevention of fibrosis in adipose tissue of obese mice, induced by HFD. In this work, HFD induced an increase of body and epididymal adipose tissue weight and also an increase of adipocyte diameter. HFD-fed mice also showed, as already described [606], an increase of fasting blood glucose, impaired glucose tolerance, an increase in serum cholesterol, triglycerides, insulin and leptin and also an increase of fat accumulation by the liver. Moreover, we observed epididymal adipose tissue fibrosis in HFD mice. These results are in agreement with “the adipose tissue expandability theory” proposed by Vidal-Puig and Virtue, which consists in the idea that WAT storage capacity may become saturated resulting in excess of fat that is released to non-adipose tissues [252]. WAT fibrosis increases rigidity of adipose tissue matrix limiting adipose tissue expansion, thereby decreasing its capability of lipid storage contributing to serum lipids and ectopic lipid accumulation in the liver and thus contributing to metabolic syndrome [591].

Moreover, we found that vildagliptin, besides improving glycemic control, also improves other serum parameters such as triglycerides, cholesterol and leptin in HFD-fed mice. Vildagliptin also improves lipid accumulated by the liver of HFD mice. The effect of vildagliptin in glycemic control is known to occur through the increase of half-life time of GLP-1 and GIP, which are known to potentiate insulin secretion by pancreatic  $\beta$ -cells, lowering blood glucose levels, HbA1c, glucagon secretion and liver glucose production [492]. Some of the other effects, namely triglycerides, cholesterol and leptin decrease can be explained by the improvement of glycemic control due to inhibition of DPP-IV [597]. Several studies described that DPP-IV inhibitors improve blood cholesterol and triglycerides, both in humans [607-609] and rodents [597,610].

Moreover, although there were no significant differences in body weight change nor adipose tissue mass we observed a decrease in fibrosis in WAT of obese mice treated with vildagliptin. These findings represent the first evidence, to our knowledge, that DPP-



IV inhibition prevents fibrosis in adipose tissue in a diet-induced obesity rodent model. This antifibrotic role of vildagliptin in non-adipose tissues has already been described by others [521,538]. This antifibrotic role will putatively decrease the stiffness of the tissue and thereby improve adipocyte ability to store lipids, and can be a cause for the amelioration of other parameters that we observed in this study, such as decrease in serum triglycerides and cholesterol and also ectopic lipid accumulation in the liver. All of these parameters are hallmarks of metabolic syndrome, so amelioration of these parameters suggests that vildagliptin could have an important role in obesity complications and thereby contributes to health improvement. In fact, it was already observed that collagen VI deficient *ob/ob* and HFD-fed mice also have less adipose tissue fibrosis [263]. These mice have more fat mass with improved insulin sensitivity, suggesting that adipose tissue fibrosis may be an important determinant of insulin sensitivity [263]. The inhibition of fibrosis in WAT decreases its rigidity and this might facilitate weight loss. In obese patients, subcutaneous adipose tissue revealed persistence of fibrosis two years after bariatric surgery [395] and adipose tissue fibrosis is even found negatively associated with weight loss induced by bariatric surgery [352]. All of these studies are important reinforcements for the role of fibrosis on adipose tissue homeostasis and its consequences during obesity process.

Regarding the mechanisms underlying the antifibrotic effect of vildagliptin in adipose tissue fibrosis, we could hypothesize that it occurs as a consequence of increased GLP-1 levels and consequently improved insulin response and glycemic control [596]. However, several studies showed that DPP-IV inhibitors are able to prevent fibrosis independently of glycemia and GLP-1 in the liver [521], in the heart [530] and in the kidney [535]. Moreover, fibrosis prevention could also be explained by anti-inflammatory effects of DPP-IV inhibitors and GLP-1 that were both described to prevent inflammation in WAT [510,611]. It is widely recognized that obesity is an inflammatory state and fibrosis is perceived by many as a process secondary to tissue inflammation [324]. But in fact little is known about this triad and the causal relationships between adipose tissue fibrosis and inflammation remain to be defined.

To better understand the putative mechanism underlying vildagliptin and fibrosis prevention in adipose tissue of obese mice, we used an *in vitro* model of 3T3-L1 preadipocytes and showed that both vildagliptin and a genetic approach of silencing DPP-IV suppress TGF $\beta$ 1-mediated stimulatory effects on the profibrotic markers:  $\alpha$ SMA, fibronectin and collagen VI and total collagen deposition. These results are in agreement with two studies that show that DPP-IV inhibitors have antifibrotic effects also *in vitro* in other cell types [522,612]. DPP-IV inhibitor, sitagliptin, decreases platelet derived growth factor-BB-mediated upregulation of TGF $\beta$ 1 and  $\alpha$ 1(I)-procollagen in activated hepatic

stellate cells [522]. Inhibitors of DPP-IV-like activity abrogate TGF $\beta$ 1-induced collagen and fibronectin in normal and keloid-derived skin fibroblasts [612]. Inhibition of DPP-IV was performed through pharmacological and genetic approaches. Genetic silencing of DPP-IV resulted in similar results to those obtained with vildagliptin, a DPP-IV inhibitor. These results show that the anti-fibrotic effects that we obtained with vildagliptin occur specifically through inhibition of catalytic function of DPP-IV, and not through non-specific, off-target effects. In fact, one study showed GLP-1-independent protective effects of a DPP-IV inhibitor in fibrosis in the kidney [535]. DPP-IV has several other substrates, such as NPY [418]. DPP-IV removes N-terminal dipeptide changing the receptor sub-type specificity from Y<sub>1</sub> (NPY<sub>1-36</sub>) to Y<sub>2</sub>/Y<sub>5</sub> (NPY<sub>3-36</sub>) [550]. Moreover, NPY has an important role in the development of adipose tissue. NPY was shown to increase proliferation and differentiation of adipocytes through NPY Y<sub>2</sub> and NPY Y<sub>5</sub> receptors [561]. It has been demonstrated that inhibition of DPP-IV facilitates the anti-lipolytic effects of NPY through Y<sub>1</sub> receptor [468]. Taking into account the NPY relevance in adipose tissue function, we hypothesized that NPY might be a possible DPP-IV substrate responsible for the antifibrotic role of vildagliptin. In this study, we showed that the vildagliptin effect occur partially through its action in NPY that in turn activates NPY Y<sub>1</sub> receptor. These results are in agreement with the “expandability theory”. If vildagliptin acts through NPY Y<sub>1</sub> receptor to inhibit fibrosis, this fibrotic inhibition might allow adipocytes to expand and accumulate lipids, thereby inhibiting lipolysis. A role of NPY in fibrosis has been previously described. It was shown that local infiltration of NPY in a swine model of chronic myocardial ischemia and hypercholesterolemia reduces fibrosis [603]. Moreover, NPY overexpression reduces the development of cardiac fibrosis in other rat model [613]. Another study observed that mouse lacking NPY Y<sub>1</sub> receptor also has a larger volume fraction of myocardial fibrosis [614], corroborating the previous result.

In summary, this study establishes that a DPP-IV inhibitor significantly protects against adipose tissue fibrosis formation and several other dysfunctions associated with obesity. The antifibrogenic activity of vildagliptin activity *in vitro* and *in vivo* adds more possibilities to the range of possible therapeutic applications of DPP-IV inhibitors.

## **CHAPTER 5**

---

### **Concluding Remarks**



## 5. Concluding remarks

Adipose tissue of obese mice and humans expands modifying its homeostasis and hypoxia and fibrosis may occur in WAT of obese mice and humans [264,265,326]. Hypoxia and fibrosis were also shown to be underlying mechanisms of adipose tissue dysfunctions [263,320].

In the present work we evaluated the effect of hypoxia in the function of adipocytes *in vitro*. Our results show that hypoxia mimetic, CoCl<sub>2</sub>, blocks adipocyte differentiation, by increasing miR-27a and miR-27b. However, hypoxia mimetic induces autophagy and increases lipid accumulation through mitochondria dysfunction and ROS production. Several studies described that hypoxia blocks PPAR $\gamma$ 2, inhibiting adipocyte differentiation [298,570]. Our results are in agreement with these studies as we observed that hypoxia mimetic downregulates PPAR $\gamma$ 2, perilipin and Pref-1, showing that hypoxia blocks adipocyte differentiation. Moreover, we observed that 3T3-L1 cells under hypoxia mimetic treatment increases miR-27a and miR-27b that are described to block adipocyte differentiation, by binding the 3'UTR of PPAR $\gamma$  mRNA [123]. Modulation of miR-27a and miR-27b in hypoxic preadipocytes might provide important clues about hypoxia role on adipogenesis and improve adipocyte function.

However, it was not clear the effect of hypoxia on lipid accumulation. We observed that CoCl<sub>2</sub> induces lipid accumulation that occurs through the increase of ROS production that is inhibited by an antioxidant, glutathione. Hypoxia favors anaerobic metabolism [571], like glycolysis, leading to a decrease in ATP and increase in lactate production . The action of antioxidants might be important to improve adipocyte function and survival. Furthermore, we also observed that CoCl<sub>2</sub> increases autophagy in 3T3-L1 preadipocytes as it was previously described in other cell types [576,577]. Autophagy is known to be increased in adipose tissue in obesity [177] and is needed to normal adipogenesis [175,176]. However, the functional role of autophagy in adipose tissue in obesity and in hypoxia-response in adipocytes should be further investigated.

Furthermore, we studied the effect of a DPP-IV inhibitor, vildagliptin, in fibrosis of adipose tissue in HFD-fed obese mice and its mechanisms *in vitro*. We showed that vildagliptin improves glucose response as expected but also decreases serum triglycerides, cholesterol and leptin and improves ectopic lipid accumulation by the liver. These effects of vildagliptin were already described by others both in human and mice and might occur as consequence of improved glucose homeostasis [597]. Moreover, we observed that vildagliptin prevents fibrosis formation in adipose tissue of HFD-fed mice. This can occur by an effect of vildagliptin in ECM of adipose tissue or it can be a consequence of the improved lipid and glucose metabolism and decreased inflammation that was already

described in WAT [510,611]. We studied the mechanisms of vildagliptin in fibrosis in 3T3-L1 preadipocytes and showed that this DPP-IV inhibitor prevents ECM remodeling in this cell line, through NPY Y<sub>1</sub> receptor activation. The protective effect of DPP-IV inhibitors in fibrosis in non-adipose tissues was already described, however, to the best of our knowledge this is the first time that a protective effect of a DPP-IV inhibitor in fibrosis in adipose tissue is described.

Taking these results together, the present study extends our understanding of the effect of hypoxia on adipocyte biology and lipid metabolism. Moreover, we provide a possible explanation for hypoxic lipogenesis, namely the importance of preadipocyte response to mitochondrial dysfunction and ROS leading to autophagy and also to lipid accumulation. In addition, we also demonstrated that vildagliptin can prevent adipose tissue fibrosis in obesity, showing that DPP-IV inhibitors might be an important class of drugs in the treatment of obesity and also in obesity-related diseases.

## **CHAPTER 6**

---

### **References**





## 6. References

1. (2000) Obesity: preventing and managing the global epidemic. Report of a WHO consultation. World Health Organ Tech Rep Ser 894: i-xii, 1-253.
2. Nuttall FQ (2015) Body Mass Index: Obesity, BMI, and Health: A Critical Review. *Nutr Today* 50: 117-128.
3. Nguyen NT, Nguyen XM, Lane J, Wang P (2011) Relationship between obesity and diabetes in a US adult population: findings from the National Health and Nutrition Examination Survey, 1999-2006. *Obes Surg* 21: 351-355.
4. Boden G, Salehi S (2013) Why does obesity increase the risk for cardiovascular disease? *Curr Pharm Des* 19: 5678-5683.
5. De Pergola G, Silvestris F (2013) Obesity as a major risk factor for cancer. *J Obes* 2013: 291546.
6. Kaur J (2014) A comprehensive review on metabolic syndrome. *Cardiol Res Pract* 2014: 943162.
7. Krude H, Biebermann H, Luck W, Horn R, Brabant G, et al. (1998) Severe early-onset obesity, adrenal insufficiency and red hair pigmentation caused by POMC mutations in humans. *Nat Genet* 19: 155-157.
8. Montague CT, Farooqi IS, Whitehead JP, Soos MA, Rau H, et al. (1997) Congenital leptin deficiency is associated with severe early-onset obesity in humans. *Nature* 387: 903-908.
9. Clement K, Vaisse C, Lahlou N, Cabrol S, Pelloux V, et al. (1998) A mutation in the human leptin receptor gene causes obesity and pituitary dysfunction. *Nature* 392: 398-401.
10. Vaisse C, Clement K, Guy-Grand B, Froguel P (1998) A frameshift mutation in human MC4R is associated with a dominant form of obesity. *Nat Genet* 20: 113-114.
11. Dina C, Meyre D, Gallina S, Durand E, Korner A, et al. (2007) Variation in FTO contributes to childhood obesity and severe adult obesity. *Nat Genet* 39: 724-726.
12. Frayling TM, Timpson NJ, Weedon MN, Zeggini E, Freathy RM, et al. (2007) A common variant in the FTO gene is associated with body mass index and predisposes to childhood and adult obesity. *Science* 316: 889-894.
13. Wing RR, Lang W, Wadden TA, Safford M, Knowler WC, et al. (2011) Benefits of modest weight loss in improving cardiovascular risk factors in overweight and obese individuals with type 2 diabetes. *Diabetes Care* 34: 1481-1486.
14. Magkos F, Fraterrigo G, Yoshino J, Luecking C, Kirbach K, et al. (2016) Effects of Moderate and Subsequent Progressive Weight Loss on Metabolic Function and Adipose Tissue Biology in Humans with Obesity. *Cell Metab* 23: 591-601.
15. Knowler WC, Barrett-Connor E, Fowler SE, Hamman RF, Lachin JM, et al. (2002) Reduction in the incidence of type 2 diabetes with lifestyle intervention or metformin. *N Engl J Med* 346: 393-403.
16. American Diabetes A (2016) 6. Obesity Management for the Treatment of Type 2 Diabetes. *Diabetes Care* 39 Suppl 1: S47-51.
17. Kusminski CM, Bickel PE, Scherer PE (2016) Targeting adipose tissue in the treatment of obesity-associated diabetes. *Nat Rev Drug Discov* 15: 639-660.
18. Sumithran P, Proietto J (2014) Benefit-risk assessment of orlistat in the treatment of obesity. *Drug Saf* 37: 597-608.

19. Smith SR, Weissman NJ, Anderson CM, Sanchez M, Chuang E, et al. (2010) Multicenter, placebo-controlled trial of lorcaserin for weight management. *N Engl J Med* 363: 245-256.
20. Verrotti A, Scaparrotta A, Agostinelli S, Di Pillo S, Chiarelli F, et al. (2011) Topiramate-induced weight loss: a review. *Epilepsy Res* 95: 189-199.
21. Greenway FL, Fujioka K, Plodkowski RA, Mudaliar S, Guttadauria M, et al. (2010) Effect of naltrexone plus bupropion on weight loss in overweight and obese adults (COR-1): a multicentre, randomised, double-blind, placebo-controlled, phase 3 trial. *Lancet* 376: 595-605.
22. Astrup A, Carraro R, Finer N, Harper A, Kunesova M, et al. (2012) Safety, tolerability and sustained weight loss over 2 years with the once-daily human GLP-1 analog, liraglutide. *Int J Obes (Lond)* 36: 843-854.
23. Pi-Sunyer X, Astrup A, Fujioka K, Greenway F, Halpern A, et al. (2015) A Randomized, Controlled Trial of 3.0 mg of Liraglutide in Weight Management. *N Engl J Med* 373: 11-22.
24. Ouchi N, Parker JL, Lugus JJ, Walsh K (2011) Adipokines in inflammation and metabolic disease. *Nat Rev Immunol* 11: 85-97.
25. Sun K, Kusminski CM, Scherer PE (2011) Adipose tissue remodeling and obesity. *J Clin Invest* 121: 2094-2101.
26. Cinti S (2012) The adipose organ at a glance. *Dis Model Mech* 5: 588-594.
27. Trayhurn P, Beattie JH (2001) Physiological role of adipose tissue: white adipose tissue as an endocrine and secretory organ. *Proc Nutr Soc* 60: 329-339.
28. Cannon B, Nedergaard J (2004) Brown adipose tissue: function and physiological significance. *Physiol Rev* 84: 277-359.
29. Nedergaard J, Bengtsson T, Cannon B (2007) Unexpected evidence for active brown adipose tissue in adult humans. *Am J Physiol Endocrinol Metab* 293: E444-452.
30. Bjorndal B, Burri L, Staalesen V, Skorve J, Berge RK (2011) Different adipose depots: their role in the development of metabolic syndrome and mitochondrial response to hypolipidemic agents. *J Obes* 2011: 490650.
31. Ishibashi J, Seale P (2010) Medicine. Beige can be slimming. *Science* 328: 1113-1114.
32. Petrovic N, Walden TB, Shabalina IG, Timmons JA, Cannon B, et al. (2010) Chronic peroxisome proliferator-activated receptor gamma (PPARgamma) activation of epididymally derived white adipocyte cultures reveals a population of thermogenically competent, UCP1-containing adipocytes molecularly distinct from classic brown adipocytes. *J Biol Chem* 285: 7153-7164.
33. Sanchez-Gurmaches J, Hung CM, Guertin DA (2016) Emerging Complexities in Adipocyte Origins and Identity. *Trends Cell Biol* 26: 313-326.
34. Gesta S, Bluher M, Yamamoto Y, Norris AW, Berndt J, et al. (2006) Evidence for a role of developmental genes in the origin of obesity and body fat distribution. *Proc Natl Acad Sci U S A* 103: 6676-6681.
35. Giorgino F, Laviola L, Eriksson JW (2005) Regional differences of insulin action in adipose tissue: insights from in vivo and in vitro studies. *Acta Physiol Scand* 183: 13-30.
36. Pittenger MF, Mackay AM, Beck SC, Jaiswal RK, Douglas R, et al. (1999) Multilineage potential of adult human mesenchymal stem cells. *Science* 284: 143-147.

## **CHAPTER 5**

---

### **Concluding Remarks**

55. Tontonoz P, Hu E, Spiegelman BM (1994) Stimulation of adipogenesis in fibroblasts by PPAR gamma 2, a lipid-activated transcription factor. *Cell* 79: 1147-1156.
56. Hu E, Tontonoz P, Spiegelman BM (1995) Transdifferentiation of myoblasts by the adipogenic transcription factors PPAR gamma and C/EBP alpha. *Proc Natl Acad Sci U S A* 92: 9856-9860.
57. Rosen ED, Sarraf P, Troy AE, Bradwin G, Moore K, et al. (1999) PPAR gamma is required for the differentiation of adipose tissue in vivo and in vitro. *Mol Cell* 4: 611-617.
58. Ren D, Collingwood TN, Rebar EJ, Wolffe AP, Camp HS (2002) PPARgamma knockdown by engineered transcription factors: exogenous PPARgamma2 but not PPARgamma1 reactivates adipogenesis. *Genes Dev* 16: 27-32.
59. Mueller C, Weaver V, Vanden Heuvel JP, August A, Cantorna MT (2003) Peroxisome proliferator-activated receptor gamma ligands attenuate immunological symptoms of experimental allergic asthma. *Arch Biochem Biophys* 418: 186-196.
60. Chawla A, Schwarz EJ, Dimaculangan DD, Lazar MA (1994) Peroxisome proliferator-activated receptor (PPAR) gamma: adipose-predominant expression and induction early in adipocyte differentiation. *Endocrinology* 135: 798-800.
61. Vernochet C, Milstone DS, Iehle C, Belmonte N, Phillips B, et al. (2002) PPARgamma-dependent and PPARgamma-independent effects on the development of adipose cells from embryonic stem cells. *FEBS Lett* 510: 94-98.
62. He W, Barak Y, Hevener A, Olson P, Liao D, et al. (2003) Adipose-specific peroxisome proliferator-activated receptor gamma knockout causes insulin resistance in fat and liver but not in muscle. *Proc Natl Acad Sci U S A* 100: 15712-15717.
63. Jones JR, Barrick C, Kim KA, Lindner J, Blondeau B, et al. (2005) Deletion of PPARgamma in adipose tissues of mice protects against high fat diet-induced obesity and insulin resistance. *Proc Natl Acad Sci U S A* 102: 6207-6212.
64. Liao W, Nguyen MT, Yoshizaki T, Favellyukis S, Patsouris D, et al. (2007) Suppression of PPAR-gamma attenuates insulin-stimulated glucose uptake by affecting both GLUT1 and GLUT4 in 3T3-L1 adipocytes. *Am J Physiol Endocrinol Metab* 293: E219-227.
65. Tamori Y, Masugi J, Nishino N, Kasuga M (2002) Role of peroxisome proliferator-activated receptor-gamma in maintenance of the characteristics of mature 3T3-L1 adipocytes. *Diabetes* 51: 2045-2055.
66. Ramji DP, Foka P (2002) CCAAT/enhancer-binding proteins: structure, function and regulation. *Biochem J* 365: 561-575.
67. Salma N, Xiao H, Imbalzano AN (2006) Temporal recruitment of CCAAT/enhancer-binding proteins to early and late adipogenic promoters in vivo. *J Mol Endocrinol* 36: 139-151.
68. Linhart HG, Ishimura-Oka K, DeMayo F, Kibe T, Repka D, et al. (2001) C/EBPalpha is required for differentiation of white, but not brown, adipose tissue. *Proc Natl Acad Sci U S A* 98: 12532-12537.
69. Tang QQ, Otto TC, Lane MD (2003) CCAAT/enhancer-binding protein beta is required for mitotic clonal expansion during adipogenesis. *Proc Natl Acad Sci U S A* 100: 850-855.
70. Tanaka T, Yoshida N, Kishimoto T, Akira S (1997) Defective adipocyte differentiation in mice lacking the C/EBPbeta and/or C/EBPdelta gene. *EMBO J* 16: 7432-7443.
71. Birsoy K, Chen Z, Friedman J (2008) Transcriptional regulation of adipogenesis by KLF4. *Cell Metab* 7: 339-347.

72. Oishi Y, Manabe I, Tobe K, Tsushima K, Shindo T, et al. (2005) Kruppel-like transcription factor KLF5 is a key regulator of adipocyte differentiation. *Cell Metab* 1: 27-39.
73. Pei H, Yao Y, Yang Y, Liao K, Wu JR (2011) Kruppel-like factor KLF9 regulates PPARgamma transactivation at the middle stage of adipogenesis. *Cell Death Differ* 18: 315-327.
74. Mori T, Sakaue H, Iguchi H, Gomi H, Okada Y, et al. (2005) Role of Kruppel-like factor 15 (KLF15) in transcriptional regulation of adipogenesis. *J Biol Chem* 280: 12867-12875.
75. Oishi Y, Manabe I, Tobe K, Ohsugi M, Kubota T, et al. (2008) SUMOylation of Kruppel-like transcription factor 5 acts as a molecular switch in transcriptional programs of lipid metabolism involving PPAR-delta. *Nat Med* 14: 656-666.
76. Li D, Yea S, Li S, Chen Z, Narla G, et al. (2005) Kruppel-like factor-6 promotes preadipocyte differentiation through histone deacetylase 3-dependent repression of DLK1. *J Biol Chem* 280: 26941-26952.
77. Tontonoz P, Kim JB, Graves RA, Spiegelman BM (1993) ADD1: a novel helix-loop-helix transcription factor associated with adipocyte determination and differentiation. *Mol Cell Biol* 13: 4753-4759.
78. Hua X, Wu J, Goldstein JL, Brown MS, Hobbs HH (1995) Structure of the human gene encoding sterol regulatory element binding protein-1 (SREBF1) and localization of SREBF1 and SREBF2 to chromosomes 17p11.2 and 22q13. *Genomics* 25: 667-673.
79. Shimomura I, Shimano H, Horton JD, Goldstein JL, Brown MS (1997) Differential expression of exons 1a and 1c in mRNAs for sterol regulatory element binding protein-1 in human and mouse organs and cultured cells. *J Clin Invest* 99: 838-845.
80. Kim JB, Spiegelman BM (1996) ADD1/SREBP1 promotes adipocyte differentiation and gene expression linked to fatty acid metabolism. *Genes Dev* 10: 1096-1107.
81. Reusch JE, Colton LA, Klemm DJ (2000) CREB activation induces adipogenesis in 3T3-L1 cells. *Mol Cell Biol* 20: 1008-1020.
82. Zhang JW, Klemm DJ, Vinson C, Lane MD (2004) Role of CREB in transcriptional regulation of CCAAT/enhancer-binding protein beta gene during adipogenesis. *J Biol Chem* 279: 4471-4478.
83. Fox KE, Fankell DM, Erickson PF, Majka SM, Crossno JT, Jr., et al. (2006) Depletion of cAMP-response element-binding protein/ATF1 inhibits adipogenic conversion of 3T3-L1 cells ectopically expressing CCAAT/enhancer-binding protein (C/EBP) alpha, C/EBP beta, or PPAR gamma 2. *J Biol Chem* 281: 40341-40353.
84. Wu Z, Wang S (2013) Role of kruppel-like transcription factors in adipogenesis. *Dev Biol* 373: 235-243.
85. Banerjee SS, Feinberg MW, Watanabe M, Gray S, Haspel RL, et al. (2003) The Kruppel-like factor KLF2 inhibits peroxisome proliferator-activated receptor-gamma expression and adipogenesis. *J Biol Chem* 278: 2581-2584.
86. Sue N, Jack BH, Eaton SA, Pearson RC, Funnell AP, et al. (2008) Targeted disruption of the basic Kruppel-like factor gene (Klf3) reveals a role in adipogenesis. *Mol Cell Biol* 28: 3967-3978.
87. Kawamura Y, Tanaka Y, Kawamori R, Maeda S (2006) Overexpression of Kruppel-like factor 7 regulates adipocytokine gene expressions in human adipocytes and inhibits glucose-induced insulin secretion in pancreatic beta-cell line. *Mol Endocrinol* 20: 844-856.

88. Cho SY, Park PJ, Shin HJ, Kim YK, Shin DW, et al. (2007) (-)-Catechin suppresses expression of Kruppel-like factor 7 and increases expression and secretion of adiponectin protein in 3T3-L1 cells. *Am J Physiol Endocrinol Metab* 292: E1166-1172.
89. Kanazawa A, Kawamura Y, Sekine A, Iida A, Tsunoda T, et al. (2005) Single nucleotide polymorphisms in the gene encoding Kruppel-like factor 7 are associated with type 2 diabetes. *Diabetologia* 48: 1315-1322.
90. Weiss MJ, Orkin SH (1995) GATA transcription factors: key regulators of hematopoiesis. *Exp Hematol* 23: 99-107.
91. Tong Q, Dalgin G, Xu H, Ting CN, Leiden JM, et al. (2000) Function of GATA transcription factors in preadipocyte-adipocyte transition. *Science* 290: 134-138.
92. Smas CM, Sul HS (1993) Pref-1, a protein containing EGF-like repeats, inhibits adipocyte differentiation. *Cell* 73: 725-734.
93. Wang Y, Kim KA, Kim JH, Sul HS (2006) Pref-1, a preadipocyte secreted factor that inhibits adipogenesis. *J Nutr* 136: 2953-2956.
94. Smas CM, Chen L, Zhao L, Latasa MJ, Sul HS (1999) Transcriptional repression of pref-1 by glucocorticoids promotes 3T3-L1 adipocyte differentiation. *J Biol Chem* 274: 12632-12641.
95. Moon YS, Smas CM, Lee K, Villena JA, Kim KH, et al. (2002) Mice lacking paternally expressed Pref-1/Dlk1 display growth retardation and accelerated adiposity. *Mol Cell Biol* 22: 5585-5592.
96. Lee K, Villena JA, Moon YS, Kim KH, Lee S, et al. (2003) Inhibition of adipogenesis and development of glucose intolerance by soluble preadipocyte factor-1 (Pref-1). *J Clin Invest* 111: 453-461.
97. Villena JA, Choi CS, Wang Y, Kim S, Hwang YJ, et al. (2008) Resistance to high-fat diet-induced obesity but exacerbated insulin resistance in mice overexpressing preadipocyte factor-1 (Pref-1): a new model of partial lipodystrophy. *Diabetes* 57: 3258-3266.
98. Zhang H, Noohr J, Jensen CH, Petersen RK, Bachmann E, et al. (2003) Insulin-like growth factor-1/insulin bypasses Pref-1/FA1-mediated inhibition of adipocyte differentiation. *J Biol Chem* 278: 20906-20914.
99. Ruiz-Hidalgo MJ, Gubina E, Tull L, Baladron V, Laborda J (2002) dlk modulates mitogen-activated protein kinase signaling to allow or prevent differentiation. *Exp Cell Res* 274: 178-188.
100. Kim KA, Kim JH, Wang Y, Sul HS (2007) Pref-1 (preadipocyte factor 1) activates the MEK/extracellular signal-regulated kinase pathway to inhibit adipocyte differentiation. *Mol Cell Biol* 27: 2294-2308.
101. Wang Y, Sul HS (2009) Pref-1 regulates mesenchymal cell commitment and differentiation through Sox9. *Cell Metab* 9: 287-302.
102. Carthew RW, Sontheimer EJ (2009) Origins and Mechanisms of miRNAs and siRNAs. *Cell* 136: 642-655.
103. Ambros V (2001) microRNAs: tiny regulators with great potential. *Cell* 107: 823-826.
104. Bartel DP (2009) MicroRNAs: target recognition and regulatory functions. *Cell* 136: 215-233.
105. Chen K, Rajewsky N (2007) The evolution of gene regulation by transcription factors and microRNAs. *Nat Rev Genet* 8: 93-103.

### **1.3.3.1.1 MicroRNA miR-27**

The miR-27 family consists of miR-27a and miR-27b, which are transcribed from different chromosomes. miR-27a and miR-27b are two highly conserved isoforms that have identical seed sequences and differ in only one nucleotide [143].

Both miR-27a and miR-27b levels are elevated in adipose tissue of genetically obese *ob/ob* mice [122]. However, the levels of pri-miR-27a are downregulated in mature adipocytes of HFD-fed obese mice comparing to chow diet-fed lean mice [121]. Moreover, the microRNAs miR-27a and miR-27b were described to impair adipocyte differentiation [121,122,144].

At the molecular level, it was demonstrated that miR-27a and miR-27b binds the 3'UTR of PPAR $\gamma$  mRNA and that both decrease during adipocyte differentiation of 3T3-L1 preadipocytes [121,123]. However, in 3T3-L1 preadipocytes, overexpression of miR-27a and miR-27b also inhibits adipogenesis by inhibiting the expression of PPAR $\gamma$  mRNA but with no alteration in PPAR $\gamma$  protein levels [122]. Additionally, miR-27 was described to suppress adipogenesis by also targeting prohibitin [144]. Prohibitin increases during differentiation and its silencing inhibits adipogenesis in 3T3-L1 preadipocytes [145]. Overexpression of miR-27a and miR-27b decreases both mRNA and protein levels of prohibitin and impairs adipocyte differentiation [144].

### **1.3.3.2 Autophagy**

Autophagy is an intracellular degradation system that targets cytoplasmic substrates for lysosomal degradation [146]. Three types of mammalian autophagy have been described: chaperone-mediated autophagy, microautophagy and macroautophagy [147]. Chaperone-mediated autophagy targets specific proteins that contain a pentapeptide motif (KFERQ) [148]. This motif is recognized by a chaperone complex that transfers the proteins to the lysosomal through the receptor lysosome-associated membrane protein 2A (LAMP2A) [149]. The proteins are degraded in the lysosomal lumen. Microautophagy involves the direct engulfment of cytosolic cargo by invagination or evagination into the lysosomal lumen for degradation [150,151]. Macroautophagy, referred here as autophagy, is the best studied type of autophagy in which cells form a double-membraned vesicle named autophagosome. Autophagosomes form around a portion of cytoplasm that engulfs proteins and organelles degrading them after fusion with the lysosome [152,153].

Autophagosome formation comprises several steps: induction of autophagosome formation; nucleation of the membrane; autophagosomal elongation; cargo selection; and autophagosome maturation and cargo degradation (Figure 1.8).

125. Tang YF, Zhang Y, Li XY, Li C, Tian W, et al. (2009) Expression of miR-31, miR-125b-5p, and miR-326 in the adipogenic differentiation process of adipose-derived stem cells. *OMICS* 13: 331-336.
126. Sun F, Wang J, Pan Q, Yu Y, Zhang Y, et al. (2009) Characterization of function and regulation of miR-24-1 and miR-31. *Biochem Biophys Res Commun* 380: 660-665.
127. Xie H, Lim B, Lodish HF (2009) MicroRNAs induced during adipogenesis that accelerate fat cell development are downregulated in obesity. *Diabetes* 58: 1050-1057.
128. Wilfred BR, Wang WX, Nelson PT (2007) Energizing miRNA research: a review of the role of miRNAs in lipid metabolism, with a prediction that miR-103/107 regulates human metabolic pathways. *Mol Genet Metab* 91: 209-217.
129. Qadir AS, Woo KM, Ryoo HM, Baek JH (2013) Insulin suppresses distal-less homeobox 5 expression through the up-regulation of microRNA-124 in 3T3-L1 cells. *Exp Cell Res* 319: 2125-2134.
130. Lee EK, Lee MJ, Abdelmohsen K, Kim W, Kim MM, et al. (2011) miR-130 suppresses adipogenesis by inhibiting peroxisome proliferator-activated receptor gamma expression. *Mol Cell Biol* 31: 626-638.
131. Yang Z, Bian C, Zhou H, Huang S, Wang S, et al. (2011) MicroRNA hsa-miR-138 inhibits adipogenic differentiation of human adipose tissue-derived mesenchymal stem cells through adenovirus EID-1. *Stem Cells Dev* 20: 259-267.
132. Oskowitz AZ, Lu J, Penforis P, Ylostalo J, McBride J, et al. (2008) Human multipotent stromal cells from bone marrow and microRNA: regulation of differentiation and leukemia inhibitory factor expression. *Proc Natl Acad Sci U S A* 105: 18372-18377.
133. Liu S, Yang Y, Wu J (2011) TNFalpha-induced up-regulation of miR-155 inhibits adipogenesis by down-regulating early adipogenic transcription factors. *Biochem Biophys Res Commun* 414: 618-624.
134. McGregor RA, Choi MS (2011) microRNAs in the regulation of adipogenesis and obesity. *Curr Mol Med* 11: 304-316.
135. Huang J, Zhao L, Xing L, Chen D (2010) MicroRNA-204 regulates Runx2 protein expression and mesenchymal progenitor cell differentiation. *Stem Cells* 28: 357-364.
136. Qin L, Chen Y, Niu Y, Chen W, Wang Q, et al. (2010) A deep investigation into the adipogenesis mechanism: profile of microRNAs regulating adipogenesis by modulating the canonical Wnt/beta-catenin signaling pathway. *BMC Genomics* 11: 320.
137. Ling HY, Ou HS, Feng SD, Zhang XY, Tuo QH, et al. (2009) CHANGES IN microRNA (miR) profile and effects of miR-320 in insulin-resistant 3T3-L1 adipocytes. *Clin Exp Pharmacol Physiol* 36: e32-39.
138. Zhu L, Chen L, Shi CM, Xu GF, Xu LL, et al. (2014) MiR-335, an adipogenesis-related microRNA, is involved in adipose tissue inflammation. *Cell Biochem Biophys* 68: 283-290.
139. Ling HY, Wen GB, Feng SD, Tuo QH, Ou HS, et al. (2011) MicroRNA-375 promotes 3T3-L1 adipocyte differentiation through modulation of extracellular signal-regulated kinase signalling. *Clin Exp Pharmacol Physiol* 38: 239-246.
140. Carrer M, Liu N, Grueter CE, Williams AH, Frisard MI, et al. (2012) Control of mitochondrial metabolism and systemic energy homeostasis by microRNAs 378 and 378\*. *Proc Natl Acad Sci U S A* 109: 15330-15335.



141. Jin W, Dodson MV, Moore SS, Basarab JA, Guan LL (2010) Characterization of microRNA expression in bovine adipose tissues: a potential regulatory mechanism of subcutaneous adipose tissue development. *BMC Mol Biol* 11: 29.
142. Kinoshita M, Ono K, Horie T, Nagao K, Nishi H, et al. (2010) Regulation of adipocyte differentiation by activation of serotonin (5-HT) receptors 5-HT<sub>2A</sub>R and 5-HT<sub>2C</sub>R and involvement of microRNA-448-mediated repression of KLF5. *Mol Endocrinol* 24: 1978-1987.
143. Zhang M, Wu JF, Chen WJ, Tang SL, Mo ZC, et al. (2014) MicroRNA-27a/b regulates cellular cholesterol efflux, influx and esterification/hydrolysis in THP-1 macrophages. *Atherosclerosis* 234: 54-64.
144. Kang T, Lu W, Xu W, Anderson L, Bacanamwo M, et al. (2013) MicroRNA-27 (miR-27) targets prohibitin and impairs adipocyte differentiation and mitochondrial function in human adipose-derived stem cells. *J Biol Chem* 288: 34394-34402.
145. Liu D, Lin Y, Kang T, Huang B, Xu W, et al. (2012) Mitochondrial dysfunction and adipogenic reduction by prohibitin silencing in 3T3-L1 cells. *PLoS One* 7: e34315.
146. Yang Z, Klionsky DJ (2010) Mammalian autophagy: core molecular machinery and signaling regulation. *Curr Opin Cell Biol* 22: 124-131.
147. Mizushima N (2004) Methods for monitoring autophagy. *Int J Biochem Cell Biol* 36: 2491-2502.
148. Dice JF (1990) Peptide sequences that target cytosolic proteins for lysosomal proteolysis. *Trends Biochem Sci* 15: 305-309.
149. Cuervo AM, Dice JF (1996) A receptor for the selective uptake and degradation of proteins by lysosomes. *Science* 273: 501-503.
150. Ahlberg J, Glaumann H (1985) Uptake--microautophagy--and degradation of exogenous proteins by isolated rat liver lysosomes. Effects of pH, ATP, and inhibitors of proteolysis. *Exp Mol Pathol* 42: 78-88.
151. Kunz JB, Schwarz H, Mayer A (2004) Determination of four sequential stages during microautophagy in vitro. *J Biol Chem* 279: 9987-9996.
152. Ravikumar B, Sarkar S, Davies JE, Futter M, Garcia-Arencibia M, et al. (2010) Regulation of mammalian autophagy in physiology and pathophysiology. *Physiol Rev* 90: 1383-1435.
153. Mizushima N, Komatsu M (2011) Autophagy: renovation of cells and tissues. *Cell* 147: 728-741.
154. Wirawan E, Vanden Berghe T, Lippens S, Agostinis P, Vandenabeele P (2012) Autophagy: for better or for worse. *Cell Res* 22: 43-61.
155. Jung CH, Ro SH, Cao J, Otto NM, Kim DH (2010) mTOR regulation of autophagy. *FEBS Lett* 584: 1287-1295.
156. Laplante M, Sabatini DM (2009) mTOR signaling at a glance. *J Cell Sci* 122: 3589-3594.
157. Sengupta S, Peterson TR, Sabatini DM (2010) Regulation of the mTOR complex 1 pathway by nutrients, growth factors, and stress. *Mol Cell* 40: 310-322.
158. Volinia S, Dhand R, Vanhaesebroeck B, MacDougall LK, Stein R, et al. (1995) A human phosphatidylinositol 3-kinase complex related to the yeast Vps34p-Vps15p protein sorting system. *EMBO J* 14: 3339-3348.

159. Kihara A, Noda T, Ishihara N, Ohsumi Y (2001) Two distinct Vps34 phosphatidylinositol 3-kinase complexes function in autophagy and carboxypeptidase Y sorting in *Saccharomyces cerevisiae*. *J Cell Biol* 152: 519-530.
160. Kuma A, Mizushima N, Ishihara N, Ohsumi Y (2002) Formation of the approximately 350-kDa Apg12-Apg5-Apg16 multimeric complex, mediated by Apg16 oligomerization, is essential for autophagy in yeast. *J Biol Chem* 277: 18619-18625.
161. Mizushima N, Kuma A, Kobayashi Y, Yamamoto A, Matsubae M, et al. (2003) Mouse Apg16L, a novel WD-repeat protein, targets to the autophagic isolation membrane with the Apg12-Apg5 conjugate. *J Cell Sci* 116: 1679-1688.
162. Hanada T, Noda NN, Satomi Y, Ichimura Y, Fujioka Y, et al. (2007) The Atg12-Atg5 conjugate has a novel E3-like activity for protein lipidation in autophagy. *J Biol Chem* 282: 37298-37302.
163. Tanida I, Ueno T, Kominami E (2004) LC3 conjugation system in mammalian autophagy. *Int J Biochem Cell Biol* 36: 2503-2518.
164. Shibata M, Yoshimura K, Tamura H, Ueno T, Nishimura T, et al. (2010) LC3, a microtubule-associated protein1A/B light chain3, is involved in cytoplasmic lipid droplet formation. *Biochem Biophys Res Commun* 393: 274-279.
165. Bjorkoy G, Lamark T, Brech A, Outzen H, Perander M, et al. (2005) p62/SQSTM1 forms protein aggregates degraded by autophagy and has a protective effect on huntingtin-induced cell death. *J Cell Biol* 171: 603-614.
166. Pankiv S, Clausen TH, Lamark T, Brech A, Bruun JA, et al. (2007) p62/SQSTM1 binds directly to Atg8/LC3 to facilitate degradation of ubiquitinated protein aggregates by autophagy. *J Biol Chem* 282: 24131-24145.
167. Babu JR, Geetha T, Wooten MW (2005) Sequestosome 1/p62 shuttles polyubiquitinated tau for proteasomal degradation. *J Neurochem* 94: 192-203.
168. Seibenhener ML, Babu JR, Geetha T, Wong HC, Krishna NR, et al. (2004) Sequestosome 1/p62 is a polyubiquitin chain binding protein involved in ubiquitin proteasome degradation. *Mol Cell Biol* 24: 8055-8068.
169. Weidberg H, Shvets E, Elazar Z (2011) Biogenesis and cargo selectivity of autophagosomes. *Annu Rev Biochem* 80: 125-156.
170. Tong J, Yan X, Yu L (2010) The late stage of autophagy: cellular events and molecular regulation. *Protein Cell* 1: 907-915.
171. Jager S, Bucci C, Tanida I, Ueno T, Kominami E, et al. (2004) Role for Rab7 in maturation of late autophagic vacuoles. *J Cell Sci* 117: 4837-4848.
172. Tanida I, Minematsu-Ikeguchi N, Ueno T, Kominami E (2005) Lysosomal turnover, but not a cellular level, of endogenous LC3 is a marker for autophagy. *Autophagy* 1: 84-91.
173. Mizushima N, Yoshimori T, Levine B (2010) Methods in mammalian autophagy research. *Cell* 140: 313-326.
174. Singh R, Xiang Y, Wang Y, Baikati K, Cuervo AM, et al. (2009) Autophagy regulates adipose mass and differentiation in mice. *J Clin Invest* 119: 3329-3339.
175. Zhang Y, Goldman S, Baerga R, Zhao Y, Komatsu M, et al. (2009) Adipose-specific deletion of autophagy-related gene 7 (*atg7*) in mice reveals a role in adipogenesis. *Proc Natl Acad Sci U S A* 106: 19860-19865.

176. Baerga R, Zhang Y, Chen PH, Goldman S, Jin S (2009) Targeted deletion of autophagy-related 5 (atg5) impairs adipogenesis in a cellular model and in mice. *Autophagy* 5: 1118-1130.
177. Kovsan J, Bluher M, Tarnovscki T, Kloting N, Kirshtein B, et al. (2011) Altered autophagy in human adipose tissues in obesity. *J Clin Endocrinol Metab* 96: E268-277.
178. Large V, Peroni O, Letexier D, Ray H, Beylot M (2004) Metabolism of lipids in human white adipocyte. *Diabetes Metab* 30: 294-309.
179. Fabbrini E, Magkos F, Mohammed BS, Pietka T, Abumrad NA, et al. (2009) Intrahepatic fat, not visceral fat, is linked with metabolic complications of obesity. *Proc Natl Acad Sci U S A* 106: 15430-15435.
180. Krssak M, Falk Petersen K, Dresner A, DiPietro L, Vogel SM, et al. (1999) Intramyocellular lipid concentrations are correlated with insulin sensitivity in humans: a <sup>1</sup>H NMR spectroscopy study. *Diabetologia* 42: 113-116.
181. El-Assaad W, Buteau J, Peyot ML, Nolan C, Roduit R, et al. (2003) Saturated fatty acids synergize with elevated glucose to cause pancreatic beta-cell death. *Endocrinology* 144: 4154-4163.
182. Sethi JK, Vidal-Puig AJ (2007) Thematic review series: adipocyte biology. Adipose tissue function and plasticity orchestrate nutritional adaptation. *J Lipid Res* 48: 1253-1262.
183. Kersten S (2001) Mechanisms of nutritional and hormonal regulation of lipogenesis. *EMBO Rep* 2: 282-286.
184. Brown CM, Layman DK (1988) Lipoprotein lipase activity and chylomicron clearance in rats fed a high fat diet. *J Nutr* 118: 1294-1298.
185. Tacke PJ, Hofker MH, Havekes LM, van Dijk KW (2001) Living up to a name: the role of the VLDL receptor in lipid metabolism. *Curr Opin Lipidol* 12: 275-279.
186. Misra KB, Kim KC, Cho S, Low MG, Bensadoun A (1994) Purification and characterization of adipocyte heparan sulfate proteoglycans with affinity for lipoprotein lipase. *J Biol Chem* 269: 23838-23844.
187. Mead JR, Irvine SA, Ramji DP (2002) Lipoprotein lipase: structure, function, regulation, and role in disease. *J Mol Med (Berl)* 80: 753-769.
188. Schaffer JE, Lodish HF (1994) Expression cloning and characterization of a novel adipocyte long chain fatty acid transport protein. *Cell* 79: 427-436.
189. Febbraio M, Abumrad NA, Hajjar DP, Sharma K, Cheng W, et al. (1999) A null mutation in murine CD36 reveals an important role in fatty acid and lipoprotein metabolism. *J Biol Chem* 274: 19055-19062.
190. Hertzler AV, Smith LA, Berg AH, Cline GW, Shulman GI, et al. (2006) Lipid metabolism and adipokine levels in fatty acid-binding protein null and transgenic mice. *Am J Physiol Endocrinol Metab* 290: E814-823.
191. Coleman RA, Lee DP (2004) Enzymes of triacylglycerol synthesis and their regulation. *Prog Lipid Res* 43: 134-176.
192. Olson AL, Pessin JE (1996) Structure, function, and regulation of the mammalian facilitative glucose transporter gene family. *Annu Rev Nutr* 16: 235-256.
193. Martin S, Parton RG (2006) Lipid droplets: a unified view of a dynamic organelle. *Nat Rev Mol Cell Biol* 7: 373-378.

194. Miura S, Gan JW, Brzostowski J, Parisi MJ, Schultz CJ, et al. (2002) Functional conservation for lipid storage droplet association among Perilipin, ADRP, and TIP47 (PAT)-related proteins in mammals, *Drosophila*, and *Dictyostelium*. *J Biol Chem* 277: 32253-32257.
195. Lu X, Gruia-Gray J, Copeland NG, Gilbert DJ, Jenkins NA, et al. (2001) The murine perilipin gene: the lipid droplet-associated perilipins derive from tissue-specific, mRNA splice variants and define a gene family of ancient origin. *Mamm Genome* 12: 741-749.
196. Brasaemle DL, Rubin B, Harten IA, Gruia-Gray J, Kimmel AR, et al. (2000) Perilipin A increases triacylglycerol storage by decreasing the rate of triacylglycerol hydrolysis. *J Biol Chem* 275: 38486-38493.
197. Brasaemle DL (2007) Thematic review series: adipocyte biology. The perilipin family of structural lipid droplet proteins: stabilization of lipid droplets and control of lipolysis. *J Lipid Res* 48: 2547-2559.
198. Nishiu J, Tanaka T, Nakamura Y (1998) Isolation and chromosomal mapping of the human homolog of perilipin (PLIN), a rat adipose tissue-specific gene, by differential display method. *Genomics* 48: 254-257.
199. Greenberg AS, Egan JJ, Wek SA, Moos MC, Jr., Londos C, et al. (1993) Isolation of cDNAs for perilipins A and B: sequence and expression of lipid droplet-associated proteins of adipocytes. *Proc Natl Acad Sci U S A* 90: 12035-12039.
200. Martinez-Botas J, Anderson JB, Tessier D, Lapillonne A, Chang BH, et al. (2000) Absence of perilipin results in leanness and reverses obesity in *Lepr(db/db)* mice. *Nat Genet* 26: 474-479.
201. Tansey JT, Sztalryd C, Gruia-Gray J, Roush DL, Zee JV, et al. (2001) Perilipin ablation results in a lean mouse with aberrant adipocyte lipolysis, enhanced leptin production, and resistance to diet-induced obesity. *Proc Natl Acad Sci U S A* 98: 6494-6499.
202. Sztalryd C, Xu G, Dorward H, Tansey JT, Contreras JA, et al. (2003) Perilipin A is essential for the translocation of hormone-sensitive lipase during lipolytic activation. *J Cell Biol* 161: 1093-1103.
203. Kern PA, Di Gregorio G, Lu T, Rassouli N, Ranganathan G (2004) Perilipin expression in human adipose tissue is elevated with obesity. *J Clin Endocrinol Metab* 89: 1352-1358.
204. Arner P (2005) Human fat cell lipolysis: biochemistry, regulation and clinical role. *Best Pract Res Clin Endocrinol Metab* 19: 471-482.
205. Carmen GY, Victor SM (2006) Signalling mechanisms regulating lipolysis. *Cell Signal* 18: 401-408.
206. Zimmermann R, Strauss JG, Haemmerle G, Schoiswohl G, Birner-Gruenberger R, et al. (2004) Fat mobilization in adipose tissue is promoted by adipose triglyceride lipase. *Science* 306: 1383-1386.
207. Haemmerle G, Lass A, Zimmermann R, Gorkiewicz G, Meyer C, et al. (2006) Defective lipolysis and altered energy metabolism in mice lacking adipose triglyceride lipase. *Science* 312: 734-737.
208. Fredrikson G, Tornqvist H, Belfrage P (1986) Hormone-sensitive lipase and monoacylglycerol lipase are both required for complete degradation of adipocyte triacylglycerol. *Biochim Biophys Acta* 876: 288-293.
209. Brodersen R, Andersen S, Vorum H, Nielsen SU, Pedersen AO (1990) Multiple fatty acid binding to albumin in human blood plasma. *Eur J Biochem* 189: 343-349.

210. Zhang Y, Proenca R, Maffei M, Barone M, Leopold L, et al. (1994) Positional cloning of the mouse obese gene and its human homologue. *Nature* 372: 425-432.
211. Ahima RS (2008) Revisiting leptin's role in obesity and weight loss. *J Clin Invest* 118: 2380-2383.
212. Kawano J, Arora R (2009) The role of adiponectin in obesity, diabetes, and cardiovascular disease. *J Cardiometab Syndr* 4: 44-49.
213. Chang YH, Chang DM, Lin KC, Shin SJ, Lee YJ (2011) Visfatin in overweight/obesity, type 2 diabetes mellitus, insulin resistance, metabolic syndrome and cardiovascular diseases: a meta-analysis and systemic review. *Diabetes Metab Res Rev* 27: 515-527.
214. Kusminski CM, McTernan PG, Kumar S (2005) Role of resistin in obesity, insulin resistance and Type II diabetes. *Clin Sci (Lond)* 109: 243-256.
215. Flier JS, Lowell B, Napolitano A, Usher P, Rosen B, et al. (1989) Adipsin: regulation and dysregulation in obesity and other metabolic states. *Recent Prog Horm Res* 45: 567-580; discussion 580-561.
216. Bluher M (2012) Vaspin in obesity and diabetes: pathophysiological and clinical significance. *Endocrine* 41: 176-182.
217. de Souza Batista CM, Yang RZ, Lee MJ, Glynn NM, Yu DZ, et al. (2007) Omentin plasma levels and gene expression are decreased in obesity. *Diabetes* 56: 1655-1661.
218. Wolf G (2007) Serum retinol-binding protein: a link between obesity, insulin resistance, and type 2 diabetes. *Nutr Rev* 65: 251-256.
219. Castan-Laurell I, Dray C, Attane C, Duparc T, Knauf C, et al. (2011) Apelin, diabetes, and obesity. *Endocrine* 40: 1-9.
220. Rohrborn D, Wronkowitz N, Eckel J (2015) DPP4 in Diabetes. *Front Immunol* 6: 386.
221. Tzanavari T, Giannogonas P, Karalis KP (2010) TNF-alpha and obesity. *Curr Dir Autoimmun* 11: 145-156.
222. Eder K, Baffy N, Falus A, Fulop AK (2009) The major inflammatory mediator interleukin-6 and obesity. *Inflamm Res* 58: 727-736.
223. Yadav H, Quijano C, Kamaraju AK, Gavrilova O, Malek R, et al. (2011) Protection from obesity and diabetes by blockade of TGF-beta/Smad3 signaling. *Cell Metab* 14: 67-79.
224. Alessi MC, Poggi M, Juhan-Vague I (2007) Plasminogen activator inhibitor-1, adipose tissue and insulin resistance. *Curr Opin Lipidol* 18: 240-245.
225. Halaas JL, Gajiwala KS, Maffei M, Cohen SL, Chait BT, et al. (1995) Weight-reducing effects of the plasma protein encoded by the obese gene. *Science* 269: 543-546.
226. Ahima RS (2006) Adipose tissue as an endocrine organ. *Obesity (Silver Spring)* 14 Suppl 5: 242S-249S.
227. Ahima RS, Prabakaran D, Mantzoros C, Qu D, Lowell B, et al. (1996) Role of leptin in the neuroendocrine response to fasting. *Nature* 382: 250-252.
228. Chen H, Charlat O, Tartaglia LA, Woolf EA, Weng X, et al. (1996) Evidence that the diabetes gene encodes the leptin receptor: identification of a mutation in the leptin receptor gene in db/db mice. *Cell* 84: 491-495.
229. Pelleymounter MA, Cullen MJ, Baker MB, Hecht R, Winters D, et al. (1995) Effects of the obese gene product on body weight regulation in ob/ob mice. *Science* 269: 540-543.

230. Scherer PE, Williams S, Fogliano M, Baldini G, Lodish HF (1995) A novel serum protein similar to C1q, produced exclusively in adipocytes. *J Biol Chem* 270: 26746-26749.
231. Hu E, Liang P, Spiegelman BM (1996) AdipoQ is a novel adipose-specific gene dysregulated in obesity. *J Biol Chem* 271: 10697-10703.
232. Maeda K, Okubo K, Shimomura I, Funahashi T, Matsuzawa Y, et al. (1996) cDNA cloning and expression of a novel adipose specific collagen-like factor, apM1 (AdiPose Most abundant Gene transcript 1). *Biochem Biophys Res Commun* 221: 286-289.
233. Nakano Y, Tobe T, Choi-Miura NH, Mazda T, Tomita M (1996) Isolation and characterization of GBP28, a novel gelatin-binding protein purified from human plasma. *J Biochem* 120: 803-812.
234. Yamauchi T, Kamon J, Ito Y, Tsuchida A, Yokomizo T, et al. (2003) Cloning of adiponectin receptors that mediate antidiabetic metabolic effects. *Nature* 423: 762-769.
235. Arita Y, Kihara S, Ouchi N, Takahashi M, Maeda K, et al. (1999) Paradoxical decrease of an adipose-specific protein, adiponectin, in obesity. *Biochem Biophys Res Commun* 257: 79-83.
236. Yamauchi T, Kamon J, Waki H, Terauchi Y, Kubota N, et al. (2001) The fat-derived hormone adiponectin reverses insulin resistance associated with both lipoatrophy and obesity. *Nat Med* 7: 941-946.
237. Berg AH, Combs TP, Du X, Brownlee M, Scherer PE (2001) The adipocyte-secreted protein Acrp30 enhances hepatic insulin action. *Nat Med* 7: 947-953.
238. Yamauchi T, Kamon J, Minokoshi Y, Ito Y, Waki H, et al. (2002) Adiponectin stimulates glucose utilization and fatty-acid oxidation by activating AMP-activated protein kinase. *Nat Med* 8: 1288-1295.
239. Kubota N, Terauchi Y, Yamauchi T, Kubota T, Moroi M, et al. (2002) Disruption of adiponectin causes insulin resistance and neointimal formation. *J Biol Chem* 277: 25863-25866.
240. Maeda N, Shimomura I, Kishida K, Nishizawa H, Matsuda M, et al. (2002) Diet-induced insulin resistance in mice lacking adiponectin/ACRP30. *Nat Med* 8: 731-737.
241. Chen H, Montagnani M, Funahashi T, Shimomura I, Quon MJ (2003) Adiponectin stimulates production of nitric oxide in vascular endothelial cells. *J Biol Chem* 278: 45021-45026.
242. Shibata R, Ouchi N, Ito M, Kihara S, Shiojima I, et al. (2004) Adiponectin-mediated modulation of hypertrophic signals in the heart. *Nat Med* 10: 1384-1389.
243. Kubota N, Yano W, Kubota T, Yamauchi T, Itoh S, et al. (2007) Adiponectin stimulates AMP-activated protein kinase in the hypothalamus and increases food intake. *Cell Metab* 6: 55-68.
244. Steppan CM, Bailey ST, Bhat S, Brown EJ, Banerjee RR, et al. (2001) The hormone resistin links obesity to diabetes. *Nature* 409: 307-312.
245. Banerjee RR, Rangwala SM, Shapiro JS, Rich AS, Rhoades B, et al. (2004) Regulation of fasted blood glucose by resistin. *Science* 303: 1195-1198.
246. Sanchez-Solana B, Laborda J, Baladron V (2012) Mouse resistin modulates adipogenesis and glucose uptake in 3T3-L1 preadipocytes through the ROR1 receptor. *Mol Endocrinol* 26: 110-127.
247. Ikeda Y, Tsuchiya H, Hama S, Kajimoto K, Kogure K (2013) Resistin affects lipid metabolism during adipocyte maturation of 3T3-L1 cells. *FEBS J* 280: 5884-5895.

248. Muse ED, Feldman DI, Blaha MJ, Dardari ZA, Blumenthal RS, et al. (2015) The association of resistin with cardiovascular disease in the Multi-Ethnic Study of Atherosclerosis. *Atherosclerosis* 239: 101-108.
249. Yang RZ, Lee MJ, Hu H, Pray J, Wu HB, et al. (2006) Identification of omentin as a novel depot-specific adipokine in human adipose tissue: possible role in modulating insulin action. *Am J Physiol Endocrinol Metab* 290: E1253-1261.
250. Schaffler A, Neumeier M, Herfarth H, Furst A, Scholmerich J, et al. (2005) Genomic structure of human omentin, a new adipocytokine expressed in omental adipose tissue. *Biochim Biophys Acta* 1732: 96-102.
251. Yang Q, Graham TE, Mody N, Preitner F, Peroni OD, et al. (2005) Serum retinol binding protein 4 contributes to insulin resistance in obesity and type 2 diabetes. *Nature* 436: 356-362.
252. Slawik M, Vidal-Puig AJ (2007) Adipose tissue expandability and the metabolic syndrome. *Genes Nutr* 2: 41-45.
253. Jacob S, Machann J, Rett K, Brechtel K, Volk A, et al. (1999) Association of increased intramyocellular lipid content with insulin resistance in lean nondiabetic offspring of type 2 diabetic subjects. *Diabetes* 48: 1113-1119.
254. Kusminski CM, Scherer PE (2012) Mitochondrial dysfunction in white adipose tissue. *Trends Endocrinol Metab* 23: 435-443.
255. Chattopadhyay M, Khemka VK, Chatterjee G, Ganguly A, Mukhopadhyay S, et al. (2015) Enhanced ROS production and oxidative damage in subcutaneous white adipose tissue mitochondria in obese and type 2 diabetes subjects. *Mol Cell Biochem* 399: 95-103.
256. Liu J, Shen W, Zhao B, Wang Y, Wertz K, et al. (2009) Targeting mitochondrial biogenesis for preventing and treating insulin resistance in diabetes and obesity: Hope from natural mitochondrial nutrients. *Adv Drug Deliv Rev* 61: 1343-1352.
257. Hotamisligil GS (2006) Inflammation and metabolic disorders. *Nature* 444: 860-867.
258. Lumeng CN, Bodzin JL, Saltiel AR (2007) Obesity induces a phenotypic switch in adipose tissue macrophage polarization. *J Clin Invest* 117: 175-184.
259. Lackey DE, Olefsky JM (2016) Regulation of metabolism by the innate immune system. *Nat Rev Endocrinol* 12: 15-28.
260. Trayhurn P (2014) Hypoxia and adipocyte physiology: implications for adipose tissue dysfunction in obesity. *Annu Rev Nutr* 34: 207-236.
261. Halberg N, Khan T, Trujillo ME, Wernstedt-Asterholm I, Attie AD, et al. (2009) Hypoxia-inducible factor 1 $\alpha$  induces fibrosis and insulin resistance in white adipose tissue. *Mol Cell Biol* 29: 4467-4483.
262. Sun K, Tordjman J, Clement K, Scherer PE (2013) Fibrosis and adipose tissue dysfunction. *Cell Metab* 18: 470-477.
263. Khan T, Muise ES, Iyengar P, Wang ZV, Chandalia M, et al. (2009) Metabolic dysregulation and adipose tissue fibrosis: role of collagen VI. *Mol Cell Biol* 29: 1575-1591.
264. Hosogai N, Fukuhara A, Oshima K, Miyata Y, Tanaka S, et al. (2007) Adipose tissue hypoxia in obesity and its impact on adipocytokine dysregulation. *Diabetes* 56: 901-911.
265. Rausch ME, Weisberg S, Vardhana P, Tortoriello DV (2008) Obesity in C57BL/6J mice is characterized by adipose tissue hypoxia and cytotoxic T-cell infiltration. *Int J Obes (Lond)* 32: 451-463.

266. Pasarica M, Sereda OR, Redman LM, Albarado DC, Hymel DT, et al. (2009) Reduced adipose tissue oxygenation in human obesity: evidence for rarefaction, macrophage chemotaxis, and inflammation without an angiogenic response. *Diabetes* 58: 718-725.
267. Crandall DL, Hausman GJ, Kral JG (1997) A review of the microcirculation of adipose tissue: anatomic, metabolic, and angiogenic perspectives. *Microcirculation* 4: 211-232.
268. Castellot JJ, Jr., Karnovsky MJ, Spiegelman BM (1982) Differentiation-dependent stimulation of neovascularization and endothelial cell chemotaxis by 3T3 adipocytes. *Proc Natl Acad Sci U S A* 79: 5597-5601.
269. Cao Y (2013) Angiogenesis and vascular functions in modulation of obesity, adipose metabolism, and insulin sensitivity. *Cell Metab* 18: 478-489.
270. Tang W, Zeve D, Suh JM, Bosnakovski D, Kyba M, et al. (2008) White fat progenitor cells reside in the adipose vasculature. *Science* 322: 583-586.
271. Cao Y (2010) Adipose tissue angiogenesis as a therapeutic target for obesity and metabolic diseases. *Nat Rev Drug Discov* 9: 107-115.
272. Trayhurn P, Wood IS (2004) Adipokines: inflammation and the pleiotropic role of white adipose tissue. *Br J Nutr* 92: 347-355.
273. Spencer M, Unal R, Zhu B, Rasouli N, McGehee RE, Jr., et al. (2011) Adipose tissue extracellular matrix and vascular abnormalities in obesity and insulin resistance. *J Clin Endocrinol Metab* 96: E1990-1998.
274. Di Girolamo M, Skinner NS, Jr., Hanley HG, Sachs RG (1971) Relationship of adipose tissue blood flow to fat cell size and number. *Am J Physiol* 220: 932-937.
275. Skurk T, Alberti-Huber C, Herder C, Hauner H (2007) Relationship between adipocyte size and adipokine expression and secretion. *J Clin Endocrinol Metab* 92: 1023-1033.
276. Brahimi-Horn MC, Pouyssegur J (2007) Hypoxia in cancer cell metabolism and pH regulation. *Essays Biochem* 43: 165-178.
277. Kabon B, Nagele A, Reddy D, Eagon C, Fleshman JW, et al. (2004) Obesity decreases perioperative tissue oxygenation. *Anesthesiology* 100: 274-280.
278. Jansson PA, Larsson A, Lonnroth PN (1998) Relationship between blood pressure, metabolic variables and blood flow in obese subjects with or without non-insulin-dependent diabetes mellitus. *Eur J Clin Invest* 28: 813-818.
279. Virtanen KA, Lonnroth P, Parkkola R, Peltoniemi P, Asola M, et al. (2002) Glucose uptake and perfusion in subcutaneous and visceral adipose tissue during insulin stimulation in nonobese and obese humans. *J Clin Endocrinol Metab* 87: 3902-3910.
280. West DB, Prinz WA, Francendese AA, Greenwood MR (1987) Adipocyte blood flow is decreased in obese Zucker rats. *Am J Physiol* 253: R228-233.
281. Karpe F, Fielding BA, Ilic V, Macdonald IA, Summers LK, et al. (2002) Impaired postprandial adipose tissue blood flow response is related to aspects of insulin sensitivity. *Diabetes* 51: 2467-2473.
282. Goossens GH, Bizzarri A, Venteclef N, Essers Y, Cleutjens JP, et al. (2011) Increased adipose tissue oxygen tension in obese compared with lean men is accompanied by insulin resistance, impaired adipose tissue capillarization, and inflammation. *Circulation* 124: 67-76.



283. Ye J, Gao Z, Yin J, He Q (2007) Hypoxia is a potential risk factor for chronic inflammation and adiponectin reduction in adipose tissue of ob/ob and dietary obese mice. *Am J Physiol Endocrinol Metab* 293: E1118-1128.
284. Sun K, Halberg N, Khan M, Magalang UJ, Scherer PE (2013) Selective inhibition of hypoxia-inducible factor 1 $\alpha$  ameliorates adipose tissue dysfunction. *Mol Cell Biol* 33: 904-917.
285. Yin J, Gao Z, He Q, Zhou D, Guo Z, et al. (2009) Role of hypoxia in obesity-induced disorders of glucose and lipid metabolism in adipose tissue. *Am J Physiol Endocrinol Metab* 296: E333-342.
286. Hodson L, Humphreys SM, Karpe F, Frayn KN (2013) Metabolic signatures of human adipose tissue hypoxia in obesity. *Diabetes* 62: 1417-1425.
287. Wang GL, Jiang BH, Rue EA, Semenza GL (1995) Hypoxia-inducible factor 1 is a basic-helix-loop-helix-PAS heterodimer regulated by cellular O<sub>2</sub> tension. *Proc Natl Acad Sci U S A* 92: 5510-5514.
288. Cummins EP, Taylor CT (2005) Hypoxia-responsive transcription factors. *Pflugers Arch* 450: 363-371.
289. Melvin A, Mudie S, Rocha S (2011) Further insights into the mechanism of hypoxia-induced NF $\kappa$ B. [corrected]. *Cell Cycle* 10: 879-882.
290. Dery MA, Michaud MD, Richard DE (2005) Hypoxia-inducible factor 1: regulation by hypoxic and non-hypoxic activators. *Int J Biochem Cell Biol* 37: 535-540.
291. Carmeliet P, Dor Y, Herbert JM, Fukumura D, Brusselmans K, et al. (1998) Role of HIF-1 $\alpha$  in hypoxia-mediated apoptosis, cell proliferation and tumour angiogenesis. *Nature* 394: 485-490.
292. Ortmann B, Druker J, Rocha S (2014) Cell cycle progression in response to oxygen levels. *Cell Mol Life Sci* 71: 3569-3582.
293. Yuan Y, Hilliard G, Ferguson T, Millhorn DE (2003) Cobalt inhibits the interaction between hypoxia-inducible factor- $\alpha$  and von Hippel-Lindau protein by direct binding to hypoxia-inducible factor- $\alpha$ . *J Biol Chem* 278: 15911-15916.
294. Hirsila M, Koivunen P, Xu L, Seeley T, Kivirikko KI, et al. (2005) Effect of desferrioxamine and metals on the hydroxylases in the oxygen sensing pathway. *FASEB J* 19: 1308-1310.
295. Triantafyllou A, Liakos P, Tsakalof A, Georgatsou E, Simos G, et al. (2006) Cobalt induces hypoxia-inducible factor-1 $\alpha$  (HIF-1 $\alpha$ ) in HeLa cells by an iron-independent, but ROS-, PI-3K- and MAPK-dependent mechanism. *Free Radic Res* 40: 847-856.
296. Ciafre SA, Niola F, Giorda E, Farace MG, Caporossi D (2007) CoCl<sub>2</sub>-simulated hypoxia in skeletal muscle cell lines: Role of free radicals in gene up-regulation and induction of apoptosis. *Free Radic Res* 41: 391-401.
297. Borenstein X, Fiszman GL, Blidner A, Vanzulli SI, Jasnis MA (2010) Functional changes in murine mammary cancer cells elicited by CoCl<sub>2</sub>-induced hypoxia. *Nitric Oxide* 23: 234-241.
298. Yun Z, Maecker HL, Johnson RS, Giaccia AJ (2002) Inhibition of PPAR  $\gamma$  2 gene expression by the HIF-1-regulated gene DEC1/Stra13: a mechanism for regulation of adipogenesis by hypoxia. *Dev Cell* 2: 331-341.
299. Yang G, Xu S, Peng L, Li H, Zhao Y, et al. (2016) The hypoxia-mimetic agent CoCl<sub>2</sub> induces chemotherapy resistance in LOVO colorectal cancer cells. *Mol Med Rep* 13: 2583-2589.

300. Lolmede K, Durand de Saint Front V, Galitzky J, Lafontan M, Bouloumie A (2003) Effects of hypoxia on the expression of proangiogenic factors in differentiated 3T3-F442A adipocytes. *Int J Obes Relat Metab Disord* 27: 1187-1195.
301. Chen B, Lam KS, Wang Y, Wu D, Lam MC, et al. (2006) Hypoxia dysregulates the production of adiponectin and plasminogen activator inhibitor-1 independent of reactive oxygen species in adipocytes. *Biochem Biophys Res Commun* 341: 549-556.
302. Wang B, Wood IS, Trayhurn P (2007) Dysregulation of the expression and secretion of inflammation-related adipokines by hypoxia in human adipocytes. *Pflugers Arch* 455: 479-492.
303. Fink T, Abildtrup L, Fogd K, Abdallah BM, Kassem M, et al. (2004) Induction of adipocyte-like phenotype in human mesenchymal stem cells by hypoxia. *Stem Cells* 22: 1346-1355.
304. Lin Q, Lee YJ, Yun Z (2006) Differentiation arrest by hypoxia. *J Biol Chem* 281: 30678-30683.
305. Cassavaugh J, Lounsbury KM (2011) Hypoxia-mediated biological control. *J Cell Biochem* 112: 735-744.
306. Wood IS, Wang B, Lorente-Cebrian S, Trayhurn P (2007) Hypoxia increases expression of selective facilitative glucose transporters (GLUT) and 2-deoxy-D-glucose uptake in human adipocytes. *Biochem Biophys Res Commun* 361: 468-473.
307. Bashan N, Burdett E, Guma A, Sargeant R, Tumiati L, et al. (1993) Mechanisms of adaptation of glucose transporters to changes in the oxidative chain of muscle and fat cells. *Am J Physiol* 264: C430-440.
308. Grosfeld A, Zilberfarb V, Turban S, Andre J, Guerre-Millo M, et al. (2002) Hypoxia increases leptin expression in human PAZ6 adipose cells. *Diabetologia* 45: 527-530.
309. Scheepers A, Doege H, Joost HG, Schurmann A (2001) Mouse GLUT8: genomic organization and regulation of expression in 3T3-L1 adipocytes by glucose. *Biochem Biophys Res Commun* 288: 969-974.
310. Lee KY, Gesta S, Boucher J, Wang XL, Kahn CR (2011) The differential role of Hif1beta/Arnt and the hypoxic response in adipose function, fibrosis, and inflammation. *Cell Metab* 14: 491-503.
311. Mazzatti D, Lim FL, O'Hara A, Wood IS, Trayhurn P (2012) A microarray analysis of the hypoxia-induced modulation of gene expression in human adipocytes. *Arch Physiol Biochem* 118: 112-120.
312. Choi S, Cho K, Kim J, Yea K, Park G, et al. (2009) Comparative proteome analysis using amine-reactive isobaric tagging reagents coupled with 2D LC/MS/MS in 3T3-L1 adipocytes following hypoxia or normoxia. *Biochem Biophys Res Commun* 383: 135-140.
313. Geiger K, Leihner A, Muendlein A, Stark N, Geller-Rhomberg S, et al. (2011) Identification of hypoxia-induced genes in human SGBS adipocytes by microarray analysis. *PLoS One* 6: e26465.
314. Perez de Heredia F, Wood IS, Trayhurn P (2010) Hypoxia stimulates lactate release and modulates monocarboxylate transporter (MCT1, MCT2, and MCT4) expression in human adipocytes. *Pflugers Arch* 459: 509-518.
315. Samuvel DJ, Sundararaj KP, Nareika A, Lopes-Virella MF, Huang Y (2009) Lactate boosts TLR4 signaling and NF-kappaB pathway-mediated gene transcription in macrophages via monocarboxylate transporters and MD-2 up-regulation. *J Immunol* 182: 2476-2484.

316. Liu C, Wu J, Zhu J, Kuei C, Yu J, et al. (2009) Lactate inhibits lipolysis in fat cells through activation of an orphan G-protein-coupled receptor, GPR81. *J Biol Chem* 284: 2811-2822.
317. Harris RB (2014) Direct and indirect effects of leptin on adipocyte metabolism. *Biochim Biophys Acta* 1842: 414-423.
318. Regazzetti C, Peraldi P, Gremeaux T, Najem-Lendom R, Ben-Sahra I, et al. (2009) Hypoxia decreases insulin signaling pathways in adipocytes. *Diabetes* 58: 95-103.
319. Jiang C, Qu A, Matsubara T, Chanturiya T, Jou W, et al. (2011) Disruption of hypoxia-inducible factor 1 in adipocytes improves insulin sensitivity and decreases adiposity in high-fat diet-fed mice. *Diabetes* 60: 2484-2495.
320. O'Rourke RW, Meyer KA, Gaston G, White AE, Lumeng CN, et al. (2013) Hexosamine biosynthesis is a possible mechanism underlying hypoxia's effects on lipid metabolism in human adipocytes. *PLoS One* 8: e71165.
321. Frayn KN, Karpe F, Fielding BA, Macdonald IA, Coppack SW (2003) Integrative physiology of human adipose tissue. *Int J Obes Relat Metab Disord* 27: 875-888.
322. Jang MK, Son Y, Jung MH (2013) ATF3 plays a role in adipocyte hypoxia-mediated mitochondria dysfunction in obesity. *Biochem Biophys Res Commun* 431: 421-427.
323. Gressner AM, Weiskirchen R (2006) Modern pathogenetic concepts of liver fibrosis suggest stellate cells and TGF-beta as major players and therapeutic targets. *J Cell Mol Med* 10: 76-99.
324. Henegar C, Tordjman J, Achard V, Lacasa D, Cremer I, et al. (2008) Adipose tissue transcriptomic signature highlights the pathological relevance of extracellular matrix in human obesity. *Genome Biol* 9: R14.
325. Mariman EC, Wang P (2010) Adipocyte extracellular matrix composition, dynamics and role in obesity. *Cell Mol Life Sci* 67: 1277-1292.
326. Spencer M, Yao-Borengasser A, Unal R, Rasouli N, Gurley CM, et al. (2010) Adipose tissue macrophages in insulin-resistant subjects are associated with collagen VI and fibrosis and demonstrate alternative activation. *Am J Physiol Endocrinol Metab* 299: E1016-1027.
327. Rosenow A, Noben JP, Bouwman FG, Mariman EC, Renes J (2013) Hypoxia-mimetic effects in the secretome of human preadipocytes and adipocytes. *Biochim Biophys Acta* 1834: 2761-2771.
328. Trayhurn P (2013) Hypoxia and adipose tissue function and dysfunction in obesity. *Physiol Rev* 93: 1-21.
329. Divoux A, Clement K (2011) Architecture and the extracellular matrix: the still unappreciated components of the adipose tissue. *Obes Rev* 12: e494-503.
330. Chun TH (2012) Peri-adipocyte ECM remodeling in obesity and adipose tissue fibrosis. *Adipocyte* 1: 89-95.
331. Schaefer L, Schaefer RM (2010) Proteoglycans: from structural compounds to signaling molecules. *Cell Tissue Res* 339: 237-246.
332. Ricard-Blum S (2011) The collagen family. *Cold Spring Harb Perspect Biol* 3: a004978.
333. Buechler C, Krautbauer S, Eisinger K (2015) Adipose tissue fibrosis. *World J Diabetes* 6: 548-553.

334. Pierleoni C, Verdenelli F, Castellucci M, Cinti S (1998) Fibronectins and basal lamina molecules expression in human subcutaneous white adipose tissue. *Eur J Histochem* 42: 183-188.
335. Harburger DS, Calderwood DA (2009) Integrin signalling at a glance. *J Cell Sci* 122: 159-163.
336. Christiaens V, Lijnen HR (2006) Role of the fibrinolytic and matrix metalloproteinase systems in development of adipose tissue. *Arch Physiol Biochem* 112: 254-259.
337. Yu Q, Stamenkovic I (2000) Cell surface-localized matrix metalloproteinase-9 proteolytically activates TGF-beta and promotes tumor invasion and angiogenesis. *Genes Dev* 14: 163-176.
338. Karsdal MA, Larsen L, Engsig MT, Lou H, Ferreras M, et al. (2002) Matrix metalloproteinase-dependent activation of latent transforming growth factor-beta controls the conversion of osteoblasts into osteocytes by blocking osteoblast apoptosis. *J Biol Chem* 277: 44061-44067.
339. Penn JW, Grobbelaar AO, Rolfe KJ (2012) The role of the TGF-beta family in wound healing, burns and scarring: a review. *Int J Burns Trauma* 2: 18-28.
340. Napolitano L (1963) The Differentiation of White Adipose Cells. An Electron Microscope Study. *J Cell Biol* 18: 663-679.
341. Scherer PE, Bickel PE, Kotler M, Lodish HF (1998) Cloning of cell-specific secreted and surface proteins by subtractive antibody screening. *Nat Biotechnol* 16: 581-586.
342. Alvarez-Llamas G, Szalowska E, de Vries MP, Weening D, Landman K, et al. (2007) Characterization of the human visceral adipose tissue secretome. *Mol Cell Proteomics* 6: 589-600.
343. Antras J, Hilliou F, Redziniak G, Pairault J (1989) Decreased biosynthesis of actin and cellular fibronectin during adipose conversion of 3T3-F442A cells. Reorganization of the cytoarchitecture and extracellular matrix fibronectin. *Biol Cell* 66: 247-254.
344. Aratani Y, Kitagawa Y (1988) Enhanced synthesis and secretion of type IV collagen and entactin during adipose conversion of 3T3-L1 cells and production of unorthodox laminin complex. *J Biol Chem* 263: 16163-16169.
345. Nakajima I, Muroya S, Tanabe R, Chikuni K (2002) Extracellular matrix development during differentiation into adipocytes with a unique increase in type V and VI collagen. *Biol Cell* 94: 197-203.
346. Spiegelman BM, Ginty CA (1983) Fibronectin modulation of cell shape and lipogenic gene expression in 3T3-adipocytes. *Cell* 35: 657-666.
347. O'Connor KC, Song H, Rosenzweig N, Jansen DA (2003) Extracellular matrix substrata alter adipocyte yield and lipogenesis in primary cultures of stromal-vascular cells from human adipose. *Biotechnol Lett* 25: 1967-1972.
348. Strissel KJ, Stancheva Z, Miyoshi H, Perfield JW, 2nd, DeFuria J, et al. (2007) Adipocyte death, adipose tissue remodeling, and obesity complications. *Diabetes* 56: 2910-2918.
349. Huber J, Loffler M, Bilban M, Reimers M, Kadl A, et al. (2007) Prevention of high-fat diet-induced adipose tissue remodeling in obese diabetic mice by n-3 polyunsaturated fatty acids. *Int J Obes (Lond)* 31: 1004-1013.
350. Mutch DM, Tordjman J, Pelloux V, Hanczar B, Henegar C, et al. (2009) Needle and surgical biopsy techniques differentially affect adipose tissue gene expression profiles. *Am J Clin Nutr* 89: 51-57.

351. Abdennour M, Reggio S, Le Naour G, Liu Y, Poitou C, et al. (2014) Association of adipose tissue and liver fibrosis with tissue stiffness in morbid obesity: links with diabetes and BMI loss after gastric bypass. *J Clin Endocrinol Metab* 99: 898-907.
352. Divoux A, Tordjman J, Lacasa D, Veyrie N, Hugol D, et al. (2010) Fibrosis in human adipose tissue: composition, distribution, and link with lipid metabolism and fat mass loss. *Diabetes* 59: 2817-2825.
353. Muir LA, Neeley CK, Meyer KA, Baker NA, Brosius AM, et al. (2016) Adipose tissue fibrosis, hypertrophy, and hyperplasia: Correlations with diabetes in human obesity. *Obesity (Silver Spring)* 24: 597-605.
354. Pasarica M, Gowronska-Kozak B, Burk D, Remedios I, Hymel D, et al. (2009) Adipose tissue collagen VI in obesity. *J Clin Endocrinol Metab* 94: 5155-5162.
355. Lackey DE, Burk DH, Ali MR, Mostaedi R, Smith WH, et al. (2014) Contributions of adipose tissue architectural and tensile properties toward defining healthy and unhealthy obesity. *Am J Physiol Endocrinol Metab* 306: E233-246.
356. McCulloch LJ, Rawling TJ, Sjöholm K, Franck N, Dankel SN, et al. (2015) COL6A3 is regulated by leptin in human adipose tissue and reduced in obesity. *Endocrinology* 156: 134-146.
357. Tartare-Deckert S, Chavey C, Monthouel MN, Gautier N, Van Obberghen E (2001) The matricellular protein SPARC/osteonectin as a newly identified factor up-regulated in obesity. *J Biol Chem* 276: 22231-22237.
358. Takahashi M, Nagaretani H, Funahashi T, Nishizawa H, Maeda N, et al. (2001) The expression of SPARC in adipose tissue and its increased plasma concentration in patients with coronary artery disease. *Obes Res* 9: 388-393.
359. Varma V, Yao-Borengasser A, Bodles AM, Rasouli N, Phanavanh B, et al. (2008) Thrombospondin-1 is an adipokine associated with obesity, adipose inflammation, and insulin resistance. *Diabetes* 57: 432-439.
360. Voros G, Maquoi E, Demeulemeester D, Clerx N, Collen D, et al. (2005) Modulation of angiogenesis during adipose tissue development in murine models of obesity. *Endocrinology* 146: 4545-4554.
361. Gomez-Ambrosi J, Catalan V, Ramirez B, Rodriguez A, Colina I, et al. (2007) Plasma osteopontin levels and expression in adipose tissue are increased in obesity. *J Clin Endocrinol Metab* 92: 3719-3727.
362. Kiefer FW, Zeyda M, Todoric J, Huber J, Geyeregger R, et al. (2008) Osteopontin expression in human and murine obesity: extensive local up-regulation in adipose tissue but minimal systemic alterations. *Endocrinology* 149: 1350-1357.
363. Nomiya T, Perez-Tilve D, Ogawa D, Gizard F, Zhao Y, et al. (2007) Osteopontin mediates obesity-induced adipose tissue macrophage infiltration and insulin resistance in mice. *J Clin Invest* 117: 2877-2888.
364. Maquoi E, Munaut C, Colige A, Collen D, Lijnen HR (2002) Modulation of adipose tissue expression of murine matrix metalloproteinases and their tissue inhibitors with obesity. *Diabetes* 51: 1093-1101.
365. Chavey C, Mari B, Monthouel MN, Bonnafous S, Anglard P, et al. (2003) Matrix metalloproteinases are differentially expressed in adipose tissue during obesity and modulate adipocyte differentiation. *J Biol Chem* 278: 11888-11896.

366. Jaworski DM, Sideleva O, Stradecki HM, Langlois GD, Habibovic A, et al. (2011) Sexually dimorphic diet-induced insulin resistance in obese tissue inhibitor of metalloproteinase-2 (TIMP-2)-deficient mice. *Endocrinology* 152: 1300-1313.
367. Unal R, Yao-Borengasser A, Varma V, Rasouli N, Labbate C, et al. (2010) Matrix metalloproteinase-9 is increased in obese subjects and decreases in response to pioglitazone. *J Clin Endocrinol Metab* 95: 2993-3001.
368. Thomas AP, Dunn TN, Oort PJ, Grino M, Adams SH (2011) Inflammatory phenotyping identifies CD11d as a gene markedly induced in white adipose tissue in obese rodents and women. *J Nutr* 141: 1172-1180.
369. Wu H, Perrard XD, Wang Q, Perrard JL, Polsani VR, et al. (2010) CD11c expression in adipose tissue and blood and its role in diet-induced obesity. *Arterioscler Thromb Vasc Biol* 30: 186-192.
370. Keophiphath M, Achard V, Henegar C, Rouault C, Clement K, et al. (2009) Macrophage-secreted factors promote a profibrotic phenotype in human preadipocytes. *Mol Endocrinol* 23: 11-24.
371. Lin, Chun TH, Kang L (2016) Adipose extracellular matrix remodelling in obesity and insulin resistance. *Biochem Pharmacol*.
372. Virtue S, Vidal-Puig A (2010) Adipose tissue expandability, lipotoxicity and the Metabolic Syndrome--an allostatic perspective. *Biochim Biophys Acta* 1801: 338-349.
373. Huang G, Ge G, Wang D, Gopalakrishnan B, Butz DH, et al. (2011) alpha3(V) collagen is critical for glucose homeostasis in mice due to effects in pancreatic islets and peripheral tissues. *J Clin Invest* 121: 769-783.
374. Bradshaw AD, Graves DC, Motamed K, Sage EH (2003) SPARC-null mice exhibit increased adiposity without significant differences in overall body weight. *Proc Natl Acad Sci U S A* 100: 6045-6050.
375. Li Y, Tong X, Rumala C, Clemons K, Wang S (2011) Thrombospondin1 deficiency reduces obesity-associated inflammation and improves insulin sensitivity in a diet-induced obese mouse model. *PLoS One* 6: e26656.
376. Morange PE, Bastelica D, Bonzi MF, Van Hoef B, Collen D, et al. (2002) Influence of t-pA and u-PA on adipose tissue development in a murine model of diet-induced obesity. *Thromb Haemost* 87: 306-310.
377. Chun TH, Inoue M, Morisaki H, Yamanaka I, Miyamoto Y, et al. (2010) Genetic link between obesity and MMP14-dependent adipogenic collagen turnover. *Diabetes* 59: 2484-2494.
378. Chun TH, Hotary KB, Sabeh F, Saltiel AR, Allen ED, et al. (2006) A pericellular collagenase directs the 3-dimensional development of white adipose tissue. *Cell* 125: 577-591.
379. Gerin I, Louis GW, Zhang X, Prestwich TC, Kumar TR, et al. (2009) Hyperphagia and obesity in female mice lacking tissue inhibitor of metalloproteinase-1. *Endocrinology* 150: 1697-1704.
380. Demeulemeester D, Collen D, Lijnen HR (2005) Effect of matrix metalloproteinase inhibition on adipose tissue development. *Biochem Biophys Res Commun* 329: 105-110.
381. Canello R, Tordjman J, Poitou C, Guilhem G, Bouillot JL, et al. (2006) Increased infiltration of macrophages in omental adipose tissue is associated with marked hepatic lesions in morbid human obesity. *Diabetes* 55: 1554-1561.

382. Shah TJ, Leik CE, Walsh SW (2010) Neutrophil infiltration and systemic vascular inflammation in obese women. *Reprod Sci* 17: 116-124.
383. Wu H, Ghosh S, Perrard XD, Feng L, Garcia GE, et al. (2007) T-cell accumulation and regulated on activation, normal T cell expressed and secreted upregulation in adipose tissue in obesity. *Circulation* 115: 1029-1038.
384. Divoux A, Moutel S, Poitou C, Lacasa D, Veyrie N, et al. (2012) Mast cells in human adipose tissue: link with morbid obesity, inflammatory status, and diabetes. *J Clin Endocrinol Metab* 97: E1677-1685.
385. Cinti S, Mitchell G, Barbatelli G, Murano I, Ceresi E, et al. (2005) Adipocyte death defines macrophage localization and function in adipose tissue of obese mice and humans. *J Lipid Res* 46: 2347-2355.
386. Misumi Y, Hayashi Y, Arakawa F, Ikehara Y (1992) Molecular cloning and sequence analysis of human dipeptidyl peptidase IV, a serine proteinase on the cell surface. *Biochim Biophys Acta* 1131: 333-336.
387. Hopsu-Havu VK, Glenner GG (1966) A new dipeptide naphthylamidase hydrolyzing glycyl-prolyl-beta-naphthylamide. *Histochemie* 7: 197-201.
388. Rasmussen HB, Branner S, Wiberg FC, Wagtmann N (2003) Crystal structure of human dipeptidyl peptidase IV/CD26 in complex with a substrate analog. *Nat Struct Biol* 10: 19-25.
389. Kikuchi M, Fukuyama K, Epstein WL (1988) Soluble dipeptidyl peptidase IV from terminal differentiated rat epidermal cells: purification and its activity on synthetic and natural peptides. *Arch Biochem Biophys* 266: 369-376.
390. Rohrborn D, Eckel J, Sell H (2014) Shedding of dipeptidyl peptidase 4 is mediated by metalloproteases and up-regulated by hypoxia in human adipocytes and smooth muscle cells. *FEBS Lett* 588: 3870-3877.
391. Ajami K, Abbott CA, Obradovic M, Gysbers V, Kahne T, et al. (2003) Structural requirements for catalysis, expression, and dimerization in the CD26/DPIV gene family. *Biochemistry* 42: 694-701.
392. Mentlein R (1999) Dipeptidyl-peptidase IV (CD26)--role in the inactivation of regulatory peptides. *Regul Pept* 85: 9-24.
393. Lambeir AM, Durinx C, Scharpe S, De Meester I (2003) Dipeptidyl-peptidase IV from bench to bedside: an update on structural properties, functions, and clinical aspects of the enzyme DPP IV. *Crit Rev Clin Lab Sci* 40: 209-294.
394. Cordero OJ, Salgado FJ, Nogueira M (2009) On the origin of serum CD26 and its altered concentration in cancer patients. *Cancer Immunol Immunother* 58: 1723-1747.
395. Gorrell MD (2005) Dipeptidyl peptidase IV and related enzymes in cell biology and liver disorders. *Clin Sci (Lond)* 108: 277-292.
396. Yazbeck R, Howarth GS, Abbott CA (2009) Dipeptidyl peptidase inhibitors, an emerging drug class for inflammatory disease? *Trends Pharmacol Sci* 30: 600-607.
397. Lamers D, Famulla S, Wronkowitz N, Hartwig S, Lehr S, et al. (2011) Dipeptidyl peptidase 4 is a novel adipokine potentially linking obesity to the metabolic syndrome. *Diabetes* 60: 1917-1925.
398. Kameoka J, Tanaka T, Nojima Y, Schlossman SF, Morimoto C (1993) Direct association of adenosine deaminase with a T cell activation antigen, CD26. *Science* 261: 466-469.

399. Cheng HC, Abdel-Ghany M, Pauli BU (2003) A novel consensus motif in fibronectin mediates dipeptidyl peptidase IV adhesion and metastasis. *J Biol Chem* 278: 24600-24607.
400. Loster K, Zeilinger K, Schuppan D, Reutter W (1995) The cysteine-rich region of dipeptidyl peptidase IV (CD 26) is the collagen-binding site. *Biochem Biophys Res Commun* 217: 341-348.
401. Engel M, Hoffmann T, Wagner L, Wermann M, Heiser U, et al. (2003) The crystal structure of dipeptidyl peptidase IV (CD26) reveals its functional regulation and enzymatic mechanism. *Proc Natl Acad Sci U S A* 100: 5063-5068.
402. Daddona PE, Kelley WN (1977) Human adenosine deaminase. Purification and subunit structure. *J Biol Chem* 252: 110-115.
403. Gorrell MD, Gysbers V, McCaughan GW (2001) CD26: a multifunctional integral membrane and secreted protein of activated lymphocytes. *Scand J Immunol* 54: 249-264.
404. Gonzalez-Gronow M, Hershfield MS, Arredondo-Vega FX, Pizzo SV (2004) Cell surface adenosine deaminase binds and stimulates plasminogen activation on 1-LN human prostate cancer cells. *J Biol Chem* 279: 20993-20998.
405. Dong RP, Tachibana K, Hegen M, Munakata Y, Cho D, et al. (1997) Determination of adenosine deaminase binding domain on CD26 and its immunoregulatory effect on T cell activation. *J Immunol* 159: 6070-6076.
406. Dong RP, Kameoka J, Hegen M, Tanaka T, Xu Y, et al. (1996) Characterization of adenosine deaminase binding to human CD26 on T cells and its biologic role in immune response. *J Immunol* 156: 1349-1355.
407. Piazza GA, Callanan HM, Mowery J, Hixson DC (1989) Evidence for a role of dipeptidyl peptidase IV in fibronectin-mediated interactions of hepatocytes with extracellular matrix. *Biochem J* 262: 327-334.
408. Pang R, Law WL, Chu AC, Poon JT, Lam CS, et al. (2010) A subpopulation of CD26+ cancer stem cells with metastatic capacity in human colorectal cancer. *Cell Stem Cell* 6: 603-615.
409. Inamoto T, Yamochi T, Ohnuma K, Iwata S, Kina S, et al. (2006) Anti-CD26 monoclonal antibody-mediated G1-S arrest of human renal clear cell carcinoma Caki-2 is associated with retinoblastoma substrate dephosphorylation, cyclin-dependent kinase 2 reduction, p27(kip1) enhancement, and disruption of binding to the extracellular matrix. *Clin Cancer Res* 12: 3470-3477.
410. Sun YX, Pedersen EA, Shiozawa Y, Havens AM, Jung Y, et al. (2008) CD26/dipeptidyl peptidase IV regulates prostate cancer metastasis by degrading SDF-1/CXCL12. *Clin Exp Metastasis* 25: 765-776.
411. Hirai K, Kotani T, Aratake Y, Ohtaki S, Kuma K (1999) Dipeptidyl peptidase IV (DPP IV/CD26) staining predicts distant metastasis of 'benign' thyroid tumor. *Pathol Int* 49: 264-265.
412. Yamaguchi U, Nakayama R, Honda K, Ichikawa H, Hasegawa T, et al. (2008) Distinct gene expression-defined classes of gastrointestinal stromal tumor. *J Clin Oncol* 26: 4100-4108.
413. de la Haba-Rodriguez J, Macho A, Calzado MA, Blazquez MV, Gomez MA, et al. (2002) Soluble dipeptidyl peptidase IV (CD-26) in serum of patients with colorectal carcinoma. *Neoplasma* 49: 307-311.
414. Abdel-Ghany M, Cheng H, Levine RA, Pauli BU (1998) Truncated dipeptidyl peptidase IV is a potent anti-adhesion and anti-metastasis peptide for rat breast cancer cells. *Invasion Metastasis* 18: 35-43.



415. Wesley UV, McGroarty M, Homoyouni A (2005) Dipeptidyl peptidase inhibits malignant phenotype of prostate cancer cells by blocking basic fibroblast growth factor signaling pathway. *Cancer Res* 65: 1325-1334.
416. Mentlein R, Gallwitz B, Schmidt WE (1993) Dipeptidyl-peptidase IV hydrolyses gastric inhibitory polypeptide, glucagon-like peptide-1(7-36)amide, peptide histidine methionine and is responsible for their degradation in human serum. *Eur J Biochem* 214: 829-835.
417. Drucker DJ, Shi Q, Crivici A, Sumner-Smith M, Tavares W, et al. (1997) Regulation of the biological activity of glucagon-like peptide 2 in vivo by dipeptidyl peptidase IV. *Nat Biotechnol* 15: 673-677.
418. Mentlein R, Dahms P, Grandt D, Kruger R (1993) Proteolytic processing of neuropeptide Y and peptide YY by dipeptidyl peptidase IV. *Regul Pept* 49: 133-144.
419. Shane R, Wilk S, Bodnar RJ (1999) Modulation of endomorphin-2-induced analgesia by dipeptidyl peptidase IV. *Brain Res* 815: 278-286.
420. Busek P, Stremenova J, Krepela E, Sedo A (2008) Modulation of substance P signaling by dipeptidyl peptidase-IV enzymatic activity in human glioma cell lines. *Physiol Res* 57: 443-449.
421. Hartrodt B, Neubert K, Fischer G, Demuth U, Yoshimoto T, et al. (1982) Degradation of beta-casomorphin-5 by proline-specific-endoropeptidase (PSE) and post-proline-cleaving-enzyme (PPCE). Comparative studies of the beta-casomorphin-5 cleavage by dipeptidyl-peptidase IV. *Pharmazie* 37: 72-73.
422. Lambeir AM, Durinx C, Proost P, Van Damme J, Scharpe S, et al. (2001) Kinetic study of the processing by dipeptidyl-peptidase IV/CD26 of neuropeptides involved in pancreatic insulin secretion. *FEBS Lett* 507: 327-330.
423. Proost P, Struyf S, Schols D, Durinx C, Wuyts A, et al. (1998) Processing by CD26/dipeptidyl-peptidase IV reduces the chemotactic and anti-HIV-1 activity of stromal-cell-derived factor-1alpha. *FEBS Lett* 432: 73-76.
424. Lambeir AM, Proost P, Durinx C, Bal G, Senten K, et al. (2001) Kinetic investigation of chemokine truncation by CD26/dipeptidyl peptidase IV reveals a striking selectivity within the chemokine family. *J Biol Chem* 276: 29839-29845.
425. Oravec T, Pall M, Roderiquez G, Gorrell MD, Ditto M, et al. (1997) Regulation of the receptor specificity and function of the chemokine RANTES (regulated on activation, normal T cell expressed and secreted) by dipeptidyl peptidase IV (CD26)-mediated cleavage. *J Exp Med* 186: 1865-1872.
426. Proost P, Menten P, Struyf S, Schutyser E, De Meester I, et al. (2000) Cleavage by CD26/dipeptidyl peptidase IV converts the chemokine LD78beta into a most efficient monocyte attractant and CCR1 agonist. *Blood* 96: 1674-1680.
427. Guan E, Wang J, Norcross MA (2004) Amino-terminal processing of MIP-1beta/CCL4 by CD26/dipeptidyl-peptidase IV. *J Cell Biochem* 92: 53-64.
428. Struyf S, Proost P, Schols D, De Clercq E, Opdenakker G, et al. (1999) CD26/dipeptidyl-peptidase IV down-regulates the eosinophil chemotactic potency, but not the anti-HIV activity of human eotaxin by affecting its interaction with CC chemokine receptor 3. *J Immunol* 162: 4903-4909.
429. Ludwig A, Schiemann F, Mentlein R, Lindner B, Brandt E (2002) Dipeptidyl peptidase IV (CD26) on T cells cleaves the CXC chemokine CXCL11 (I-TAC) and abolishes the

- stimulating but not the desensitizing potential of the chemokine. *J Leukoc Biol* 72: 183-191.
430. Drucker DJ (2006) The biology of incretin hormones. *Cell Metab* 3: 153-165.
431. Kreymann B, Williams G, Ghatel MA, Bloom SR (1987) Glucagon-like peptide-1 7-36: a physiological incretin in man. *Lancet* 2: 1300-1304.
432. Creutzfeldt WO, Kleine N, Willms B, Orskov C, Holst JJ, et al. (1996) Glucagonostatic actions and reduction of fasting hyperglycemia by exogenous glucagon-like peptide I(7-36) amide in type I diabetic patients. *Diabetes Care* 19: 580-586.
433. Kieffer TJ, McIntosh CH, Pederson RA (1995) Degradation of glucose-dependent insulinotropic polypeptide and truncated glucagon-like peptide 1 in vitro and in vivo by dipeptidyl peptidase IV. *Endocrinology* 136: 3585-3596.
434. Delgado-Aros S, Kim DY, Burton DD, Thomforde GM, Stephens D, et al. (2002) Effect of GLP-1 on gastric volume, emptying, maximum volume ingested, and postprandial symptoms in humans. *Am J Physiol Gastrointest Liver Physiol* 282: G424-431.
435. Challa TD, Beaton N, Arnold M, Rudofsky G, Langhans W, et al. (2012) Regulation of adipocyte formation by GLP-1/GLP-1R signaling. *J Biol Chem* 287: 6421-6430.
436. Liu R, Li N, Lin Y, Wang M, Peng Y, et al. (2016) Glucagon Like Peptide-1 Promotes Adipocyte Differentiation via the Wnt4 Mediated Sequestering of Beta-Catenin. *PLoS One* 11: e0160212.
437. Sanz C, Vazquez P, Blazquez C, Barrio PA, Alvarez Mdel M, et al. (2010) Signaling and biological effects of glucagon-like peptide 1 on the differentiation of mesenchymal stem cells from human bone marrow. *Am J Physiol Endocrinol Metab* 298: E634-643.
438. Vendrell J, El Bekay R, Peral B, Garcia-Fuentes E, Megia A, et al. (2011) Study of the potential association of adipose tissue GLP-1 receptor with obesity and insulin resistance. *Endocrinology* 152: 4072-4079.
439. Bertin E, Arner P, Bolinder J, Hagstrom-Toft E (2001) Action of glucagon and glucagon-like peptide-1-(7-36) amide on lipolysis in human subcutaneous adipose tissue and skeletal muscle in vivo. *J Clin Endocrinol Metab* 86: 1229-1234.
440. Nogueiras R, Perez-Tilve D, Veyrat-Durebex C, Morgan DA, Varela L, et al. (2009) Direct control of peripheral lipid deposition by CNS GLP-1 receptor signaling is mediated by the sympathetic nervous system and blunted in diet-induced obesity. *J Neurosci* 29: 5916-5925.
441. Davies MJ, Bergenstal R, Bode B, Kushner RF, Lewin A, et al. (2015) Efficacy of Liraglutide for Weight Loss Among Patients With Type 2 Diabetes: The SCALE Diabetes Randomized Clinical Trial. *JAMA* 314: 687-699.
442. Inoue K, Maeda N, Kashine S, Fujishima Y, Kozawa J, et al. (2011) Short-term effects of liraglutide on visceral fat adiposity, appetite, and food preference: a pilot study of obese Japanese patients with type 2 diabetes. *Cardiovasc Diabetol* 10: 109.
443. Cummings BP, Stanhope KL, Graham JL, Baskin DG, Griffen SC, et al. (2010) Chronic administration of the glucagon-like peptide-1 analog, liraglutide, delays the onset of diabetes and lowers triglycerides in UCD-T2DM rats. *Diabetes* 59: 2653-2661.
444. Shao Y, Yuan G, Zhang J, Guo X (2015) Liraglutide reduces lipogenic signals in visceral adipose of db/db mice with AMPK activation and Akt suppression. *Drug Des Devel Ther* 9: 1177-1184.

445. Baggio LL, Drucker DJ (2007) Biology of incretins: GLP-1 and GIP. *Gastroenterology* 132: 2131-2157.
446. Rask E, Olsson T, Soderberg S, Holst Jj J, Tura A, et al. (2004) Insulin secretion and incretin hormones after oral glucose in non-obese subjects with impaired glucose tolerance. *Metabolism* 53: 624-631.
447. Kim SJ, Nian C, McIntosh CH (2011) Adipocyte expression of the glucose-dependent insulinotropic polypeptide receptor involves gene regulation by PPARgamma and histone acetylation. *J Lipid Res* 52: 759-770.
448. Weaver RE, Donnelly D, Wabitsch M, Grant PJ, Balmforth AJ (2008) Functional expression of glucose-dependent insulinotropic polypeptide receptors is coupled to differentiation in a human adipocyte model. *Int J Obes (Lond)* 32: 1705-1711.
449. Song DH, Getty-Kaushik L, Tseng E, Simon J, Corkey BE, et al. (2007) Glucose-dependent insulinotropic polypeptide enhances adipocyte development and glucose uptake in part through Akt activation. *Gastroenterology* 133: 1796-1805.
450. Kim SJ, Nian C, McIntosh CH (2007) Activation of lipoprotein lipase by glucose-dependent insulinotropic polypeptide in adipocytes. A role for a protein kinase B, LKB1, and AMP-activated protein kinase cascade. *J Biol Chem* 282: 8557-8567.
451. McIntosh CH, Bremsak I, Lynn FC, Gill R, Hinke SA, et al. (1999) Glucose-dependent insulinotropic polypeptide stimulation of lipolysis in differentiated 3T3-L1 cells: wortmannin-sensitive inhibition by insulin. *Endocrinology* 140: 398-404.
452. Getty-Kaushik L, Song DH, Boylan MO, Corkey BE, Wolfe MM (2006) Glucose-dependent insulinotropic polypeptide modulates adipocyte lipolysis and reesterification. *Obesity (Silver Spring)* 14: 1124-1131.
453. Gogebakan O, Andres J, Biedasek K, Mai K, Kuhnen P, et al. (2012) Glucose-dependent insulinotropic polypeptide reduces fat-specific expression and activity of 11beta-hydroxysteroid dehydrogenase type 1 and inhibits release of free fatty acids. *Diabetes* 61: 292-300.
454. Miyawaki K, Yamada Y, Ban N, Ihara Y, Tsukiyama K, et al. (2002) Inhibition of gastric inhibitory polypeptide signaling prevents obesity. *Nat Med* 8: 738-742.
455. McClean PL, Irwin N, Cassidy RS, Holst JJ, Gault VA, et al. (2007) GIP receptor antagonism reverses obesity, insulin resistance, and associated metabolic disturbances induced in mice by prolonged consumption of high-fat diet. *Am J Physiol Endocrinol Metab* 293: E1746-1755.
456. Althage MC, Ford EL, Wang S, Tso P, Polonsky KS, et al. (2008) Targeted ablation of glucose-dependent insulinotropic polypeptide-producing cells in transgenic mice reduces obesity and insulin resistance induced by a high fat diet. *J Biol Chem* 283: 18365-18376.
457. Pathak V, Gault VA, Flatt PR, Irwin N (2015) Antagonism of gastric inhibitory polypeptide (GIP) by palmitoylation of GIP analogues with N- and C-terminal modifications improves obesity and metabolic control in high fat fed mice. *Mol Cell Endocrinol* 401: 120-129.
458. Nasteska D, Harada N, Suzuki K, Yamane S, Hamasaki A, et al. (2014) Chronic reduction of GIP secretion alleviates obesity and insulin resistance under high-fat diet conditions. *Diabetes* 63: 2332-2343.
459. Asmar M, Simonsen L, Madsbad S, Stallknecht B, Holst JJ, et al. (2010) Glucose-dependent insulinotropic polypeptide may enhance fatty acid re-esterification in subcutaneous abdominal adipose tissue in lean humans. *Diabetes* 59: 2160-2163.

460. Everitt BJ, Hokfelt T, Terenius L, Tatemoto K, Mutt V, et al. (1984) Differential co-existence of neuropeptide Y (NPY)-like immunoreactivity with catecholamines in the central nervous system of the rat. *Neuroscience* 11: 443-462.
461. Yang K, Guan H, Arany E, Hill DJ, Cao X (2008) Neuropeptide Y is produced in visceral adipose tissue and promotes proliferation of adipocyte precursor cells via the Y1 receptor. *FASEB J* 22: 2452-2464.
462. Silva AP, Xapelli S, Grouzmann E, Cavadas C (2005) The putative neuroprotective role of neuropeptide Y in the central nervous system. *Curr Drug Targets CNS Neurol Disord* 4: 331-347.
463. Zheng F, Kim YJ, Chao PT, Bi S (2013) Overexpression of neuropeptide Y in the dorsomedial hypothalamus causes hyperphagia and obesity in rats. *Obesity (Silver Spring)* 21: 1086-1092.
464. Kim YJ, Bi S (2016) Knockdown of neuropeptide Y in the dorsomedial hypothalamus reverses high-fat diet-induced obesity and impaired glucose tolerance in rats. *Am J Physiol Regul Integr Comp Physiol* 310: R134-142.
465. Morgan DG, Kulkarni RN, Hurley JD, Wang ZL, Wang RM, et al. (1998) Inhibition of glucose stimulated insulin secretion by neuropeptide Y is mediated via the Y1 receptor and inhibition of adenylyl cyclase in RIN 5AH rat insulinoma cells. *Diabetologia* 41: 1482-1491.
466. Kuo LE, Kitlinska JB, Tilan JU, Li L, Baker SB, et al. (2007) Neuropeptide Y acts directly in the periphery on fat tissue and mediates stress-induced obesity and metabolic syndrome. *Nat Med* 13: 803-811.
467. Rosmaninho-Salgado J, Marques AP, Estrada M, Santana M, Cortez V, et al. (2012) Dipeptidyl-peptidase-IV by cleaving neuropeptide Y induces lipid accumulation and PPAR-gamma expression. *Peptides* 37: 49-54.
468. Kos K, Baker AR, Jernas M, Harte AL, Clapham JC, et al. (2009) DPP-IV inhibition enhances the antilipolytic action of NPY in human adipose tissue. *Diabetes Obes Metab* 11: 285-292.
469. Valet P, Berlan M, Beauville M, Crampes F, Montastruc JL, et al. (1990) Neuropeptide Y and peptide YY inhibit lipolysis in human and dog fat cells through a pertussis toxin-sensitive G protein. *J Clin Invest* 85: 291-295.
470. Ahmad S, Wang L, Ward PE (1992) Dipeptidyl(amino)peptidase IV and aminopeptidase M metabolize circulating substance P in vivo. *J Pharmacol Exp Ther* 260: 1257-1261.
471. Karagiannides I, Torres D, Tseng YH, Bowe C, Carvalho E, et al. (2008) Substance P as a novel anti-obesity target. *Gastroenterology* 134: 747-755.
472. Fu J, Liu B, Liu P, Liu L, Li G, et al. (2011) Substance P is associated with the development of obesity, chronic inflammation and type 2 diabetes mellitus. *Exp Clin Endocrinol Diabetes* 119: 177-181.
473. Wang LH, Zhou SX, Li RC, Zheng LR, Zhu JH, et al. (2012) Serum levels of calcitonin gene-related peptide and substance P are decreased in patients with diabetes mellitus and coronary artery disease. *J Int Med Res* 40: 134-140.
474. Gross K, Karagiannides I, Thomou T, Koon HW, Bowe C, et al. (2009) Substance P promotes expansion of human mesenteric preadipocytes through proliferative and antiapoptotic pathways. *Am J Physiol Gastrointest Liver Physiol* 296: G1012-1019.

475. Miegueu P, St-Pierre DH, Lapointe M, Poursharifi P, Lu H, et al. (2013) Substance P decreases fat storage and increases adipocytokine production in 3T3-L1 adipocytes. *Am J Physiol Gastrointest Liver Physiol* 304: G420-427.
476. Bouchard L, Faucher G, Tchernof A, Deshaies Y, Lebel S, et al. (2009) Comprehensive genetic analysis of the dipeptidyl peptidase-4 gene and cardiovascular disease risk factors in obese individuals. *Acta Diabetol* 46: 13-21.
477. Zillessen P, Celner J, Kretschmann A, Pfeifer A, Racke K, et al. (2016) Metabolic role of dipeptidyl peptidase 4 (DPP4) in primary human (pre)adipocytes. *Sci Rep* 6: 23074.
478. Lessard J, Pelletier M, Biertho L, Biron S, Marceau S, et al. (2015) Characterization of dedifferentiating human mature adipocytes from the visceral and subcutaneous fat compartments: fibroblast-activation protein alpha and dipeptidyl peptidase 4 as major components of matrix remodeling. *PLoS One* 10: e0122065.
479. Han R, Wang X, Bachovchin W, Zukowska Z, Osborn JW (2015) Inhibition of dipeptidyl peptidase 8/9 impairs preadipocyte differentiation. *Sci Rep* 5: 12348.
480. Sell H, Bluher M, Kloting N, Schlich R, Willems M, et al. (2013) Adipose dipeptidyl peptidase-4 and obesity: correlation with insulin resistance and depot-specific release from adipose tissue in vivo and in vitro. *Diabetes Care* 36: 4083-4090.
481. Zheng T, Liu Y, Qin S, Liu H, Zhang X, et al. (2016) Increased plasma dipeptidyl peptidase-4 activities are associated with high prevalence of diabetic nephropathy in Chinese patients with newly diagnosed type 2 diabetes: A cross-sectional study. *Diab Vasc Dis Res* 13: 127-136.
482. Kirino Y, Kamimoto T, Sato Y, Kawazoe K, Minakuchi K, et al. (2009) Increased plasma dipeptidyl peptidase IV (DPP IV) activity and decreased DPP IV activity of visceral but not subcutaneous adipose tissue in impaired glucose tolerance rats induced by high-fat or high-sucrose diet. *Biol Pharm Bull* 32: 463-467.
483. Conarello SL, Li Z, Ronan J, Roy RS, Zhu L, et al. (2003) Mice lacking dipeptidyl peptidase IV are protected against obesity and insulin resistance. *Proc Natl Acad Sci U S A* 100: 6825-6830.
484. Ben-Shlomo S, Zvibel I, Varol C, Spektor L, Shlomain A, et al. (2013) Role of glucose-dependent insulinotropic polypeptide in adipose tissue inflammation of dipeptidylpeptidase 4-deficient rats. *Obesity (Silver Spring)* 21: 2331-2341.
485. Kirino Y, Sato Y, Kamimoto T, Kawazoe K, Minakuchi K, et al. (2009) Interrelationship of dipeptidyl peptidase IV (DPP4) with the development of diabetes, dyslipidaemia and nephropathy: a streptozotocin-induced model using wild-type and DPP4-deficient rats. *J Endocrinol* 200: 53-61.
486. Marguet D, Baggio L, Kobayashi T, Bernard AM, Pierres M, et al. (2000) Enhanced insulin secretion and improved glucose tolerance in mice lacking CD26. *Proc Natl Acad Sci U S A* 97: 6874-6879.
487. Yasuda N, Nagakura T, Yamazaki K, Inoue T, Tanaka I (2002) Improvement of high fat-diet-induced insulin resistance in dipeptidyl peptidase IV-deficient Fischer rats. *Life Sci* 71: 227-238.
488. Frerker N, Raber K, Bode F, Skripuletz T, Nave H, et al. (2009) Phenotyping of congenic dipeptidyl peptidase 4 (DP4) deficient Dark Agouti (DA) rats suggests involvement of DP4 in neuro-, endocrine, and immune functions. *Clin Chem Lab Med* 47: 275-287.

489. Mulvihill EE, Drucker DJ (2014) Pharmacology, physiology, and mechanisms of action of dipeptidyl peptidase-4 inhibitors. *Endocr Rev* 35: 992-1019.
490. Kulasa K, Edelman S (2010) Saxagliptin: the evidence for its place in the treatment of type 2 diabetes mellitus. *Core Evid* 5: 23-37.
491. van Bloemendaal L, Ten Kulve JS, la Fleur SE, Ijzerman RG, Diamant M (2014) Effects of glucagon-like peptide 1 on appetite and body weight: focus on the CNS. *J Endocrinol* 221: T1-16.
492. Elahi D, McAloon-Dyke M, Fukagawa NK, Meneilly GS, Sclater AL, et al. (1994) The insulinotropic actions of glucose-dependent insulinotropic polypeptide (GIP) and glucagon-like peptide-1 (7-37) in normal and diabetic subjects. *Regul Pept* 51: 63-74.
493. Shimizu S, Hosooka T, Matsuda T, Asahara S, Koyanagi-Kimura M, et al. (2012) DPP4 inhibitor vildagliptin preserves beta-cell mass through amelioration of endoplasmic reticulum stress in C/EBPB transgenic mice. *J Mol Endocrinol* 49: 125-135.
494. Capuano A, Sportiello L, Maiorino MI, Rossi F, Giugliano D, et al. (2013) Dipeptidyl peptidase-4 inhibitors in type 2 diabetes therapy--focus on alogliptin. *Drug Des Devel Ther* 7: 989-1001.
495. Pi-Sunyer FX, Schweizer A, Mills D, Dejager S (2007) Efficacy and tolerability of vildagliptin monotherapy in drug-naive patients with type 2 diabetes. *Diabetes Res Clin Pract* 76: 132-138.
496. Plosker GL (2014) Sitagliptin: a review of its use in patients with type 2 diabetes mellitus. *Drugs* 74: 223-242.
497. Keating GM (2010) Vildagliptin: a review of its use in type 2 diabetes mellitus. *Drugs* 70: 2089-2112.
498. Dhillon S (2015) Saxagliptin: A Review in Type 2 Diabetes. *Drugs* 75: 1783-1796.
499. McGill JB (2012) Linagliptin for type 2 diabetes mellitus: a review of the pivotal clinical trials. *Ther Adv Endocrinol Metab* 3: 113-124.
500. Kim SH, Jung E, Yoon MK, Kwon OH, Hwang DM, et al. (2016) Pharmacological profiles of gemigliptin (LC15-0444), a novel dipeptidyl peptidase-4 inhibitor, in vitro and in vivo. *Eur J Pharmacol* 788: 54-64.
501. Nishio S, Abe M, Ito H (2015) Anagliptin in the treatment of type 2 diabetes: safety, efficacy, and patient acceptability. *Diabetes Metab Syndr Obes* 8: 163-171.
502. Keating GM (2015) Alogliptin: a review of its use in patients with type 2 diabetes mellitus. *Drugs* 75: 777-796.
503. Scott LJ (2015) Teneligliptin: a review in type 2 diabetes. *Clin Drug Investig* 35: 765-772.
504. Kaku K (2015) First novel once-weekly DPP-4 inhibitor, trelagliptin, for the treatment of type 2 diabetes mellitus. *Expert Opin Pharmacother* 16: 2539-2547.
505. Evans PM, Bain SC (2016) Omarigliptin for the treatment of type 2 diabetes mellitus. *Expert Opin Pharmacother* 17: 1947-1952.
506. Tan X, Hu J (2016) Evogliptin: a new dipeptidyl peptidase inhibitor for the treatment of type 2 diabetes. *Expert Opin Pharmacother* 17: 1285-1293.
507. Thomas L, Eckhardt M, Langkopf E, Tadayyon M, Himmelsbach F, et al. (2008) (R)-8-(3-amino-piperidin-1-yl)-7-but-2-ynyl-3-methyl-1-(4-methyl-quinazolin-2-ylmethyl)-3,7-dihydro-purine-2,6-dione (BI 1356), a novel xanthine-based dipeptidyl peptidase 4

- inhibitor, has a superior potency and longer duration of action compared with other dipeptidyl peptidase-4 inhibitors. *J Pharmacol Exp Ther* 325: 175-182.
508. Keating GM (2014) Vildagliptin: a review of its use in type 2 diabetes mellitus. *Drugs* 74: 587-610.
509. Sudre B, Broqua P, White RB, Ashworth D, Evans DM, et al. (2002) Chronic inhibition of circulating dipeptidyl peptidase IV by FE 999011 delays the occurrence of diabetes in male Zucker diabetic fatty rats. *Diabetes* 51: 1461-1469.
510. Dobrian AD, Ma Q, Lindsay JW, Leone KA, Ma K, et al. (2011) Dipeptidyl peptidase IV inhibitor sitagliptin reduces local inflammation in adipose tissue and in pancreatic islets of obese mice. *Am J Physiol Endocrinol Metab* 300: E410-421.
511. Lamont BJ, Drucker DJ (2008) Differential antidiabetic efficacy of incretin agonists versus DPP-4 inhibition in high fat fed mice. *Diabetes* 57: 190-198.
512. Souza-Mello V, Gregorio BM, Cardoso-de-Lemos FS, de Carvalho L, Aguila MB, et al. (2010) Comparative effects of telmisartan, sitagliptin and metformin alone or in combination on obesity, insulin resistance, and liver and pancreas remodelling in C57BL/6 mice fed on a very high-fat diet. *Clin Sci (Lond)* 119: 239-250.
513. Fukuda-Tsuru S, Kakimoto T, Utsumi H, Kiuchi S, Ishii S (2014) The novel dipeptidyl peptidase-4 inhibitor teneligliptin prevents high-fat diet-induced obesity accompanied with increased energy expenditure in mice. *Eur J Pharmacol* 723: 207-215.
514. Shimasaki T, Masaki T, Mitsutomi K, Ueno D, Gotoh K, et al. (2013) The dipeptidyl peptidase-4 inhibitor des-fluoro-sitagliptin regulates brown adipose tissue uncoupling protein levels in mice with diet-induced obesity. *PLoS One* 8: e63626.
515. Flock G, Baggio LL, Longuet C, Drucker DJ (2007) Incretin receptors for glucagon-like peptide 1 and glucose-dependent insulinotropic polypeptide are essential for the sustained metabolic actions of vildagliptin in mice. *Diabetes* 56: 3006-3013.
516. Shirakawa J, Fujii H, Ohnuma K, Sato K, Ito Y, et al. (2011) Diet-induced adipose tissue inflammation and liver steatosis are prevented by DPP-4 inhibition in diabetic mice. *Diabetes* 60: 1246-1257.
517. Kern M, Kloting N, Niessen HG, Thomas L, Stiller D, et al. (2012) Linagliptin improves insulin sensitivity and hepatic steatosis in diet-induced obesity. *PLoS One* 7: e38744.
518. Boschmann M, Engeli S, Dobberstein K, Budziarek P, Strauss A, et al. (2009) Dipeptidyl-peptidase-IV inhibition augments postprandial lipid mobilization and oxidation in type 2 diabetic patients. *J Clin Endocrinol Metab* 94: 846-852.
519. Kato H, Nagai Y, Ohta A, Tenjin A, Nakamura Y, et al. (2015) Effect of sitagliptin on intrahepatic lipid content and body fat in patients with type 2 diabetes. *Diabetes Res Clin Pract* 109: 199-205.
520. Foley JE, Jordan J (2010) Weight neutrality with the DPP-4 inhibitor, vildagliptin: mechanistic basis and clinical experience. *Vasc Health Risk Manag* 6: 541-548.
521. Klein T, Fujii M, Sandel J, Shibasaki Y, Wakamatsu K, et al. (2014) Linagliptin alleviates hepatic steatosis and inflammation in a mouse model of non-alcoholic steatohepatitis. *Med Mol Morphol* 47: 137-149.
522. Kaji K, Yoshiji H, Ikenaka Y, Noguchi R, Aihara Y, et al. (2014) Dipeptidyl peptidase-4 inhibitor attenuates hepatic fibrosis via suppression of activated hepatic stellate cell in rats. *J Gastroenterol* 49: 481-491.

523. Takahashi A, Asakura M, Ito S, Min KD, Shindo K, et al. (2013) Dipeptidyl-peptidase IV inhibition improves pathophysiology of heart failure and increases survival rate in pressure-overloaded mice. *Am J Physiol Heart Circ Physiol* 304: H1361-1369.
524. Picatoste B, Ramirez E, Caro-Vadillo A, Iborra C, Ares-Carrasco S, et al. (2013) Sitagliptin reduces cardiac apoptosis, hypertrophy and fibrosis primarily by insulin-dependent mechanisms in experimental type-II diabetes. Potential roles of GLP-1 isoforms. *PLoS One* 8: e78330.
525. Miyoshi T, Nakamura K, Yoshida M, Miura D, Oe H, et al. (2014) Effect of vildagliptin, a dipeptidyl peptidase 4 inhibitor, on cardiac hypertrophy induced by chronic beta-adrenergic stimulation in rats. *Cardiovasc Diabetol* 13: 43.
526. Chua S, Lee FY, Tsai TH, Sheu JJ, Leu S, et al. (2014) Inhibition of dipeptidyl peptidase-IV enzyme activity protects against myocardial ischemia-reperfusion injury in rats. *J Transl Med* 12: 357.
527. Lenski M, Kazakov A, Marx N, Bohm M, Laufs U (2011) Effects of DPP-4 inhibition on cardiac metabolism and function in mice. *J Mol Cell Cardiol* 51: 906-918.
528. Bostick B, Habibi J, Ma L, Aroor A, Rehmer N, et al. (2014) Dipeptidyl peptidase inhibition prevents diastolic dysfunction and reduces myocardial fibrosis in a mouse model of Western diet induced obesity. *Metabolism* 63: 1000-1011.
529. Chaykovska L, von Websky K, Rahnenfuhrer J, Alter M, Heiden S, et al. (2011) Effects of DPP-4 inhibitors on the heart in a rat model of uremic cardiomyopathy. *PLoS One* 6: e27861.
530. Connelly KA, Zhang Y, Advani A, Advani SL, Thai K, et al. (2013) DPP-4 inhibition attenuates cardiac dysfunction and adverse remodeling following myocardial infarction in rats with experimental diabetes. *Cardiovasc Ther* 31: 259-267.
531. Marques C, Mega C, Goncalves A, Rodrigues-Santos P, Teixeira-Lemos E, et al. (2014) Sitagliptin prevents inflammation and apoptotic cell death in the kidney of type 2 diabetic animals. *Mediators Inflamm* 2014: 538737.
532. Kanasaki K, Shi S, Kanasaki M, He J, Nagai T, et al. (2014) Linagliptin-mediated DPP-4 inhibition ameliorates kidney fibrosis in streptozotocin-induced diabetic mice by inhibiting endothelial-to-mesenchymal transition in a therapeutic regimen. *Diabetes* 63: 2120-2131.
533. Liu WJ, Xie SH, Liu YN, Kim W, Jin HY, et al. (2012) Dipeptidyl peptidase IV inhibitor attenuates kidney injury in streptozotocin-induced diabetic rats. *J Pharmacol Exp Ther* 340: 248-255.
534. Gangadharan Komala M, Gross S, Zaky A, Pollock C, Panchapakesan U (2015) Linagliptin Limits High Glucose Induced Conversion of Latent to Active TGFs through Interaction with CIM6PR and Limits Renal Tubulointerstitial Fibronectin. *PLoS One* 10: e0141143.
535. Min HS, Kim JE, Lee MH, Song HK, Kang YS, et al. (2014) Dipeptidyl peptidase IV inhibitor protects against renal interstitial fibrosis in a mouse model of ureteral obstruction. *Lab Invest* 94: 598-607.
536. Li J, Guan M, Li C, Lyv F, Zeng Y, et al. (2014) The dipeptidyl peptidase-4 inhibitor sitagliptin protects against dyslipidemia-related kidney injury in Apolipoprotein E knockout mice. *Int J Mol Sci* 15: 11416-11434.
537. Williams KH, Vieira De Ribeiro AJ, Prakoso E, Veillard AS, Shackel NA, et al. (2015) Circulating dipeptidyl peptidase-4 activity correlates with measures of hepatocyte apoptosis and



- fibrosis in non-alcoholic fatty liver disease in type 2 diabetes mellitus and obesity: A dual cohort cross-sectional study. *J Diabetes* 7: 809-819.
538. Hirakawa H, Zempo H, Ogawa M, Watanabe R, Suzuki J, et al. (2015) A DPP-4 inhibitor suppresses fibrosis and inflammation on experimental autoimmune myocarditis in mice. *PLoS One* 10: e0119360.
539. Tatemoto K, Carlquist M, Mutt V (1982) Neuropeptide Y--a novel brain peptide with structural similarities to peptide YY and pancreatic polypeptide. *Nature* 296: 659-660.
540. Pedrazzini T, Pralong F, Grouzmann E (2003) Neuropeptide Y: the universal soldier. *Cell Mol Life Sci* 60: 350-377.
541. Schwartz TW, Fuhlendorff J, Kjems LL, Kristensen MS, Vervelde M, et al. (1990) Signal epitopes in the three-dimensional structure of neuropeptide Y. Interaction with Y1, Y2, and pancreatic polypeptide receptors. *Ann N Y Acad Sci* 611: 35-47.
542. Michel MC, Beck-Sickinger A, Cox H, Doods HN, Herzog H, et al. (1998) XVI. International Union of Pharmacology recommendations for the nomenclature of neuropeptide Y, peptide YY, and pancreatic polypeptide receptors. *Pharmacol Rev* 50: 143-150.
543. Medeiros Mdos S, Turner AJ (1996) Metabolism and functions of neuropeptide Y. *Neurochem Res* 21: 1125-1132.
544. Silva AP, Cavadas C, Grouzmann E (2002) Neuropeptide Y and its receptors as potential therapeutic drug targets. *Clin Chim Acta* 326: 3-25.
545. Fredriksson R, Lagerstrom MC, Lundin LG, Schiöth HB (2003) The G-protein-coupled receptors in the human genome form five main families. Phylogenetic analysis, paralogue groups, and fingerprints. *Mol Pharmacol* 63: 1256-1272.
546. Holliday ND, Michel MC, Cox H (2004) NPY receptor subtypes and their signal transduction. In: M. C. Michel, editor. *Neuropeptide Y and related peptides*. In: Springer-Verlag Berlin Heidelberg, pp 45-73.
547. Blomqvist AG, Herzog H (1997) Y-receptor subtypes--how many more? *Trends Neurosci* 20: 294-298.
548. Larhammar D, Salaneck E (2004) Molecular evolution of NPY receptor subtypes. *Neuropeptides* 38: 141-151.
549. Eva C, Keinanen K, Monyer H, Seeburg P, Sprengel R (1990) Molecular cloning of a novel G protein-coupled receptor that may belong to the neuropeptide receptor family. *FEBS Lett* 271: 81-84.
550. Grundemar L, Krstenansky JL, Hakanson R (1993) Activation of neuropeptide Y1 and neuropeptide Y2 receptors by substituted and truncated neuropeptide Y analogs: identification of signal epitopes. *Eur J Pharmacol* 232: 271-278.
551. Rose PM, Fernandes P, Lynch JS, Frazier ST, Fisher SM, et al. (1995) Cloning and functional expression of a cDNA encoding a human type 2 neuropeptide Y receptor. *J Biol Chem* 270: 22661-22664.
552. Bard JA, Walker MW, Branchek TA, Weinshank RL (1995) Cloning and functional expression of a human Y4 subtype receptor for pancreatic polypeptide, neuropeptide Y, and peptide YY. *J Biol Chem* 270: 26762-26765.
553. Gehlert DR, Schober DA, Beavers L, Gadski R, Hoffman JA, et al. (1996) Characterization of the peptide binding requirements for the cloned human pancreatic polypeptide-preferring receptor. *Mol Pharmacol* 50: 112-118.

554. Gerald C, Walker MW, Criscione L, Gustafson EL, Batzl-Hartmann C, et al. (1996) A receptor subtype involved in neuropeptide-Y-induced food intake. *Nature* 382: 168-171.
555. Serradeil-Le Gal C, Lafontan M, Raufaste D, Marchand J, Pouzet B, et al. (2000) Characterization of NPY receptors controlling lipolysis and leptin secretion in human adipocytes. *FEBS Lett* 475: 150-156.
556. Hausman GJ, Barb CR, Dean RG (2008) Patterns of gene expression in pig adipose tissue: insulin-like growth factor system proteins, neuropeptide Y (NPY), NPY receptors, neurotrophic factors and other secreted factors. *Domest Anim Endocrinol* 35: 24-34.
557. Gericke MT, Kosacka J, Koch D, Nowicki M, Schroder T, et al. (2009) Receptors for NPY and PACAP differ in expression and activity during adipogenesis in the murine 3T3-L1 fibroblast cell line. *Br J Pharmacol* 157: 620-632.
558. Baker SB, Cohen M, Kuo L, Johnson M, Al-Attar A, et al. (2009) The role of the neuropeptide Y2 receptor in liporemodeling: neuropeptide Y-mediated adipogenesis and adipose graft maintenance. *Plast Reconstr Surg* 123: 486-492.
559. Shi YC, Lin S, Castillo L, Aljanova A, Enriquez RF, et al. (2011) Peripheral-specific y2 receptor knockdown protects mice from high-fat diet-induced obesity. *Obesity (Silver Spring)* 19: 2137-2148.
560. Han R, Kitlinska JB, Munday WR, Gallicano GI, Zukowska Z (2012) Stress hormone epinephrine enhances adipogenesis in murine embryonic stem cells by up-regulating the neuropeptide Y system. *PLoS One* 7: e36609.
561. Rosmaninho-Salgado J, Cortez V, Estrada M, Santana MM, Goncalves A, et al. (2012) Intracellular mechanisms coupled to NPY Y2 and Y5 receptor activation and lipid accumulation in murine adipocytes. *Neuropeptides* 46: 359-366.
562. Kos K, Harte AL, James S, Snead DR, O'Hare JP, et al. (2007) Secretion of neuropeptide Y in human adipose tissue and its role in maintenance of adipose tissue mass. *Am J Physiol Endocrinol Metab* 293: E1335-1340.
563. Martinez JA, Aguado M, Fruhbeck G (2000) Interactions between leptin and NPY affecting lipid mobilization in adipose tissue. *J Physiol Biochem* 56: 1-8.
564. Bradley RL, Mansfield JP, Maratos-Flier E (2005) Neuropeptides, including neuropeptide Y and melanocortins, mediate lipolysis in murine adipocytes. *Obes Res* 13: 653-661.
565. Turtzo LC, Marx R, Lane MD (2001) Cross-talk between sympathetic neurons and adipocytes in coculture. *Proc Natl Acad Sci U S A* 98: 12385-12390.
566. Castan I, Valet P, Quideau N, Voisin T, Ambid L, et al. (1994) Antilipolytic effects of alpha 2-adrenergic agonists, neuropeptide Y, adenosine, and PGE1 in mammal adipocytes. *Am J Physiol* 266: R1141-1147.
567. Margareto J, Aguado M, Oses-Prieto JA, Rivero I, Monge A, et al. (2000) A new NPY-antagonist strongly stimulates apoptosis and lipolysis on white adipocytes in an obesity model. *Life Sci* 68: 99-107.
568. Li R, Guan H, Yang K (2012) Neuropeptide Y potentiates beta-adrenergic stimulation of lipolysis in 3T3-L1 adipocytes. *Regul Pept* 178: 16-20.
569. Labelle M, Boulanger Y, Fournier A, St Pierre S, Savard R (1997) Tissue-specific regulation of fat cell lipolysis by NPY in 6-OHDA-treated rats. *Peptides* 18: 801-808.
570. Kim KH, Song MJ, Chung J, Park H, Kim JB (2005) Hypoxia inhibits adipocyte differentiation in a HDAC-independent manner. *Biochem Biophys Res Commun* 333: 1178-1184.

571. Brahimi-Horn MC, Pouyssegur J (2007) Oxygen, a source of life and stress. *FEBS Lett* 581: 3582-3591.
572. Semenza GL (2003) Targeting HIF-1 for cancer therapy. *Nat Rev Cancer* 3: 721-732.
573. Park YS, Huang Y, Park YJ, David AE, White L, et al. (2010) Specific down regulation of 3T3-L1 adipocyte differentiation by cell-permeable antisense HIF1alpha-oligonucleotide. *J Control Release* 144: 82-90.
574. Krishnan J, Danzer C, Simka T, Ukropec J, Walter KM, et al. (2012) Dietary obesity-associated Hif1alpha activation in adipocytes restricts fatty acid oxidation and energy expenditure via suppression of the Sirt2-NAD+ system. *Genes Dev* 26: 259-270.
575. Takanabe R, Ono K, Abe Y, Takaya T, Horie T, et al. (2008) Up-regulated expression of microRNA-143 in association with obesity in adipose tissue of mice fed high-fat diet. *Biochem Biophys Res Commun* 376: 728-732.
576. Gui L, Liu B, Lv G (2016) Hypoxia induces autophagy in cardiomyocytes via a hypoxia-inducible factor 1-dependent mechanism. *Exp Ther Med* 11: 2233-2239.
577. Bellot G, Garcia-Medina R, Gounon P, Chiche J, Roux D, et al. (2009) Hypoxia-induced autophagy is mediated through hypoxia-inducible factor induction of BNIP3 and BNIP3L via their BH3 domains. *Mol Cell Biol* 29: 2570-2581.
578. Priyanka A, Anusree SS, Nisha VM, Raghu KG (2014) Curcumin improves hypoxia induced dysfunctions in 3T3-L1 adipocytes by protecting mitochondria and down regulating inflammation. *Biofactors* 40: 513-523.
579. Chen Y, Azad MB, Gibson SB (2009) Superoxide is the major reactive oxygen species regulating autophagy. *Cell Death Differ* 16: 1040-1052.
580. Hashimoto T, Yokokawa T, Endo Y, Iwanaka N, Higashida K, et al. (2013) Modest hypoxia significantly reduces triglyceride content and lipid droplet size in 3T3-L1 adipocytes. *Biochem Biophys Res Commun* 440: 43-49.
581. Ren H, Cao Y, Zhao Q, Li J, Zhou C, et al. (2006) Proliferation and differentiation of bone marrow stromal cells under hypoxic conditions. *Biochem Biophys Res Commun* 347: 12-21.
582. Sano S, Izumi Y, Yamaguchi T, Yamazaki T, Tanaka M, et al. (2014) Lipid synthesis is promoted by hypoxic adipocyte-derived exosomes in 3T3-L1 cells. *Biochem Biophys Res Commun* 445: 327-333.
583. Chen SZ, Xu X, Ning LF, Jiang WY, Xing C, et al. (2015) miR-27 impairs the adipogenic lineage commitment via targeting lysyl oxidase. *Obesity (Silver Spring)* 23: 2445-2453.
584. Vankoningsloo S, Piens M, Lecocq C, Gilson A, De Pauw A, et al. (2005) Mitochondrial dysfunction induces triglyceride accumulation in 3T3-L1 cells: role of fatty acid beta-oxidation and glucose. *J Lipid Res* 46: 1133-1149.
585. Vankoningsloo S, De Pauw A, Houbion A, Tejerina S, Demazy C, et al. (2006) CREB activation induced by mitochondrial dysfunction triggers triglyceride accumulation in 3T3-L1 preadipocytes. *J Cell Sci* 119: 1266-1282.
586. Wang W, Zhang Y, Lu W, Liu K (2015) Mitochondrial reactive oxygen species regulate adipocyte differentiation of mesenchymal stem cells in hematopoietic stress induced by arabinosylcytosine. *PLoS One* 10: e0120629.
587. Lee H, Lee YJ, Choi H, Ko EH, Kim JW (2009) Reactive oxygen species facilitate adipocyte differentiation by accelerating mitotic clonal expansion. *J Biol Chem* 284: 10601-10609.

588. Lin Y, Berg AH, Iyengar P, Lam TK, Giacca A, et al. (2005) The hyperglycemia-induced inflammatory response in adipocytes: the role of reactive oxygen species. *J Biol Chem* 280: 4617-4626.
589. Talior I, Tennenbaum T, Kuroki T, Eldar-Finkelman H (2005) PKC-delta-dependent activation of oxidative stress in adipocytes of obese and insulin-resistant mice: role for NADPH oxidase. *Am J Physiol Endocrinol Metab* 288: E405-411.
590. Boren J, Brindle KM (2012) Apoptosis-induced mitochondrial dysfunction causes cytoplasmic lipid droplet formation. *Cell Death Differ* 19: 1561-1570.
591. Vidal-Puig A (2013) Adipose tissue expandability, lipotoxicity and the metabolic syndrome. *Endocrinol Nutr* 60 Suppl 1: 39-43.
592. Kitlinska J, Lee EW, Li L, Pons J, Estes L, et al. (2003) Dual role of dipeptidyl peptidase IV (DPP IV) in angiogenesis and vascular remodeling. *Adv Exp Med Biol* 524: 215-222.
593. Ruiz P, Zacharievich N, Shenkin M (1998) Multicolor cytoenzymatic evaluation of dipeptidyl peptidase IV (CD26) function in normal and neoplastic human T-lymphocyte populations. *Clin Diagn Lab Immunol* 5: 362-368.
594. Stulc T, Sedo A (2010) Inhibition of multifunctional dipeptidyl peptidase-IV: is there a risk of oncological and immunological adverse effects? *Diabetes Res Clin Pract* 88: 125-131.
595. Yu DM, Wang XM, McCaughan GW, Gorrell MD (2006) Extraenzymatic functions of the dipeptidyl peptidase IV-related proteins DP8 and DP9 in cell adhesion, migration and apoptosis. *FEBS J* 273: 2447-2460.
596. Drucker DJ, Nauck MA (2006) The incretin system: glucagon-like peptide-1 receptor agonists and dipeptidyl peptidase-4 inhibitors in type 2 diabetes. *Lancet* 368: 1696-1705.
597. Ferreira L, Teixeira-de-Lemos E, Pinto F, Parada B, Mega C, et al. (2010) Effects of sitagliptin treatment on dysmetabolism, inflammation, and oxidative stress in an animal model of type 2 diabetes (ZDF rat). *Mediators Inflamm* 2010: 592760.
598. Shah Z, Kampfrath T, Deiuliis JA, Zhong J, Pineda C, et al. (2011) Long-term dipeptidyl-peptidase 4 inhibition reduces atherosclerosis and inflammation via effects on monocyte recruitment and chemotaxis. *Circulation* 124: 2338-2349.
599. Amori RE, Lau J, Pittas AG (2007) Efficacy and safety of incretin therapy in type 2 diabetes: systematic review and meta-analysis. *JAMA* 298: 194-206.
600. Woessner JF, Jr. (1961) The determination of hydroxyproline in tissue and protein samples containing small proportions of this imino acid. *Arch Biochem Biophys* 93: 440-447.
601. de Almeida LP, Zala D, Aebischer P, Deglon N (2001) Neuroprotective effect of a CNTF-expressing lentiviral vector in the quinolinic acid rat model of Huntington's disease. *Neurobiol Dis* 8: 433-446.
602. Xu Q, Norman JT, Shrivastav S, Lucio-Cazana J, Kopp JB (2007) In vitro models of TGF-beta-induced fibrosis suitable for high-throughput screening of antifibrotic agents. *Am J Physiol Renal Physiol* 293: F631-640.
603. Matyal R, Sakamuri S, Wang A, Mahmood E, Robich MP, et al. (2013) Local infiltration of neuropeptide Y as a potential therapeutic agent against apoptosis and fibrosis in a swine model of hypercholesterolemia and chronic myocardial ischemia. *Eur J Pharmacol* 718: 261-270.
604. Grouzmann E, Cressier F, Walker P, Hofbauer K, Waeber B, et al. (1994) Interactions between NPY and its receptor: assessment using ant-NPY antibodies. *Regul Pept* 54: 439-444.

605. Rizzo M, Rizvi AA, Spinass GA, Rini GB, Berneis K (2009) Glucose lowering and anti-atherogenic effects of incretin-based therapies: GLP-1 analogues and DPP-4-inhibitors. *Expert Opin Investig Drugs* 18: 1495-1503.
606. Collins S, Martin TL, Surwit RS, Robidoux J (2004) Genetic vulnerability to diet-induced obesity in the C57BL/6J mouse: physiological and molecular characteristics. *Physiol Behav* 81: 243-248.
607. Matikainen N, Manttari S, Schweizer A, Ulvestad A, Mills D, et al. (2006) Vildagliptin therapy reduces postprandial intestinal triglyceride-rich lipoprotein particles in patients with type 2 diabetes. *Diabetologia* 49: 2049-2057.
608. Tremblay AJ, Lamarche B, Deacon CF, Weisnagel SJ, Couture P (2011) Effect of sitagliptin therapy on postprandial lipoprotein levels in patients with type 2 diabetes. *Diabetes Obes Metab* 13: 366-373.
609. Eliasson B, Moller-Goede D, Eeg-Olofsson K, Wilson C, Cederholm J, et al. (2012) Lowering of postprandial lipids in individuals with type 2 diabetes treated with alogliptin and/or pioglitazone: a randomised double-blind placebo-controlled study. *Diabetologia* 55: 915-925.
610. Gault VA, Lennox R, Flatt PR (2015) Sitagliptin, a dipeptidyl peptidase-4 inhibitor, improves recognition memory, oxidative stress and hippocampal neurogenesis and upregulates key genes involved in cognitive decline. *Diabetes Obes Metab* 17: 403-413.
611. Lee YS, Park MS, Choung JS, Kim SS, Oh HH, et al. (2012) Glucagon-like peptide-1 inhibits adipose tissue macrophage infiltration and inflammation in an obese mouse model of diabetes. *Diabetologia* 55: 2456-2468.
612. Thielitz A, Vetter RW, Schultze B, Wrenger S, Simeoni L, et al. (2008) Inhibitors of dipeptidyl peptidase IV-like activity mediate antifibrotic effects in normal and keloid-derived skin fibroblasts. *J Invest Dermatol* 128: 855-866.
613. Michalkiewicz M, Zhao G, Jia Z, Michalkiewicz T, Racadio MJ (2005) Central neuropeptide Y signaling ameliorates N(omega)-nitro-L-arginine methyl ester hypertension in the rat through a Y1 receptor mechanism. *Hypertension* 45: 780-785.
614. Costoli T, Sgoifo A, Stilli D, Flugge G, Adriani W, et al. (2005) Behavioural, neural and cardiovascular adaptations in mice lacking the NPY Y1 receptor. *Neurosci Biobehav Rev* 29: 113-123.